MULTIFOCAL CHOROIDITIS

Clinical, immunologic and genetic aspects

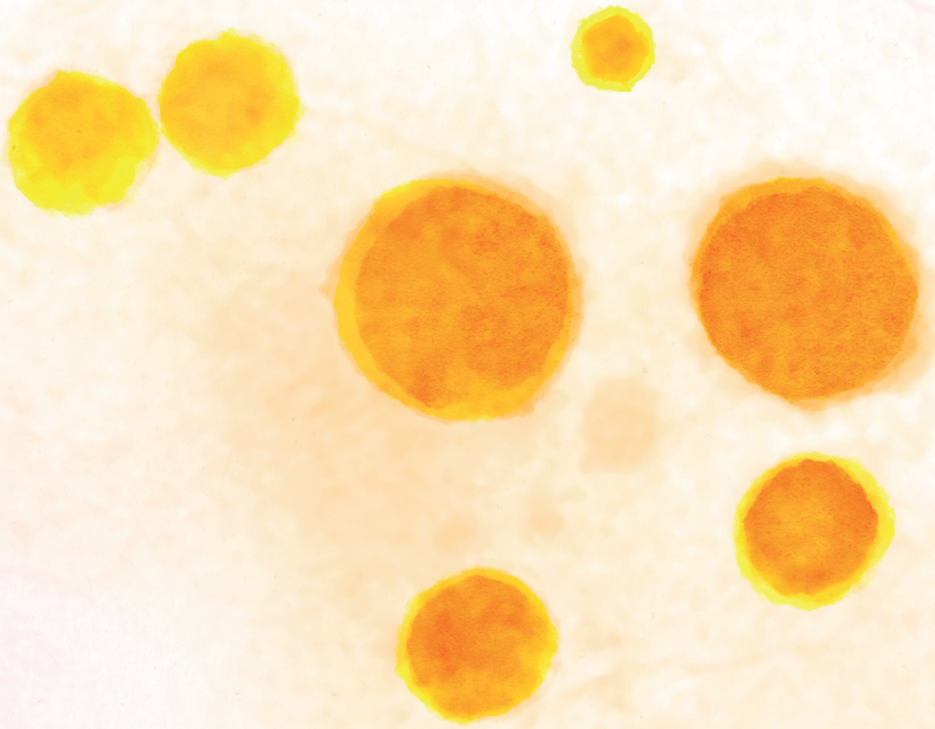

EVIANNE DE GROOT

Multifocal choroiditis

Clinical, immunologic and genetic aspects

Evianne Laura de Groot

Colofon

Cover and layout: Erwin Timmerman
Layout and printed by: Optima Grafische Communicatie (www.ogc.nl)
ISBN: 978-94-6361-853-3

The research described in this thesis was financially supported by het Oogfonds, Dr. F.P. Fischer Stichting, Stichting Beheer het Schild, Landelijke Stichting voor Blinden en Slechtzienden, Rotterdamse Stichting Blindenbelangen, Corona Noodfonds, Algemene Nederlandse Vereniging Ter Voorkoming Van Blindheid en het Louise Rottinghuis Fonds. Publication of this thesis was financially supported by Rotterdamse Stichting Blindenbelangen, Blindenhulp, Landelijke Stichting voor Blinden en Slechtzienden, Théa Pharma, Visser contactlenzen, Chipsoft, Infection & Immunity Utrecht, Oculenti, Rockmed, Tramedico, and Bayer.

Multifocal choroiditis
Clinical, immunologic and genetic aspects

Multifocale choroïditis
Klinische, immunologische en genetische aspecten
(met een samenvatting in het Nederlands)

Proefschrift

ter verkrijging van de graad van doctor aan de
Universiteit Utrecht
op gezag van de

rector magnificus, prof.dr. H.R.B.M. Kummeling,

ingevolge het besluit van het college voor promoties
in het openbaar te verdedigen op
donderdag 29 juni 2023 des middags te 2.15 uur

door

Evianne Laura de Groot
geboren op 24 februari 1994
te Leiderdorp

Promotoren:
Prof. dr. J.H. de Boer
Prof. dr. C.B. Hoyng

Copromotoren:
Dr. J. Ossewaarde-van Norel
Dr. J.J.W. Kuiper

Beoordelingscommissie:
Prof. dr. D. Hamann (voorzitter)
Prof. dr. C.C.W. Klaver
Prof. dr. J.H. Veldink
Dr. M.E.J. van Velthoven
Prof. dr. S.M. Imhof

Paranimfen:
Sara Lopes van den Broek
Wilbert Tomey

TABLE OF CONTENT

LIST OF ABBREVIATIONS

ADA	Adalimumab
AF	Allele frequency
AMD	Age-related macular degeneration
APMPPE	Acute posterior multifocal placoid pigment epitheliopathy
APOC1	Apolipoprotein C-I
APOF	Apolipoprotein F
AU	Arbitrary units
AUMC	Amsterdam University Medical Center
AZA	Azathioprine
AZOOR	Acute zonal occult outer retinopathy
B	Beta
BCVA	Best-corrected visual acuity
BSCR	Birdshot chorioretinopathy
BVZ	Bevacizumab
C3	Complement component 3
CBC	Complete blood count
CFH	Complement factor H
CI	Confidence interval
CMFC	Central multifocal choroiditis
CNV	Choroidal neovascularization
CP	Cyclophosphamide
CS	Corticosteroids
CsA	Cyclosporine
CSC	Central serous chorioretinopathy
C-section	Caesarean section
D	Diopters
DMARD	Disease-modifying antirheumatic drug
EDI	Enhanced depth imaging
EMC	Erasmus Medical Center
EZ	Ellipsoid zone
F2	Prothrombin
FA	Fluorescein angiography
FAF	Fundus autofluorescence
FDR	False discovery rate
FGA	Fibrinogen alpha chain
FH	Factor H
FHR	Factor H-related

GA	Gestational age
GH-QoL	General health quality of life
GIPR	Gastric inhibitory polypeptide receptor
GLD	Greatest linear dimension
GWAS	Genome-wide association study
HLA	Human leukocyte antigen
HRC	Haplotype Reference Consortium
HWE	Hardy-Weinberg equilibrium
ICGA	Indocyanine green angiography
ICP	Intrahepatic cholestasis of pregnancy
IL10	Interleukin 10
IMT	Immunomodulatory therapy
IOP	Intraocular pressure
IQR	Interquartile range
LBW	Low birth weight
LD	Linkage disequilibrium
LFMN	Mean lymphocyte fluorescence
LogMAR	Logarithm of the Minimum Angle of Resolution
LRT	Likelihood ratio test
LUMC	Leiden University Medical Center
MAF	Minor allele frequency
MEWDS	Multiple evanescent white dot syndrome
MFC	Multifocal choroiditis
MFMN	Mean monocyte fluorescence
MHC	Major histocompatibility complex
MMF	Mycophenolate mofetil
MMI	Multimodal imaging
MON	Number of monocytes
MONE	Absolute number of monocytes without blasts
MPA	Mycophenolic acid
MTX	Methotrexate
NBS	Nijmegen Biomedical Study
NEI-VFQ-25	National Eye Institute Visual Function Questionnaire 25
NFCV	Coefficient of variance as percentage of the mean of the FL3-fluorescence of neutrophil granulocytes
NFMN	Mean FL3-fluorescence of neutrophil granulocytes
NIR	Near-infrared
NIU	Non-infectious uveitis
NPX	Normalized Protein eXpression

OR	Odds ratio
PC	Principal Components
PEA	Proximity extension assay
PIC	Punctate inner choroidopathy
PICC	Primary inflammatory choriocapillaropathy
PIMN	Platelet granularity
PMON	The number of monocytes as percentage of all leukocytes
PMONE	The number of monocytes without blasts as percentage of all leukocytes
POHS	Presumed ocular histoplasmosis syndrome
PPM	Persistent placoid maculopathy
QC	Quality control
QoL	Quality of life
Radboudumc	Radboud University Medical Center
RBCFMN	Mean erythrocyte fluorescence
RBZ	Ranibizumab
RPC	Relentless placoid chorioretinitis
RPE	Retinal pigment epithelium
SAIGE	Scalable and Accurate Implementation of GEneralized
SC	Serpiginous choroiditis
SD	Standard deviation
(SD-)OCT	(Spectral-domain) Optical coherence tomography
(SD-)OCTA	(Spectral-domain) Optical coherence tomography angiography
SE	Spherical equivalent
SF36	Short Form Health Survey 36-items
SLC	Serpiginous-like choroiditis
SLE	Systemic lupus erythematosus
SNP	Single nucleotide polymorphism
TA	Triamcinolone acetonide
TNF	Tumor necrosis factor
UMCG	University Medical Center Groningen
UMCU	University Medical Centre Utrecht
UPOD	Utrecht Patient Oriented Database
VA	Visual acuity
VEGF	Vascular endothelial growth factor
VR-QoL	Vision-related quality of life

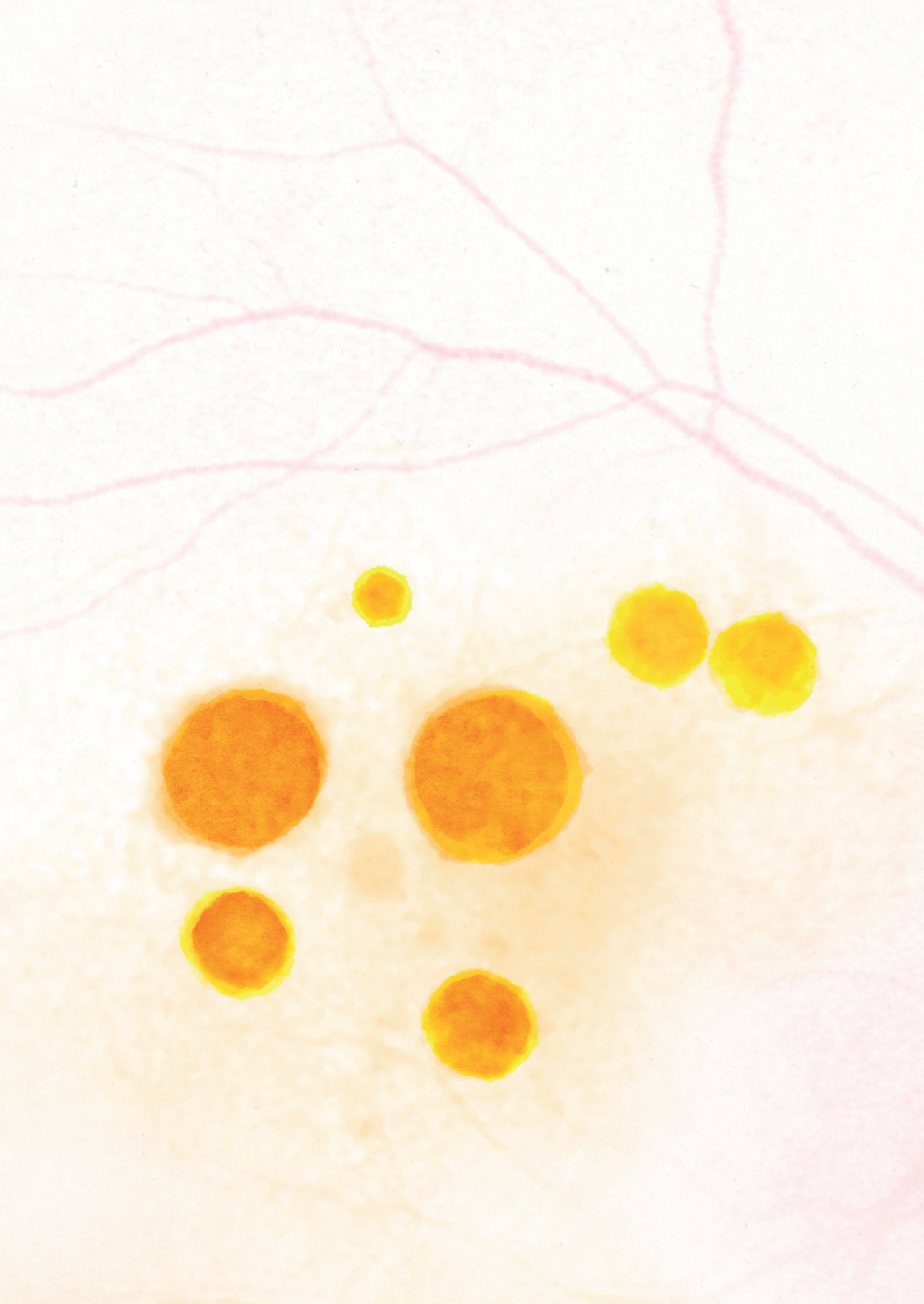

Chapter 1

General introduction

Multifocal choroiditis (MFC) is a relatively rare form of non-infectious uveitis predominantly targeting young women with myopia. MFC belongs to the group of primary inflammatory choriocapillaropathies as introduced by Herbort and colleagues.[1] This potentially sight-threatening disease targets young and otherwise healthy women in their reproductive phase of life. Due to the low prevalence, the current knowledge regarding this disease is very limited. The disease mechanisms underlying MFC are unknown and prior research is restricted to small and targeted genetic studies. Moreover, the course of disease is variable and it is not yet possible to predict this course on patient-level hindering the development of adequate monitoring and treatment strategies. This thesis focuses on three aims:

1. To improve the clinical outcomes of MFC by investigating the efficacy of current therapies and explore clinical risk factors for increased relapse rate.
2. To explore imaging characteristics that can aid in early recognition of disease activity and can help to distinguish inflammation from secondary choroidal neovascularization (CNV).
3. To determine genetic and immunologic risk factors to gain insight into the pathophysiology underlying this disease.

EPIDEMIOLOGY AND DEMOGRAPHICS

The diagnosis of MFC is relatively rare though exact numbers regarding the incidence and prevalence of this group of disease entities are not available. This is mainly since (inter)national registries are lacking and there is no international consensus on the classification criteria and to what extent disease entities should be included in MFC.[2] Though, based on the report of a single center, the incidence is roughly estimated to be around 1.6 persons per million population per year.[3] For the majority of the patients, the first disease presentation occurs during the 2nd-4th decade of life.[4-6] A clear predominance for the female gender is reported with frequencies varying from 71-93%.[3,5-7] MFC is mainly reported in Caucasian subjects though it is also observed in patients from other ethnicities.[8-11] There is an indisputable association between MFC and myopia, yet the clinical relevance and pathophysiological origin of this relationship is unknown. Essex and colleagues reported a median spherical equivalent of -4.6 Diopters (D) and 84% of the patients had myopia, which is similar to the observations in other reports.[4-6,11]

SUBTYPE CLASSIFICATION

In this thesis, we introduce the term central MFC (cMFC) to refer to 4 forms of primary inflammatory choriocapillaritis: “idiopathic multifocal choroiditis”, “punctate inner choroidopathy”, “serpiginous choroiditis” and “relentless placoid chorioretinitis” (**Figure 1.1**). These diagnoses have in common that the choriocapillaris is affected in the macular area and all disease entities are idiopathic and without an association with systemic diseases or other ocular syndromes.[2,12]

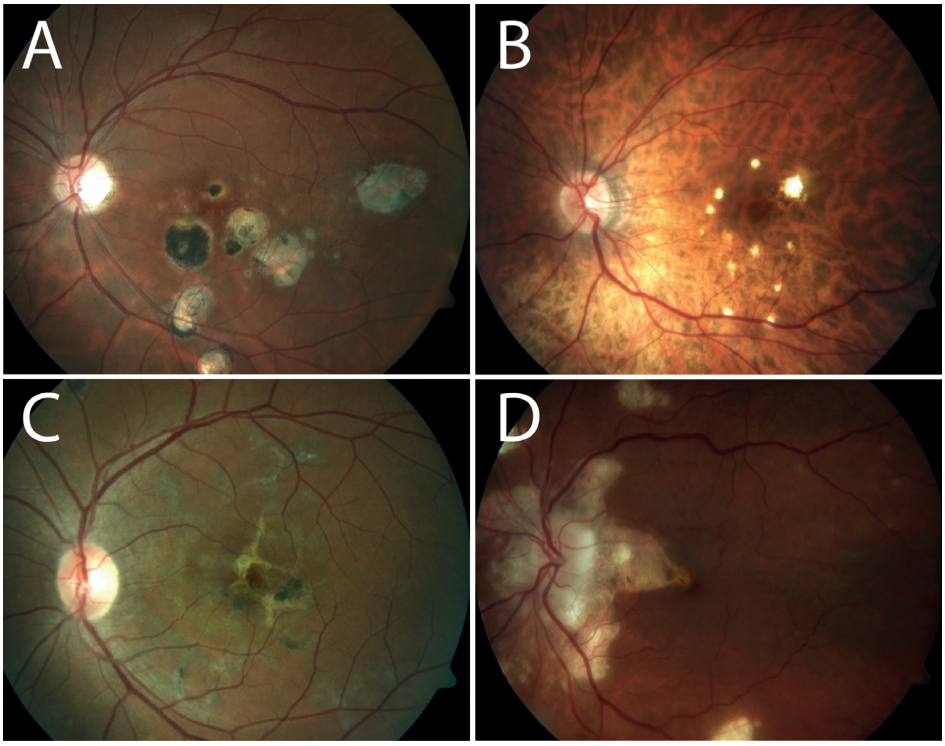

Figure 1.1. Subtypes of central multifocal choroiditis. **A.** Idiopathic multifocal choroiditis **B.** Punctate inner choroidopathy **C.** Relentless placoid chorioretinitis **D.** Serpiginous choroiditis.

Idiopathic MFC and PIC

Idiopathic MFC and punctate inner choroidopathy (PIC) are two very similar disease entities and many even advocate that both represent an identical disease entity. Recently, the SUN working group has developed criteria for PIC and MFC with panuveitis. In this thesis, the diagnoses of PIC and idiopathic MFC followed these criteria with minor adjustments based on consensus recommendation by an expert panel comprising Dutch uveitis- and/or retina-specialists.[8,9,13] Patients were diagnosed with PIC following the criteria 1) chorioretinal lesions were located within the posterior

pole with or without involvement of the mid-peripheral retina but without involvement of the peripheral retina, 2) no cells in the anterior chamber or vitreous were observed, and 3) predominant lesions size was <250µm with a punctate appearance (**Figure 1.1-B**). Idiopathic MFC was diagnosed if 1) chorioretinal lesions were located both in the posterior pole and extending to the peripheral retina, and/or 2) cells were observed in the anterior chamber or vitreous, and 3) predominant lesion size was >125µm with a round appearance (**Figure 1.1-A**). Even though it is not clear if idiopathic MFC and PIC are truly different disease entities, we have adopted both subtypes separately in this thesis.

Serpiginous choroiditis

Serpiginous choroiditis (SC) is considered to be on the more severe end of the spectrum of cMFC. Different types of SC can be distinguished of which the peripapillary form is the most common type (80%) where usually a unifocal lesion grows around the optic disc progressing in a serpentine pattern (**Figure 1.1-D**).[14] The macular form is less frequent but visual prognosis is often worse due to the early involvement of the macular area.[14] SC generally affects older patients without a predominance for the female gender, is almost always bilateral and the frequency of secondary CNV is less high compared to idiopathic MFC and PIC.[15] Serpiginous choroiditis must be differentiated from serpiginous-like choroiditis (SLC), also known as multifocal serpignoid choroiditis, which is linked to an infectious etiology.[14-19] SLC is thought to be the result of an immunological reaction to various organisms of which *Mycobacterium tuberculosis* is most frequent followed by *Toxoplasma gondii*.[14] Consequently, SLC is more prevalent in patients from tuberculosis-endemic regions and should additionally be treated with anti- tuberculous antibiotics.[14,20] The diagnosis of SLC is outside the scope of this thesis.

Relentless placoid chorioretinitis

Relentless placoid chorioretinitis (RPC) was first described by Jonas et al. as a clinical entity presenting with features of both serpiginous choroiditis and acute posterior multifocal placoid pigment epitheliopathy (APMPPE)(**Figure 1.1-C**).[14,18,21] Other names that can be found in the literature are "*ampiginous choroiditis*" or "*atypical APMPPE*".[18,22] In classical APMPPE, the disease is self-limiting and has a prodromal viral flu-like illness.[23] In RPC, the distribution of the lesions is similar to APMPPE but even more widespread and is, in contrast to APMPPE, not monophasic. Both APMPPE and RPC affect relatively young patients but RPC has the chronic and relapsing character of serpiginous choroiditis whereas APMPPE does not.[18,21]

Rare variants and overlapping forms of choriocapillaritis

A very rare form of choroiditis or choroidopathy is persistent placoid maculopathy (PPM). Patients typically present with a large placoid hypopigmented white plaque in the fovea sparing the peripapillary areas corresponding with large lobular areas of hypofluorescence on ICG (**Figure 1.2-A**). Literature is scarce regarding this disease entity with only a few cases available[24] and some consider it to be a subtype of SC.[14,24] A link with cerebral vasculitis has been described and therefore neurological examination, especially when neurological symptoms are present, is advised.[24]

Additionally, idiopathic multifocal choroiditis can present simultaneously with other diagnoses. The most common mixed forms are the combination with acute zonal occult outer retinopathy (AZOOR)[25] and multiple evanescent white dot syndrome (MEWDS) (**Figure 1.2-B)**.[26] MEWDS typically occurs in young women, is self-limiting and many patients have an antecedent influenza-like illness.[27] Recently, the idea of two separate forms of MEWDS was suggested by Esselfie and colleagues,[28] where the primary form is the true self-limiting disease with an influenza-like prodrome and secondary MEWDS or EpiMEWDS occurs as a result of an underlying disease (for example MFC) that caused disruption of the outer retina to subsequently induce MEWDS as an epiphenomenon (**Figure 1.2-C)**.[26]

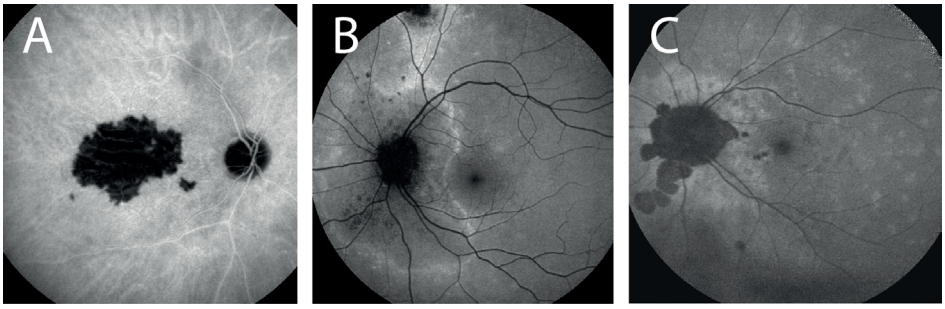

Figure 1.2. A. A case with bilateral persistent placoid maculopathy with a relapse 4 years after initial presentation complicated with a pons infarct most likely due to cerebral vasculitis. **B.** A case with multifocal choroiditis in combination with acute zonal occult outer retinopathy. **C.** A case presenting with recurrent episodes of multiple evanescent white dots syndrome with subsequently the development of chorioretinal lesions matching multifocal choroiditis.

DIFFERENTIAL DIAGNOSES

Other diagnoses can have a similar ocular presentation and should therefore be ruled out in these patients by appropriate diagnostic laboratory testing, chest imaging and anterior chamber fluid analysis if indicated. In particular, patients should be checked for infectious causes of chorioretinitis, including toxoplasmosis, syphilis and tuberculosis, and other alternative diagnoses e.g. sarcoidosis, Birdshot chorioretinopathy and

inflammatory bowel syndrome. Moreover, especially during the inactive stage of disease, PIC and idiopathic MFC lesions will become atrophic and can resemble myopic patchy atrophy. It is even suggested that cMFC patients are often misdiagnosed as myopic patchy atrophy, resulting in an underestimation of the prevalence of cMFC.[29,30] Therefore, it is important to monitor patients with myopia and to be aware of signs that could indicate idiopathic MFC/PIC on multimodal imaging, as will be discussed later in this general introduction, since the prevalence of secondary CNV is much higher in cMFC and the management differs.[29]

SYMPTOMS AND NATURAL COURSE OF DISEASE

The disease is bilateral for the majority of the patients, with reported values varying between 54-88%.[6,31-33] The most frequent reported symptoms during the active stage of the disease are blurred vision, metamorphopsia, scotomas, photopsia, photophobia and floaters.[2,12] cMFC often has a chronic and relapsing character resulting is numerous lesions in the fundus of the eye. A relapse of disease activity can either develop at a different location in the choriocapillaris, resulting in a new chorioretinal lesion, or at the edges of existing chorioretinal atrophy, resulting in growth of the area of chorioretinal atrophy. The local inflammatory process will most likely become quiescent over time, though unfortunately the inflammatory process often has already resulted in irreversible damage to the RPE and the photoreceptors in the form of atrophy. In contrast to other resembling diagnoses, cMFC is often not self-limiting and deterioration of the visual function over time, especially if left untreated, is not rare.[7,31] Moreover, the prevalence of secondary CNV is exceptionally high compared to other non-infectious uveitis entities and increases the risk of irreversible damage of the retina. The incidence of secondary CNV is reported to be between 22 and 81%.[5,7,11] Most patients have already developed this complication before the initial presentation at the ophthalmologist, or will develop secondary CNV within the first year after the first presentation.[6] Essex et al. report that 81% of the patients had developed secondary CNV at baseline and, from the patients without secondary CNV, an additional 22% of the patients developed this complication in a mean follow-up time of 4.5 years.[5] On the contrary, de prevalence of secondary CNV in serpiginous choroiditis is reported to be less high and occurs in 10-25% of the patients.[14] The visual acuity (VA) at presentation is variable depending on the disease localization and complications and can range from almost completely preserved to severely distorted. Moderate vision loss (VA ≤20/50) is reported in 30-55% of the eyes and severe vision loss (VA ≤20/200) in 17-38% of the eyes. However, it must be pointed out that most literature reporting on visual function is relatively outdated.[7,11,31,34] The natural course of disease can be relatively favorable with long time periods between

relapses of disease activity. Unfortunately, the disease often demonstrates many relapses of disease activity and requires long-term treatment with immunomodulatory therapy. Moreover, even in the absence of observed disease activity, enlargement of the chorioretinal lesions is observed, most likely due to subclinical and unrecognized disease activity.[30,35,36]

TERMINOLOGY

Varying and overlapping nomenclature, specifically concerning the diagnosis idiopathic MFC, has resulted in confusion amongst ophthalmologists. Many different names have been established over the years to describe this idiopathic syndrome of recurrent inflammatory activity of the choriocapillaris in young myopic females. The number of different names was that high, that Essex and colleagues even dedicated an Editorial to it.[37] Unfortunately, the term multifocal choroiditis or MFC in the more literal sense can describe any type of multifocal inflammatory choroidal disease with various causes, in contrast to the specific idiopathic syndrome we intend in this thesis. In 1970, the term MFC was used to describe patients with presumed ocular histoplasmosis syndrome (POHS).[38] Unfortunately, the term POHS is still used by many European ophthalmologists to describe this idiopathic syndrome, even though these patients are from non–Histoplasma endemic regions and do not have a positive histoplasmin skin antigen test. Other diagnostic terms developed over the years include "*pseudo-POHS", "multifocal inner choroiditis", "recurrent multifocal choroiditis", "peripheral multifocal chorioretinitis", "multifocal choroidopathy", "multifocal choroiditis with panuveitis", "disseminated inner choroiditis"* and many others.[37] To complicate matters even further, Watzke and colleagues described a similar idiopathic syndrome in 1984, almost identical to the definition of idiopathic MFC but called it punctate inner choroidopathy.[39] Over the years, the use of this term became reserved for patients with smaller lesions clustered at the posterior pole and without cells in the anterior chamber and vitreous.[37]

CMFC AS A PART OF THE "WHITE DOT SYNDROMES"

The overarching term "fungal dot syndromes" was first introduced in 2000 and was renamed shortly after to "white dot syndromes". This term describes a heterogeneous group of inflammatory diseases originally considered to reside in the deep retina and the choroid.[1,20] These inflammatory diseases have in common that multiple white-yellowish lesions can be observed in the fundus of the eye, hence the name "white dot syndromes". At the time of the introduction of this term, the knowledge of the pathophysiology of

these inflammatory diseases was limited, and considering the similar appearance in the fundus, it was assumed that all these disease entities belonged to one disease spectrum. However, nowadays we know that both the aetiology as well as the specific targeted structures differ for these disease entities.[1] Unfortunately, even though ”white dot syndromes” is not accurate and not very specific either, it is still a term that is frequently used in clinical practice and in the literature. Recently, Herbort and colleagues proposed a new classification system specifically focusing on the targeted structures and the aetiology of the various disease entities.[1] In the context of this classification system, this thesis focuses on the non-self-limiting disease entities within the group of primary choriocapillaritis. A schematic representation of this classification system is depicted in **Table 1.1.**

Table 1.1. Classification of choroiditis according to location of lesions, pathophysiology and clinicopathology[1]

Choriocapillary vessels		Choroidal stroma		*Targeted structures*
Choriocapillary non-perfusion		Stromal infiltration of inflammatory cells		*Pathophysiological mechanism*
Primary	Secondary	Primary	Secondary	*Aetiology*
Multiple Evanescent White Dot Syndrome	Serpiginous-like choroiditis	Birdshot chorioretinopathy	Sarcoidosis chorioretinitis	*Diagnosis*
Acute Posterior Multifocal Placoid Pigment Epitheliopathy	Acute syphilitic posterior placoid chorioretinitis	Vogt-Koyanagi-Harada Disease	Syphilitic chorioretinitis	
Idiopathic multifocal choroiditis		Sympathetic ophthalmia	Tuberculosis chorioretinitis	
Punctate inner choroidopathy				
Serpiginous choroiditis				

IMAGING TECHNIQUES

Different imaging techniques are available to monitor patients with cMFC with the goal to detect disease activity in an early stage. The literature regarding which imaging characteristics are useful for the recognition of disease activity is scarce and mostly limited to cross-sectional studies. Therefore, it is uncertain to what extent the imaging characteristics associated with disease activity are reversible or that these imaging characteristics will remain present even when the disease has become inactive. Here,

we discuss the different imaging techniques that are valuable in cMFC and we will give an overview of the imaging characteristics that are described to be associated with disease activity in cMFC.

Fundus photography

Fundus photography is the oldest imaging modality visualizing the fundus of the eye by using white light. New active lesions can be observed as creamy-like spots with vague borders on fundus photography (**Figure 1.3-A**) and hemorrhage can be observed in case of active CNV.[2,40] Inactive lesions are typically described as punched-out lesions with sharp boundaries often demonstrating hyperpigmentation. The role of fundus photography in cMFC is limited since this imaging modality is not very sensitive to diagnose subtle disease activity but can be used to roughly monitor growth of the chorioretinal lesions as indicator for disease activity.

Near-infrared imaging

Near-infrared (NIR) imaging or infrared reflectance imaging uses light with a long excitation wavelength (~820 nm diode laser).[41] The clinical utilization is restricted since disease activity cannot be recognized on NIR imaging, though it is suggested that lesions will be visible on the NIR images before they can be recognized on fundus pictures or fundus autofluorescence (FAF) imaging. Therefore, NIR imaging is suggested to have a higher sensitivity for the early detection of lesions than fundus photography or FAF imaging.[42]

Fundus autofluorescence

Blue-light fundus autofluorescence (FAF) (Heidelberg Spectralis®; excitation peak 488nm, emission peak 610nm) is a non-invasive imaging modality that visualizes the autofluorescent lipofuscin in retinal pigment epithelium (RPE) cells.[43] In cMFC, most lesions appear hypoautofluorescent due to severely affected and atrophic retinal pigment epithelium (RPE) resulting in loss of RPE cells and thus absence of lipofuscin (**Figure 1.3-B**). In cMFC also an increased autofluorescence signal can be observed, though the underlying cause of this phenomenon is not completely clear. Some authors believe this is caused by a reduction of the "photoreceptor screen" due to loss of photoreceptor outer segments resulting in better observation of the autofluorescence signal.[43] Others suggest that inflammation increases the amount of lipofuscin in the RPE cells, which subsequently increases the autofluorescence signal.[44]

Fluorescein and indocyanine green angiography

Both fluorescein angiography (FA) as indocyanine green angiography (ICGA) are invasive imaging techniques based on the intravenous injection of fluorescein and/

or ICG respectively. A fluorescent dye (fluorescein and indocyanine green) is injected intravenously and is excited by a light or laser beam of a specific wavelength using a fundus camera or a scanning laser ophthalmoscope that detects the fluorescent emission light after passing a filter. Thus, the retinal and choroidal perfusion can be examined with both fluorescent dyes. Moreover, leakage of these dyes into the retina or choroid can be observed and, finally, staining of the tissue can occur during the angiogram.[45] The atrophic lesions are well visualized by showing a window defect on the fluorescein angiogram. The role of FA is limited for choroidal diseases since the sodium fluorescein molecule is very small and therefore immediately extravasates out of the choroidal vessels. Moreover, the blue light used in FA (Heidelberg Spectralis®; excitation peak 494nm, emission peak 521nm) is partially absorbed by the melanin in the RPE and choroid and therefore FA is mainly suitable to visualize the (sub)retinal structures and not the choroidal structures.[45] The main role of FA is the diagnosis of secondary CNV because, in that case, the fluorescein molecules will leak out of the neovascular choroidal vessels above the RPE (most CNVs in cMFC are type II lesions or so called classical CNVs). Therefore, an active CNV can be visualized as a gradually increasing hyperfluorescence over time (**Figure 1.3-C+D**).

The majority of the ICG molecules are bound to large size blood proteins and therefore remain intravascularly in the retina.[43] On the contrary, in the choriocapillaris, the molecules will extravasate through the large fenestrations and fill the choroidal stroma, where the dye will slowly be washed out. Moreover, the NIR light used in ICGA has a long wave-length (Heidelberg Spectralis®; excitation peak 789nm, emission peak 814nm) and is therefore able to penetrate the RPE making this imaging modality particular useful in visualizing the choroid.[45] In ICGA, the most important observation is hypofluorescent areas at the location of the lesion and this is assumed to represent choriocapillary non-perfusion (**Figure 1.3-E**).[43,45] Both atrophic lesions as well as lesions with active inflammation can demonstrate hypofluorescence. Suggested signs of inflammation in a lesion on ICGA imaging are an increase in the size of the hypofluorescent area with blurry boundaries.[20,43]

Spectral-domain optical coherence tomography

Spectral-domain optical coherence tomography (SD-OCT) is based on NIR light that is absorbed and backscattered in various degrees by the different boundaries between cells and cell layers in the retina and choroid.[46] This makes it possible to distinguish the different retinal layers and to visualize the consequences of the choriocapillary non-perfusion on the retinal layers in cMFC.

One of the first signs that is considered to represent choriocapillary non- or hypoperfusion due to inflammation occurs in the ellipsoid zone (EZ) layer. This layer represents the junction between the inner and outer segment of photoreceptors. Specifically the photoreceptors are very sensitive for ischemia due to their high energy consumption to convert light into electrical signals.[47] Thus, one of the first signs of inflammation is considered EZ disruption near or at the location of the active inflammatory lesions. In later stages, when the inflammatory lesions have become atrophic scars, the RPE and the outer segment of the photoreceptors can even completely disappear (**Figure 1.3-G+H**).[40] Some authors suggest that also an increase in the thickness of the choroid/choriocapillaris can be observed in the inflammatory lesions referred to as the "sponge sign".[48,49] Moreover, secondary CNV can be identified on SD-OCT imaging but it can still difficult to distinguish secondary CNV from inflammatory lesions since sub- or intraretinal fluid is often absent in the early stage of the CNV.[50,51]

Spectral-domain optical coherence tomography angiography

Spectral-domain optical coherence tomography angiography (SD-OCTA) is a relatively new imaging technique. This technique relies on the consecutive performance of many OCT scans and the comparison between these scans. Differences between the scans is considered motion of erythrocytes and thus blood flow.[52] This information is processed using an algorithm to create images of vessels and the static surrounding areas. In theory, this imaging modality is capable of visualizing hypoperfusion in the choriocapillaris and can identify secondary CNV (**Figure 1.3-F**). SD-OCTA is a promising imaging technique but knowledge regarding the clinical performance in cMFC is limited.[51,53-55]

TREATMENT OF CMFC

Systemic immunomodulatory treatment

The treatment strategy for cMFC focuses on the suppression of the immune system to treat the inflammatory processes in the choriocapillaris and prohibit subsequent damage to the choroidal and retinal structures.[43,46] The treatment strategy can be considered as a stepwise approach and the treatment is escalated in case disease activity is insufficiently controlled with the current therapy. The first step is the start of systemic glucocorticosteroid therapy to rapidly control the inflammation. Usually, prednisolone at a dosage of 1mg/kg per day with a maximum dosage of 60mg/day is initiated which will be tapered over the course of 4-6 months and can be discontinued if the disease remains quiescent. Long-term treatment with glucocorticosteroids, even at relatively low dosages, should be avoided given the concerns regarding the long-term safety and to prevent the development of severe side-effects including

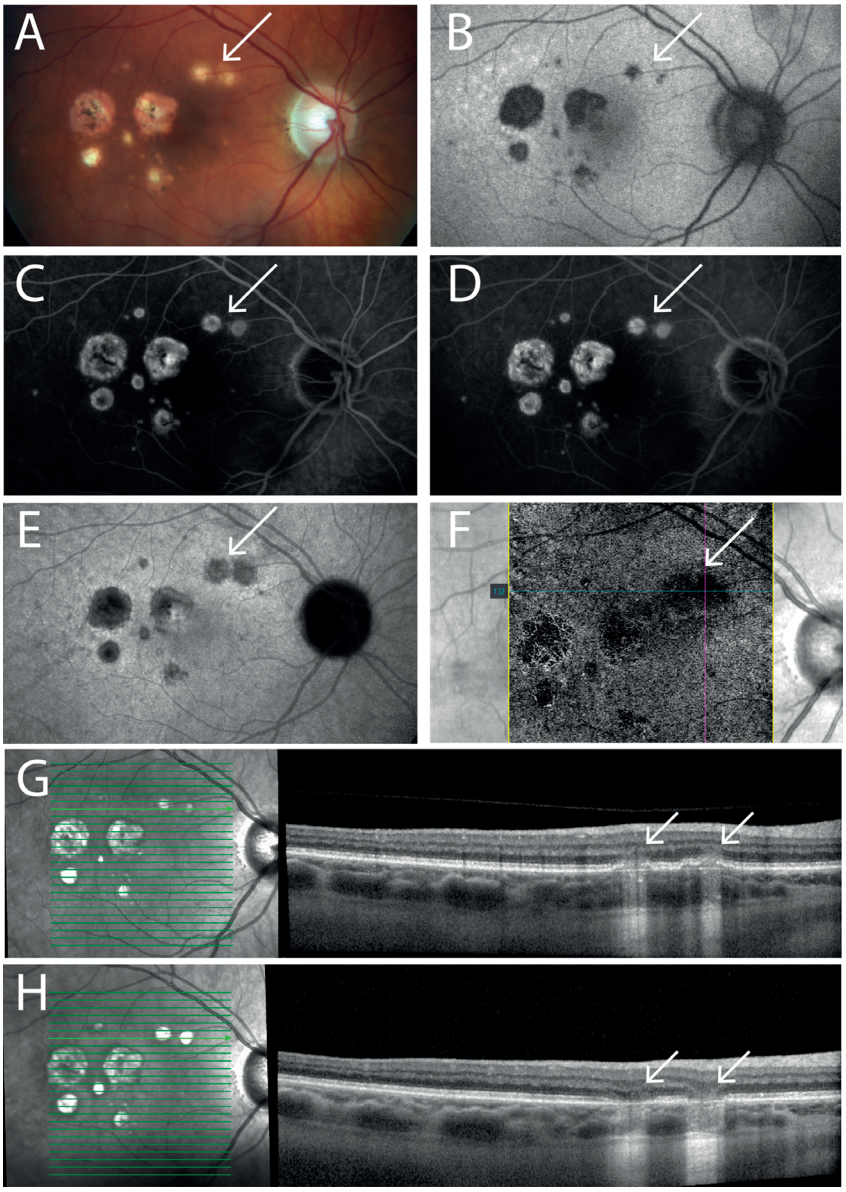

Figure 1.3. Multimodal imaging in cMFC. The different imaging modalities are demonstrated in a patient diagnosed with MFC in an active stage (**A-G**) and inactive stage (**H**). The two active lesions are indicated with the white arrows. **A.** Fundus picture shows the active lesions as creamy-like spots with vague borders; **B.** Fundus autofluorescence picture demonstrate atrophy (hypoautofluorescence) of the retinal pigment epithelium (RPE) at the location of the disease activity but the affected area is limited compared to other imaging modalities. **C+D.** Fluorescein angiography images in the early (**C**) and late (**D**) phases demonstrating minimal leakage in the late phase. **E.** Indocyanine green angiography picture at the late phase (30 minutes). The active lesions are observed as large hypofluorescent areas with vague borders. **F.** Optical coherence tomography angiography demonstrates large areas of hypoperfusion of the choriocapillaris under the lesions larger in size compared to FAF and fundus pictures. **G+H.** Optical coherence tomography during the active (**G**) and inactive (**H**) stages of disease. During the active stage, hyperreflective material accumulates below the RPE resulting in the disruption of the ellipsoid zone (EZ) and RPE. In the inactive stage atrophic areas can be observed with the disappearance of the EZ and RPE.

osteoporosis, systemic hypertension, hyperglycaemia and psychological burdens. If the patient develops a relapse of disease activity during the tapering period or shortly after the prednisolone is discontinued, the initiation of corticosteroid-sparing immunomodulatory therapy (IMT) including disease-modifying antirheumatic drugs (DMARDs) or biological therapy is often considered. Even though the literature on the effectiveness of DMARDs in cMFC is scarce and limited to case reports,[56,57] it is universally accepted as safe and effective for other forms of non-infectious uveitis.[58-61] The most commonly used DMARDs are azathioprine (AZA), methotrexate (MTX), mycophenolate mofetil (MMF) and cyclosporine. If monotherapy with a DMARD is ineffective, the next step could be to increase the dosage of the DMARD if possible. If this is not sufficient to control the disease, treatment with either the combination of two types of DMARD or the combination of a biological agent and a DMARD can be considered. Biological agents including adalimumab and infliximab are potentially very effective and are increasingly imbedded in the treatment of non-infectious uveitis.[62-65] Positive results are also observed in cMFC, though literature is limited to case reports and therefore caution is advised when prescribing these agents.[25,66-68]

Anti-vascular endothelial growth factor therapy

Secondary CNV is a frequent complication affecting up to 81% of patients with cMFC.[5] The effectiveness of intravitreal anti-vascular endothelial growth factor (VEGF) injections to treat CNV is particularly well investigated in patients with age-related macular degeneration (AMD). Since the introduction of intravitreal anti-VEGF injections, the visual outcome of affected eyes improved dramatically.[69] Even though treatment with anti-VEGF is less thoroughly investigated in non-AMD diagnoses, cohort studies report beneficial effects of treatment with anti-VEGF therapy in cMFC. Therefore, this treatment is universally accepted as standard practice for secondary CNV in patients with cMFC.[70-74]

Note that simultaneously treating the inflammatory component with immunomodulatory therapy (IMT) and if applicable the complication of secondary CNV with intravitreal anti-VEGF injections is not standardized practice. Still many ophthalmologists consider the administration of intravitreal anti-VEGF injections for the complication of secondary CNV the principal treatment option for cMFC and only consider treatment with immunomodulatory therapy (prednisolone/DMARDs) in select and severe cases.

SHARED DECISION-MAKING

The approach of shared decision-making is gaining importance in clinical practice. Central in this approach is that both the treating physician and the patient jointly decide

what the best treatment option is. Especially for the treatment of patients with cMFC this concept is of upmost importance since most patients are relatively young and otherwise healthy individuals. Due to the rarity of the disease and the fact that the pathophysiology of cMFC is still widely unknown, there is no absolute evidence that immunomodulatory therapy is effective in cMFC. On the other hand, side-effects are reported frequently for both prednisolone and DMARDs.[60] The quality of life of patients with cMFC has never been explored but is of interest to identify possible relations with disease activity and immunomodulatory therapy.

CMFC AND PREGNANCY

Since cMFC predominantly develops in women in the second to fourth decade of life, patients often become pregnant or want to become pregnant. During pregnancy, various immunological and hormonal changes take place favoring the maternal tolerance of the fetus. Generally, the immune system becomes more tolerant during pregnancy and, as a result, most autoimmune diseases become quiescent during pregnancy.[75,76] Literature regarding the course of disease during pregnancy and in the postpartum period in cMFC patients, is scarce and limited to case studies.[77-79] In non-infectious uveitis in general, a decline in the relapse rate is observed during the second and third trimester of the pregnancy.[80-83] Treating pregnant patients can be challenging because several DMARDs are contra-indicated due to safety reasons for the fetus. Moreover, anti-VEGF is considered potentially teratogenic and embryo-fetotoxic. Therefore, treatment with intravitreal anti-VEGF injections is advised to be avoided in pregnancy, especially in the first trimester.[78,84,85] Consequently, pre-conception counseling should be considered by the treating ophthalmologist.

PATHOPHYSIOLOGY – WHERE DO WE STAND

The pathophysiological mechanism driving cMFC is not completely understood. A few genetic and functional case studies have been performed, though in most cases with a limited number of patients and only using a targeted approach. Most ideas concerning the pathophysiological mechanism is still based on clinical observations and the analysis of multimodal imaging results.

Primary targeted structures in cMFC: the chicken or the egg discussion

Currently there is an ongoing debate regarding what the primary targeted structure is in cMFC. Some ophthalmologists advocate that initially the outer segments of the

photoreceptors are targeted in this disease and thus that cMFC is an outer retinal inflammation instead of a choroidal inflammation.[40] They substantiate this statement by the fact that the first signs of active inflammation is the disruption of the outer nuclear layer and the outer segment photoreceptor layer on SD-OCT images (**Figure 1.2G**). Increasing choroidal thickness and the accumulation of material under the RPE are thought to represent the recruitment of inflammatory cells as a consequence of the inflammation of the outer segment of the photoreceptors. Therefore, these authors reason that the hypofluorescent areas on ICGA are the result of infiltration of inflammatory cells in the choriocapillaris rather than a sign of non-perfusion due to choriocapillaritis.[40] Whereas others[47] believe cMFC to be a primary choriocapillaritis, where the primary targets are the choriocapillary vessels. The choriocapillaris provides the outer retina of oxygen and nutrients and, due to capillary non- or hypoperfusion resulting from the choriocapillaritis, the outer retinal structures will endure ischemia. This is supported by a case report demonstrating a decreased choroidal blood flow measured with laser speckle flowgraphy during an active stage of disease in a patient with PIC.[49] Particularly the outer segments of the photoreceptors are sensitive for ischemia and therefore, as these authors propose, will be the first to demonstrate irregularities on SD-OCT imaging.[47] SD-OCT imaging does not provide structural imaging of the choroid or choriocapillaris and thus is not able to visualize abnormalities in the choriocapillaris. Due to the lack of histopathological studies, all theories are based on clinicopathological observations and it cannot be determined with certainty what the primary targeted structure is in cMFC.

The role of myopia: clue for pathogenesis?

From clinical practice, we know that cMFC, and particularly the subtypes idiopathic MFC and PIC, is associated with myopia. Herbort and colleagues hypothesize that myopia leads to structural changes in the choriocapillaris, Bruch's membrane and the RPE, leading to an increased fragility of this complex. It is suggested that due to this fragility, these structures are prone to be targeted by inflammatory diseases[86] and therefore especially patients with myopia will develop idiopathic MFC and PIC. Moreover, they have suggested that the choriocapillaris of myopic eyes is more sensitive for ischemia which could also contribute to the association between cMFC and myopia. Others have demonstrated that the prevalence of myopia is higher in children with inflammatory diseases.[87] Moreover, Lin et al.[87] have demonstrated that genes involved in inflammation are upregulated in myopia using animal models. Currently, most studies exploring the association between myopia and inflammation are experimental animal studies and due to the complex and multifactorial nature of both inflammatory processes and the process of myopia, it remains challenging to unravel all the aspects of this relationship.

Genetic architecture of cMFC

The knowledge concerning the genetic architecture of cMFC is limited to small cohort studies using a targeted approach. Ferrara and colleagues[88] reported an association between MFC and multiple single nucleotide polymorphisms (SNPs) in the *complement factor H (CFH)* gene, known to be associated with AMD. Factor H (FH) is a regulator of the alternative complement pathway and therefore this genetic predisposition supports an immune-mediated mechanism in cMFC. Atan and colleagues[89] investigated the association between SNPs in the *Interleukin 10* (*IL10*) gene and *tumor necrosis factor (TNF)* gene, known to be associated with uveitis. This study discovered an association with a single SNP in the *IL10* gene and this association was only found in patients with MFC, not in patients diagnosed with PIC. No associations were found with SNPs in the *TNF* gene. Lastly, few studies explored an association with the *human leukocyte antigen* (*HLA*) regions, specifically the *HLA-DR2* region since this region is thought to be related to the phenotypically similar POHS in patients with positive histoplasmin skin antigen test in the United States.[90-93] The results are inconclusive since both decreased and increased allele frequencies in *HLA-DR2* are reported.[89,94,95]

Over the last decades, genome-wide association studies (GWAS) have helped to reveal genetic structures for many traits. One of the first successful GWAS was performed for AMD and has contributed largely to the current knowledge concerning the pathophysiology for this multifactorial trait.[96] In contrast to Mendelian traits involving rare mutations, this type of analysis works particularly well for multifactorial diseases. In this type of diseases, the genetic susceptibility is considered to be mediated predominantly by common variants that each have a small contribution to the phenotypic trait.

There are many locations with genomic variation within the genome.[97] Most genomic variation consists of common variants, also known as single nucleotide polymorphisms (SNPs). The principle of a GWAS is to compare allele frequencies between groups (mostly individuals with and without a certain trait) for SNPs throughout the genome. A strong deviation in the frequency for a certain SNP implicates that either the SNP itself or a genetic locus in proximity of the SNP is associated with the studied trait. In a GWAS, allele frequencies of thousands to millions of SNPs are compared between patients with and without a certain trait. The association results of all the SNPs are summarized in a *Manhattan plot* (**Figure 1.4**), where every single dot represent the association result for a single SNP.[97] SNPs are considered associated with a trait if the result of the association test exceeds a certain threshold (for most GWAS this threshold is set at $P<5.0\times10^{-8}$). Linkage disequilibrium (LD) is the phenomenon were SNPs are not in equilibrium and are associated with each other in the population more frequently than one would expect based on random selection (often these SNPs are located in proximity of each other).

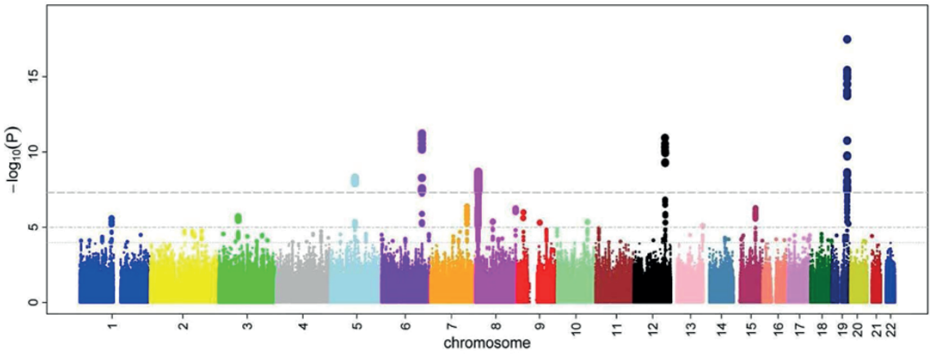

Figure 1.4. An illustration of a Manhattan plot commonly used to summarize and visualize the results of a genome-wide association study. In this plot the chromosomes are on the x-axis and are represented in various colors. Each dot represents the association results of a single nucleotide polymorphism (SNP) with an explored trait. The y-axis represents the $-\log_{10}$ of the p-value of the association test and thus the higher a SNP is plotted in the Manhattan plot the lower the p-value is of the association test (i.e. stronger associated with the trait). Picture originates from Ikram MK et al (2010).[98]

This information of LD can be used for the imputation of SNPs and consequently not all SNPs have to be directly genotyped but, based on the LD, many SNPs can also be predicted. Once an associated SNP is discovered in a GWAS, the true associated variation can be that specific SNP but most likely, the true association is near and correlated with the associated SNP found in the GWAS.[97]

Functional studies in cMFC

Research regarding the pathophysiological mechanism driving cMFC is limited to targeted genetic studies and no literature exists on functional evaluation of the immune system. Several methods exists to explore the biological pathways and blood cells involved in a disease process. Proteomics refer to the detection and quantification of proteins and this can be explored using several techniques including proximity extension assay technology (PEA). Multiplex immunoassays such as Olink PEA enables the measurement of many proteins in a small amount of blood and even low abundant proteins, including chemokines and interleukins, can be measured with great accuracy.[99,100]

The exploration of the blood cell composition and morphological blood cell characteristics using automated hematocytometry is another approach to further unravel to pathophysiology of cMFC. The Utrecht Patient Oriented Database (UPOD) is a research facility that stores the results of a hematology analyzer, a machine that uses spectrophotometry, electrical impedance, laser light scattering (multi angle polarized scatter separation), and 3-color fluorescent technologies to report on morphological parameters of red blood cells, platelets and leukocytes.[101,102]

AIM AND OUTLINE OF THE THESIS

The overarching aim of this thesis is to identify clinical and genetic risk factors of cMFC. These risk factors will help to increase the understanding of the pathophysiological mechanism of cMFC and can be used to improve the monitoring and treatment of patients with cMFC.

Part 1. Clinical aspects of cMFC

The first part of this thesis will focus on the clinical aspects of cMFC including the treatment strategies and clinical risk factors for an increased relapse rate.

In **Chapter 2**, we describe the results of a prospective 2-year follow up study. In this study we describe the course of disease in a large cohort of patients. Moreover, the aim is to determine clinical characteristics that are associated with an increase in the relapse rate.

Chapter 3 and **Chapter 4** focus on the evaluation of treatment strategies. In **Chapter 3**, we evaluate the effectiveness of IMT in patients with cMFC. In **Chapter 4**, we describe the clinical course of disease before and after the initiation of adalimumab, a tumor necrosis factor-alpha antagonist.

Predominantly relative young females are affected in this disease and thus pregnancies occur frequently. In **Chapter 5**, we describe the course of disease during pregnancy and report on the available treatment strategies during pregnancy.

Part 2. Multimodal imaging characteristics of cMFC

This part comprises **Chapter 6** where we evaluate six different imaging modalities. In this chapter, we will explore differences in imaging-related characteristics between an active and inactive stage of disease and we attempt to find imaging-related variables that are able to distinguish inflammatory lesions from secondary CNV.

Part 3. Immunological and genetic risk factors of cMFC

In **Chapter 7**, we evaluate morphological blood cell characteristics between patients with cMFC and control subjects using readily available data stored in the Utrecht Patient Oriented Database. In **Chapter 8**, we describe the incidental finding of distorted blood cell characteristics after the performance of fluorescein angiography.

In **Chapter 9**, we describe the results of a genome-wide association analysis in patients with idiopathic MFC and PIC from 6 Dutch academic centers including a targeted

validation in an independent cohort. Additionally, we evaluated the concentrations of 370 proteins incorporated in the Explore 384 Inflammation II panel from Olink® in a selection of treatment-naïve patients. In **Chapter 10**, we explore if the genetic association discovered in chapter 9 is also present in other subtypes of cMFC including serpiginous choroiditis and relentless placoid chorioretinitis.

REFERENCES

1. Neri P, Herbort CP, Hedayatfar A, et al. “White dot syndromes”, an inappropriate and outdated misnomer. Int Ophthalmol. 2022;42(1):1-6.
2. Tavallali A, Yannuzzi LA. Idiopathic multifocal choroiditis. J Ophthalmic Vis Res. 2016;11(4):429-432.
3. Jones NP. The Manchester Uveitis Clinic: The first 3000 patients--epidemiology and casemix. Ocul Immunol Inflamm. 2015;23(2):118-126.
4. Fung AT, Pal S, Yannuzzi NA, et al. Multifocal choroiditis without panuveitis; Clinical Characteristics and Progression. Retina. 2014;34(1):98-107.
5. Essex RW, Wong J, Fraser-Bell S, et al. Punctate inner choroidopathy: Clinical Features and Outcomes. Arch Ophthalmol. 2010;128(8):982-987.
6. Niederer RL, Gilbert R, Lightman SL, Tomkins-Netzer O. Risk Factors for Developing Choroidal Neovascular Membrane and Visual Loss in Punctate Inner Choroidopathy. Ophthalmology. 2018;125(2):288-294.
7. Thorne JE, Wittenberg S, Jabs DA, et al. Multifocal Choroiditis with Panuveitis. Incidence of Ocular Complications and of Loss of Visual Acuity. Ophthalmology. 2006;113(12):2310-2316.
8. The Standardization of Uveitis Nomenclature (SUN) Working group. Classification criteria for multifocal choroiditis with panuveitis. Am J Ophthalmol. 2021;228:152-158.
9. The Standardization of Uveitis Nomenclature (SUN) Working group. Classification Criteria for Punctate Inner Choroiditis. Am J Ophthalmol. 2021;228:275-280.
10. Gerstenblith AT, Thorne JE, Sobrin L, et al. Punctate Inner Choroidopathy. A Survey Analysis of 77 Persons. Ophthalmology. 2007;114(6).
11. Zhang X, Wen F, Zuo C, et al. Clinical features of punctate inner choroidopathy in Chinese patients. Retina. 2011;31(8):1680-1691.
12. Ahnood D, Madhusudhan S, Tsaloumas MD, Waheed NK, Keane PA, Denniston AK. Punctate inner choroidopathy: A review. Surv Ophthalmol. 2017;62(2):113-126.
13. Gilbert RM, Niederer RL, Kramer M, et al. Differentiating Multifocal Choroiditis and Punctate Inner Choroidopathy: A Cluster Analysis Approach. Am J Ophthalmol. 2020;213:244-251.
14. Dutta Majumder P, Biswas J, Gupta. Enigma of serpiginous choroiditis. Indian J Ophthalmol. 2019;67:325-333.
15. The Standardization of Uveitis Nomenclature (SUN) Working group. Classification Criteria for Serpiginous Choroiditis. Am J Ophthalmol. 2021;228:126-133.
16. The Standardization of Uveitis Nomenclature (SUN) Working Group. Classification criteria for tubercular uveitis. Am J Ophthalmol. 2021;228:142-514.
17. Kawali A, Bavaharan B, Sanjay S, Mohan A, Mahendradas P, Shetty R. Serpiginous-Like Choroiditis (SLC)–Morphology and Treatment Outcomes. Ocul Immunol Inflamm. 2020;28(4):667-675.
18. Nazari Khanamiri H, Rao NA. Serpiginous choroiditis and infectious multifocal serpiginoid choroiditis. Surv Ophthalmol. 2013;58(3):203-232.
19. Cunningham ET, Gupta A, Zierhut M. The creeping choroiditides-serpiginous and multifocal serpiginoid choroiditis. Ocul Immunol Inflamm. 2014;22(5):345-348.
20. Herbort CP, Neri P, Papasavvas I. Clinicopathology of non-infectious choroiditis: evolution of its appraisal during the last 2–3 decades from “white dot syndromes” to precise classification. J Ophthalmic Inflamm Infect. 2021;11(1).
21. Jones EB, Jampol LM, Yannuzzi LA, et al. Relentless placoid chorioretinitis. Arch Ophthalmol. 2000;118:931-938.

22. Jyotirmay B, Jafferji SS, Sudharshan S, Kalpana B. Clinical profile, treatment, and visual outcome of ampiginous choroiditis. Ocul Immunol Inflamm. 2010;18(1):46-51.
23. The Standardization of Uveitis Nomenclature (SUN) Working group. Classification criteria for acute posterior multifocal placoid pigment epitheliopathy. Am J Ophthalmol. 2021;228:174-181.
24. Kolomeyer AM, Brucker AJ. Persistent Placoid Maculopathy: A Systematic Review. Retina. 2018;38(10):1881-1895.
25. Neri P, Ricci F, Giovannini A, et al. Successful treatment of an overlapping choriocapillaritis between multifocal choroiditis and acute zonal occult outer retinopathy (AZOOR) with adalimumab (HumiraTM). Int Ophthalmol. 2014;34(2):359-364.
26. Serrar Y, Cahuzac A, Gascon P, et al. COMPARISON OF PRIMARY AND SECONDARY FORMS OF MULTIPLE. Retina. 2022;42(12):2368-2378.
27. The Standardization of Uveitis Nomenclature (SUN) Working group. Classification Criteria For Multiple Evanescent White Dot Syndrome. Am J Ophthalmol. 2021;228:198-204.
28. Essilfie J, Bacci T, Abdelhakim AH, et al. Are There Two Forms of Multiple Evanescent White Dot Syndrome? Retina. 2022;42(2):227-235.
29. Hady SK, Xie S, Freund KB, et al. Prevalence and Characteristics of Multifocal Choroiditis/Punctate Inner Choroidopathy in Pathologic Myopia Eyes With Patchy Atrophy. Retina. 2022;42(4):669-678.
30. Chen YC, Chen YL, Chen SN. Chorioretinal Atrophy in Punctate Inner Choroidopathy/multifocal Choroiditis: A Five-year Follow-up Study. Ocul Immunol Inflamm. 2021;00(00):1-6.
31. Kedhar SR, Thorne JE, Wittenberg S, Jabs DA. Multifocal choroiditis with Panuveitis and Punctate Inner Choroidopathy: Comparison of Clinical Characteristics at Presentation. Retina. 2007;27(9):1174-1179.
32. Borrego-Sanz L, Gómez-Gómez A, Gurrea-Almela M, et al. Visual acuity loss and development of ocular complications in white dot syndromes: a longitudinal analysis of 3 centers. Graefe□s Arch Clin Exp Ophthalmol. 2019;257(11):2505-2516.
33. Brown J. J, Folk JC, Reddy C V., Kimura AE. Visual prognosis of multifocal choroiditis, punctate inner choroidopathy, and the diffuse subretinal fibrosis syndrome. Ophthalmology. 1996;103(7):1100-1105.
34. Leung TG, Moradi A, Liu D, et al. Clinical features and incidence rate of ocular complications in punctate inner choroidopathy. Retina. 2014;34(8):1666-1674.
35. Erba S, Cozzi M, Xhepa A, Cereda M, Staurenghi G, Invernizzi A. Distribution and Progression of Inflammatory Chorioretinal Lesions Related to Multifocal Choroiditis and Their Correlations with Clinical Outcomes at 24 Months. Ocul Immunol Inflamm. 2022;30(2):409-416.
36. Hua R, Liu L, Chen L. Evaluation of the progression rate of atrophy lesions in punctate inner choroidopathy (PIC) based on autofluorescence analysis. Photodiagnosis Photodyn Ther. 2014;11(4):565-569.
37. Essex RW, Wong J, Jampol LM, Bird AC. Editorial Idiopathic Multifocal Choroiditis : A Comment on Present and Past Nomenclature. Retina. 2013;33(1):1-4.
38. Krill AE, Archer D. Choroidal Neovascularization in Multifocal (Presumed Histoplasmin) Choroiditis. Arch Ophthalmol. 1970;84(5):595-604.
39. Watzke RC, Packer AJ, Folk JC, Benson WE, Burgess D, Ober RR. Punctate Inner Choroidopathy. Am J Ophthalmol. 1984;98(5):572-584.
40. Zhang X, Zuo C, Li M, Chen H, Huang S, Wen F. Spectral-domain optical coherence tomographic findings at each stage of punctate inner choroidopathy. Ophthalmology. 2013;120(12):2678-2683.
41. Abdolrahimzadeh S, Ciancimino C, Grassi F, Sordi E, Fragiotta S, Scuderi G. Near-Infrared Reflectance Imaging in Retinal Diseases Affecting Young Patients. J Ophthalmol. 2021;2021.

42. Li J, Li Y, Li H, Zhang L. Imageology features of different types of multifocal choroiditis. BMC Ophthalmol. 2019;19(1):1-7.
43. Papasavvas I, Herbort CPJ. Diagnosis and Treatment of Primary Inflammatory Choriocapillaropathies (PICCPs): A Comprehensive Overview. Medicina (B Aires). 2022;58(2):165.
44. Munk MR, Jung JJ, Biggee K, et al. Idiopathic multifocal choroiditis/punctate inner choroidopathy with acute photoreceptor loss or dysfunction out of proportion to clinically visible lesions. Retina. 2015;35(2):334-343.
45. Herbort CP. Fluorescein and Indocyanine Green Angiography for Uveitis. Middle East Afr J Ophthalmol. 2009;16(4):168-187.
46. Mrejen S, Spaide RF. Optical coherence tomography: Imaging of the choroid and beyond. Surv Ophthalmol. 2013;58(5):387-429.
47. Herbort CP, Tugal-Tutkun I, Mantovani A, Neri P, Khairallah M, Papasavvas I. Advances and potential new developments in imaging techniques for posterior uveitis Part 2: invasive imaging methods. Eye. 2021;35(1):52-73.
48. Giuffrè C, Marchese A, Fogliato G, et al. The Sponge sign: A novel feature of inflammatory choroidal neovascularization. Eur J Ophthalmol. Published online 2020.
49. Hirooka K, Saito W, Hashimoto Y, Saito M, Ishida S. Increased macular choroidal blood flow velocity and decreased choroidal thickness with regression of punctate inner choroidopathy. BMC Ophthalmol. 2014;14(1):1-8.
50. Hoang Q V., Cunningham ET, Sorenson JA, Freund KB. The “pitchfork sign”: A distinctive optical coherence tomography finding in inflammatory choroidal neovascularization. Retina. 2013;33(5):1049-1055.
51. Pohlmann D, Pleyer U, Joussen AM, Winterhalter S. Optical coherence tomography angiography in comparison with other multimodal imaging techniques in punctate inner choroidopathy. Br J Ophthalmol. 2019;103:60-66.
52. Dingerkus VLS, Munk MR, Brinkmann MP, et al. Optical coherence tomography angiography (OCTA) as a new diagnostic tool in uveitis. J Ophthalmic Inflamm Infect. 2019;9(1).
53. Zahid S, Chen KC, Jung JJ, et al. OPTICAL COHERENCE TOMOGRAPHY ANGIOGRAPHY of CHORIORETINAL LESIONS DUE to IDIOPATHIC MULTIFOCAL CHOROIDITIS. Retina. 2017;37(8):1451-1463.
54. Levison AL, Baynes KM, Lowder CY, Kaiser PK, Srivastava SK. Choroidal neovascularisation on optical coherence tomography angiography in punctate inner choroidopathy and multifocal choroiditis. Br J Ophthalmol. 2017;101:616-622.
55. Cheng L, Chen X, Weng S, et al. Spectral-Domain Optical Coherence Tomography Angiography Findings in Multifocal Choroiditis With Active Lesions. Am J Ophthalmol. 2016;169:145-161.
56. Goldberg NR, Lyu T, Moshier E, Godbold J, Jabs DA. Success with single-agent immunosuppression for multifocal choroidopathies. Am J Ophthalmol. 2014;158(6):1310-1317.
57. Turkcuoglu P, Chang PY, Rentiya ZS, et al. Mycophenolate mofetil and fundus autofluorescence in the management of recurrent punctate inner choroidopathy. Ocul Immunol Inflamm. 2011;19(4):286-292.
58. Dick AD, Rosenbaum JT, Al-Dhibi HA, et al. Guidance on Noncorticosteroid Systemic Immunomodulatory Therapy in Noninfectious Uveitis: Fundamentals Of Care for UveitiS (FOCUS) Initiative. Ophthalmology. 2018;125(5):757-773.
59. Galor A, Jabs DA, Leder HA, et al. Comparison of Antimetabolite Drugs as Corticosteroid-Sparing Therapy for Noninfectious Ocular Inflammation. Ophthalmology. 2008;115(10):1826-1832.
60. Jabs DA. Immunosuppression for the Uveitides. Ophthalmology. 2018;125(2):193-202.

61. Nederlands Oogheelkundig Gezelschap, Federatie Medische Specialisten. Uveitis. Published online 2012.
62. Jaffe GJ, Dick AD, Brézin AP, et al. Adalimumab in patients with active noninfectious uveitis. N Engl J Med. 2016;375(10):932-943.
63. Nguyen QD, Merrill PT, Jaffe GJ, et al. Adalimumab for prevention of uveitic flare in patients with inactive non-infectious uveitis controlled by corticosteroids (VISUAL II): a multicentre, double-masked, randomised, placebo-controlled phase 3 trial. Lancet. 2016;388:1183-1192.
64. LaMattina KC, Goldstein DA. Adalimumab for the treatment of uveitis. Expert Rev Clin Immunol. 2017;13(3):181-188.
65. Shmueli O, Amer R. Outcomes of adalimumab therapy in refractory punctate inner choroidopathy and multifocal choroiditis. Graefe's Arch Clin Exp Ophthalmol. 2022;(0123456789).
66. Llorenç V, Molins B, Rey A, Mesquida M, Adán A. Adalimumab in serpiginous choroiditis. Ocul Immunol Inflamm. 2013;21(3):237-240.
67. Chinchurreta Capote A, Requena Jiménez JM, Lorenzo Soto M, Romero Gómez C, García De Lucas MD. Effectiveness of adalimumab for refractory serpiginous choroiditis. Ocul Immunol Inflamm. 2014;22(5):405-408.
68. Asano S, Tanaka R, Kawashima H, Kaburaki T. Relentless Placoid Chorioretinitis: A Case Series of Successful Tapering of Systemic Immunosuppressants Achieved with Adalimumab. Case Rep Ophthalmol. 2019;10:145-152.
69. Rosenfeld PJ, Brown DM, Heier JS, et al. Ranibizumab for Neovascular Age-Related Macular Degeneration. N Engl J Med. 2006;355(14):1419-1431.
70. Parodi MB, Iacono P, Mansour A, et al. INTRAVITREAL BEVACIZUMAB FOR JUXTAFOVEAL CHOROIDAL NEOVASCULARIZATION SECONDARY TO MULTIFOCAL CHOROIDITIS. Retina. 2013;33:953-956.
71. Zhang H, Liu ZL, Sun P, Gu F. Intravitreal bevacizumab as primary treatment of choroidal neovascularization secondary to punctate inner choroidopathy: Results of a 1-year prospective trial. Retina. 2012;32(6):1106-1113.
72. Mansour AM, Arevalo JF, Ziemssen F, et al. Long-term Visual Outcomes of Intravitreal Bevacizumab in Inflammatory Ocular Neovascularization. Am J Ophthalmol. 2009;148(2):310-316.e2.
73. Menezo V, Cuthbertson F, Downes SM. Positive response to intravitreal ranibizumab in the treatment of choroidal neovascularization secondary to punctate inner choroidopathy. Retina. 2010;30(9):1400-1404.
74. Rouvas A, Petrou P, Douvali M, et al. Intravitreal ranibizumab for the treatment of inflammatory choroidal neovascularization. Retina. 2011;31(5):871-879.
75. Chiam NPY, Lim LLP. Uveitis and Gender: The Course of Uveitis in Pregnancy. J Ophthalmol. 2014;2014:1-10.
76. Grotting LA, Papaliodis GN. A Review of the Course and Treatment of Non-Infectious Uveitis during Pregnancy. Semin Ophthalmol. 2017;32(1):75-81.
77. Rao VG, Rao GS, Narkhede NS. Flare up of choroiditis and choroidal neovasculazation associated with punctate inner choroidopathy during early pregnancy. Indian J Ophthalmol. 2011;59(2):145-148.
78. Fossum P, Couret C, Briend B, Weber M, Lagarce L. Safety of intravitreal injection of ranibizumab in early pregnancy: A series of three cases. Eye. 2018;32(4):830-832.
79. Sim DA, Sheth HG, Kaines A, Tufail A. Punctate inner choroidopathy-associated choroidal neovascular membranes during pregnancy. Eye. 2008;22(5):725-727.
80. Chiam NPY, Hall AJH, Stawell RJ, Busija L, Lim LLP. The course of uveitis in pregnancy and postpartum. Br J Ophthalmol. 2013;97(10):1284-1288.

81. Kump LI, Cervantes-Castañeda RA, Androudi SN, Foster CS, Christen WG. Patterns of exacerbations of chronic non-infectious uveitis in pregnancy and puerperium. Ocul Immunol Inflamm. 2006;14(2):99-104.
82. Rabiah PK, Vitale AT. Noninfectious uveitis and pregnancy. Am J Ophthalmol. 2003;136(1):91-98.
83. Verhagen FH, Braakenburg AM, Kremer T, Drylewicz J, Rothova A, de Boer JH. Reduced number of relapses of human leucocyte antigen-B27-associated uveitis during pregnancy. Acta Ophthalmol. 2017;95(8):e798-e799.
84. Peracha ZH, Rosenfeld PJ. Anti-vascular endothelial growth factor therapy in pregnancy: What we know, what we don't know, and what we don't know we don't know. Retina. 2016;36(8):1413-1417.
85. Polizzi S, Mahajan VB. Intravitreal Anti-VEGF Injections in Pregnancy: Case Series and Review of Literature. J Ocul Pharmacol Ther. 2015;31(10):605-610.
86. Herbort CP, Papadia M, Neri P. Myopia and inflammation. J Ophthalmic Vis Res. 2011;6(4):270-283.
87. Lin HJ, Wei CC, Chang CY, et al. Role of Chronic Inflammation in Myopia Progression: Clinical Evidence and Experimental Validation. EBioMedicine. 2016;10:269-281.
88. Ferrara DC, Takahashi BS, Yannuzzi LA, et al. Analysis of major alleles associated with age-related macular degeneration in patients with multifocal choroiditis: Strong association with complement factor H. Arch Ophthalmol. 2008;126(11):1562-1566.
89. Atan D, Fraser-Bell S, Plskova J, et al. Punctate Inner choroidopathy and multifocal choroiditis with panuveitis share haplotypic associations with IL10 and TNF loci. Investig Ophthalmol Vis Sci. 2011;52(6):3573-3581.
90. Braley RE, Meredith TA, Aaberg TM, Koethe SM, Witkowski JA. The prevalence of HLA-b7 in presumed ocular histoplasmosis. Am J Ophthalmol. 1978;85:859-861.
91. Meredith TA, Smith RE, Braley RE, Witkowski JA, Koethe SM. The prevalence of HLA-b7 in presumed ocular histoplasmosis in patients with peripheral atrophic scars. Am J Ophthalmol. 1978;86:325-328.
92. Meredith TA, Smith RE. ASSOCIATION OF HLA-DRw2 ANTIGEN WITH PRESUMED OCULAR HISTOPLASMOSIS. Am J Ophthalmol. 1980;89:70-76.
93. Dabil H, Kaplan HJ, Duffy BF, Phelan DL, Mohanakumar T, Jaramillo A. Association of the HLA-DR15/HLA-DQ6 haplotype with development of choroidal neovascular lesions in presumed ocular histoplasmosis syndrome. Hum Immunol. 2003;64(10):960-964.
94. Spaide RF, Skerry JE, Yannuzzi LA, Derosa JT. Lack of the HLA-DR2 specificity in multifocal choroiditis and panuveitis. Br J Ophthalmol. 1990;74(9):536-537.
95. Ongkosuwito J V., Tilanus MGJ, Van der Lelij A, et al. Amino acid residue 67 (isoleucine) of HLA-DRB is associated with POHS. Investig Ophthalmol Vis Sci. 2002;43(6):1725-1729.
96. Klein RJ, Zeiss C, Chew EY, et al. Complement Factor H Polymorphism in Age-Related Macular Degeneration. Science (80-). 2005;308(5720):385-389.
97. Uffelmann E, Huang QQ, Munung NS, et al. Genome-wide association studies. Nat Rev Methods Prim. 2021;1(1).
98. Kamran Ikram M, Xueling S, Jensen RA, et al. Four novel loci (19q13, 6q24, 12q24, and 5q14) influence the microcirculation In vivo. PLoS Genet. 2010;6(10):1-12.
99. Zhong W, Edfors F, Gummesson A, Bergström G, Fagerberg L, Uhlén M. Next generation plasma proteome profiling to monitor health and disease. Nat Commun. 2021;12(1):1-12.
100. Sobsey CA, Ibrahim S, Richard VR, et al. Targeted and Untargeted Proteomics Approaches in Biomarker Development. Proteomics. 2020;20(9):1-15.

101. Ten Berg MJ, Huisman A, Van Den Bemt PMLA, Schobben AFAM, Egberts ACG, Van Solinge WW. Linking laboratory and medication data: New opportunities for pharmacoepidemiological research. Clin Chem Lab Med. 2007;45(1):13-19.
102. den Harder AM, de Jong PA, de Groot MCH, et al. Commonly available hematological biomarkers are associated with the extent of coronary calcifications. Atherosclerosis. 2018;275:166-173.

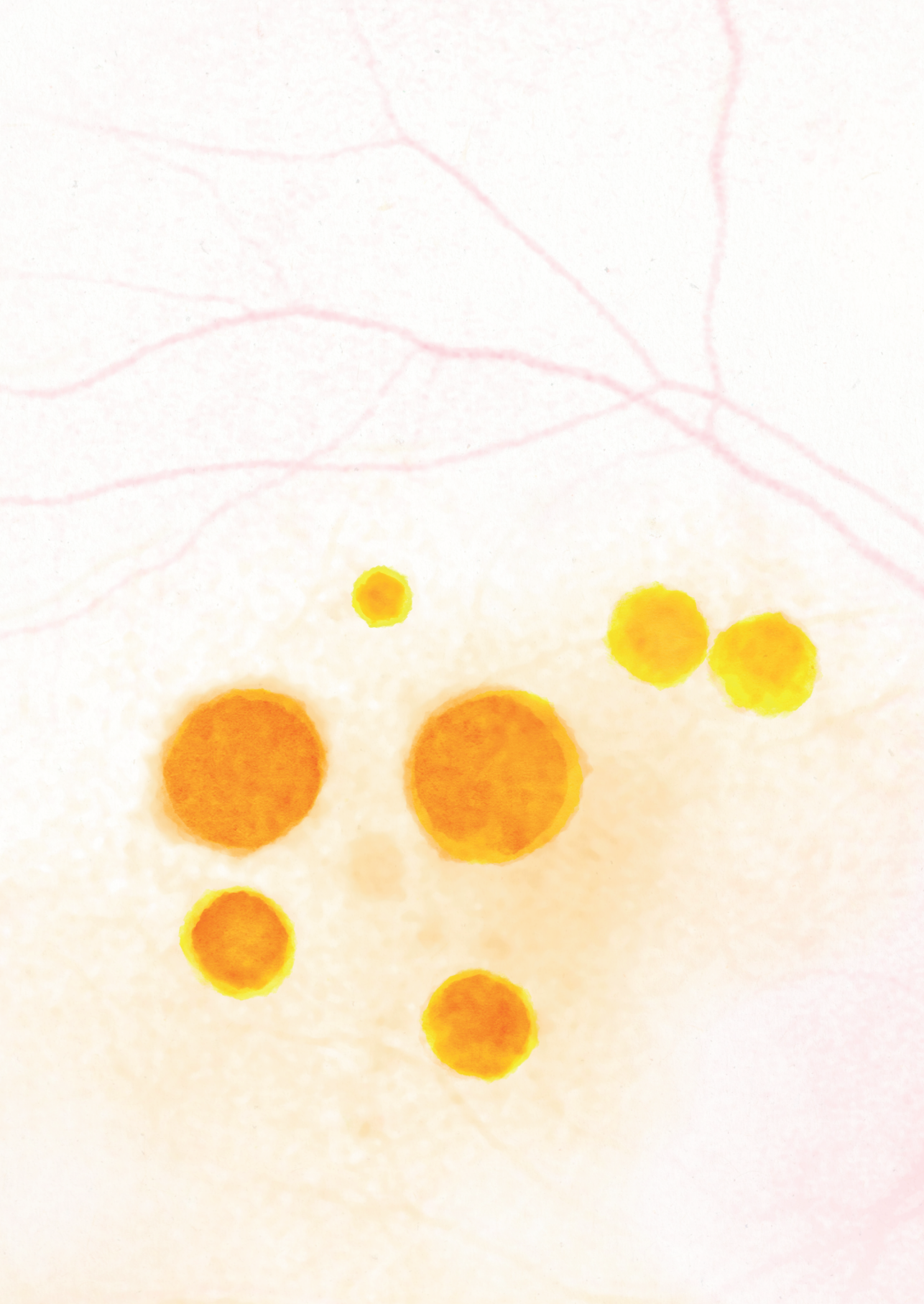

Chapter 2

Idiopathic Multifocal Choroiditis and Punctate Inner Choroidopathy – Evaluation of Risk Factors for Increased Relapse Rate: A 2-Year Prospective Observational Cohort Study

Evianne L. de Groot
Joke H. de Boer
Jeannette Ossewaarde-van Norel

Ophthalmologica 2022;245(5):476-486. doi: 10.1159/000526663.

ABSTRACT

Introduction

The aim of this study was to describe the course of disease in patients with idiopathic multifocal choroiditis (MFC) and punctate inner choroidopathy (PIC) and to identify risk factors associated with an increased relapse rate of disease activity.

Methods

In this prospective observational cohort study, demographical and clinical data were collected concerning the relapses rate of disease activity, the conclusions of the multimodal imaging results, treatment, complications, and self-reported quality of life. Disease activity was defined as new inflammatory lesions or active inflammation in preexisting chorioretinal lesions either with or without active choroidal neovascularization (CNV). Linear regression analysis was performed to identify risk factors associated with an increased relapse rate.

Results

In total, 122 eyes of 82 patients (93% females) were included with a median age (IQR) of 45 (37–54) years. A history of secondary CNV was present in 66% of the eyes. During follow-up, the best-corrected visual acuity remained stable despite a median relapse rate (IQR) of 1.0 (0.25–3). Cycles of oral corticosteroids were given in 59% of the patients, 72% were treated at baseline or started treatment during follow-up with a disease-modifying antirheumatic drug (DMARD), and 35% with a biological agent in addition to the DMARD. Both a history of secondary CNV (B = 1.2, 95% CI: 0.7–1.7, $p = 3.6 \times 10{-}5$) and high myopia (<−6 diopters) (B = 0.6, 95% CI: 0.1–1.1, p = 0.02) independently increased the relapse rate of disease activity.

Discussion/Conclusion

A history of secondary CNV and high myopia were associated with an increased relapse rate of disease activity. Moreover, the results of this study emphasize the challenging character of treating patients with MFC/PIC.

INTRODUCTION

Central multifocal choroiditis (cMFC) is part of the spectrum of the white dot syndromes or more specifically of the group of primary inflammatory choriocapillaris.[1] cMFC is characterized by inflammation of the choriocapillaris resulting in the typical white dots in the fundus of the eye. cMFC comprises several subtypes including punctate inner choroidopathy (PIC), idiopathic multifocal choroiditis (MFC), serpiginous choroiditis, and relentless placoid chorioretinitis. cMFC has a chronic and relapsing character often resulting in the development and growth of multiple chorioretinal lesions and frequently patients develop secondary choroidal neovascularization (CNV) (**Figure 2.1**).[2,3] Interestingly, over 90% of the cases are reported in women and over 85% of the patients are myopic.[4,5] The nature of the association between cMFC and myopia is not yet determined and requires further research. As mentioned, cMFC comprises different subtypes including the closely resembling subtypes PIC and idiopathic MFC. The literature is inconclusive if these subtypes should be considered as separate subtypes, or both subtypes represent an identical disease entity. Recently, several attempts have been made to create classification criteria for both PIC and MFC though most cases present with overlapping criteria.[4-6] As many others, the authors believe that these subtypes most likely belong to one disease entity. Future genetic and protein profiling studies exploring the pathophysiological mechanism are needed to provide more clear evidence on this matter. Even though the pathophysiological mechanism is still largely unknown, increasing evidence points toward a dysregulation of the immune system. Involvement of the immune system is supported by both small genetic studies[7,8] and the efficacy of immunomodulatory therapy for this disease.[7-11] Nevertheless, the severity of the course of disease and the demand for immunomodulatory therapy differ between patients. Subsequently, it is difficult to predict the course of disease in individual patients and practice personalized medicine. Moreover, the quality of life in these relatively young patients and the effect of treatment have not yet been evaluated. In this study, we aim to describe the clinical course of disease and self-reported quality of life during 24 months of follow-up in a large cohort of patients and to identify risk factors associated with an increased relapse rate.

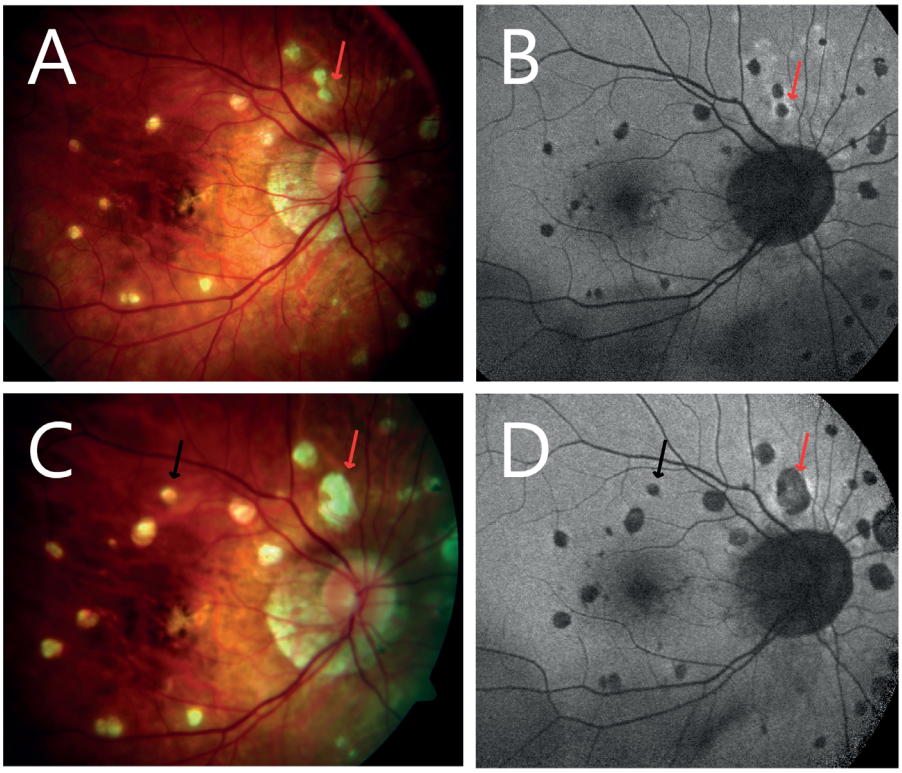

Figure 2.1. Substantial growth of chorioretinal lesions in 24 months of follow-up (red arrows) and the development of new chorioretinal lesion (black arrow). **A&B.** Fundus picture (**A**) and fundus autofluorescence picture (**B**) taken at baseline. **C&D.** Both the fundus picture (**C**) and the fundus autofluorescence picture (**D**) demonstrate growth of the chorioretinal lesions.

METHODS

Design and Study Population

This was a 2-year prospective observational cohort study in patients with idiopathic MFC and PIC, carried out between January 2019 and September 2021 in the outpatient clinic of the University Medical Centre (UMC) Utrecht, The Netherlands. Additionally, patients were asked to fill out questionnaires regarding the self-reported quality of life at the start and end of follow-up. This study is in adherence to the Declaration of Helsinki and its further amendments. All study participants provided written informed consent for using their medical data for research purpose and a subset of participants provided written informed consent for filling out the questionnaires. The Institutional Review Board of the University Medical Centre (UMC) of Utrecht approved this study (*METC number 20-269*). The UMC Utrecht is a tertiary referral center specialized in the care of patients with inflammatory ocular diseases. A standardized care protocol was developed within

the expertise of the team of uveitis specialists outlining the diagnostics, treatment options, and follow-up regime for these patients (**Suppl. Figure 2.1a and 2.1b**). Patients were diagnosed with cMFC when they presented with chorioretinal lesions within the posterior pole without papillitis and retinal vasculitis. Other frequent causes of posterior uveitis were ruled out by obtaining the medical history, routine laboratory diagnostics, and chest X-ray. These alternate diagnoses consist of ocular tuberculosis, toxoplasmosis, sarcoidosis, uveitis associated with inflammatory bowel disease, Birdshot chorioretinopathy, lymphoma, and other viral and bacterial ocular infections. When indicated routine diagnostic workup was extended with a (positron emission tomography-) computed tomography or an anterior chamber tap with aqueous humor analysis. Patients with cMFC were included if they were diagnosed with the subtypes idiopathic MFC and PIC, visited the outpatient clinic between January 2019 and June 2019, and were ≥18 years old. Patients diagnosed with other subtypes of cMFC such as serpiginous choroiditis and relentless placoid chorioretinitis were excluded from this study.

Data Collection

The start of follow-up was a visit in the outpatient clinic in the first 6 months of 2019 and the follow-up duration was 24 months with a maximum follow-up time deviation of 3 months. At each follow-up moment, patients underwent routine ophthalmological examination including Snellen best-corrected visual acuity (BCVA), slit-lamp examination, fundus biomicroscopy, and indirect ophthalmoscopy. Routine retinal imaging consisted of enhanced depth imaging scans on the spectral-domain optical coherence tomography (SD-OCT) including the TruTrack Active Eye Tracking technology and 30° near-infrared imaging of the fundus (Spectralis HRA-OCT; Heidelberg Engineering, Heidelberg, Germany/FF 450 plus; Carl Zeiss Meditec, Jena, Germany). When indicated retinal imaging was extended with fluorescein and indocyanine green angiography, 55° fundus auto fluorescence (FAF) images (Spectralis HRA-OCT; Heidelberg Engineering), color fundus images (FF 450 plus; Carl Zeiss Meditec), and OCT angiography (SD-OCT Angioplex Cirrus HD-OCT 5000; Carl Zeiss Meditec). The affected area of the posterior pole was measured with the Region Finder software (Spectralis HRA-OCT; Heidelberg Engineering). This software allows semiautomatic identification and quantification of atrophic areas on FAF images. Collected data consisted of demographic and clinical data and included patient characteristics, relapses of disease activity of choroidal inflammation, reactivation of CNV, or the development of new CNV sites, treatment, and complications. Disease activity was defined as new inflammatory lesions or active inflammation in preexisting chorioretinal lesions either with or without active CNV. Choroidal inflammation was scored based on imaging parameters including (1) focal increase of the choriocapillaris thickness below the lesion and/or (2) new focal elevation

of the RPE with underlying material and increased penetration of light through the inner choroid with or without retinal infiltration and/or (3) new RPE/EZ disruption on the SD-OCT (**Figure 2.2**). On the late-phase ICGA imaging (4) areas of hypofluorescence can be observed, which are not well circumscribed with vague edges and are greater in size compared to the FAF images. New or reactivation of a CNV was scored in case (1) new intraretinal or subretinal fluid developed in the neovascular complex visualized with SD-OCT (atrophic cysts in scars not included) and/or (2) when growth of the neovascular complex was observed with decreased penetration of light through the inner choroid on SD-OCT and/or (3) leakage on the fluorescein angiography and/or (4) in case a new vascular network was observed on OCT angiography. When patients presented with residual activity or reactivation of CNV without an active choroidal inflammation, this was not scored as disease activity. Inactive stage of disease is defined as no disease activity for at least 3 months while treated with ≤7.5 mg oral prednisolone, or in case of ocular corticosteroid injections, the last injection was <3 months ago. A relapse of disease activity was defined as the observation of disease activity after reaching an inactive stage of disease. Within the first 6 months of follow-up, all patients received an invitation to fill out a set of questionnaires concerning the self-reported quality of life. The set comprised two questionnaires: the Dutch translation of the National Eye Institute Visual Function Questionnaire 25 (NEI-VFQ-25), a standardized questionnaire reporting on the vision-related quality of life (VR-QoL), and the Dutch translation of the Short Form Health Survey 36-items (SF36), a standardized questionnaire reporting on the quality of life in relation to the patients' general health (GH-QoL). The NEIVFQ-25 reports on the VR-QoL within 12 domains and the SF-36 reports on the GH-QoL within 8 domains (for specification of the domains, see **Table 2.3**). The questionnaires were filled out again in the last 6 months of follow-up.

Data Analysis

To determine clinical characteristics associated with the relapse rate during the 24 months of follow-up, data of the most active eye were used in case of bilateral disease. We compared the affected area in the posterior pole on 55° FAF imaging exclusively for patients with available date at baseline (±3 months) and at the 24 months of follow-up (±3 months). The Snellen BCVA was converted to the logarithm of the minimum angle of resolution equivalent for analysis. The answers from the NEI-VFQ-25 and SF-36 questionnaires were converted to a 0-100 points scale where 0 corresponds with the worst and 100 with the best QoL-related outcome. The scores of the domains of the NEI-VFQ-25 questionnaires were compared to a reference group within the working population,[12] and the scores of the domains of the SF-36 questionnaires were compared to a Dutch reference group.[13]

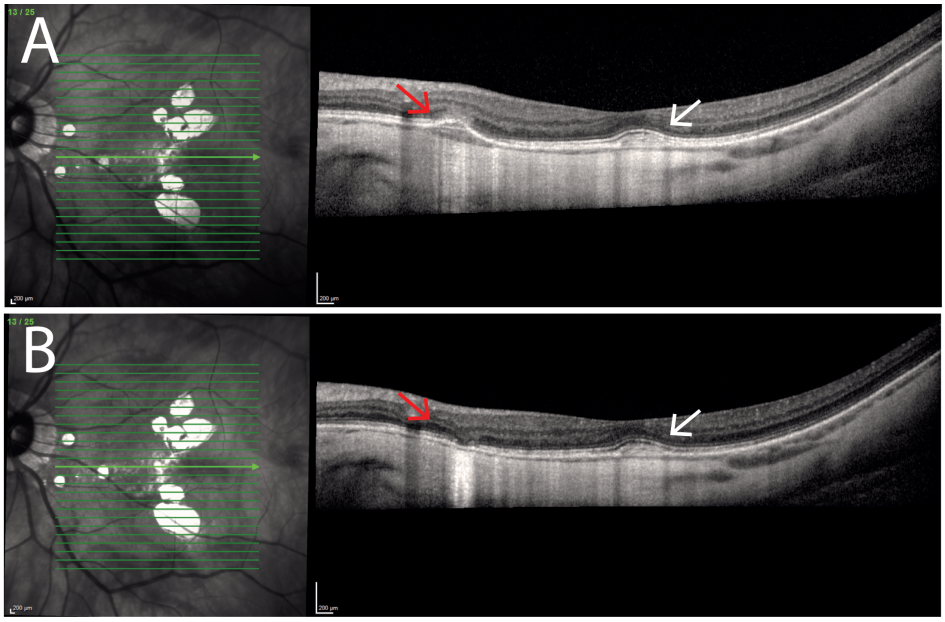

Figure 2.2. Relapse of disease activity in one of the lesions visualized with the EDI SD-OCT. **A.** Inflammatory activity in one of the lesions is observed (red arrow) and is characterized by an increased choroidal thickness beneath the lesion, focal elevation of the RPE with breakthrough of the underlying material into the retinal structures. The white arrow depicts an inactive pre-existent CNV scar. **B.** Six weeks after increasing the dose of the DMARD and administering a periocular triamcinolone, the lesion does not show signs of inflammation (red arrow). The choroidal thickness normalized and the sub-RPE material disappeared. The CNV scar has remained inactive (white arrow).
EDI SD-OCT, Enhanced depth imaging spectral-domain optical coherence tomography; RPE, retinal pigment epithelium; CNV, choroidal neovascularization; DMARD, disease-modifying antirheumatic drugs.

Statistical Approach

Data analyses were performed in RStudio version 1.2.5001 (RStudio Team, Boston, USA) and R version 3.6.1 (R Foundation for Statistical Computing, Austria). Between-group differences for continuous variables were compared with the Student's *t* test and for categorical variables with the $\chi 2$ test with false discovery rate correction at 5% to correct for multiple testing. For longitudinal analysis the paired sample *t* test was used. Normality of the data was tested using the Shapiro-Wilk's method, and in case of non-normal distributed data, the nonparametric variant of the statistical tests was performed. To evaluate the survival time until a relapse of disease activity, we used Kaplan-Meier curves of the survival R package.[14] Multivariate linear regression analysis was performed to evaluate the effect of clinical characteristics on the quality of life scores of the different domains of the NEI-VFQ-25 and SF-36 questionnaires. Relapse rate, treatment with IMT, treatment with prednisolone, age, and gender were incorporated in these models, and false discovery rate correction at 5% was applied as indicated. To identify the clinical factors associated with the relapse rate, univariate linear regression analyses were performed and significant parameters resulting from the univariate

analyses were used for a multivariate linear regression analysis. Multicollinearity was checked with the variance inflation factor. A p value of <0.05 was accepted as indicating statistical significance.

RESULTS

Study Population

A total of 91 patients with PIC and idiopathic MFC were included in this study. Nine patients were lost to follow-up with several reasons including referral back to the initial ophthalmologist (n = 3) or no follow-up visit at 24 ± 3 months (n = 6); thus, the study group consisted of 82 patients. The median age was 45 years (interquartile range (IQR) 37–54) and 76 (93%) patients were female. The baseline characteristics of the patients are demonstrated in **Table 2.1**.

Longitudinal Analysis

In total, 135 relapses of active choroiditis occurred in 61 patients with a median (IQR) number of relapses of 1.0 (0.25–3) per patient. In 25% of the relapses the patient experienced symptoms at the time the relapse was diagnosed. In 41% of the relapses, the active choroiditis was accompanied by active secondary CNV (of which in 10% of the relapses a new CNV site developed, and 31% of the relapses the CNV reactivated). **Figure 2.3a** visualizes the relapse-free survival time in all patients and **Figure 2.3b** displays the survival curves for the patients grouped by whether the patients had a history of secondary CNV. For 24 patients (36 eyes) fundus autofluorescence imaging was available both at baseline and at 24 months of follow-up. In these patients, there was a significant increase of the median (IQR) affected area between baseline (5.5 (1.5–13.6) mm^2) and after 24 months of follow-up (6.0 (2.7–15.9) mm^2) ($P_{\text{Wilcoxon signed-rank test}} = 2.0 \times 10^{-5}$) (**Figure 2.1b and 2.1d**). This corresponds with a total median (IQR) growth of the affected area of 0.8 (0.2–2.0) mm^2 during follow-up. In eyes of patients with (n = 19) and without (n = 17) treatment with disease-modifying antirheumatic drugs (DMARDs) or biologicals at baseline, the median growth was 0.4 (0.1–2.3) mm^2 and 0.9 (0.4–1.7) mm^2, respectively ($P_{\text{Wilcoxon rank sum test}} = 0.51$). The median (IQR) percentage increase was 13.4% (5.8–18.4%) versus 22.5% (12.7–51.7%) in eyes of patients with treatment with DMARDs or biologicals at baseline versus patients without treatment($P_{\text{Wilcoxon rank sum test}} = 0.03$).

The median BCVA (IQR) in logarithm of the minimum angle of resolution at baseline and after 24 months of follow-up was 0.034 (0.061–0.26) and 0.018 (−0.061 to 0.21), respectively ($P_{\text{Wilcoxon signed-rank test}} = 0.20$). **Table 2.2** demonstrates the treatment initiated during follow-up and complications that occurred during follow-up. In summary, 59%

Table 2.1. Patient characteristics at baseline of patients with idiopathic multifocal choroiditis and punctate inner choroidopathy

	n = 82 patients / 122 eyes	
Median age start follow-up (IQR)	45	[37 - 54]
Median age first complaints (IQR)	37	[28 - 45]
Female, n (%) of all patients	76	(93)
Bilateral disease, n (%) of all patients	40	(49)
History of CNV, n (%) of affected eyes	81	(66)
Median BCVA (in LogMAR) [IQR] of affected eyes	0.034	[-0.06 – 0.26]
BCVA <20/50, n (%) of affected eyes	20	(16)
BCVA <20/200, n (%) of affected eyes	13	(11)
Median refractive error [IQR] of affected eyes	-5.50	[-8.3 – -2.9]
History of anterior uveitisa, n (%) of affected eyes	10	(8)
History of vitritisa, n (%) of affected eyes	10	(8)
History of EpiMEWDS, n (%) of affected eyes	4	(3)
Median lesion number in the posterior poleb (IQR) of affected eyes	6	[3-13]
Lesions limited to the posterior pole, n (%) of affected eyes	60	(49)
Median affected area in posterior poleb (mm2) (IQR)	4.1	[1.4 – 11.0]
Treatment with oral prednisolone, n (%) of all patients	30	(37)
Steroidsparing immunomodulatory therapy, n (%) of all patients		
• None	34	(41)
• DMARDc	41	(50)
• Biologicalsd + DMARD	7	(9)

IQR, interquartile range; CNV, choroidal neovascularization; BCVA, best-corrected visual acuity; LogMAR, Logarithm of the Minimum Angle of Resolution; EpiMEWDS, Epiphenomenon of a secondary Multiple Evanescent White Dot Syndrome reaction; DMARD, disease-modifying antirheumatic drugs.

[a] Vitritis was defined as more than 1+ cells in the vitreous, anterior uveitis was defined as more than ½+ cells in the anterior chamber.

[b] Affected area and lesion number in the posterior pole was measured on the first available 55 degree fundus autofluorescence imaging during follow-up. Data was missing for 7 patients.

[c] Mycophenolate mofetil (n=20), ciclosporin (n=7), methotrexate (n=4), azathioprine (n=4), ciclosporin+mycophenolate mofetil (n=5), tacrolimus (n=1).

[d] All patients treated with a biological were treated with adalimumab.

of the patients were treated with oral cycles of prednisolone during follow-up, 21% of the patients started treatment with a DMARD, and 26% of the patients started treatment with a biological agent in addition to a DMARD. Complications occurred in 13% of the eyes and for the majority consisted of a temporary steroid-induced ocular hypertension.

Self-Reported Quality of Life

From the 82 study participants, 46 (56%) filled out the questionnaires concerning the quality of life at baseline. The results are demonstrated in **Table 2.3**. The study population scored significantly lower on almost all domains of the NEI-VFQ-25 compared to the reference group except for the domains “Social functioning” and “Color vision.” On the

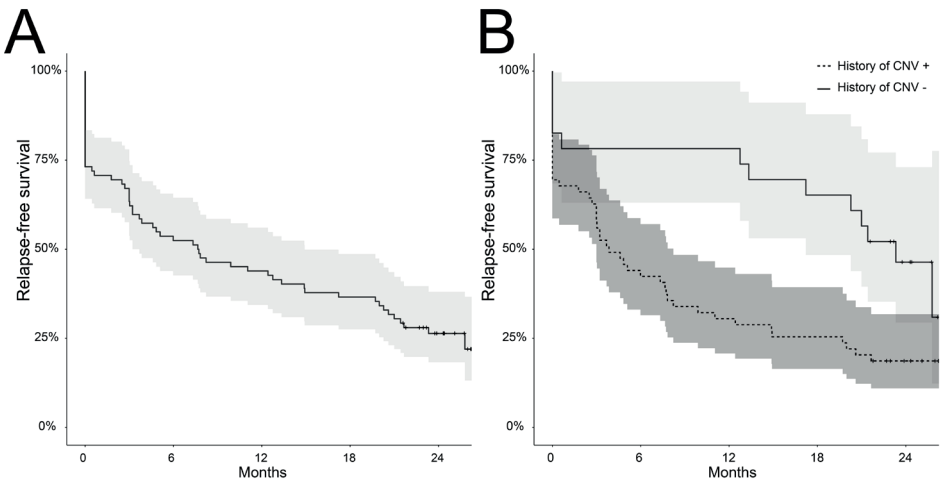

Figure 2.3. Relapse-free survival visualized with Kaplan-Meier curves including 95% confidence intervals.
A. Relapse-free survival plot of all patients **B**. Relapse-free survival plot of the patients grouped by a history of secondary CNV.
CNV, choroidal neovascularization.

contrary, on the domains of the SF-36, the study population only scored significantly lower for the domains "General health" and "Vitality/Energy" and scored significantly higher on the domain "Physical functioning." Forty-one of the 46 patients filled out the questionnaires once more at 24 months of follow-up. Multivariate linear regression analysis revealed that treatment with IMT (DMARD or DMARD + biological) significantly decreased the quality of life scores of the domains of "Distance vision" and "Driving" though after correction for multiple testing none remained significant. The relapse rate during follow-up and treatment with prednisolone did not influence the self-reported quality of life (**Suppl. Table 2.1**).

Clinical Characteristics

We evaluated whether clinical characteristics could be identified that were associated with the number of relapses of disease activity during the 24 months of follow-up (**Table 2.4**). These analyses revealed that both a history of secondary CNV and high myopia significantly increased the relapse rate of patients during follow-up. High myopia was defined as a refractive error of more than −6 diopters. Multivariate linear regression analysis revealed that both a history of secondary CNV and high myopia independently significantly increased the relapse rate (**Table 2.4**). No multicollinearity was observed between myopia and a history of secondary CNV. A history of secondary CNV increased the relapse rate with 1.2 relapses (95% CI: 0.7–1.7, $P = 3.6 \times 10^{-5}$), and high myopia increased the relapse rate with 0.6 relapses (95% CI: 0.1–1.1, $P = 0.02$).

Table 2.2. Treatment and complications during follow-up in patients with idiopathic multifocal choroiditis and punctate inner choroidopathy

	n=82 patients n=122 eyes	
Systemic corticosteroids, n (%) of all patients		
1 cycle of oral prednisolone	31	(38)
≥2 cycles of oral prednisolone	17	(21)
Systemic DMARDs, n (%) of all patients		
Start DMARD[a]	17	(21)
Switch DMARD	34	(42)
Reason for switch, n (%) of all switches (n=46)		
No disease control	30	(65)
Side-effects	15	(33)
Pregnancy	1	(2)
Stop DMARD		
Side-effects	6	(7)
Disease control	2	(2)
Systemic biological therapy, n (%) of all patients		
Start biological[b]	21	(26)
Corticosteroid injections, n (%) of all eyes		
Periocular triamcinolone	20	(16)
Parabulbar betamethasone	20	(16)
Intravitreal triamcinolone	5	(4)
Dexamethasone implant	1	(1)
Anti-VEGF therapy, n (%) of all eyes	48	(39)
Median [IQR] number of injections of all eyes with at least 1 injection	7	4-12
Complications, n (%) of all eyes		
Steroid-induced ocular hypertension	7	(6)
Ocular hypotony	1	(1)
Cataract extraction	3	(2)
Reversible ptosis	4	(3)

DMARDs, disease modifying antirheumatic drugs; VEGF, vascular endothelial growth factor; IQR, interquartile range.
[a] Mycophenolate mofetil (n=8), ciclosporin (n=3), methotrexate (n=3), azathioprine (n=3)
[b] All patients started treatment with adalimumab

DISCUSSION AND CONCLUSION

In this study, we described the course of disease in the 24 months of follow-up in patients with idiopathic MFC and PIC. We discovered that the self-reported quality of life in these patients is substantially decreased compared to healthy controls. Moreover, we identified that a history of secondary CNV and high myopia both independently increased the relapse rate of disease activity.

Previously, it was suggested that the development of secondary CNV is the result of a chronic and severe inflammatory process in the choriocapillaris.[15,16] This inflammation results in hypoperfusion of the choriocapillaris visualized as hypofluorescent areas on indocyanine green angiography. These areas of hypoperfusion are often larger

Table 2.3. The results of the quality of life–related questionnaires of patients with idiopathic multifocal choroiditis and punctate inner choroidopathy compared to healthy control subjects

	Scale	Idiopathic MFC/PIC				Ref[a]		P_{adj}-value[b]
		Median	(range)	Mean	(SD)	Mean	(SD)	
NEI-VFQ-25 baseline			**n=46**			**n =511**		
General health	0-100	65	(25-100)	62	(15)	80	(17)	4.2×10^{-10}
General vision	0-100	74	(40-85)	70	(12)	79	(16)	7.4×10^{-6}
Ocular pain	0-100	88	(38-100)	81	(17)	88	(15)	0.02
Near vision activities	0-100	83	(33-100)	80	(16)	92	(13)	7.4×10^{-6}
Distance vision (n=45)	0-100	83	(42-100)	80	(16)	92	(11)	7.4×10^{-6}
Social functioning	0-100	100	(33-100)	95	(14)	98	(8)	0.14
Mental Health	0-100	75	(20-95)	75	(17)	88	(10)	5.2×10^{-6}
Role difficulties	0-100	75	(19-100)	75	(20)	93	(13)	5.3×10^{-7}
Dependency	0-100	100	(50-100)	94	(12)	99	(6)	0.03
Driving (n=41)	0-100	75	(33-100)	70	(17)	89	(11)	1.6×10^{-7}
Color vision	0-100	100	(50-100)	98	(9)	98	(9)	0.94
Peripheral vision	0-100	100	(25-100)	84	(21)	93	(15)	7.8×10^{-3}
Composite score (n=40)	0-100	86	(51-96)	83	(11)	91	(7)	2.9×10^{-6}
SF-36 baseline			**n=46**			**n=1742**		
Physical functioning	0-100	95	(35-100)	90	(15)	83	(23)	6.6×10^{-3}
Role limitations – physical	0-100	100	(0-100)	74	(40)	76	(36)	0.78
Bodily pain	0-100	82	(21-100)	78	(21)	75	(23)	0.36
General health	0-100	60	(20-100)	58	(21)	71	(21)	1.8×10^{-4}
Vitality/Energy	0-100	63	(15-100)	60	(20)	69	(19)	5.4×10^{-3}
Social functioning	0-100	89	(0-100)	81	(23)	84	(22)	0.50
Mental health	0-100	78	(40-100)	76	(14)	77	(17)	0.84
Role limitations – emotional	0-100	100	(0-100)	82	(36)	82	(33)	0.94

NEI-VFQ-25, national eye institute visual function questionnaire 25; SF-36, Short Form Health Survey 36-items.
[a] Reference group for NEI-VFQ-25: Hirneiß et al. Graefes Arch. Clin. Exp. Ophthalmol. 2010; Reference group for SF-36: Aaronson et al. J. Clin Epidemiol 1998
[b] Student's t-test after 5% false discovery rate correction for multiple testing

and more widespread than one would expect based on color fundus imaging and ophthalmological examination.[17] Probably both the inflammatory environment in the choriocapillaris and the subsequent hypoperfusion of the choriocapillaris contribute to the trigger for neoangiogenesis and the development of secondary CNV. In line with this hypothesis, only patients presenting with severe inflammation in the choriocapillaris and severe hypoperfusion will develop secondary CNV. This could possibly explain the observed association between a history of secondary CNV and the increased relapse rate of disease activity in these patients, though we must take into account that it can still be challenging to distinguish choroidal inflammation and secondary CNV activity on multimodal imaging especially in the absence of fluorescein and indocyanine green angiography.[18,19] However, considering the extensive treatment of secondary CNV in

Table 2.4. Clinical characteristics associated with relapse rate of disease activity during follow-up in patients with idiopathic multifocal choroiditis and punctate inner choroidopathy.

	Univariate			*Multivariate*		
	B	**95% CI**	***P*-value**	**B**	**95% CI**	***P*-value**
Age start follow-up	-0.012	-0.036 – 0.012	0.34			
Age start of symptoms	0.007	-0.015 – 0.029	0.54			
Female gender	-0.233	-1.31 – 0.85	0.67			
Bilateral disease	-0.149	-0.71 – 0.42	0.60			
History of CNV	1.167	0.31 – 1.72	7.5×10^{-5}	1.192	0.65 – 1.73	3.6×10^{-5}
High myopia[a]	0.557	0.0025-1.11	0.049	0.599	0.10 – 1.10	0.02
History of anterior uveitis	-0.806	-1.80 – 0.19	0.11			
History of vitritis	0.600	-0.40 – 1.60	0.24			
History of EpiMEWDS	0.314	-1.00 – 1.62	0.64			
Affected area in the posterior pole[b]	-0.020	-0.04 – 0.002	0.07			
Lesion number in the posterior pole[b,c]						
• 2-5	-0.537	-1.63 – 0.56	0.33			
• >5	-0.397	-1.43 – 0.64	0.45			
Lesions limited to the posterior pole	-0.246	-0.81 – 0.32	0.39			
Therapy at baseline[c]						
• DMARD	-0.178	-0.77 – 0.41	0.55			
• DMARD + biological	-0.749	-1.81 – 0.31	0.16			

B, beta; CI, confidence interval; CNV, choroidal neovascularization; EpiMEWDS, Epiphenomenon of a secondary Multiple Evanescent White Dot Syndrome reaction; DMARD, disease-modifying antirheumatic drug.

[a] High myopia was defined as a refractive error of more than or equal to -6 diopters.

[b] Affected area and lesion number in the posterior pole was measured on the first available 55 degree fundus autofluorescence imaging during follow-up. Data was missing for 7 patients.

[c] Reference was set at: Lesion number=1, therapy at baseline=no DMARD or biological agent

these patients (**Suppl. Figure 2.1B**), especially compared to the treatment of myopic CNV, it is highly unlikely that secondary CNV reactivates in the absence of choroidal inflammation.[20] In addition, we found that high myopia is associated with an increased relapse rate. As hypothesized by Herbort et al.,[15] myopia causes structural changes to the choriocapillaris, Bruch's membrane, and the retinal pigment epithelium, resulting in an increased fragility of this complex. Due to this increased fragility, this complex is eminently prone to be targeted by inflammatory diseases. This could perhaps also explain why predominantly myopic patients are affected. However, due to the complex and multifactorial nature of both inflammatory processes and the process of myopia, it remains challenging to unravel all the aspects of this relationship. The risk factors of high myopia and the history of secondary CNV are probably also related to each other (no correlation was observed in this study) since the choriocapillaris of myopic eyes is

more sensitive for hypoperfusion and ischemia. This could probably also explain why in idiopathic MFC and PIC the prevalence of secondary CNV is much higher than other forms of uveitis without an association with myopia.[15] In line with the results of this study, one could debate if a patient developed secondary CNV at the first presentation and has high myopia, immunosuppressive therapy with DMARDs and biologicals should be initiated more timely to decrease the number of relapses of disease activity, since the course of disease is expected to be more severe.

The results we report at baseline and during the 24 months of follow-up are relatively favorable in comparison to the literature. We report a better preserved BCVA, less patients had bilateral disease, and less complications occurred.[2,21-23] Moreover, compared to the literature, the reported annual growth of chorioretinal lesions was fewer.[24] Several reasons could explain these positive outcomes. In this study, the patients were closely monitored with multimodal imaging and many relapses of disease activity were diagnosed even before the patient developed symptoms. In our opinion, an asymptomatic inflammatory process in the choriocapillaris should be treated to avoid the development of new chorioretinal lesions and substantial growth of existing lesions (more than expected as part of the natural history of lesions) and to avoid the development or reactivation of secondary CNV. Moreover, most of the patients in our study population did not demonstrate cells in the vitreous of anterior chamber and could therefore be classified as "multifocal choroiditis without panuveitis" a term introduced by Fung and colleagues.[25] Since vitritis and anterior uveitis are considered risk factors for the development of several complications including glaucoma, cystoid macular edema, and cataract,[21] this could partly also explain our relatively positive outcomes. Even though the outcomes are relatively favorable, this study also confirms that the treatment of patients with idiopathic MFC and PIC can be challenging. In a considerable proportion of the patients, there was incomplete response to treatment with a DMARD and a biological was added to the treatment regime. Even though in the literature monotherapy with a DMARD is described as effective as steroid-sparing treatment,[9,10] this study shows that in more than one-third of the patients, DMARD monotherapy is insufficient to achieve long-term steroid-free remission. Treatment with biologicals seems to be very effective in this patient group though the literature is limited to small case series.[26-28] However, in this study, we did not observe an association between treatment with biologicals and a decrease in the relapse rate, probably due to the low number of cases.

Although the disease is considered to be eye-limited without an association with a systemic disease, the majority of the patients report a decreased quality of life on a wide variety of domains including the domain "General health." This group of patients has a

worse perception of their quality of life than one would expect based on the visual acuity and disease localization. Perhaps this is the result of the relatively young age of disease manifestation in combination with the recurrent and chronic character of the disease and the frequent necessity of systemic immunomodulatory therapy. Even though we did not find a clear association between the quality of life and relapse rate, treatment with oral prednisolone, and immunomodulatory therapy, this could possibly be attributed to the limited number of patients that filled out the questionnaires. Moreover, Pearlman et al.[29] described an increased prevalence of self-reported autoimmune diseases in patients with white dot syndromes and their families. Thus, another explanation could be that patients with idiopathic MFC and PIC are more likely to develop other autoimmune diseases affecting the general health of the patients.[29] We compared our results with a study carried out in the UMC Utrecht including patients with non-infectious uveitis (NIU).[30] Patients with idiopathic MFC and PIC scored significantly higher on almost all domains of the NEI-VFQ compared to NIU patients (**Suppl. Table 2.2**). Thus, even though the vision-related quality of life is decreased in patients with idiopathic MFC and PIC, this patient group still scored higher than patients with NIU.

Strengths of this study are its prospective nature and the relatively high number of included patients considering the low prevalence of the disease. Diagnostics and treatment are standardized in our tertiary referral center for inflammatory eye disorders. To preserve homogeneity within the group of patients, only patients with the subtypes idiopathic MFC and PIC were included. This study was executed during the COVID-19 pandemic. Fortunately, for the majority of the follow-up time, limited restrictions were present for ophthalmological visitation and none of the patients structurally canceled their appointments during the COVID-19 pandemic. However at onset of the pandemic uveitis specialists were reluctant to start treatment with immunomodulatory therapy because of the unknown effect on COVID-19 progression and response to COVID-19 vaccines.

In summary, our data demonstrate that both a history of secondary CNV and high myopia are associated with an increased relapse rate in patients with PIC and idiopathic MFC. Moreover, the results of this study emphasize the challenging character of monitoring and treating patients with idiopathic MFC and PIC.

REFERENCES

1. Neri P, Herbort CP, Hedayatfar A, et al. “White dot syndromes”, an inappropriate and outdated misnomer. Int Ophthalmol. 2022;42(1):1-6.
2. Essex RW, Wong J, Fraser-Bell S, et al. Punctate inner choroidopathy: Clinical Features and Outcomes. Arch Ophthalmol. 2010;128(8):982-987.
3. Zhang X, Wen F, Zuo C, et al. Clinical features of punctate inner choroidopathy in Chinese patients. Retina. 2011;31(8):1680-1691.
4. The Standardization of Uveitis Nomenclature (SUN) Working group. Classification Criteria for Punctate Inner Choroiditis. Am J Ophthalmol. 2021;228:275-280.
5. The Standardization of Uveitis Nomenclature (SUN) Working group. Classification criteria for multifocal choroiditis with panuveitis. Am J Ophthalmol. 2021;228:152-158.
6. Gilbert RM, Niederer RL, Kramer M, et al. Differentiating Multifocal Choroiditis and Punctate Inner Choroidopathy: A Cluster Analysis Approach. Am J Ophthalmol. 2020;213:244-251.
7. Atan D, Fraser-Bell S, Plskova J, et al. Punctate Inner choroidopathy and multifocal choroiditis with panuveitis share haplotypic associations with IL10 and TNF loci. Investig Ophthalmol Vis Sci. 2011;52(6):3573-3581.
8. Ferrara DC, Takahashi BS, Yannuzzi LA, et al. Analysis of major alleles associated with age-related macular degeneration in patients with multifocal choroiditis: Strong association with complement factor H. Arch Ophthalmol. 2008;126(11):1562-1566.
9. de Groot EL, ten Dam-van Loon NH, de Boer JH, Ossewaarde-van Norel J. The efficacy of corticosteroid-sparing immunomodulatory therapy in treating patients with central multifocal choroiditis. Acta Ophthalmol. 2020;98(8):816-821.
10. Goldberg NR, Lyu T, Moshier E, Godbold J, Jabs DA. Success with single-agent immunosuppression for multifocal choroidopathies. Am J Ophthalmol. 2014;158(6):1310-1317.
11. Turkcuoglu P, Chang PY, Rentiya ZS, et al. Mycophenolate mofetil and fundus autofluorescence in the management of recurrent punctate inner choroidopathy. Ocul Immunol Inflamm. 2011;19(4):286-292.
12. Hirneiß C, Schmid-Tannwald C, Kernt M, Kampik A, Neubauer AS. The NEI VFQ-25 vision-related quality of life and prevalence of eye disease in a working population. Graefe’s Arch Clin Exp Ophthalmol. 2010;248(1):85-92.
13. Aaronson NK, Muller M, Cohen PDA, et al. Translation, validation, and norming of the Dutch language version of the SF-36 Health Survey in community and chronic disease populations. J Clin Epidemiol. 1998;51(11):1055-1068.
14. Therneau TM. A Package for Survival Analysis in R. R package version 3.2-11. Published online 2021.
15. Herbort CP, Papadia M, Neri P. Myopia and inflammation. J Ophthalmic Vis Res. 2011;6(4):270-283.
16. Niederer RL, Gilbert R, Lightman SL, Tomkins-Netzer O. Risk Factors for Developing Choroidal Neovascular Membrane and Visual Loss in Punctate Inner Choroidopathy. Ophthalmology. 2018;125(2):288-294.
17. Herbort CP, Neri P, Papasavvas I. Clinicopathology of non-infectious choroiditis: evolution of its appraisal during the last 2–3 decades from “white dot syndromes” to precise classification. J Ophthalmic Inflamm Infect. 2021;11(1).
18. Cheng L, Chen X, Weng S, et al. Spectral-Domain Optical Coherence Tomography Angiography Findings in Multifocal Choroiditis With Active Lesions. Am J Ophthalmol. 2016;169:145-161.

19. Pohlmann D, Pleyer U, Joussen AM, Winterhalter S. Optical coherence tomography angiography in comparison with other multimodal imaging techniques in punctate inner choroidopathy. Br J Ophthalmol. 2019;103:60-66.
20. Ohno-Matsui K, Ikuno Y, Lai TYY, Gemmy Cheung CM. Diagnosis and treatment guideline for myopic choroidal neovascularization due to pathologic myopia. Prog Retin Eye Res. 2018;63(October 2017):92-106.
21. Kedhar SR, Thorne JE, Wittenberg S, Jabs DA. Multifocal choroiditis with Panuveitis and Punctate Inner Choroidopathy: Comparison of Clinical Characteristics at Presentation. Retina. 2007;27(9):1174-1179.
22. Leung TG, Moradi A, Liu D, et al. Clinical features and incidence rate of ocular complications in punctate inner choroidopathy. Retina. 2014;34(8):1666-1674.
23. Thorne JE, Wittenberg S, Jabs DA, et al. Multifocal Choroiditis with Panuveitis. Incidence of Ocular Complications and of Loss of Visual Acuity. Ophthalmology. 2006;113(12):2310-2316.
24. Chen YC, Chen YL, Chen SN. Chorioretinal Atrophy in Punctate Inner Choroidopathy/multifocal Choroiditis: A Five-year Follow-up Study. Ocul Immunol Inflamm. 2021;00(00):1-6.
25. Fung AT, Pal S, Yannuzzi NA, et al. Multifocal choroiditis without panuveitis; Clinical Characteristics and Progression. Retina. 2014;34(1):98-107.
26. de Groot EL, Ossewaarde - van Norel J, Ho L, ten Dam - van Loon NH, de Boer JH. The efficacy of adalimumab in treating patients with central multifocal choroiditis. Am J Ophthalmol Case Reports. 2020;20:100921.
27. Neri P, Ricci F, Giovannini A, et al. Successful treatment of an overlapping choriocapillaritis between multifocal choroiditis and acute zonal occult outer retinopathy (AZOOR) with adalimumab (HumiraTM). Int Ophthalmol. 2014;34(2):359-364.
28. Shmueli O, Amer R. Outcomes of adalimumab therapy in refractory punctate inner choroidopathy and multifocal choroiditis. Graefe's Arch Clin Exp Ophthalmol. 2022;(0123456789).
29. Pearlman RB, Golchet PR, Feldmann MG, et al. Increased Prevalence of Autoimmunity in Patients With White Spot Syndromes and Their Family Members. Arch Ophthalmol. 2009;127(7):869-874.
30. Verhagen FH, Wijnhoven R, Ossewaarde-Van Norel J, et al. Prevalence and characteristics of ocular pain in non-infectious uveitis: A quality of life study. Br J Ophthalmol. 2018;102(8):1160-1166.

SUPPLEMENTARY DATA

Supplemental Table 2.1. Outcomes of multivariable linear regression analysis of risk factors for quality of life scores

	Relapse rate			IMT[a] (yes/no)			Prednisolone[b] (yes/no)		
NEI-VFQ-25 n=41	**B**	**95% CI**	***P*-value**	**B**	**95% CI**	***P*-value**	**B**	**95% CI**	***P*-value**
General health	1.6	-2.7 – 5.9	0.45	-5.0	-15.1 – 5.1	0.32	-1.1	-12.6 – 10.3	0.85
General vision	-0.7	-4.1 – 2.8	0.69	0.2	-7.9 – 8.2	0.97	3.0	-6.2 – 12.2	0.51
Ocular pain	-4.1	-8.6 – 0.7	0.08	-2.6	-13.4 – 8.0	0.61	-5.1	-18.3 – 7.0	0.39
Near vision activities (n=40)	-1.3	-6.0 – 3.5	0.59	-4.6	-15.7 – 6.5	0.41	-4.6	-17.2 – 8.0	0.46
Distance vision (n=39)	-1.3	-4.7 – 2.1	0.45	-8.8	-16.6 – -1.1	0.03[c]	-0.9	-9.5 – 7.6	0.83
Social functioning	0.7	-2.5 – 3.9	0.67	0.1	-7.1 – 7.3	0.97	-2.9	-11.1 – 5.2	0.47
Mental Health	-2.9	-6.9 – 1.1	0.15	-2.0	-11.4 – 7.4	0.67	-0.7	-11.3 – 10.0	0.90
Role difficulties	-3.9	-9.6 – 1.8	0.18	-9.8	-23.2 – 3.5	0.14	-3.4	-18.7 – 11.8	0.65
Dependency	-0.2	-3.4 – 2.9	0.88	-4.1	-11.4 – 3.2	0.26	-1.7	-10.1 – 6.6	0.68
Driving (n=39)	-3.6	-8.8 – 1.6	0.17	-13.7	-26.4 – -1.0	0.04[c]	-3.0	-16.8 – 10.8	0.66
Color vision	-0.3	-3.0 – 2.3	0.80	-3.5	-9.7 – 2.6	0.26	-3.0	-10.0 – 4.1	0.40
Peripheral vision	-1.5	-7.1 – 4.0	0.58	-1.4	-14.5 – 11.6	0.83	4.7	-10.1 – 19.6	0.52
Overall composite score	-1.6	-4.4 – 1.3	0.28	-6.0	-12.7 – -0.7	0.08	-0.0	-7.3 – 7.2	1.0
SF-36 n=41	**B**	**95% CI**	**P-value**	**B**	**95% CI**	**P-value**	**B**	**95% CI**	**P-value**
Physical functioning	1.7	-2.2 – 5.6	0.38	2.3	-6.8 – 11.4	0.61	-2.2	-12.6 – 8.1	0.66
Role limitations – physical	-0.1	-10.0 – 9.9	0.99	-8.5	-31.7 – 14.7	0.46	-17.0	-43.5 – 9.4	0.20
Bodily pain	-0.0	-6.0 – 5.9	0.99	8.7	-5.2 – 22.7	0.21	2.4	-13.5 – 18.3	0.76
General health	0.6	-5.8 – 6.9	0.86	-8.2	-23.1 – 6.6	0.27	-3.7	-20.6 – 13.3	0.66
Vitality/Energy	0.1	-4.6 – 4.9	0.95	-4.9	-16.1 – 6.3	0.38	4.0	-8.8 – 16.7	0.53
Social functioning	-1.9	-6.8 – 3.1	0.45	-2.7	-14.2 – 8.9	0.64	2.1	-11.0 – 15.3	0.75
Mental health	-1.0	-4.5 – 2.5	0.55	-1.2	-9.4 – 7.0	0.76	4.0	-5.3 – 13.3	0.39
Role limitations – emotional	4.4	-4.7 – 13.5	0.33	-0.2	-21.5 – 21.0	0.98	-24.0	-48.2 – 0.3	0.05

The results of multivariate linear regression analyses to evaluate the influence of clinical characteristics on the domain scores of the NEI-VFQ and SF questionnaires. Gender and age were also incorporated in the linear models (results not shown). Categorical variables were converted to dummy variables and as default the value 0 was set as reference (IMT: no=0/yes=1, prednisolone: no=0/yes=1)

B, Regression coefficient; CI, confidence interval; IMT, corticosteroid-sparing immunomodulatory treatment; NEI-VFQ, National Eye Institute Visual Function Questionnaire; SF, Short Form Health Survey; DMARD, disease-modifying antirheumatic drug.

[a] IMT: DMARD or DMARD+biological therapy

[b] Prednisolone: yes in case the patient was treated with at least 1 cycle of oral prednisolone during the 24 months of follow-up.

[c] Significant at nominal level, after 5% false discovery rate correction for multiple testing none remained significant.

Supplemental Table 2.2. Results of the SF-36 and NEI-VFQ-25 questionnaires in patients with idiopathic multifocal choroiditis and punctate inner choroidopathy compared to a reference group with non-infectious uveitis.

		Idiopathic MFC/PIC	**NIU[a]**	
	Scale	Mean (SD)	Mean (SD)	P_{adj}-value[b]
NEI-VFQ-25		**n=50**	**n=147**	
General health	0-100	62 (15)	46 (23)	9.5×10^{-6}
General vision	0-100	70 (12)	64 (15)	0.01
Ocular pain	0-100	81 (17)	72 (24)	0.02
Near vision activities	0-100	80 (16)	72 (23)	0.01
Distance vision activities (n=49)	0-100	80 (16)	70 (23)	4.2×10^{-3}
Social functioning	0-100	95 (14)	88 (18)	0.02
Mental Health	0-100	75 (17)	72 (20)	0.45
Role difficulties	0-100	75 (20)	65 (27)	0.02
Dependency	0-100	94 (12)	88 (21)	0.01
Driving (n=46)	0-100	70 (17)	74 (20)	0.46
Color vision	0-100	98 (9)	92 (17)	7.2×10^{-3}
Peripheral vision	0-100	84 (21)	75 (27)	0.02
SF-36		**n=50**	**n=147**	
Physical functioning	0-100	90 (15)	81 (24)	0.02
Role limitations – physical	0-100	74 (40)	65 (43)	0.51
Bodily pain	0-100	78 (21)	47 (15)	2.5×10^{-12}
General health	0-100	58 (21)	60 (21)	0.39
Vitality/Energy	0-100	60 (20)	63 (21)	0.16
Social functioning	0-100	81 (23)	82 (24)	0.69
Mental health	0-100	76 (14)	78 (17)	0.39
Role limitations – emotional	0-100	82 (36)	83 (34)	0.78

MFC, multifocal choroiditis; PIC, punctate inner choroidopathy; NIU, non-infectious uveitis; NEI-VFQ, National Eye Institute Visual Function Questionnaire; SF, Short Form Health Survey.

[a] Reference group consists of 147 patients with non-infectious uveitis from the UMC Utrecht[30]

[b] Student's T-test with false discovery rate correction at 5% to correct for multiple testing.

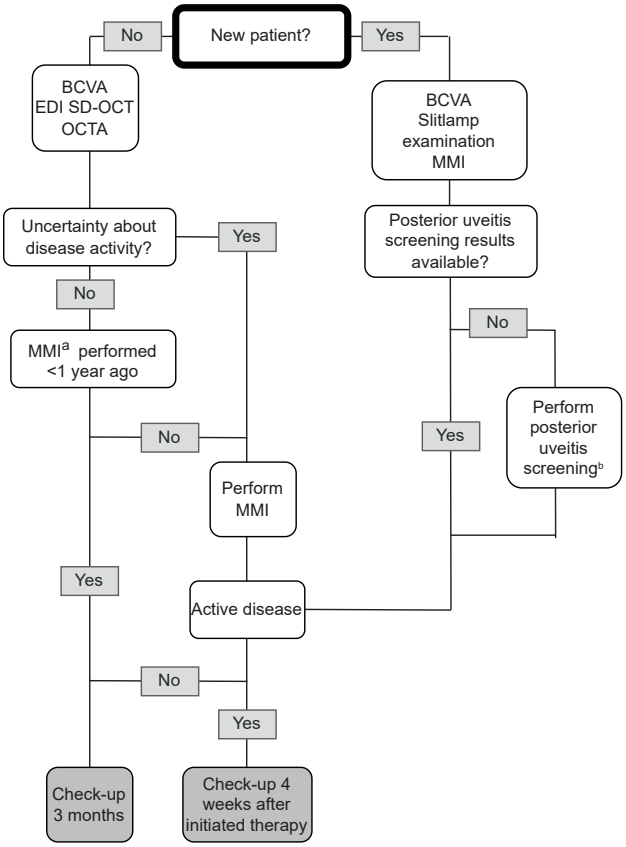

Supplemental Figure 2.1a. Flowchart of the diagnostic procedures in patients with idiopathic multifocal choroiditis and punctate inner choroidopathy.
BCVA, best-corrected visual acuity; EDI SD-OCT, enhanced depth imaging spectral-domain optical coherence tomography; OCTA, optical coherence tomography angiography; MMI, multimodal imaging modalities.
[a] Multimodal imaging (MMI) consists of fundus photography, fundus autofluorescence imaging, fluorescein angiography, indocyanine green angiography, *EDI SD*-OCT and OCTA.
[b] Posterior uveitis screening consists of a X-ray of the chest and optionally computed tomography, Soluble Interleukine-2 receptor, angiotensin converting enzyme, human leukocyte antigen A29 typing, QuantiFERON-TB, Treponema antibody test.

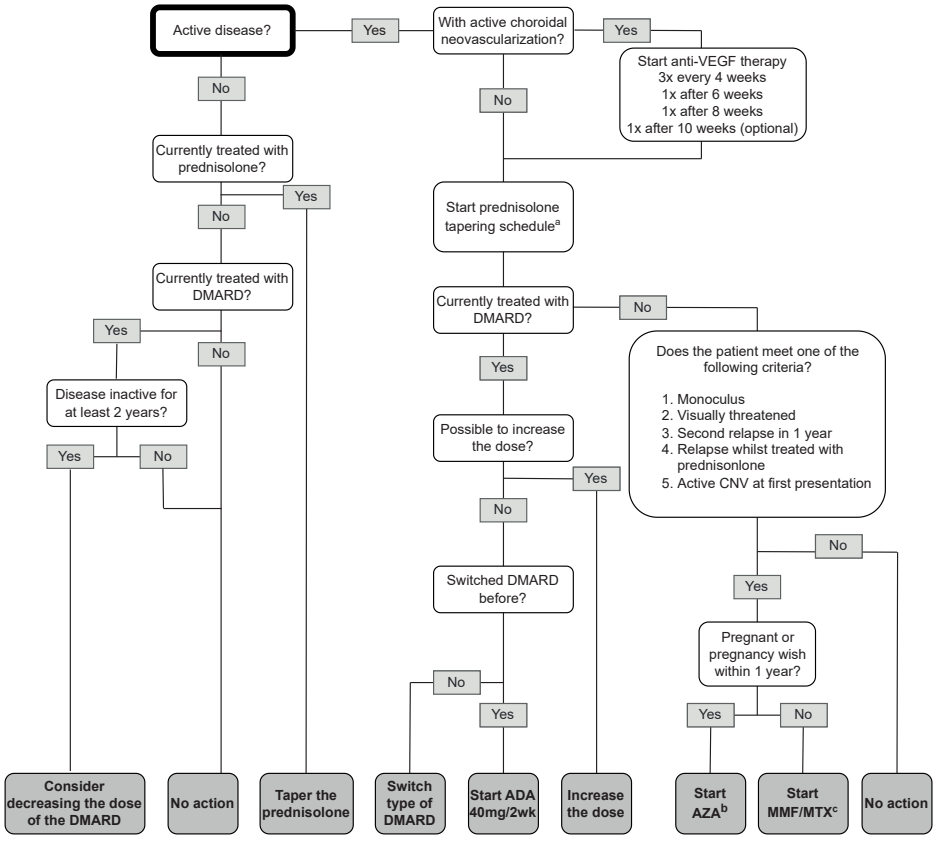

Supplemental Figure 2.1b. Flowchart of the therapeutic interventions in patients with idiopathic multifocal choroiditis and punctate inner choroidopathy.

VEGF, anti-vascular endothelial growth factor; DMARD, disease-modifying antirheumatic drugs; CNV, choroidal neovascularization; ADA, adalimumab; AZA, azathioprine; MMF, mycophenolate mofetil; MTX, methotrexate.

[a] Standard tapering schedule consisted of 3 days 60mg, 1 week 40 mg, 1 week 30mg, 1 week 20mg, 1 week 17,5mg, 1 week 15mg, 1 week 12,5 mg, 1 week 10mg, 1 months 7,5mg, 1 month 5mg, 1 month 2,5 mg and 1 month 2,5mg every other day.

[b] Azathioprine dose: 6TGN levels > 300 picomole/8 x 10^8 RBC, 6-MMP levels < 5700 picomole/8 x 10^8 RBC .

[c] First choice: mycophenolate mofetil dose 2000-3000 mg/day, second choice: MTX dose 15-25mg/week.

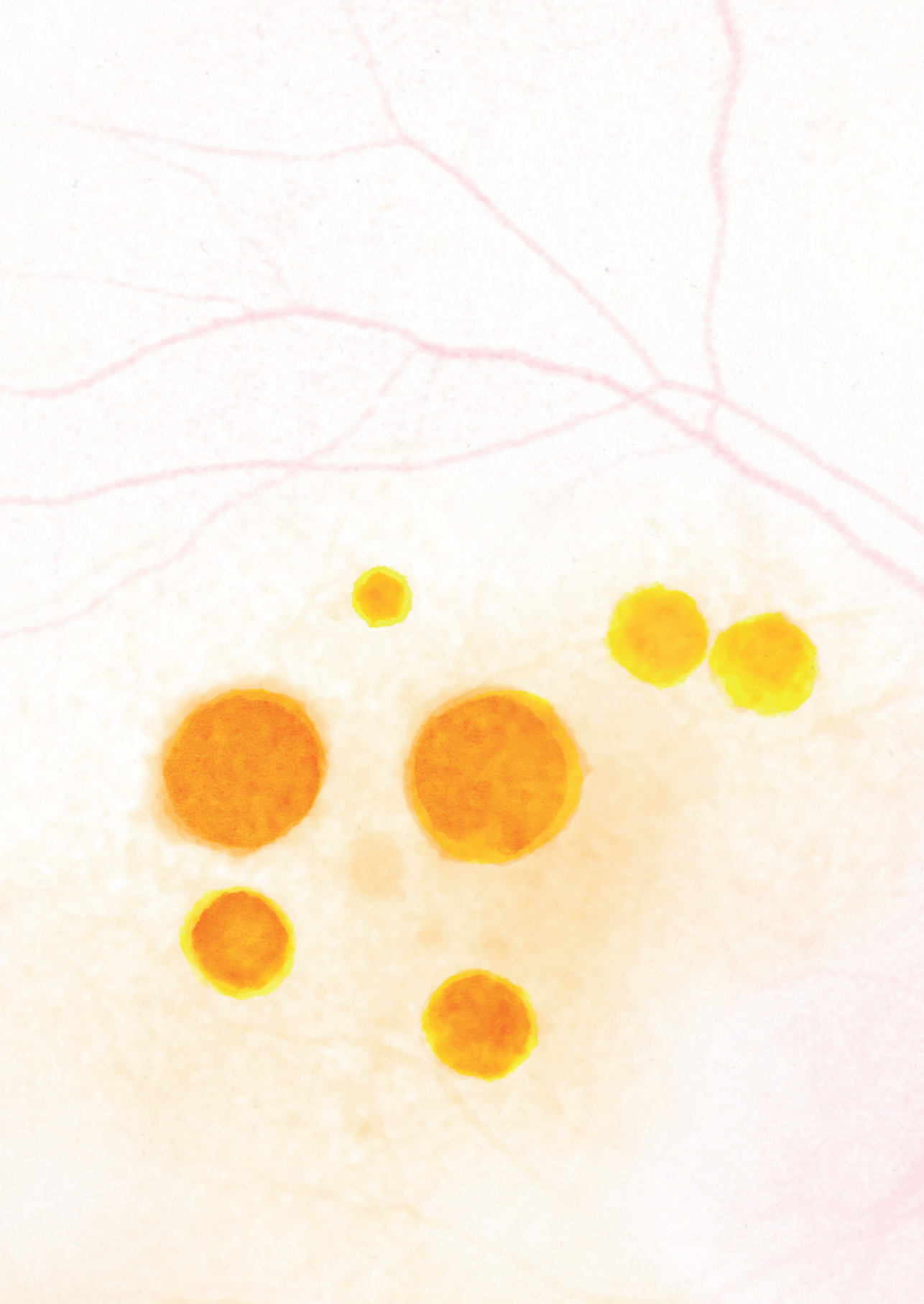

Chapter 3

The efficacy of corticosteroid-sparing immunomodulatory therapy in treating patients with central multifocal choroiditis

Evianne L. de Groot
Ninette H. ten Dam-van Loon
Joke H. de Boer
Jeannette Ossewaarde-van Norel

Acta Ophthalmol. 2020;98(8):816-821. doi: 10.1111/aos.14473

ABSTRACT

Purpose

To evaluate the efficacy of corticosteroid-sparing immunomodulatory therapy (IMT) in patients with recurrent and/or sight-threatening central multifocal choroiditis (MFC).

Methods

This was a retrospective cohort study in a tertiary uveitis centre including all patients with MFC who have been treated with IMT for at least 12 months. Clinical data and imaging results were collected regarding the period prior to the start of IMT and at 3, 6, 12 and – where available – 24 months after the start of IMT. Main outcome measure was the number of annual recurrences of choroiditis with or without active choroidal neovascularization before and after the start of IMT. Secondary outcomes were the percentage of patients with (steroid-free) remission and the median time between the start of IMT and (steroid-free) remission.

Results

Thirty-two patients (39 eyes) were included. At the start of IMT, none of the patients were in (steroid-free) remission. At 24 months, the probability of achieving remission and steroid-free remission was 88,5% and 50%, respectively. The median time to achieve remission and steroid-free remission was 21 and 83 weeks, respectively. In 17 patients (20 eyes) with available clinical data and imaging results for ≥ 12 months prior to the start of IMT, the mean number of recurrences/year decreased significantly from 1.40 ± 0.81 at baseline to 0.49 ± 0.47 ($p = 0.001$) after the start of IMT.

Conclusions

Preventive therapy with IMT should be considered in patients with recurrent and/or sight-threatening MFC to decrease the number of recurrences/year and to increase the prospects of achieving either remission or steroid-free remission.

INTRODUCTION

Central multifocal choroiditis (MFC) is a rare form of noninfectious posterior uveitis most commonly seen in the second to fourth decade of life in Caucasian women with myopia.[1] Several subtypes of MFC have been described based on the phenotypic presentation, including punctate inner choroidopathy (PIC) and multifocal choroiditis without panuveitis, though they are considered to be slightly different clinical presentations of the same disease entity. The aetiology of these subtypes remains unclear, and no association with a systemic disease has been identified.[1] Symptoms of MFC can include metamorphopsia, floaters, decreased vision and scotoma.[2] Moreover, patients typically develop numerous central choroidal spots that usually form atrophic scars, without signs of ocular inflammation. A common complication is the development of choroidal neovascularization (CNV) in – or adjacent to – one or more of these choroidal spots.[3-6] Fluorescein angiography (FA), indocyanine green angiography (ICG), optical coherence tomography (OCT) and optical coherence tomography angiography (OCTA) can be used in order to diagnose and monitor the disease (**Figure 3.1**).[1] The current treatment for MFC consists of systemic corticosteroids in the early stage of the disease in order to control the inflammatory component; in the case of active CNV, this treatment can be combined with intravitreal injections of anti-vascular endothelial growth factor (anti-VEGF).[7-10] Corticosteroid-sparing immunomodulatory therapy (IMT) is widely used for treating noninfectious uveitis to achieve disease control and minimize corticosteroid-related side-effects.[9,11-14] Recently, the inflammatory component was proposed to trigger the onset and growth of CNV in MFC, suggesting that IMT such as methotrexate and mycophenolate mofetil may be used as a preventive treatment for MFC.[1] To date, however, the potential value of using IMT in central MFC has been investigated in retrospective case studies involving only small cohort sizes.[15,16] Therefore, the aim of this study was to retrospectively evaluate the effect of IMT in a relatively large group of patients with central MFC.

PATIENTS AND METHODS

This study was performed in accordance with the tenets of the Declaration of Helsinki regarding research involving human subjects and approved by the University Medical Center Utrecht institutional review board.

Study population

This retrospective cohort study was performed at the University Medical Center (UMC) Utrecht in Utrecht, the Netherlands. We included patients presenting with idiopathic central choroiditis who were treated for at least 12 months with IMT. Central multifocal choroiditis was diagnosed in case of the presence of idiopathic punctate choroidal or chorioretinal spots or punched-out lesions within the temporal vascular arcades without signs of intraocular inflammation. In addition, patients who were treated consecutively with more than one immunosuppressive drug were included only if at least one agent was administered for at least three consecutive months. We excluded patients who were diagnosed with an infectious cause of uveitis (f.e. toxoplasmosis), birdshot chorioretinopathy, or had suspected systemic and/or ocular sarcoidosis; patients with anterior uveitis (based on the SUN criteria with a score > 0),[17] ≥1 + vitreous cells (based on the National Health Institute grading system for vitreous cells),[18] retinal vasculitis, and/or papillitis; and eyes with a best-corrected visual acuity (BCVA) (LogMAR) of 20/1200 (1.79) or worse. Secondly, we excluded patients who were treated with IMT for less than 12 months.

Data collection

Clinical data and imaging results were collected regarding the period from 1988 through 20 July 2018. Imaging modalities included FA-ICGA and SD-OCT (Spectralis HRA + OCT; Heidelberg Engineering, Heidelberg, Germany). Data were collected for the period prior to the start with IMT and at 3, 6, 12 and – where available – 24 months of follow-up after the start of IMT. Data regarding the patient's ophthalmic history prior to presentation at the UMC Utrecht were reviewed in selected cases in which recurrences were documented and all relevant imaging results were available. If this data were incomplete or inconclusive, this time period was not included in this study. In cases involving more than one immunosuppressive agent, all agents were included in the analysis. When a biological agent was added to the treatment regime, only the data regarding the period without treatment with the biological agent were used.

Outcome measures

Patients who were treated with IMT and ≤ 10 mg prednisolone and developed no new choroidal lesions, no growth of existing lesions, no new CNV site, or reactivation of

an existing CNV site based on FA-ICG or SD-OCT imaging for at least 3 months were defined as being in remission. Steroid-free remission was defined as remission without treatment with steroids for at least 3 months. A recurrence of choroiditis was defined as the presence of new choroidal lesions or the growth of any existing choroidal lesions visible on OCT or FA-ICG after previous by imaging confirmed remission. A recurrence of CNV was defined as follows: (1a) dye leakage from an existing subretinal neovascular lesion visible on FA-ICG; or (1b) subretinal and/or intraretinal fluid visible on OCT; or (1c) evidence of a growing subretinal neovascular complex on OCT; and 2) CNV that had been documented previously as inactive based on imaging. Intraretinal fluid in the context of atrophic cysts due to scarring was left out of account. The primary outcome was the difference between the number of recurrences/year measured before the start of IMT and the number of recurrences/year measured after the start of IMT. The number of recurrences was further classified as whether or not an active site of CNV was present. Because no statistical correction could be performed in patients with bilateral disease, the analysis was repeated by analysing only the first affected eye in the patients with bilateral disease. In addition, the following secondary outcomes were recorded: BCVA; the percentage of patients who achieved remission and the median time to achieve remission; the percentage of patients who achieved steroid-free remission and the median time to achieve steroid-free remission; the number of anti-VEGF injections/year before and after the start of IMT; the number of patients with treatment escalation to a combination of IMT and biologicals within 12 months of follow-up; the percentage of patients who received high-dose IMT at 24 months of follow-up; the percentage of patients who were treated with two immunomodulatory agents at 24 months of follow-up; and the percentage of patients who switched their type of immunomodulatory agent during follow-up. BCVA was converted to LogMAR (logarithm of the minimum angle of resolution) values for analysis, and is presented as both Snellen and LogMAR values. The IMT was prescribed at standard doses (methotrexate: 15–20 mg/week, mycophenolate mofetil: 2000 mg/day, mycophenolate sodium: 1440 mg/day and azathioprine: 1–3 mg/kg/day). A trough serum level of ≥ 0.10 mg/L was used for cyclosporine treatment. High-dose IMT was defined as follows: methotrexate > 20 mg/week, mycophenolate mofetil > 2000 mg/day, mycophenolate sodium > 1440 mg/day and azathioprine > 3 mg/kg/day.

Statistical analysis

All statistical analyses were performed using SPSS for Windows version 25.0 (IBM Corp., Armonk, NY, USA). The number of recurrences/year before and after the start of IMT was calculated by dividing the total number of recurrences in the given period by the total number of years in the given period and was compared using the Wilcoxon signed-rank test. Differences with a p-value ≤ 0.05 were considered significant. The probability to

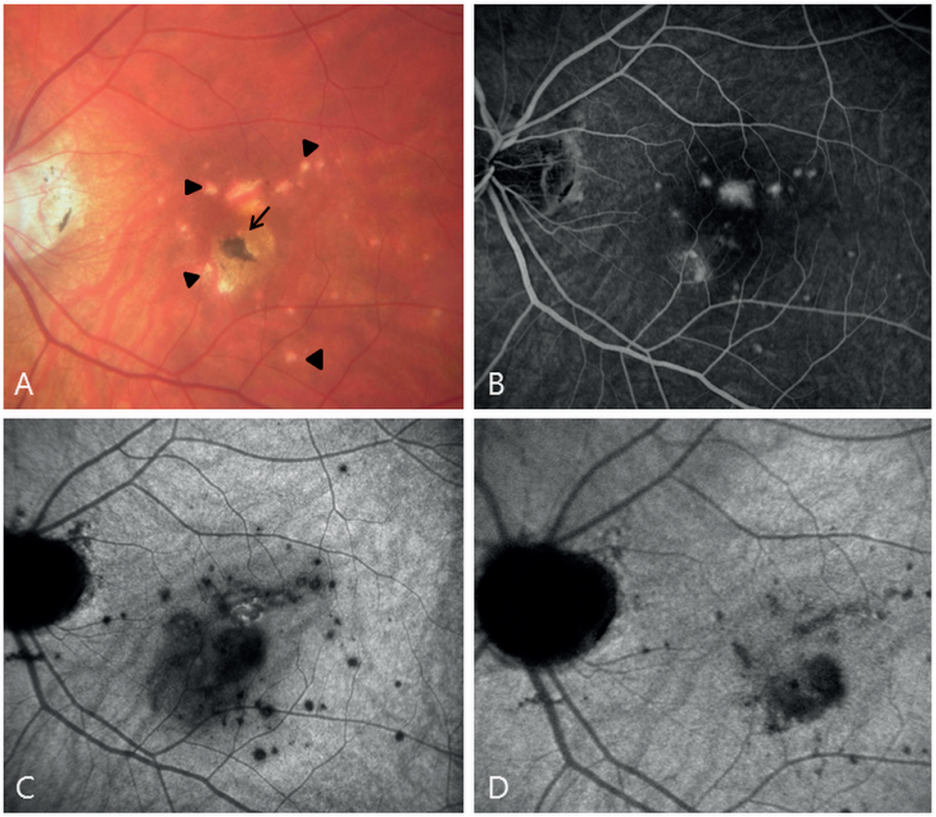

Figure 3.1. Central multifocal choroiditis in the left eye. (**A**) Colour fundus photograph taken during an active stage of the disease, showing multiple spots in the posterior pole (arrowheads) and a hyperpigmented spot in the centre (arrow). (**B**) Fluorescein angiography image at 4 min during an active stage of the disease, showing leakage of multiple active CNV sites. (**C**) Indocyanine green angiography (ICGA) image at 31 min during an active stage of the disease, showing a hypodense area with vague boundaries corresponding with choroidal inflammation. (**D**) ICGA image at 31 min during an inactive stage of the disease, showing a reduction in the hypodense area with sharp boundaries.

achieve (steroid-free) remission and the time to (steroid-free) remission was estimated using the Kaplan–Meier method.

RESULTS

Baseline characteristics

A total of 34 patients with 48 affected eyes were identified. Two patients were excluded because IMT was discontinued within 12 months (in one patient due to side-effects and in one patient due to inefficacy). Of the remaining 32 patients and 44 eyes, five eyes of five patients with bilateral disease were excluded because the BCVA (LogMAR) was ≤ 20/1200 (1.79) prior to the first presentation in the UMC Utrecht. Thus, a total of 39

eyes in 32 patients were included in the final analysis (**Table 3.1**). Of the 32 patients, 12 patients (36%) presented with bilateral disease. Thirty of the 32 patients (94%) were female. Seventeen of the 39 eyes (44%) had high myopia with a spherical equivalent (SE) over -6.0 dioptres (D), and 20 eyes (51%) had mild to moderate myopia with a SE up to -6.0 D. The mean (±SD) age at presentation was 33.4 ± 9.3 years (range: 21-56 years) (**Table 3.1**).

Table 3.1. Patient characteristics (n=32 patients)

Eyes, n[a]	39
Age at presentation in years, mean (range)	33.4 (18-56)
Female patients, n (%)	30 (94)
CNV present prior to first consult[b], n (%)	22 (56)
BCVA at presentation, mean (range)	20/38 (20/400 – 20/9.4)
Bilateral disease, n (%)	12 (36)
High myopia[c], n (%)	17 (44)
BCVA ≤20/1200 (0.02) in one eye, n (%)	5 (16)

CNV, choroidal neovascularization; BCVA, best-corrected visual acuity.
[a] Does not include the five eyes with a BCVA (LogMAR) ≤ 20/1200 (1.79)
[b] First consult refers to the first consult at UMC Utrecht.
[c] High myopia is defined as a spherical equivalent over -6 diopters.

Annual recurrences

A total of 20 eyes (in 17 patients) had a follow-up period of at least 12 months both before and after the start of IMT, and we determined the change in the mean number of recurrences/year of disease activity for these cases. In this group, the median follow-up period before IMT and after the start of IMT was 23 months (range: 14–256 months) and 59 months (range: 15– 109 months), respectively. Data regarding recurrences prior to the first presentation in the UMC Utrecht were judged eligible for 3 patients; thus, these recurrences were included in the final analysis. When analysing 1 eye per patient, the mean (±SD) number of recurrences/year before the start of IMT was 1.40 ± 0.81. After the start of IMT, this number was significantly lower (0.49 ±0.47; $p = 0.002$). Our analysis of the number of recurrences/year is summarized in **Table 3.2**. We also analysed the number of recurrences/year separately for choroiditis with active CNV and choroiditis without active CNV, revealing that the number of recurrences/year for choroiditis with active CNV decreased significantly after the start of IMT, from 0.73 ± 0.76 to 0.17 ± 0.25 ($p = 0.008$). In contrast, although the mean number of recurrences/year for choroiditis without active CNV decreased from 0.67 ± 0.68 to 0.32 ± 0.30, this difference was not significant ($p = 0.234$). Similar results were obtained when all affected eyes were analysed (**Table 3.2**). The number of anti-VEGF injections decreased significantly when

analysing one eye per patient, but this decrease lost its significance when analysing all affected eyes (**Table 3.2**).

Table 3.2. Summary of the number of recurrences/year and the number of anti-VEGF injections/year in the subgroup of patients with ≥12 months of follow-up data before and after the start of IMT.

	17 eyes of 17 patients			20 eyes of 17 patients		
	Before IMT	After IMT	*P*-value[a]	Before IMT	After IMT	*P*-value[a]
Total recurrences[b]/year	1.40±0.81	0.49±0.47	**0.002**	1.25±0.83	0.45±0.45	**0.001**
Number of recurrences	49	34		59	38	
Recurrences with active CNV/year	0.73±0.76	0.17±0.25	**0.008**	0.63±0.73	0.16±0.24	**0.011**
Number of recurrences	21	10		25	12	
Recurrences without active CNV/year	0.67±0.68	0.32±0.30	0.234	0.62±0.65	0.29±0.30	0.136
Number of recurrences	28	24		34	26	
Anti-VEGF injections[c]/year	3.34±3.46	1.98±2.92	**0.041**	2.87±3.40	1.75±2.76	0.071
Number of injections	81	155		81	161	

VEGF, vascular endothelial growth factor; IMT, corticosteroid-sparing immunomodulatory therapy; CNV, choroidal neovascularization.

[a] Wilcoxon signed rank test.

[b] Total, number of recurrences/year of choroiditis with CNV + number of recurrences/year of choroiditis without CNV.

[c] Anti-VEGF injections included bevacizumab, ranibizumab, and aflibercept.

Remission and steroid-free remission

Next, we measured the time between the start of IMT and (steroid-free) remission. The median time after the start of IMT to achieve remission and steroid-free remission was 21 and 83 weeks, respectively. At 2 years of follow-up, the probability of achieving remission and steroid-free remission was 88.5% and 50%, respectively (**Figure 3.2**). Mean Snellen BCVA (LogMAR) improved from 20/31 (0.19) at the start of IMT to 20/28 (0.15) at 3 months of follow-up and remained stable with a mean Snellen (LogMAR) BCVA of 20/27 (0.13) at 24 months of follow-up. In one patient, treatment was escalated to the combination of IMT and biological treatment within the first 12 months of follow-up. Twenty-three of the 32 patients had 24 months of follow-up. At 24 months of follow-up, 4/23 patients (17%) required two immunomodulatory agents in order to achieve remission, and an additional four patients (17%) required high-dose IMT. Moreover, in 15/32 patients (47%) the type of agent of IMT was switched within the first 24 months either because of treatment failure (i.e. no remission was achieved) or because the patient developed intolerable objective and/or subjective side effects. In some cases, the dose of IMT could not be increased due to side effects.

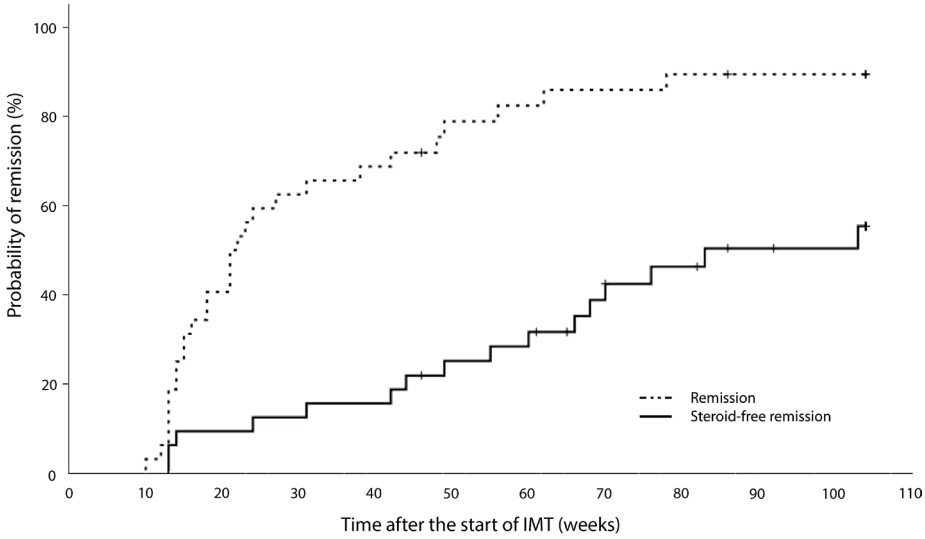

Figure 3.2. Time to remission and steroid-free remission. A Kaplan-Meier graph illustrates the time between the start of IMT and the probability of achieving remission (interrupted line) and steroid-free remission (continuing line). Censoring is indicated by small vertical lines.

DISCUSSION

In our opinion, treatment with IMT is recommended in patients with recurrent and/or sight-threatening central MFC in order to prevent cumulative damage from recurrent disease and to avoid corticosteroid-related side-effects. In this study, we accepted 10 mg/day of prednisolone as the maximum maintenance dose, as suggested by guidelines.[13,17]

Our retrospective analysis revealed a significant decrease in both the total number of recurrences/year and the number of recurrences/year of choroiditis with active CNV following the start of IMT. This finding is consistent with a previous report of 8 patients with recurrent PIC, which also found a significant reduction in the frequency of recurrences after starting mycophenolate mofetil therapy.[15] A recent study documented a significant reduction of the risk of the development of a choroidal neovascular membrane in the subgroup of 14 patients treated with IMT before the development of CNV.[9] Another study[16] evaluated the success of mycophenolate mofetil monotherapy in a cohort of 27 patients with various multifocal choroidopathies, including birdshot chorioretinitis, multifocal choroiditis with panuveitis and – relevant to our study – six patients with PIC; the authors reported a 95% success rate after 2 years of follow-up. Success was defined as no disease activity while treated with ≤ 10 mg/day prednisolone. The 95% success rate is similar to our finding that the probability of achieving remission is 88.5% at 24 months of follow-up. Moreover, 21% of the patients required a second immunosuppressive agent

in order to achieve remission, which is similar to our results in which 17% of patients required a second immunosuppressive agent. Twenty-four months after the start of IMT, mean BCVA (LogMAR) in our cohort was 20/27 (0.13), which is relatively high compared to other studies.[3,5,15,16] This difference may be due to the relatively early detection and more timely treatment of the disease which is a result of increased awareness among ophthalmologists and/or improvements in retinal imaging over the past decade. In particular, the eye-tracking function on the Heidelberg SD-OCT and improved quality of the ICGA on the Heidelberg scanning laser ophthalmoscope (with reduced stray light compared to conventional ICG) provide a more accurate means of monitoring disease activity and recognizing a recurrence early, possibly resulting in better long-term visual acuity. In half of the patients, at least one year with multiple recurrences passed by before IMT was initiated. One could argue that this period is relatively long and earlier intervention should be considered in the future. This observance can be explained by the fact that for this retrospective study, a large timeframe was assessed with a change of clinical practice over time.

A strength of this study is the relatively large, homogeneous study cohort including 32 patients with central MFC for whom clinical data were available after the start of IMT. To the best of our knowledge, this is the first study of this size to evaluate the efficacy of IMT on the long term exclusively in patients with central MFC. Moreover, data were available for at least 12 months – and in some cases, 24 months – after the start of IMT, thus providing important insight into the long-term course of the disease after the start of IMT.

Despite these strengths, our study has several possible limitations that warrant discussion, and as with any retrospective cohort study, the results should be interpreted in the context of these limitations. First, although the sample size is relatively large compared to previously published studies regarding central MFC,[15,16] the sample size is still a limitation of the study.

Second, we chose for a longitudinal (within-subject) study design instead of cross-sectional study design. Therefore, a control group is not applicable and thus the natural course of disease is not taken into account. Though, in our opinion within-subject study design is the best method considering the available data. Only a selective group of MFC patients have an indication for preventive treatment with IMT. When comparing these results to a control group (patients without treatment with IMT and often without indication for preventive treatment), it will inevitably causes distortion of the results. This study focused exclusively on patients with sight-threatening and/or recurrent

central MFC, and thus, the results are most applicable to this specific subgroup of patients with central MFC.

Third, the observed decrease in the number of annual recurrences in the choroiditis cases both with and without active CNV after the start of IMT is likely an underestimation. Since 2011, most patients treated with IMT are closely monitored using the eye-tracker system on the OCT machine, thereby allowing for the early identification and treatment of subclinical recurrences of choroiditis, rather than treating only clinically identifiable recurrences (which present mostly with active CNV). Thus, it is reasonable to assume that the number of recurrences before 2011 (and often prior to the start of IMT) is likely an underestimation due to unreported subclinical recurrences.

Fourth, choroidal neovascularization (CNV) develops in a relatively large percentage of patients, ranging from 45.2% to 76.9%,[3,5,6] and CNV can result in permanent vision loss. Distinguishing between an active CNV site and an inflammatory lesion is often difficult; literature suggests OCTA can be used to distinguish an inflammatory lesion and CNV though unfortunately this imaging modality was not yet available during the timeframe of this study. For this reason, at least one preventive injection of anti-VEGF often was given in cases with an active inflammatory lesion. Moreover, in the case of active CNV, neither the number nor the frequency of injections is standardized and varied both between patients and over time; thus, our results regarding anti-VEGF injections should be interpreted with caution.

Finally, patient-centred outcomes should also be considered. For example, it is unclear to what extent preserving vision in a patient with central MFC improves quality of life, as well as whether this is sufficient to offset the extent to which preventive treatment with IMT can potentially decrease the patient's quality of life. Moreover, no data are currently available regarding the impact of IMT on quality of life in patients with central MFC, and additional research is needed in order to evaluate the overall effects of IMT in these patients.

CONCLUSIONS

In summary, we report that after the start of preventive treatment with IMT, the number of recurrences/year significantly decreased, BCVA stabilized, and the number of patients who achieved (steroid-free) remission increased. We therefore conclude that preventive treatment with IMT should be considered as a treatment option in patients with recurrent and/or sight-threatening central MFC.

REFERENCES

1. Ahnood D, Madhusudhan S, Tsaloumas MD, Waheed NK, Keane PA, Denniston AK. Punctate inner choroidopathy: A review. Surv Ophthalmol. 2017;62(2):113-126. doi:10.1016/j.survophthal.2016.10.003
2. Tavallali A, Yannuzzi LA. Idiopathic multifocal choroiditis. J Ophthalmic Vis Res. 2016;11(4):429-432. doi:10.4103/2008-322X.194141
3. Kedhar SR, Thorne JE, Wittenberg S, Jabs DA. Multifocal choroiditis with Panuveitis and Punctate Inner Choroidopathy: Comparison of Clinical Characteristics at Presentation. Retina. 2007;27(9):1174-1179. doi:10.1097/IAE.0b013e318068de72
4. Baxter SL, Pistilli M, Pujari SS, et al. Risk of choroidal neovascularization among the uveitides. Am J Ophthalmol. 2013;156:468-477.
5. Leung TG, Moradi A, Liu D, et al. Clinical features and incidence rate of ocular complications in punctate inner choroidopathy. Retina. 2014;34(8):1666-1674. doi:10.1097/IAE.0000000000000125
6. Fung AT, Pal S, Yannuzzi NA, et al. Multifocal choroiditis without panuveitis; Clinical Characteristics and Progression. Retina. 2014;34(1):98-107. doi:10.1097/IAE.0b013e31829234cb
7. Barth T, Zeman F, Helbig H, Gamulescu MA. Intravitreal anti-VEGF treatment for choroidal neovascularization secondary to punctate inner choroidopathy. Int Ophthalmol. 2018;38(3):923-931. doi:10.1007/s10792-017-0536-0
8. Parodi MB, Iacono P, Mansour A, et al. INTRAVITREAL BEVACIZUMAB FOR JUXTAFOVEAL CHOROIDAL NEOVASCULARIZATION SECONDARY TO MULTIFOCAL CHOROIDITIS. Retina. 2013;33:953-956.
9. Niederer RL, Gilbert R, Lightman SL, Tomkins-Netzer O. Risk Factors for Developing Choroidal Neovascular Membrane and Visual Loss in Punctate Inner Choroidopathy. Ophthalmology. 2018;125(2):288-294. doi:10.1016/j.ophtha.2017.09.002
10. Chen SN, Chen YL, Yang BCL. Long-Term Outcome of Punctate Inner Choroidopathy or Multifocal Choroiditis with Active Choroidal Neovascularization Managed with Intravitreal Bevacizumab. Ocul Immunol Inflamm. 2020;28(1):33-38. doi:10.1080/09273948.2019.1588335
11. Jabs DA, Rosenbaum JT, Foster CS, et al. Guidelines for the use of immunosuppressive drugs in patients with ocular inflammatory disorders: Recommendations of an expert panel. Am J Ophthalmol. 2000;130(4):492-513. doi:10.1016/S0002-9394(00)00659-0
12. Galor A, Jabs DA, Leder HA, et al. Comparison of Antimetabolite Drugs as Corticosteroid-Sparing Therapy for Noninfectious Ocular Inflammation. Ophthalmology. 2008;115(10):1826-1832. doi:10.1016/j.ophtha.2008.04.026
13. Dick AD, Rosenbaum JT, Al-Dhibi HA, et al. Guidance on Noncorticosteroid Systemic Immunomodulatory Therapy in Noninfectious Uveitis: Fundamentals Of Care for UveitiS (FOCUS) Initiative. Ophthalmology. 2018;125(5):757-773. doi:10.1016/j.ophtha.2017.11.017
14. Jabs DA. Immunosuppression for the Uveitides. Ophthalmology. 2018;125(2):193-202. doi:10.1016/j.ophtha.2017.08.007
15. Turkcuoglu P, Chang PY, Rentiya ZS, et al. Mycophenolate mofetil and fundus autofluorescence in the management of recurrent punctate inner choroidopathy. Ocul Immunol Inflamm. 2011;19(4):286-292. doi:10.3109/09273948.2011.580072
16. Goldberg NR, Lyu T, Moshier E, Godbold J, Jabs DA. Success with single-agent immunosuppression for multifocal choroidopathies. Am J Ophthalmol. 2014;158(6):1310-1317. doi:10.1016/j.ajo.2014.08.039

17. Jabs DA, Nussenblatt RB, Rosenbaum JT, et al. Standardization of uveitis nomenclature for reporting clinical data. Results of the first international workshop. Am J Ophthalmol. 2005;140(3):509-516. doi:10.1016/j.ajo.2005.03.057
18. Nussenblatt RB, Palestine AG, Chan CC, Roberge F. Standardizatlon of Vitreal inflammatory Activity in Intermediate and Posterior Uveitis. Ophthalmology. 1985;92(4):467-471. doi:10.1016/S0161-6420(85)34001-0

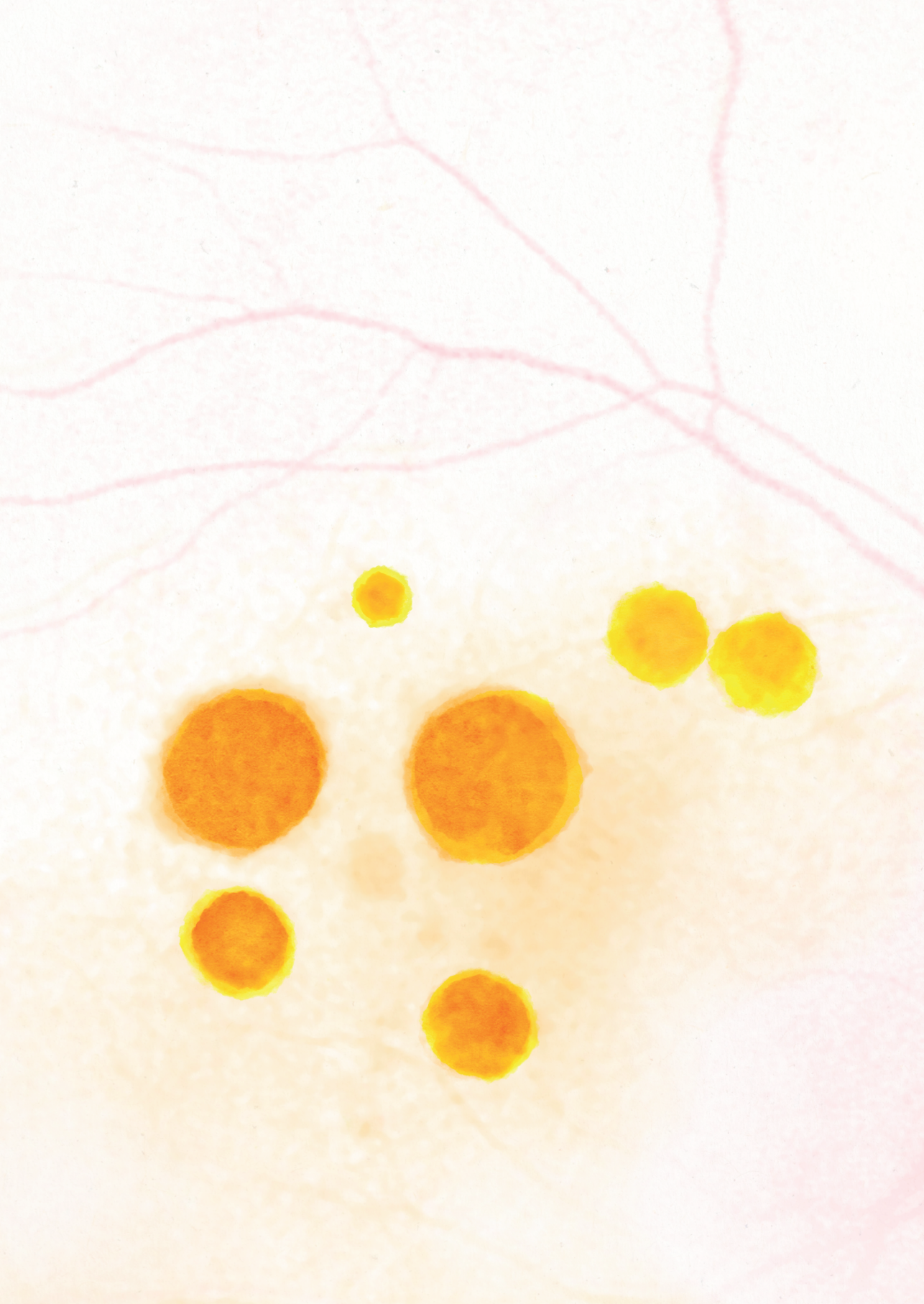

Chapter 4

The efficacy of adalimumab in treating patients with central multifocal choroiditis

Evianne L. de Groot
Jeannette Ossewaarde-van Norel
Lintje Ho
Ninette H. ten Dam-van Loon
Joke H. de Boer

Am J Ophthalmol Case Rep. 2020; 20: 100921

ABSTRACT

Purpose

To evaluate the efficacy of adalimumab in patients with central multifocal choroiditis (cMFC) refractory to conventional corticosteroid-sparing immunomodulatory agents (IMT).

Methods

Medical records were reviewed from all patients with cMFC and treated with adalimumab with follow-up of at least 12 months. The study focused on the 12 months prior to and after the start of adalimumab. The imaging results were independently evaluated by two ophthalmologists. The main outcomes were the number of patients without a relapse of disease activity in 12 months after the start of adalimumab and the ability to stop the systemic corticosteroids to evaluate the corticosteroid-sparing effect.

Results

Twelve patients (18 eyes) were included. In 8/12 (67%) patients no relapse of disease activity was observed in the 12 months after the start of adalimumab. In 9/12 patients the systemic corticosteroid treatment could be stopped and in an additional 2 patients tapered to ≤7,5mg daily. In the 12 months before the start of adalimumab, the patients experienced a median of 3 (range 2–4) relapses of disease activity. Nine patients experienced relapses while treated with a combination of systemic corticosteroids (mean dose 13,6 mg; range 5–25 mg) and IMT. Moreover, 3 patients treated with IMT, experienced relapses after tapering and stopping the systemic corticosteroids. In all eyes (n = 5) with CNV before the start of adalimumab, the intravitreal anti-VEGF injections could be stopped after the start of adalimumab.

Conclusions and importance

Adalimumab may be effective in patients with cMFC refractory to IMT and may be considered as a treatment option in patients with cMFC.

INTRODUCTION

Central multifocal choroiditis (cMFC), a rare idiopathic inflammatory condition, is part of the wider spectrum of the "white dot syndromes".[1] The term cMFC is introduced by the authors to cover all subtypes of idiopathic inflammation of the choroid in the posterior pole, including punctate inner choroidopathy (PIC), multifocal choroiditis (MFC) without panuveitis,[2] persistent placoid maculopathy (PPM) and serpiginous choroiditis (SC). The most frequent complication is the formation of secondary choroidal neovascularization (CNV) presumed to be triggered by a low-grade, often asymptomatic, level of inflammation.[3,4] The pathophysiology of cMFC is largely unknown but a dysregulation of the immune system is a proposed disease mechanism.[5,6] Moreover, this disease is predominantly observed in young Caucasian women with myopia without an association with a systemic disease.[7] During the active stage of disease, a short course of oral corticosteroids is often prescribed.[1,8] In severe or sight-threatening cases, preventive treatment with corticosteroid-sparing immunomodulatory therapy (IMT) is suggested to prevent retinal damage caused either by the relapsing choroiditis or by scarring due to the complication of secondary CNV.[8-11] Treatment with conventional IMT, such as mycophenolate mofetil and azathioprine, is generally accepted to be safe and effective for noninfectious ocular inflammatory diseases.[12-14] In cMFC, though evidence is scarce, these agents are suggested to decline the number of relapses of the choroiditis and reduce the number of relapses with active CNV.[9,11,15,16] In our experience, though conventional IMT is generally effective, few patients with cMFC have an insufficient response to these agents. Since adalimumab is increasingly prescribed and proven to be effective in treatment for noninfectious uveitis,[12,17-19] we aim to explore the efficacy of adalimumab in patients with cMFC with an insufficient response to conventional IMT.

MATERIALS AND METHODS

A single center retrospective observational cohort study was performed at the University Medical Center (UMC) Utrecht, the Netherlands. This study was conducted with approval of the University Medical Center Utrecht institutional review board and in accordance with the tenets of the Declaration of Helsinki. Written informed consent was given by all participants.

Study population

All patients were diagnosed with cMFC and presented with choroidal scars in the posterior pole within the temporal arcades with no to minimum vitreous cells (grading score ≤1+ following the National Institute of Health grading system for vitreous cells), and without

papillitis, vasculitis or anterior uveitis (SUN criteria 0).[20,21] All patients had a diagnostic work-up to rule out tuberculosis and sarcoidosis (and when clinically indicated other less frequent causes for posterior uveitis, such as birdshot chorioretinopathy). Subtypes of central cMFC included punctate inner choroidopathy (PIC), idiopathic multifocal choroiditis, serpiginous-like choroiditis, and persistent placoid maculopathy. All patients were treated with adalimumab and followed for at least 12 months after the start of adalimumab.

Data collection

Clinical data between January 2014 and December 2019 was collected and focused on the 12 months before and after the start of adalimumab. Data of all affected eyes was obtained by reviewing the medical chart and by the evaluation of imaging results including optical coherence tomography (SD-OCT), fundus color pictures, fundus autofluorescence pictures and fluorescein and indocyanine green angiography (FA-ICG) (Spectralis HRA + OCT; Heidelberg Engineering, Heidelberg, Germany). The imaging results were presented anonymously and evaluated for disease activity of choroiditis and CNV by two ophthalmologists (JO-vN and LH) who were masked for all data from the medical records.

Outcome measures

The main outcome measure was the number of patients without a (sub)clinical relapse of disease activity in the 12 months after the start of adalimumab. A relapse of disease activity was assessed solely on imaging results and was defined as either 1. the development of new inflammatory lesions or CNV or 2. growth and/or reactivation of pre-existing inflammatory lesions or CNV (vague boundaries of the lesions on 20 minute ICG images/blurred boundaries or growth of subretinal lesions on OCT/leakage on FA images) after previous quiescent disease confirmed by imaging (**Figure 4.1**). Moreover, the ability to taper and stop the prednisolone without disease reactivation was assessed in order to evaluate the corticosteroid-sparing effect. Secondary outcomes included visual acuity (VA), adalimumab related side-effects, dose reduction of IMT after the start of adalimumab, the number of relapses of disease activity in the 12 months before the start of adalimumab including corresponding dose of prednisolone and finally the number of intravitreal anti-VEGF injections before and after the start of adalimumab. The presence of disease activity 12 months prior to the start of adalimumab was considered to be a relapse. Corticosteroid-sparing agents included methotrexate (MTX), azathioprine (AZA), mycophenolate mofetil (MMF)/mycophenolic acid (MPA), cyclosporine (CsA), and cyclophosphamide (CP). VA was converted to LogMAR (logarithm of the minimum angle of resolution) values for analysis and is presented as both LogMAR value and the Snellen equivalent. The Wilcoxon signed-rank test was conducted to analyze the change in VA.

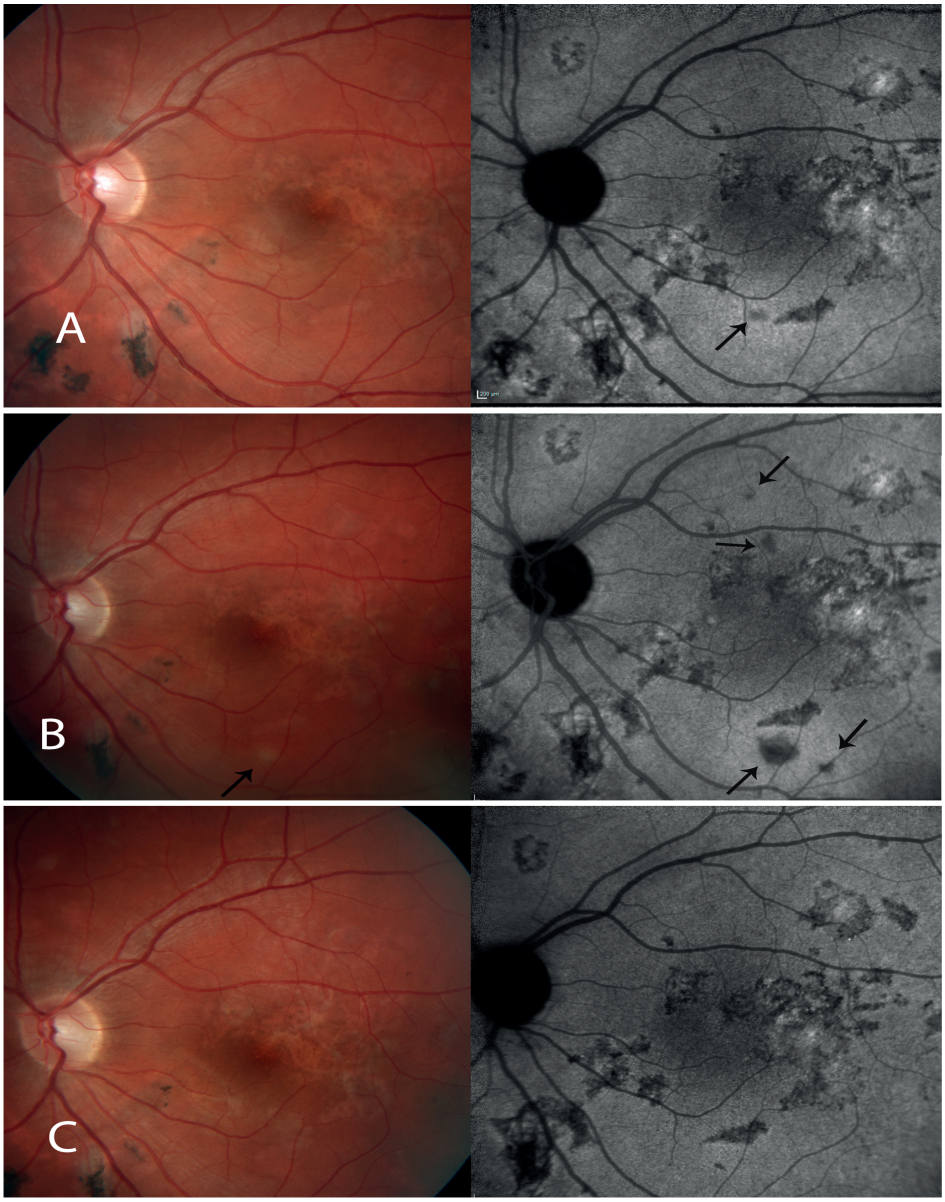

Figure 4.1 Case 6 presenting with a relapse of disease activity Indocyanine green (ICG) pictures at 30 minutes and fundus pictures taken **A + B**. before the start of adalimumab whilst treated with ciclosporin A 200mg, mycophenolate mofetil 2000mg and prednisolone 10mg daily and **C.** during treatment with adalimumab 40mg/2 weeks, mycophenolate mofetil 2000mg and prednisolone 7.5mg daily **A.** 4 months before the start of adalimumab with almost complete quiescent disease except for one spot of choroiditis (black arrow). **B.** One month before the start of adalimumab, ICG angiography shows a relapse of disease activity with multiple spots of choroiditis (black arrows) and the fundus image shows one white-yellowish lesion (black arrow). **C.** Eight months after the start of adalimumab, imaging shows complete remission of disease activity.

RESULTS

Baseline characteristics

Twelve patients (18 eyes) were included in this cohort study. The reason for starting adalimumab was treatment failure with conventional IMT in 10 patients and subjective side-effects experienced at sub-therapeutic doses of conventional IMT in 2 patients. All patients were treated with adalimumab (subcutaneously with a loading dose of 80mg, 40mg one week later and subsequently with 40mg every two weeks). The patient characteristics at the start of treatment with adalimumab are described in **Table 4.1**.

Table 4.1. Patient characteristics at the start of treatment with adalimumab

Patients (eyes)	12	(18)
Female gender, n (%)	10	(83)
Age in years, mean (range)	44.3	(22-74)
VA, mean of all eyes (range)	20/30	(20/125 – 20/17)
Refractive error of all eyes		
High myopia[a], n (%)	2	(11)
Mild to moderate myopia[b], n (%)	11	(61)
Hypermetropia, n (%)	5	(28)
CNV, n (%) of all eyes	5	(28)
Bilateral disease, n (%) of all patients	6	(50)

VA, visual acuity; D, dioptrics; CNV, choroidal neovascularization.
[a]High myopia: refractive error over -6D.
[b]Mild to moderate myopia: refractive error between 0 and -6D.

Visual acuity

The logMAR VA (Snellen equivalent) of the affected eyes did not change significantly during follow-up and was 0.17 (20/30) at the start of adalimumab and 0.18 (20/30) at 12 months follow-up.

Efficacy of adalimumab

In the 12 months before the start of adalimumab, all patients had at least two relapses of disease activity (median: 3 relapses, range 2–4). In the 12 months after the start of adalimumab, no subclinical or clinical relapse of disease activity was observed in 8/12 (67%) patients (**Table 4.2**; **Figure 4.2a**). Two patients experienced a single minor subclinical relapse of disease activity after the start of adalimumab, resulting in a temporary dose escalation to adalimumab weekly for one month in case 3 and a single bevacizumab injection in case 4. In an additional 2 cases symptomatic relapses of disease activity were observed despite treatment with adalimumab (**Table 4.2**). Case 12, although less severe than prior to the start of adalimumab, still experienced 2 relapses

of disease activity of the choroiditis. Case 10 presented with 3 relapses and adalimumab was considered ineffective and was stopped after 10 months. (**Table 4.2**). While treated with adalimumab, the systemic corticosteroids could be stopped in 9/12 (75%) patients. In 3 patients the systemic corticosteroids was not stopped 12 months after the start of adalimumab because of persistent disease activity (case 10 and 12) and on patient request despite disease inactivity (case 6). The mean daily dose of prednisolone was tapered from 17mg at the start of adalimumab to 2mg 12 months after the start of adalimumab (**Figure 4.2b**). This is in contrast to before the start of adalimumab where 9/12 (75%) of the patients experienced a relapse of disease activity whilst treated with prednisolone (mean daily dose: 13 mg range 5–25mg). The remaining 3 patients experienced a relapse of disease activity after tapering the prednisolone completely (**Table 4.2**).

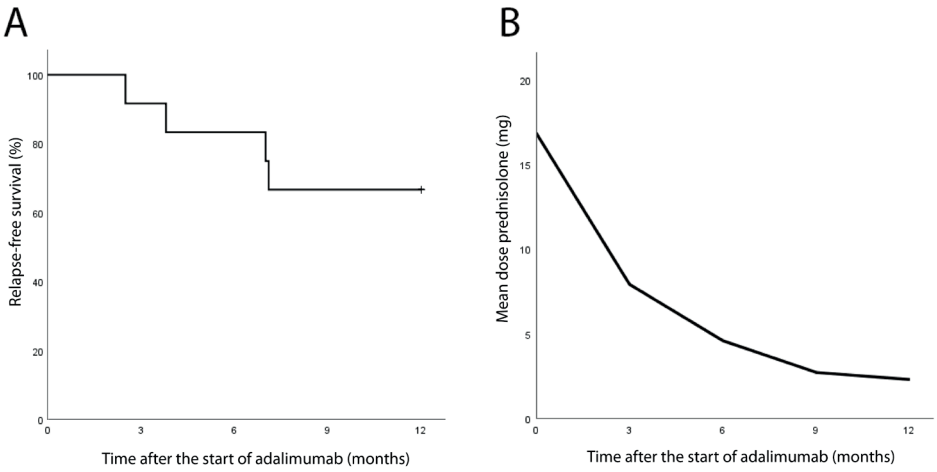

Figure 4.2 Efficacy of adalimumab **2A.** The relapse-free survival is presented as a percentage of the patients during the first 12 months of follow-up after the start of adalimumab. **2B.** The mean dose of prednisolone is presented at the start of adalimumab, and after 3, 6, 9 and 12 months of follow-up.

IMT

Patients were concomitant treated with IMT for the synergistic effect and to avoid the formation of antibodies against adalimumab. A dose reduction of ≥50% of the conventional IMT was achieved in 6/12 (50%) patients 12 months after the start of adalimumab.

Intravitreal anti-VEGF injections

In the 5 eyes with CNV, the treatment with intravitreal anti-VEGF injections could be extended and stopped after the start of adalimumab.

Table 4.2. Overview of treatment with adalimumab, conventional IMT, corticosteroids and anti-VEGF injections

			12 months before start of adalimumab				12 months after start of adalimumab			
Case/ age	**Diagnosis**	**Eye**	IMT[a]	Relapses	Pred-nisolone (mg)[b]	Anti-VEGF injections	IMT	Relapses	Pred-nisolone (mg)[c]	Anti-VEGF injections
1/23	Idiopathic MFC	OS	MMF	2[d]	5	0	MMF	0	0	0
2/44	Idiopathic MFC (CNV+)	OS	MPA, CsA	2	0	0	MTX	0	0	0
3/45	Idiopathic MFC (CNV+)	OD	MMF, CsA, MTX	3	0	1	AZA	1[e]	0	0
4/46	Idiopathic MFC (CNV+)	OD	MTX, AZA, MMF	3	0	5	MMF	1[f]	0	2[g]
5/22	Idiopathic MFC (CNV+)	OD	AZA+CsA, MMF+CsA	2	10	8	MPA	0	0	2[g]
6/23	Idiopathic MFC	ODS	AZA, MMF, MMF+CsA	3	10	0	MMF	0	7.5	0
7/54	Idiopathic MFC	ODS	MTX	3[d]	25	0	AZA	0	0	0
8/22	PIC (CNV+)	OS	AZA, MMF	3[d]	17.5	10	MMF	0	0	0
9/64	Serpiginous-like choroiditis	ODS	MMF, CP[h], AZA, MTX, MTX+CsA	4	20	1[i]	None[j]	0	0	0
10/74	Serpiginous-like choroiditis	ODS	MMF	2[d]	10	0	MMF	3	15	3[g]
11/66	Persistent placoid maculopathy	ODS	MTX, MPA, MPA+CsA MPA+MTX	2	10	0	MPA	0	0	0
12/48	Persistent placoid maculopathy	ODS	MMF, CP	3	15	0	MTX	2	7.5	0

IMT, corticosteroid-sparing immunomodulatory therapy; VEGF, vascular endothelial growth factor; MFC, multifocal choroiditis; MMF, mycophenolate mofetil; CNV, choroidal neovascularization; MPA; mycophenolic acid; CsA, ciclosporin A; MTX, methotrexate; AZA, azathioprine; CP, cyclophosphamide.

[a] All corticosteroid-sparing agents administered in the UMC Utrecht before the start of adalimumab. [b] Dose of prednisone in mg at the time a relapse of disease activity occurred. The highest dose is mentioned in case of multiple relapses. [c] Dose of prednisone in mg at 12 months after the start of adalimumab. [d] Less than 12 months of follow-up were present prior to the start of adalimumab. For case 1 and 8, 11 months of follow-up was present, for case 10 this was 5 months and for case 7 this was 7 months. [e] Due to a subclinical relapse of choroiditis 7 months after the start of adalimumab, the dose of adalimumab was temporarily increased to 40mg weekly for one month. [f] Subclinical activity of CNV 2.5 months after the start of adalimumab, treated with a single anti-VEGF injection. [g] In case 4 and 5, two anti-VEGF injections were administered within 3 months after the start of adalimumab as part of a treat and extent strategy. Case 10 was suspected for the development of CNV 9 months after the start of adalimumab though in retrospect this was not confirmed. [h] Intravenously administration of 750 mg/m2 per dose. A total of 6 doses were administered. [i] A single prophylactic anti-VEGF injection was administered without the development of CNV. [j] Patient discontinued conventional immunosuppressive agent, on its own initiative, due to side-effects.

Side effects of adalimumab

In general, treatment with adalimumab was well tolerated. Case 9 and 12 were treated with monthly cyclophosphamide infusions for 6 months just before the start of adalimumab. Case 9 developed a pneumocystis jiroveci pneumonia and urosepsis within 2 months and case 12 a perforated diverticulitis within 3.5 months after the start of adalimumab. In both cases there was no direct relation between the adverse events and treatment with adalimumab.

DISCUSSION

We report that in the majority of the patients with cMFC, no clinical relapse of disease activity occurred in the 12 months after the start of adalimumab. Moreover, in the majority of the patients, adalimumab had a steroid sparing effect. In particular, the younger patients with idiopathic MFC and PIC, frequently with pre-existent CNV, responded fast and well to adalimumab. On the contrary, the four patients diagnosed with persistent placoid maculopathy and serpiginous-like choroiditis without CNV, who were somewhat older, responded less well.

Treatment with conventional IMT is supported by a few studies and in our experience, it has shown to be effective in the majority of the patients.[9,15,16] Nevertheless, a minority of the patients continue to endure sight-threatening relapses of disease activity despite treatment with adequately dosed conventional immunosuppressive agents. These patients remain steroid-dependent often requiring a dose of corticosteroids above the safety dose of 7.5 mg prednisolone daily.[14] Due to the negative long-term effects of low-dose prednisolone, steroid dependency is considered to be an indication for additional immunomodulating treatment including biologicals such as adalimumab. The efficacy of adalimumab in patients with cMFC is not well described. A few case reports and small case series are available evaluating the safety and efficacy of adalimumab in serpiginous choroiditis,[22-24] persistent placoid chorioretinitis[25] and MFC in combination with acute zonal occult outer retinopathy.[26] None of these studies included patients with PIC or idiopathic multifocal choroiditis. In most cases, though not all, adalimumab was reported to be effective, which is in line with the results of our study. All patients were concomitantly treated with IMT for synergistic effect as well as prohibition of the formation of anti-drug antibodies to adalimumab, though literature is conflicting concerning the latter indication.[27]

In our study, intravitreal anti-VEGF injections were extended and discontinued after the initiation of treatment with adalimumab. We hypothesize that chronic or recurrent

inflammatory activity in the choroid is a trigger for ongoing or new choroidal neovascular activity, requiring intravitreal anti-VEGF injections.[3,4] Removing the inflammatory trigger is, in our opinion, a prerequisite to be able to permanently discontinue intravitreal anti-VEGF therapy in cMFC subtypes that are accompanied by CNVs.

Drawbacks of the current study were its retrospective nature and the low number of patients. We performed a within-patient study (i.e. longitudinal assessment) without the use of a control group to avoid the risk of a selection bias.

Strengths of our study are the homogeneous study population with standard treatment of 40mg adalimumab every two weeks with a standard follow-up of 12 months. Secondly, because of the lack of evidence in literature on the efficacy of adalimumab in cMFC, a relatively rare disease, the current series, though small, can be informative for ophthalmologist treating this potentially blinding disease in young patients. Thirdly, since relapses of choroiditis and CNV are often subtle and subject to subjective interpretation, imaging results were evaluated by two independent ophthalmologists. Eye-tracking technology in the OCT ensured an accurate assessment of changes in the outer retina, subretinal space and choroidal thickness.

In conclusion, adalimumab is potentially an effective treatment in patients with cMFC, in whom treatment with conventional IMT failed due to ineffectiveness or side effects.

REFERENCES

1. Ahnood D, Madhusudhan S, Tsaloumas MD, Waheed NK, Keane PA, Denniston AK. Punctate inner choroidopathy: A review. Surv Ophthalmol. 2017;62(2):113-126.
2. Fung AT, Pal S, Yannuzzi NA, et al. Multifocal choroiditis without panuveitis; Clinical Characteristics and Progression. Retina. 2014;34(1):98-107.
3. Agarwal A, Invernizzi A, Singh RB, et al. An update on inflammatory choroidal neovascularization: epidemiology, multimodal imaging, and management. J Ophthalmic Inflamm Infect. 2018;8(1):13.
4. Dhingra N, Kelly S, Majid MA, Bailey CB, Dick AD. Inflammatory choroidal neovascular membrane in posterior uveitis-pathogenesis and treatment. Indian J Ophthalmol. 2010;58(1):3-10.
5. Ferrara DC, Takahashi BS, Yannuzzi LA, et al. Analysis of major alleles associated with age-related macular degeneration in patients with multifocal choroiditis: Strong association with complement factor H. Arch Ophthalmol. 2008;126(11):1562-1566.
6. Atan D, Fraser-Bell S, Plskova J, et al. Punctate Inner choroidopathy and multifocal choroiditis with panuveitis share haplotypic associations with IL10 and TNF loci. Investig Ophthalmol Vis Sci. 2011;52(6):3573-3581.
7. Leung TG, Moradi A, Liu D, et al. Clinical features and incidence rate of ocular complications in punctate inner choroidopathy. Retina. 2014;34(8):1666-1674.
8. Niederer RL, Gilbert R, Lightman SL, Tomkins-Netzer O. Risk Factors for Developing Choroidal Neovascular Membrane and Visual Loss in Punctate Inner Choroidopathy. Ophthalmology. 2018;125(2):288-294.
9. Turkcuoglu P, Chang PY, Rentiya ZS, et al. Mycophenolate mofetil and fundus autofluorescence in the management of recurrent punctate inner choroidopathy. Ocul Immunol Inflamm. 2011;19(4):286-292.
10. Galor A, Jabs DA, Leder HA, et al. Comparison of Antimetabolite Drugs as Corticosteroid-Sparing Therapy for Noninfectious Ocular Inflammation. Ophthalmology. 2008;115(10):1826-1832.
11. Uraki T, Namba K, Mizuuchi K, et al. Cyclosporine and prednisolone combination therapy as a potential therapeutic strategy for relentless placoid chorioretinitis. Am J Ophthalmol Case Reports. 2019;14:87-91.
12. Dick AD, Rosenbaum JT, Al-Dhibi HA, et al. Guidance on Noncorticosteroid Systemic Immunomodulatory Therapy in Noninfectious Uveitis: Fundamentals Of Care for UveitiS (FOCUS) Initiative. Ophthalmology. 2018;125(5):757-773.
13. Jabs DA, Rosenbaum JT, Foster CS, et al. Guidelines for the use of immunosuppressive drugs in patients with ocular inflammatory disorders: Recommendations of an expert panel. Am J Ophthalmol. 2000;130(4):492-513.
14. Jabs DA. Immunosuppression for the Uveitides. Ophthalmology. 2018;125(2):193-202.
15. Goldberg NR, Lyu T, Moshier E, Godbold J, Jabs DA. Success with single-agent immunosuppression for multifocal choroidopathies. Am J Ophthalmol. 2014;158(6):1310-1317.
16. de Groot EL, ten Dam-van Loon NH, de Boer JH, Ossewaarde-van Norel J. The efficacy of corticosteroid-sparing immunomodulatory therapy in treating patients with central multifocal choroiditis. Acta Ophthalmol. 2020;98(8):816-821.
17. Suhler EB, Adán A, Brézin AP, et al. Safety and Efficacy of Adalimumab in Patients with Noninfectious Uveitis in an Ongoing Open-Label Study: VISUAL III. Ophthalmology. 2018;125:1075-1087.
18. Nguyen QD, Merrill PT, Jaffe GJ, et al. Adalimumab for prevention of uveitic flare in patients with inactive non-infectious uveitis controlled by corticosteroids (VISUAL II): a multicentre, double-masked, randomised, placebo-controlled phase 3 trial. Lancet. 2016;388:1183-1192.

19. LaMattina KC, Goldstein DA. Adalimumab for the treatment of uveitis. Expert Rev Clin Immunol. 2017;13(3):181-188.
20. Nussenblatt RB, Palestine AG, Chan CC, Roberge F. Standardizatlon of Vitreal inflammatory Activity in Intermediate and Posterior Uveitis. Ophthalmology. 1985;92(4):467-471.
21. Jabs DA, Nussenblatt RB, Rosenbaum JT, et al. Standardization of uveitis nomenclature for reporting clinical data. Results of the first international workshop. Am J Ophthalmol. 2005;140(3):509-516.
22. Noda K, Oishi A, Uji A, Tanaka S, Tsujikawa A. Limited efficacy of adalimumab in the acute phase of serpiginous choroiditis refractory to corticosteroid and cyclosporine, a case report. BMC Ophthalmol. 2019;19:95.
23. Chinchurreta Capote A, Requena Jiménez JM, Lorenzo Soto M, Romero Gómez C, García De Lucas MD. Effectiveness of adalimumab for refractory serpiginous choroiditis. Ocul Immunol Inflamm. 2014;22(5):405-408.
24. Llorenç V, Molins B, Rey A, Mesquida M, Adán A. Adalimumab in serpiginous choroiditis. Ocul Immunol Inflamm. 2013;21(3):237-240.
25. Asano S, Tanaka R, Kawashima H, Kaburaki T. Relentless Placoid Chorioretinitis: A Case Series of Successful Tapering of Systemic Immunosuppressants Achieved with Adalimumab. Case Rep Ophthalmol. 2019;10:145-152.
26. Neri P, Ricci F, Giovannini A, et al. Successful treatment of an overlapping choriocapillaritis between multifocal choroiditis and acute zonal occult outer retinopathy (AZOOR) with adalimumab (HumiraTM). Int Ophthalmol. 2014;34(2):359-364.
27. Qiu Y, Mao R, Chen B li, et al. Effects of Combination Therapy With Immunomodulators on Trough Levels and Antibodies Against Tumor Necrosis Factor Antagonists in Patients With Inflammatory Bowel Disease: A Meta-analysis. Clin Gastroenterol Hepatol. 2017;15(9):1359-1372.e6.

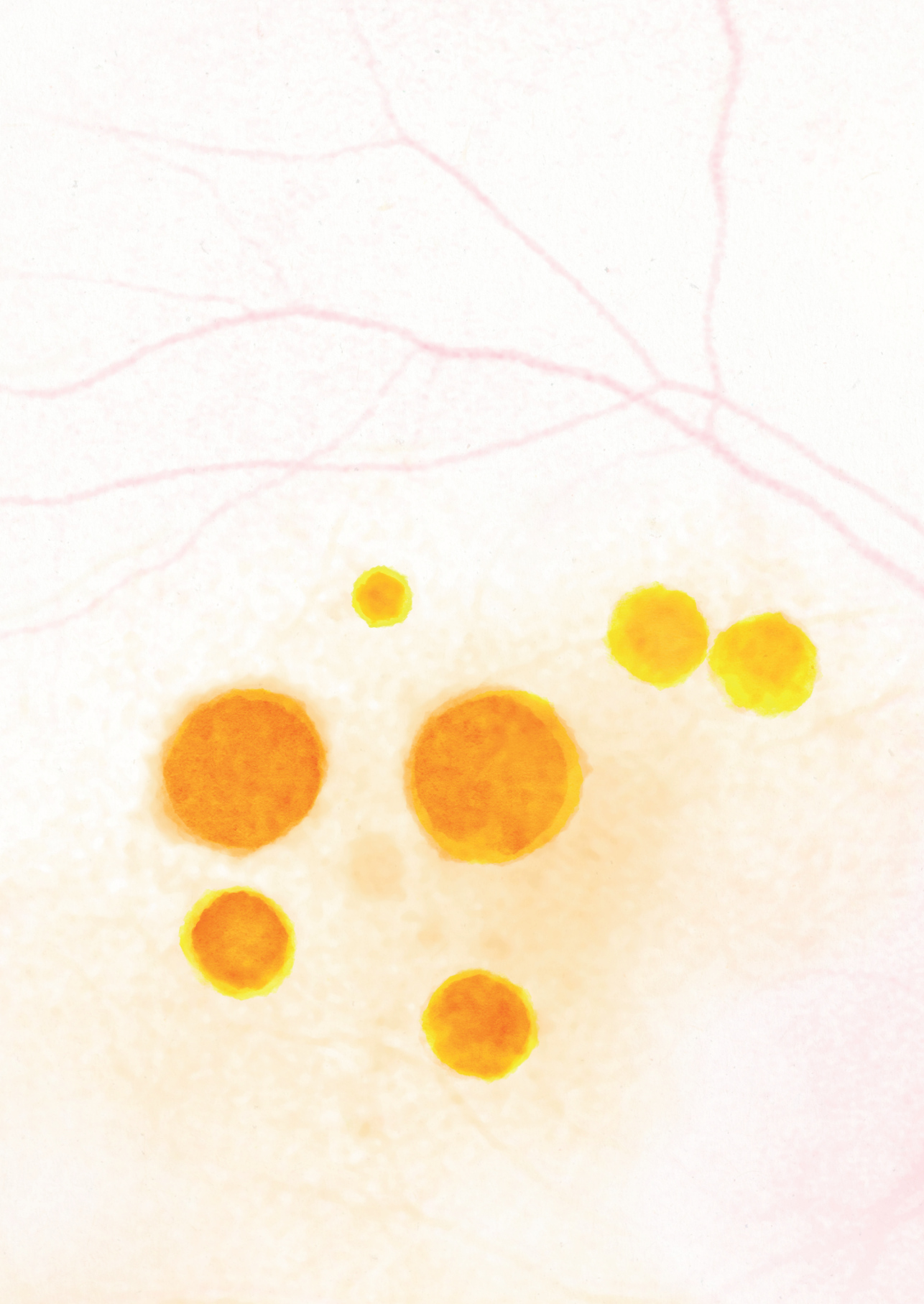

Chapter 5

Idiopathic multifocal choroiditis and punctate inner choroidopathy: an evaluation in pregnancy

Evianne L. de Groot
Ramon A. C. van Huet
Kitty W. M. Bloemenkamp
Joke H. de Boer
Jeannette Ossewaarde-van Norel

Acta Ophthalmol. 2022;100(1):82-88. doi: 10.1111/aos.14898

ABSTRACT

Purpose

To evaluate the clinical course of idiopathic multifocal choroiditis (MFC) and punctate inner choroidopathy (PIC) and the efficacy and safety of treatment options during pregnancy.

Methods

Patients with MFC or PIC and a pregnancy in 2011-2019 from two academic centres were enrolled. For the most recent pregnancy, data on best-corrected visual acuity (BCVA) before and after pregnancy, relapse rate in pregnancy and postpartum period and obstetric, maternal and neonatal outcomes were collected. Treatment regimens consisted of a wait-and-see regime and an immunosuppressive treatment regime with systemic corticosteroids and/or azathioprine, both combined with intravitreal antivascular endothelial growth factor injections when indicated.

Results

Sixteen women (26 affected eyes) were included. Median Snellen BCVA was 20/19 before pregnancy and 20/18 after delivery. In seven pregnancies a wait-and-see regime and in nine pregnancies an immunosuppressive treatment regime was carried out. Fourteen intravitreal anti-VEGF injections were given in six pregnancies. The relapse rate during pregnancy was 44% and in the postpartum period 31%. Maternal/obstetrical and fetal complications occurred in 31% and 13% of the pregnancies, respectively. Fifteen healthy children were born and one pregnancy ended in a stillbirth in a patient with a complicated obstetrical history. One patient treated with azathioprine developed intrahepatic cholestasis of pregnancy (ICP).

Conclusions

Among women with MFC and PIC BCVA remained stable during pregnancy despite a relapse rate of 44% in pregnancy. No major maternal, obstetric and fetal complications occurred in pregnant patients treated with systemic corticosteroids, azathioprine or intravitreal anti-VEGF injections, though one patient developed ICP while treated with azathioprine.

INTRODUCTION

Idiopathic multifocal choroiditis (MFC) and punctate inner choroidopathy (PIC) are rare types of noninfectious posterior uveitis within the spectrum of white dot syndromes. Both MFC and PIC are characterized by a relapsing inflammatory activity in the choroid in the posterior pole resulting in multiple chorioretinal scars within the temporal vascular arcades. The disease predominantly affects young women with myopia often in their reproductive years.[1] Inflammation, even without symptoms, is thought to trigger the development and reactivation of choroidal neovascularization (CNV), which is considered the most frequent complication in MFC and PIC.[2,3] CNV demands treatment with intravitreal antivascular endothelial growth factor (VEGF) injections to minimize irreversible retinal damage. There are two viewpoints on how the inflammatory component in MFC and PIC can best be treated. The first treatment strategy is based on the wait-and-see principle, where patients are only treated in case of active choroidal inflammation for a relatively short period with periocular, intraocular or systemic corticosteroids. The second treatment strategy is focused on a continuous suppression of the immune system with disease-modifying antirheumatic drugs (DMARDs), if necessary in combination with systemic corticosteroids, sometimes biologicals are used. As a result, the number of relapses of inflammation and reactivation of CNV is proposed to decline.[4-6]

Pregnancy is well known to be associated with numeral immunological and hormonal changes, favouring the maternal tolerance of the fetus.[7,8] Most studies regarding noninfectious uveitis demonstrate a decline of disease activity during the second and third trimester of pregnancy with an increase in the relapse rate within the first 6 months postpartum to the prepregnancy situation.[9-12] However, these studies did not specifically investigate patients with MFC and PIC, but noninfectious uveitis in general. Since anti-VEGF is considered to be potentially teratogenic and embryo-fetotoxic, treatment with intravitreal anti-VEGF injections is advised to be avoided in pregnancy, especially in the first trimester.[13-15] Therefore, it is of utmost importance to prohibit the development or reactivation of CNV during pregnancy in patients with MFC and PIC. Treatment with azathioprine (AZA), a steroid-sparing immunomodulatory agent, is recognized to be safe in pregnancy though complications have been described.[16] Therefore, whether or not a patient is treated with AZA during pregnancy, is a shared decision of the ophthalmologist, the obstetrician and the patient. Due to the rarity of the disease, and the fact that pregnant women are excluded from medication trials for several reasons,[17] literature is scarce regarding different treatment options for MFC and PIC during pregnancy. A few case series have been described for the different treatment options, varying from treatment with intravitreal anti-VEGF injections, corticosteroid

therapy and an observational approach.[15,18,19] This retrospective cohort study aims to contribute to the knowledge concerning the course of MFC and PIC during pregnancy and the postpartum period and to evaluate different treatment options for pregnant women.

PATIENTS AND METHODS

For this retrospective multicentre cohort study, patients treated in two tertiary academic centres (the University Medical Center Utrecht, Utrecht, the Netherlands, and the Radboud University Medical Center, Nijmegen, the Netherlands) were included. This study received institutional review board approval from both the University Medical Center Utrecht and the Radboud University Medical Center and was performed in accordance with the tenets of the Declaration of Helsinki regarding research involving human subjects. All participants provided written informed consent.

Study participants

Patients with PIC were included as well as patients with MFC in case they presented with chorioretinal scars within the temporal vascular arcades without other signs of ocular inflammation, including no vasculitis, no papillitis and no cells in the anterior chamber or vitreous. The diagnosis of PIC was made in patients with chorioretinal scars situated exclusively within the temporal vascular arcades. In case patients had chorioretinal scars both within and outside the temporal vascular arcades, the diagnosis of MFC was made. Other frequent causes of posterior uveitis including tuberculosis and sarcoidosis were ruled out, as well as Birdshot chorioretinopathy. Patients with MFC and PIC, who were pregnant between 2011 and 2019, were included.

Data collection

Data were distracted from the medical records for the period between 12 months before pregnancy and 6 months after delivery. In case of multiple pregnancies, only the most recent pregnancy was included. Collected data consisted of maternal, fetal and neonatal variables, ophthalmic information before, during and after pregnancy (best-corrected visual acuity (BCVA), number of relapses of disease activity), imaging results on the Heidelberg Spectralis® (Heidelberg engineering, Heidelberg, Germany) including spectral domain optical coherence tomography (SD-OCT) and fluorescein and indocyanine angiography (FA-ICGA) and information regarding treatment regimens. Treatment regimens were divided into a wait-and-see regime and an immunosuppressive treatment regime consisting of treatment with systemic corticosteroids and/or azathioprine. In both treatment regimens, patients with a relapse of disease activity during pregnancy

were generally treated with intravitreal anti-VEGF injections in case of secondary CNV, after careful consideration of the risks for the fetus versus the benefits for the patient, and/or periocular or intravitreal corticosteroid injections in case of active inflammation.

Outcome measures

To evaluate disease activity during pregnancy, we analysed whether a relapse of disease activity occurred before pregnancy, during pregnancy or in the postpartum period. A relapse of disease activity was defined as either the development of new choroidal inflammatory lesions or new CNV, or the growth of pre-existent choroidal scars due to choroidal inflammation or reactivation of CNV after previously inactive disease confirmed by imaging (SD-OCT and if available FA-ICGA). In case of a relapse of disease activity, the fetus's gestational age in weeks and initiated treatment were points of interest.

To evaluate the efficacy and safety of different treatment regimens in pregnancy, the main outcome measures were the BCVA of the mother before and after pregnancy as well as maternal, fetal and obstetrical complications during the pregnancy and postpartum period. The characteristics and clinical outcomes examined for women with MFC and PIC were maternal age and obstetrical complications including gestational diabetes, gestational hypertension, intrahepatic cholestasis of pregnancy (ICP), delivery before 37 weeks[20] and mode of delivery, including caesarean section for ophthalmic indication. Evaluated maternal ocular complications included elevated intraocular pressure, cataract and subretinal bleeding of CNV induced by Valsalva manoeuvre during labour. Evaluated fetal complications were miscarriages, birth defects, still birth, birth weight <2500 g,[21] early-onset neonatal sepsis and neonatal hypoglycaemia.

Best-corrected visual acuity was recorded in Snellen values. Best-corrected visual acuity was converted to LogMAR (logarithm of the minimum angle of resolution) values in order to perform the Wilcoxon signed-rank test and patients were case-wise excluded when data were missing. A p-value <0.05 was considered significant.

RESULTS

Study participants

Sixteen women (26 affected eyes) with MFC (n = 9) and PIC (n = 7) with a pregnancy between 2011 and 2019 were identified. The median age at the start of the pregnancy was 35 years (range 24–41). Bilateral disease was present in 10/16 women (63%), and 11/16 women (69%) had developed the complication of CNV at any point before the start of pregnancy. In seven patients a wait-and-see regime was carried out, and nine patients

received immunosuppressive treatment during pregnancy. Immunosuppressive treatment consisted of low-to-medium-dose oral corticosteroids in three patients, azathioprine in one patient and a combination of low-to-medium-dose corticosteroids and azathioprine in the remaining five patients. All patients treated with azathioprine received weight-based doses varying between 100 and 200 mg/day (**Table 5.1**). In advance, an alternative DMARD such as mycophenolate mofetil or methotrexate was switched to azathioprine because of the wish to become pregnant in three patients (**Table 5.2**).

Relapse during pregnancy and postpartum period

The number of relapses in the 12 months prior to pregnancy, during pregnancy and postpartum period are demonstrated in **Table 5.2**. **Figure 5.1** illustrates an example of a case with relapses of disease activity during pregnancy and in the postpartum period. The percentage of patients with relapse-free survival over the time course of 40 weeks after conception is demonstrated in **Figure 5.2A**. In 7/16 pregnancies (44%), a relapse of disease activity occurred, demanding for prompt treatment. When analysing the treatment regimens separately, in 3/9 (33%) pregnancies with patients receiving an immunosuppressive treatment regime and in 4/7 (57%) of the pregnancies with patients receiving a wait-and-see regime, a relapse of disease activity was observed (**Table 5.2, Figure 5.2B**). In 5/16 (31%) pregnancies, a relapse of disease activity occurred in the postpartum period, though in two pregnancies no complete follow-up of 6 months was available (**Table 5.2**).

Intravitreal anti-VEGF injections in pregnancy

A total number of 14 intravitreal anti-VEGF injections were given in six pregnancies. Thirteen intravitreal anti-VEGF injections with ranibizumab and one intravitreal injection with bevacizumab were administered. In general, intravitreal anti-VEGF injections were not given in the first trimester except for one patient. In this case, the shared decision was made to continue treatment with intravitreal anti-VEGF injections in the first trimester to preserve vision despite the pregnancy (**Table 5.1**).

Visual acuity

Best-corrected visual acuity prior to pregnancy and after delivery was available for 13 pregnancies (20 eyes). The median Snellen BCVA measured in the visit prior to the start of pregnancy was 20/19. This is not significantly different from the median Snellen BCVA of 20/18 measured in the first consult after delivery (**Table 5.3**). When evaluating both treatment regimens separately, no significant difference was observed (wait-and-see regime $p = 0.78$, immunosuppressive treatment $p = 0.58$).

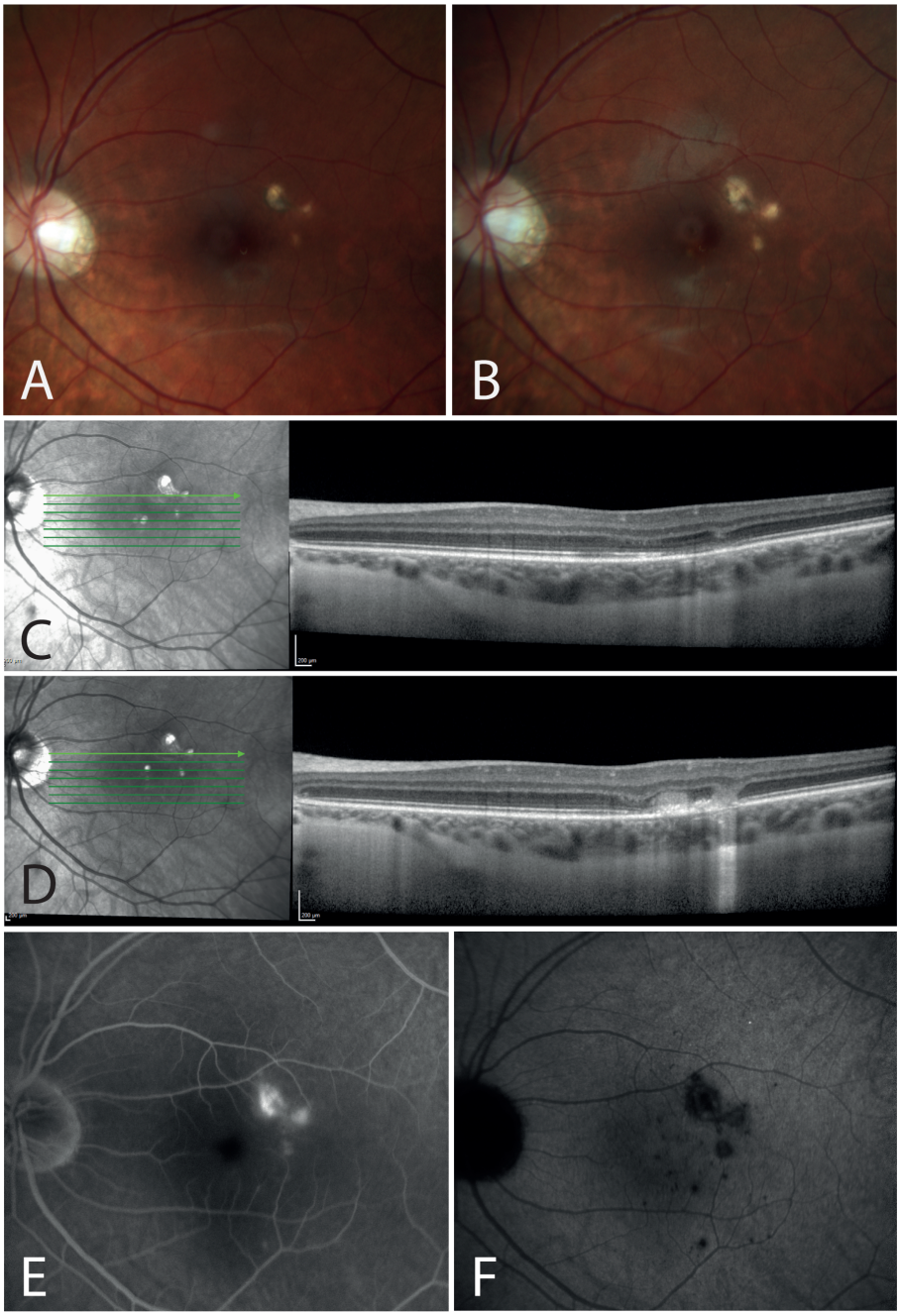

Figure 5.1 Disease activity in pregnancy and postpartum period in case 8. (**A, B**) Colour fundus pictures taken at gestational age (GA) of 5 weeks (**A**) and 11 weeks postpartum (B) showing growth of central choroidal lesions during pregnancy and the postpartum period. (**C, D**) Optical coherence tomography scans on the Heidelberg Spectralis® with eye-tracker function. (**C**) No disease activity at GA 10 weeks. (**D**) A relapse of disease activity at GA of 20 weeks. (**E, F**) A relapse of disease activity at 11 weeks postpartum. Fluorescein (**E**) and indocyanine green (**F**) pictures at 20 min showing (**E**) leakage of active CNV and (**F**) dark choroidal lesions with blurred boundaries indicating inflammatory activity.

Table 5.1. Maternal, obstetrical and fetal complications during pregnancy and postpartum period including initiated medical treatment in pregnancy

		Medical treatment in pregnancy in mg (GA in weeks)				Complications during pregnancy and 6 months postpartum	
Case	*Diagnose*	*DMARD*	*Systemic corticosteroids (prednisolone)*[a]	*Subconjunctival (SC)/ intravitreal injection (IVI) TA*	*Anti-VEGF intravitreal injection*	*Maternal and obstetrical complications*	*Fetal complications*
1	MFC	AZA 150	7,5	-	-	None	None
2	PIC	AZA 100	7,5-12,5	-	-	Gestational hypertension + diabetes[b]	None
3	PIC	AZA 100	17,5-20	TA SC (8)[c]	-	None	None
4	MFC	AZA 200	20	-	RZB (5, 11, 20, 25, 30)	Placental abruption	Intrauterine fetal death[d]
5	MFC	AZA 125	10	-	-	Intrahepatic cholestasis	Late preterm birth+LBW[e]
6	MFC	-	10	-	-	None	None
7	PIC	AZA 100	-	-	-	None	None
8	MFC	-	5-15	TA IVI (20)	RZB (30, 37)	Elevated IOP	None
9	MFC	-	7.5-12,5	TA SC (6) TA IVI (9+13)	-	None	None
10	MFC	-	-	TA IVI (24)	½ RZB[f] (32) 1 RZB (36)	None	None
11	PIC	-	-	TA IVI (33)	RZB (33+37)	None	None
12	PIC	-	-	-	RZB (27)	None	None
13	PIC	-	-	-	BVZ (2) RZB (20)	C-section[g]	None
14	MFC	-	-	-	-	None[h]	None[h]
15	PIC	-	-	-	-	None	None
16	MFC	-	-	-	-	None[h]	None[h]

GA, gestational age; DMARD, disease-modifying antirheumatic drug; TA, triamcinolone acetonide; VEGF, vascular endothelial growth factor; MFC, idiopathic multifocal choroiditis; PIC, punctate inner choroidopathy; AZA, azathioprine; RZB, ranibizumab; LBW, low birth weight; NA, not available; IOP, intraocular pressure; C-section, caesarean section; BVZ, bevacizumab.

[a] The minimum and maximum dose of prednisolone during pregnancy.

[b] Two months prior to the start of the pregnancy, the weight of the patient was 110kg (243 LBS).

[c] Subjective relapse of disease activity. After subconjunctival TA complaints did not improve and a relapse of disease activity was never objectified.

[d] Intrauterine fetal death at a gestational age of 33 weeks due to a placental abruption. Obstetrical history of multiple miscarriages and 2 intrauterine fetal deaths, all prior to the diagnosis of MFC. Histopathology of the three placentas of the stillborn children demonstrated similar abnormalities with unknown origin.

[e] Late preterm birth at GA 36+6 with a low birth weight of 2240 grams.

[f] In consultation with the patient and the partner of the patient, the shared decision was made to administer ½ a dose of ranibizumab at GA of 32 weeks.

[g] Ophthalmic indication for cesarean section due to active choroidal neovascularization with risk of bleeding.

[h] No complete follow-up of six months is available in the postpartum period (case 14 has 5,5 months of follow-up and case 16 has 4 months of follow-up).

Table 5.2. Summary of the number of relapses of disease activity in the 12 months before pregnancy, during pregnancy and in the postpartum period

	12 months before pregnancy			During pregnancy			6 months postpartum
Case	Systemic CS[a]	DMARD	Relapses	Systemic CS[a]	DMARD	Relapses (GA)	Relapses
1	+	MMF → AZA	0	+	AZA	0	1 (24)
2	+/-	-	1	+	AZA	0	0
3	+/-	MMF → AZA	2	+	AZA	0	0
4	+/-	MMF → MTX → AZA	1	+	AZA	1 (5)[b]	0
5	+	AZA	0	+	AZA	0	0
6	+/-	-	1	+	-	0	1 (26)
7	+/-	AZA[c]	1	-	AZA	0	0
8	NA[d]	NA[d]	NA[d]	+	-	1 (20)[b]	1 (11)
9	+/-	MMF → AZA[e]	1	+	-	1 (6)[b]	0
10	-	-	1	-	-	2 (24 + 32)	0
11	NA[d]	NA[d]	NA[4]	-	-	1 (33)	0
12	-	-	0	-	-	1 (27)	0
13	NA[d]	NA[d]	NA[4]	-	-	2 (9 + 20)	0
14	-	-	0	-	-	0	1 (6)[f]
15	-	-	0	-	-	0	2 (3 + 20)
16	-	-	1	-	-	0	0[f]

CS, corticosteroids; DMARD, disease-modifying antirheumatic drug; GA, gestational age; MMF, mycophenolate mofetil; MTX, methotrexate; AZA, azathioprine; NA, not available.

[a] Treatment with systemic corticosteroids: maintenance dose of prednisolone (+), prednisolone in tapering schedule (+/-), no prednisolone (-)

[b] A relapse of disease activity occurred while treated with prednisolone. At the time of a relapse of disease activity, the doses were 20mg (case 4), 15mg (case 8) and 7,5mg (case 9).

[c] Azathioprine was started 5 months prior to pregnancy.

[d] No information was present concerning the period before pregnancy. Case 8 was referred to the UMCU Utrecht at GA of 5 weeks, case 13 was referred to the Radboud UMC at GA of 9 weeks and case 11 presented for the first time with symptoms during the third trimester of pregnancy.

[e] Azathioprine was discontinued prior to the start of the pregnancy due to intolerance (elevated liver enzymes).

[f] No complete follow-up of six months is available in the postpartum period (case 14 has 5,5 months of follow-up and case 16 has 4 months of follow-up).

Maternal, obstetric and fetal outcomes

A total of 16 pregnancies resulted in the birth of 15 healthy children. Maternal/obstetrical complications occurred in 5/16 (31%) pregnancies. One patient developed an elevated intraocular pressure following an intravitreal corticosteroid injection. Nonocular complications included a placental abruption in one patient, gestational hypertension and diabetes in one patient and ICP in one patient. Moreover, in one patient an elective caesarean section was performed because of an active CNV with increased risk of subretinal bleeding during Valsalva manoeuvre (**Table 5.1**). Fetal complications occurred in 2/16 (13%) of the unborn children. One pregnancy resulted in a stillbirth at a gestational age of 33 weeks due to a placental abruption and one infant was born late

preterm with a birth weight of 2240 g but was otherwise healthy. None of the infants had birth defects or suffered from complications in the neonatal period (**Table 5.1**).

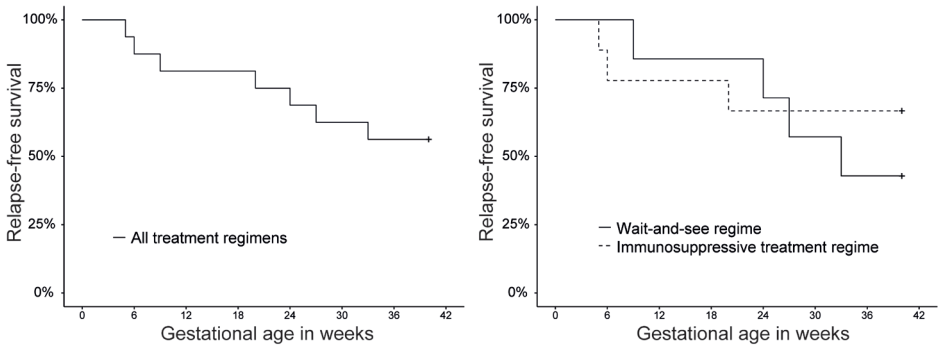

Figure 5.2 Relapse-free survival during pregnancy. (**A**) Demonstrates the relapse-free survival during pregnancy of all treatment regimens. (**B**) Demonstrates the relapse-free survival during pregnancy split out in treatment regimens. The continuing line represents the patients treated with a wait-and-see regime, the dashed line represents the patients treated with an immunosuppressive treatment regime with systemic corticosteroids and/or azathioprine.

Table 5.3. Summary of visual functioning before pregnancy and after delivery of 20 eyes[a]

	Before pregnancy		After delivery		*P*-value
	Median	(range)	Median	(range)	
LogMAR BCVA	-0.02	(-0.15-1.30)	-0.04	(-0.18-1.78)	0.86[b]
Snellen BCVA	20/19	(20/14-20/400)	20/18	(20/13-20/1200)	NA
Time to consult in weeks[c]	4	(0-25)	8	(2-15)	NA

BCVA, best-corrected visual acuity; NA, not applicable.

[a] Missing data prior to pregnancy for 6 eyes

[b] Wilcoxon signed-rank test

[c] The time in weeks between the moment of evaluation of BCVA prior to the start of pregnancy and after delivery

DISCUSSION

In this study, we report that in 44% of the pregnancies a relapse of disease activity occurred demanding for prompt treatment. Remarkable was the higher relapse rate in the women with a wait-and-see regime compared to the women with an immunosuppressive treatment regime, though due to the small number of patients no direct conclusions can be drawn from this observation. Despite these relapses of disease activity, the median BCVA remained stable throughout the pregnancy and no difference was observed between treatment regimens. Surprisingly, a considerable proportion of the relapses of disease activity occurred in the third trimester of pregnancy whereas most studies regarding uveitis in general, report a decline in uveitis activity in the second and third trimester.[9-11]

We report that none of the infants had birth defects and the majority of the children were healthy term infants. The reported rate of the different maternal, obstetrical and fetal complications does not seem notably higher than the overall complication rate in the general population.[22-32] One pregnancy ended in a stillbirth due to a placental abruption. The obstetrical history of this patient before this pregnancy was complicated and stated four miscarriages and two stillborn children with unknown cause all prior to the diagnosis of MFC.

Literature on the use of intravitreal anti-VEGF injections during pregnancy is scarce. The signal protein VEGF plays an important role in the embryo implantation and the development of the lungs, kidneys and central nervous system of the fetus.[14] Keeping this in mind, it is reasonable that anti-VEGF can potentially harm the fetus particularly during the development of the vital organs in the first trimester. One publication summarizes 20 cases of pregnant women who were treated with intravitreal anti-VEGF injections (18 with bevacizumab and two with ranibizumab) during pregnancy. In three pregnancies a miscarriage was observed, all treated with bevacizumab within 5 weeks of gestational age (GA).[13] To understand the difference between ranibizumab on the one hand, and aflibercept and bevacizumab on the other hand, one should take the pharmacological differences into account. Firstly, ranibizumab has the shortest half-life and therefore is most rapidly cleared when entering the systemic circulation. Due to the short period of drug exposure in ranibizumab, it affects the plasma level of free VEGF molecules for the shortest time period.[14,33] Secondly, aflibercept has the highest affinity with VEGF and therefore leads to the most dramatic suppression of free VEGF molecules in the plasma.[33] Thirdly, ranibizumab does not have a Fc fragment and therefore is not expected to be able to bind to the neonatal Fc receptor. It is proposed that this receptor is important for transporting the antibodies (f.e. bevacizumab) over the placental barrier to the fetus.[34] Based on this theory, ranibizumab will not reach the fetal circulation, for it will not pass the placental barrier, in contrast to bevacizumab and aflibercept.

Treatment with steroid-sparing immunomodulatory therapy in pregnancy is contraindicated for some agents including mycophenolate mofetil and methotrexate. On the contrary, no increase in the rate of miscarriages and congenital malformations is observed in pregnant patients treated with azathioprine, cyclosporine, tacrolimus and anti-tumour necrosis factor inhibitors and thus treatment with these agents is considered to be safe in pregnancy.[16] Literature regarding the influence of azathioprine on the prevalence of low-birth weight, preterm birth and small for gestational age is conflicting.[35,36] In our study, one patient treated with azathioprine developed the complication of ICP and spontaneously delivered preterm an infant with a low-birth

weight. Two case reports documented a similar finding in patients treated with azathioprine for Vogt–Koyanagi–Harada disease and Crohn's disease.[37,38]

This retrospective study comes with several limitations. Firstly, the number of patients was small and more importantly, limited to patients treated in tertiary academic centres. As a result, it is possible that the real-life relapse rate is lower than the reported relapse rate due to selection bias. Secondly, we report that the median BCVA remained stable throughout follow-up despite multiple relapses. Though, for a more thorough evaluation of the visual function in these patients, central visual field tests should be performed and evaluated before and after pregnancy to monitor the number and size of the scotomas due to the chorioretinal scars. Thirdly, it is possible that minor relapses of disease activity are missed during pregnancy since fluorescein and indocyanine green angiography is preferably not performed during pregnancy, though can be performed in urgent cases. Both fluorescein and indocyanine green are classified as a category C drug by the Food and Drug Administration indicating that it is unknown to what extent it will harm the fetus. Though indocyanine green has proven to be harmless for nonophthalmic indications, many ophthalmologists remain reluctant to use it.[39]

Despite the limitations of this study, this is the first study of this extent to report on the course of disease and different treatment options in pregnancy specifically for patients with MFC and PIC. We expect that the current data are of great value for clinicians dealing with this blinding disease and could be helpful in the process of shared decision-making.

In conclusion, we report that BCVA remained stable during pregnancy despite a considerable relapse rate of 44% in pregnancy. Overall, no major maternal, obstetrical and fetal complications were observed in patients treated with corticosteroids, azathioprine or intravitreal anti-VEGF injections, though one patient developed ICP while treated with azathioprine. We emphasize no conclusions can be drawn based on these results, due to the small number of patients. The optimal medical treatment of MFC and PIC during pregnancy should be established by the ophthalmologist together with the obstetrician considering the health of the unborn child and the risk of loss of visual function in the mother. Moreover, at all times medical treatment should be established within the concept op shared decision-making.

REFERENCES

1. Ahnood D, Madhusudhan S, Tsaloumas MD, Waheed NK, Keane PA, Denniston AK. Punctate inner choroidopathy: A review. Surv Ophthalmol. 2017;62(2):113-126.
2. Dhingra N, Kelly S, Majid MA, Bailey CB, Dick AD. Inflammatory choroidal neovascular membrane in posterior uveitis-pathogenesis and treatment. Indian J Ophthalmol. 2010;58(1):3-10.
3. Agarwal A, Invernizzi A, Singh RB, et al. An update on inflammatory choroidal neovascularization: epidemiology, multimodal imaging, and management. J Ophthalmic Inflamm Infect. 2018;8(1):13.
4. Turkcuoglu P, Chang PY, Rentiya ZS, et al. Mycophenolate mofetil and fundus autofluorescence in the management of recurrent punctate inner choroidopathy. Ocul Immunol Inflamm. 2011;19(4):286-292.
5. Goldberg NR, Lyu T, Moshier E, Godbold J, Jabs DA. Success with single-agent immunosuppression for multifocal choroidopathies. Am J Ophthalmol. 2014;158(6):1310-1317.
6. de Groot EL, ten Dam-van Loon NH, de Boer JH, Ossewaarde-van Norel J. The efficacy of corticosteroid-sparing immunomodulatory therapy in treating patients with central multifocal choroiditis. Acta Ophthalmol. 2020;98(8):816-821.
7. Chiam NPY, Lim LLP. Uveitis and Gender: The Course of Uveitis in Pregnancy. J Ophthalmol. 2014;2014:1-10.
8. Grotting LA, Papaliodis GN. A Review of the Course and Treatment of Non-Infectious Uveitis during Pregnancy. Semin Ophthalmol. 2017;32(1):75-81.
9. Rabiah PK, Vitale AT. Noninfectious uveitis and pregnancy. Am J Ophthalmol. 2003;136(1):91-98.
10. Kump LI, Cervantes-Castañeda RA, Androudi SN, Foster CS, Christen WG. Patterns of exacerbations of chronic non-infectious uveitis in pregnancy and puerperium. Ocul Immunol Inflamm. 2006;14(2):99-104.
11. Chiam NPY, Hall AJH, Stawell RJ, Busija L, Lim LLP. The course of uveitis in pregnancy and postpartum. Br J Ophthalmol. 2013;97(10):1284-1288.
12. Verhagen FH, Braakenburg AM, Kremer T, Drylewicz J, Rothova A, de Boer JH. Reduced number of relapses of human leucocyte antigen-B27-associated uveitis during pregnancy. Acta Ophthalmol. 2017;95(8):e798-e799.
13. Polizzi S, Mahajan VB. Intravitreal Anti-VEGF Injections in Pregnancy: Case Series and Review of Literature. J Ocul Pharmacol Ther. 2015;31(10):605-610.
14. Peracha ZH, Rosenfeld PJ. Anti-vascular endothelial growth factor therapy in pregnancy: What we know, what we don't know, and what we don't know we don't know. Retina. 2016;36(8):1413-1417.
15. Fossum P, Couret C, Briend B, Weber M, Lagarce L. Safety of intravitreal injection of ranibizumab in early pregnancy: A series of three cases. Eye. 2018;32(4):830-832.
16. Skorpen CG, Hoeltzenbein M, Tincani A, et al. The EULAR points to consider for use of antirheumatic drugs before pregnancy, and during pregnancy and lactation. Ann Rheum Dis. 2016;75(5):795-810.
17. Illamola SM, Bucci-Rechtweg C, Costantine MM, Tsilou E, Sherwin CM, Zajicek A. Inclusion of pregnant and breastfeeding women in research – efforts and initiatives. Br J Clin Pharmacol. 2018;84(2):215-222.
18. Sim DA, Sheth HG, Kaines A, Tufail A. Punctate inner choroidopathy-associated choroidal neovascular membranes during pregnancy. Eye. 2008;22(5):725-727.

19. Rao VG, Rao GS, Narkhede NS. Flare up of choroiditis and choroidal neovasculazation associated with punctate inner choroidopathy during early pregnancy. Indian J Ophthalmol. 2011;59(2):145-148.
20. World Health Organization. WHO recommendations on interventions to improve preterm birth outcomes. Published online 2015.
21. World Health Organization. Guidelines on optimal feeding of low birth-weight infants in low-and middle-income countries. Geneva WHO. Published online 2011:16-45.
22. Wilcox AJ, Weinberg CR, O'Conner JF, et al. Incidence of Early Loss of Pregnancy. N Engl J Med. 1988;319:189-194.
23. Beck S, Wojdyla D, Say L, et al. The worldwide incidence of preterm birth: A systematic review of maternal mortality and morbidity. Bull World Health Organ. 2010;88(1):31-38.
24. Ammon Avalos L, Galindo C, Li DK. A systematic review to calculate background miscarriage rates using life table analysis. Birth Defects Res Part A - Clin Mol Teratol. 2012;94(6):417-423.
25. Blencowe H, Cousens S, Oestergaard MZ, et al. National, regional, and worldwide estimates of preterm birth rates in the year 2010 with time trends since 1990 for selected countries: A systematic analysis and implications. Lancet. 2012;379(9832):2162-2172.
26. Gillon TER, Pels A, Von Dadelszen P, MacDonell K, Magee LA. Hypertensive disorders of pregnancy: A systematic review of international clinical practice guidelines. PLoS One. 2014;9(12):1-20.
27. Williamson C, Geenes V. Intrahepatic cholestasis of pregnancy. Obstet Gynecol. 2014;124(1):120-133.
28. Zhu Y, Zhang C. Prevalence of Gestational Diabetes and Risk of Progression to Type 2 Diabetes: a Global Perspective. Curr Diab Rep. 2016;16(1):1-11.
29. Eades CE, Cameron DM, Evans JMM. Prevalence of gestational diabetes mellitus in Europe: A meta-analysis. Diabetes Res Clin Pract. 2017;129(0):173-181.
30. Shen M, Smith GN, Rodger M, White RR, Walker MC, Wen SW. Comparison of risk factors and outcomes of gestational hypertension and pre-eclampsia. PLoS One. 2017;12(4):1-13.
31. Magnus MC, Wilcox AJ, Morken NH, Weinberg CR, Håberg SE. Role of maternal age and pregnancy history in risk of miscarriage: Prospective register based study. BMJ. 2019;364:1-8.
32. Smith DD, Rood KM. Intrahepatic cholestasis of pregnancy. Clin Obstet Gynecol. 2020;63(1):134-151.
33. Avery RL, Castellarin AA, Steinle NC, et al. Systemic pharmacokinetics following intravitreal injections of ranibizumab, bevacizumab or aflibercept in patients with neovascular amd. Br J Ophthalmol. 2014;98(12):1636-1641.
34. Krohne TU, Holz FG, Meyer CH. Essentials in Ophthalmology: Anti-Angiogenic Therapy in Ophthalmology. (Stahl A, ed.). Springer International Publishing; 2016.
35. Saavedra MÁ, Sánchez A, Morales S, Ángeles U, Jara LJ. Azathioprine during pregnancy in systemic lupus erythematosus patients is not associated with poor fetal outcome. Clin Rheumatol. 2015;34(7):1211-1216.
36. Plauborg AV, Hansen AV, Garne E. Use of azathioprine and corticosteroids during pregnancy and birth outcome in women diagnosed with inflammatory bowel disease. Birth Defects Res Part A - Clin Mol Teratol. 2016;106(6):494-499.
37. Ingolotti M, Schlaen BA, Roig Melo-Granados EA, García HR, Partida JAA. Azathioprine during the first trimester of pregnancy in a patient with Vogt-Koyanagi-Harada disease: A multimodal imaging follow-up study. Am J Case Rep. 2019;20:300-305.
38. Lauterbach R, Linder R, Vitner D, Solt I. Azathioprine-induced cholestasis of pregnancy-A new insight on azathioprine safety in pregnancy. Eur J Obstet Gynecol Reprod Biol. 2020;250:271-272.

39. Fineman MS. Safety of Indocyanine Green Angiography During Pregnancy. Arch Ophthalmol. 2001;119(3):353.

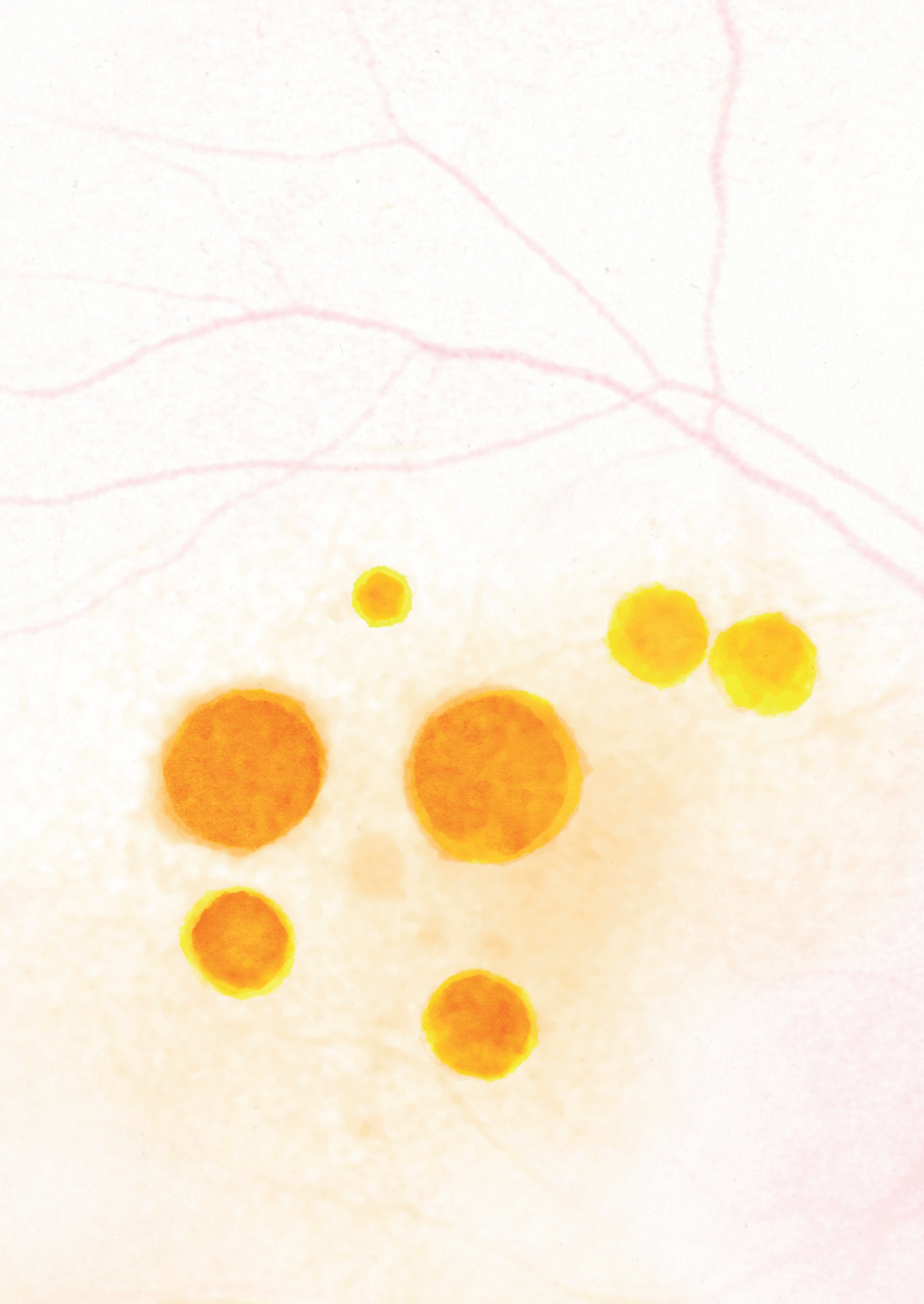

Chapter 6

Increased choroidal thickness as a marker for disease activity in idiopathic multifocal choroiditis using a multimodal imaging approach

Evianne L. de Groot
Ninette H. ten Dam-van Loon
Carlyn V. Kouwenberg
Joke H. de Boer
Jeannette Ossewaarde-van Norel

Adapted version accepted for publication in the American Journal of Ophthalmology

ABSTRACT

Purpose

To identify characteristics on multimodal imaging (MMI) in idiopathic MFC that can identify inflammatory activity and distinguish CNV activity from inflammatory activity.

Design

Prospective multimodal imaging study

Methods

MMI consisted of spectral-domain optical coherence tomography (angiography) (SD-OCT(A)), fundus autofluorescence, fundus photography, infrared imaging and fluorescein- and indocyanine green angiography (FA-ICGA). MMI characteristics obtained during active and inactive disease were compared within the same lesion. Secondly, MMI characteristics were compared between active inflammatory lesions with and without CNV activity.

Results

Fifty patients (110 lesions) were included. In 96 lesions without CNV activity, the mean focal choroidal thickness was increased during the active disease (205µm) compared to the inactive disease (180µm) (*P*=<0.001). Lesions with inflammatory activity typically demonstrated moderately reflective material located sub-retinal pigment epithelium (RPE) and/or in the outer retina with disruption of the ellipsoid zone. During the inactive stage of the disease, the material disappeared or became hyperreflective and fused with the RPE. During the active stage of the disease, the area of hypoperfusion in the choriocapillaris significantly increased visualized on both ICGA and SD-OCTA. CNV activity in 14 lesions was associated with subretinal material with a mixed reflectivity and choroidal hyporeflectivity on SD-OCT and leakage on FA. SD-OCTA identified vascular structures in all active CNV lesions and in 24% of lesions without CNV activity (showing old, quiescent CNV membranes).

Conclusion

Inflammatory activity in idiopathic MFC was associated with one or more typical MMI characteristics, such as focally increased choroidal thickness, which can be used by clinicians to improve monitoring of idiopathic MFC patients.

INTRODUCTION

Idiopathic multifocal choroiditis (MFC) is part of the spectrum of the "white dot syndromes" and is considered a primary inflammatory choriocapillaropathy (PICC).[1,2] Idiopathic MFC is a relapsing disease and predominantly affects Caucasian women with myopia in their second to fourth decade of life.[3,4] Typical features for idiopathic MFC are the inflammatory lesions that arise in the posterior pole at the level of the outer retina, the retinal pigment epithelium (RPE), and the choriocapillaris and the complication of secondary choroidal neovascularization (CNV). Both the inflammatory lesions and secondary CNV can be visualized and monitored using multimodal imaging (MMI) including spectral-domain optical coherence tomography (SD-OCT), spectral-domain optical coherence tomography angiography (SD-OCTA), fundus autofluorescence (FAF), and fluorescein- and indocyanine green angiography (FA-ICGA).[3,5] Monitoring and subsequently treating disease activity, even when the patient is still asymptomatic, is considered to be indicated since subclinical inflammatory disease activity can trigger the development and reactivation of secondary CNV. Moreover, subclinical inflammatory activity results in growth of the chorioretinal lesions over the years, which is, considering the young age at the first time of presentation, unfavorable.[6-8]

Currently, the evidence regarding which MMI characteristics can identify inflammatory activity is scarce and mostly limited to descriptive studies.[9-15] It can especially be challenging to recognize inflammatory activity in pre-existing lesions, since the local retinal structure is already distorted. Previous studies have suggested several imaging characteristics that are associated with disease activity including increased focal choroidal thickness on SD-OCT,[11,15] choroidal hyperreflectivity on SD-OCT[16,17] and the presence of a hyperautofluorescent margin surrounding a lesion on FAF.[10,18,19] However, most studies are cross-sectional and do not compare the same lesion over time during the active and inactive stages of disease. Therefore, it is uncertain to what extent these observed alterations during the active disease are reversible, or that they will remain altered once the inactive stage of the disease is achieved. Moreover, it is challenging to distinguish inflammatory activity from CNV activity. However, this distinction is of upmost importance, since the appropriate treatment for both conditions differs.

Therefore, the aim of this study is to identify imaging characteristics that are able to detect inflammatory activity. We will explore this by comparing the MMI results obtained during the active stage of disease with the results obtained during the inactive stage within the same patient. Moreover, we aim to find imaging characteristics distinguishing CNV activity from inflammatory activity. These imaging characteristics will ultimately help clinicians to improve the monitoring and treatment of patients with idiopathic MFC.

METHODS

This is a single-center prospective observational cohort study performed at the University Medical Center Utrecht, Utrecht, the Netherlands. The study was performed in accordance with the tenets of Helsinki and approval for this study was waived by the institutional review board. All study participants provided written informed consent to use medical data for research purposes.

Study population

All patients were diagnosed with idiopathic MFC following the SUN criteria[20,21] with the additional criteria of posterior pole involvement and the absence of retinal vasculitis and papillitis. Alternative diagnoses were ruled out by diagnostic work-up including but not limited to tuberculosis, sarcoidosis, toxoplasmosis and birdshot chorioretinopathy. Patients with other forms of idiopathic choroiditis including serpiginous choroiditis and relentless placoid chorioretinitis were excluded. Patients with idiopathic MFC were included in this study if two sets of multimodal imaging were present. The modalities ICGA, SD-OCT and SD-OCTA had to be available in both multimodal imaging sets to be eligible for inclusion.

Image acquisition and processing

After pupil dilatation, all imaging modalities were performed consecutively and consisted of Enhanced Depth Imaging (EDI) SD-OCT with TruTrack Active Eye Tracking®, FA-ICGA, FAF, near-infrared imaging (NIR) (Spectralis HRA-OCT; Heidelberg Engineering, Heidelberg, Germany), color fundus photography (FF 450 plus; Carl Zeiss Meditec, Jena, Germany) and SD-OCTA (SD-OCT Angioplex Cirrus HD-OCT 5000; Carl Zeiss Meditec, Jena, Germany). The imaging results of the SD-OCT existed of one volume of 20° x 20° (25 horizontal b-scans averaged nine times) and two volumes of 20° x 5° covering the macular area (seven horizontal and seven vertical b-scans averaged 25 times). For acquiring FA-ICGA images, patients received standard dye dose of 4ml of 100mg/ml sodium fluorescein and 4ml of 5mg/ml indocyanine green. Information of the early and late phase was obtained and pictures were taken up until 30 minutes after injection of the dye. The Cirrus Angioplex has an A-scan rate of 68,000 per second and the AngioPlex software uses an algorithm (the “Optical Micro Angiography Complex”) which is based on both amplitude and phase differences between consecutive b-scans. Both 6x6mm and 3x3mm SD-OCTA images from the macular area were obtained.

Assessment of disease activity

The assessment of disease activity consisted of several steps. Step 1. an ETDRS-grid overlay was added to the ICGA image of 20 minutes for both imaging sets by grader EG.

The location of the ETDRS-grid was determined based on the foveal pit visualized on SD-OCT. All lesions with a diameter of more than 150µm within the ETDRS-grid on the ICGA image of both sets were numbered with a maximum of 6 lesions per eye. If more lesions could be identified, the lesions showing the most dynamism between the 2 sets were selected. Step 2. two experienced uveitis and/or retina specialists (JO and NtD) assessed all lesions independently for the presence of inflammatory activity and CNV activity. Assessment was based on all available imaging results in combination with the information in the medical records regarding symptoms, ophthalmic examination, ophthalmic medical history and treatment. The lesions were scored as either active inflammation without active CNV, active inflammation with active CNV or inactive. Disagreement was resolved by discussion. Lesions that were scored as active in one imaging set and inactive in the other imaging set, were selected for further analysis (**Figure 6.1**). In addition, for all the lesions that were scored as inflammation without active CNV, we evaluated if the lesions had signs of pre-existing and inactive CNV. This evaluation was based on all available imaging and information from the medical records.

Image analysis

All imaging modalities were graded separately by the graders EG and CK (SD-OCTA by graders JO and EG). All imaging results were evaluated independently and in case of disagreement this was resolved by discussion. Continuous variables were remeasured when values deviated by more than 20%, otherwise results were averaged. All graders were masked for the outcome of the disease activity assessment, information from the medical records and the results of the other imaging modalities. For a detailed description and examples of the imaging characteristics see **Supplemental table 6.1** and **Supplemental figures 6.1-3**. The focal choroidal thickness was measured directly underneath the lesion at an identical location in both imaging sets. In addition, the choroidal thickness was measured at a single location distant from the lesions (at 3mm extrafoveal, first or last line of the 20º x 20º horizontal SD-OCT scan) also at an identical location in both imaging sets. SD-OCTA scans were evaluated for the presence of vascular structures and flow void and we first assessed all slabs dynamically. To assess the presence and morphology of vascular structures on SD-OCTA in more detail, we evaluated a segmentation slab ranging from 80µm above the RPE to 29µm below the RPE (slab was adjusted for individual cases if needed to improve assessment). To assess the presence and extensiveness of flow void in the choriocapillaris, a segmentation slab ranging from 29µm to 49µm below the RPE was evaluated. Imaging characteristics regarding ICGA were evaluated on an image obtained in the late phase (30±10 minutes). To grade fluorescence patterns on FA, early (30s to 2 min) and late phase (10-20 min) images were evaluated.

Statistical analysis

Data analyses were performed in RStudio version 1.2.5001 (RStudio Team, Boston, USA) and R version 3.6.1 (R Foundation for Statistical Computing, Austria). Imaging characteristics were compared between the active and inactive stage of the disease using the Wilcoxon signed-rank test (continuous variables) or McNemar test (categorical variables). Imaging characteristics between inflammatory lesions with and without CNV activity were compared using the chi-square test (or fisher exact test) for categorical variables and the Wilcoxon Rank-Sum Test for continuous variables. Correlation between variables were evaluated using the pearson correlation coefficient. FDR of 5% was used for correcting for multiple testing. A p-value of ≤0.05 was considered significant.

RESULTS

Study participants

Multimodal imaging of 50 idiopathic MFC patients were obtained during the active and inactive stage of the disease. In total 110 chorioretinal lesions were included that were imaged during both the active and inactive stage of disease (**Figure 6.1**). Of these lesions, 96 were graded as lesions with inflammatory activity and without CNV activity and 14 lesions were graded as inflammatory activity with CNV activity. **Figure 6.1** shows a complete overview of the process of patient and lesion selection. The patient characteristics are summarized in **Table 6.1**.

Table 6.1. Patient characteristics

	Patients n=50 **Affected eyes n=71**
Age, mean (SD)	43.7 (11.8)
Female gender, n (%)	47 (94)
Bilateral disease, n (%)	21 (42)
History of CNV, n (%) of all eyes	57 (80)
Number of lesions per eye, median [IQR]	3 [2 - 5.5]
Refractive error (D), mean (SD) of all affected eyes	-5.0 (4.3)
BCVA (LogMAR), median [IQR] of all affected eyes	0.027 [-0.06 – 0.20]
Time (days) between imaging sets, mean (SD)	386 (224)

SD, standard deviation; IQR, interquartile range; CNV, choroidal neovascularization; D, dioptres; BCVA, best-corrected visual acuity; LogMAR, Logarithm of the Minimum Angle of Resolution.

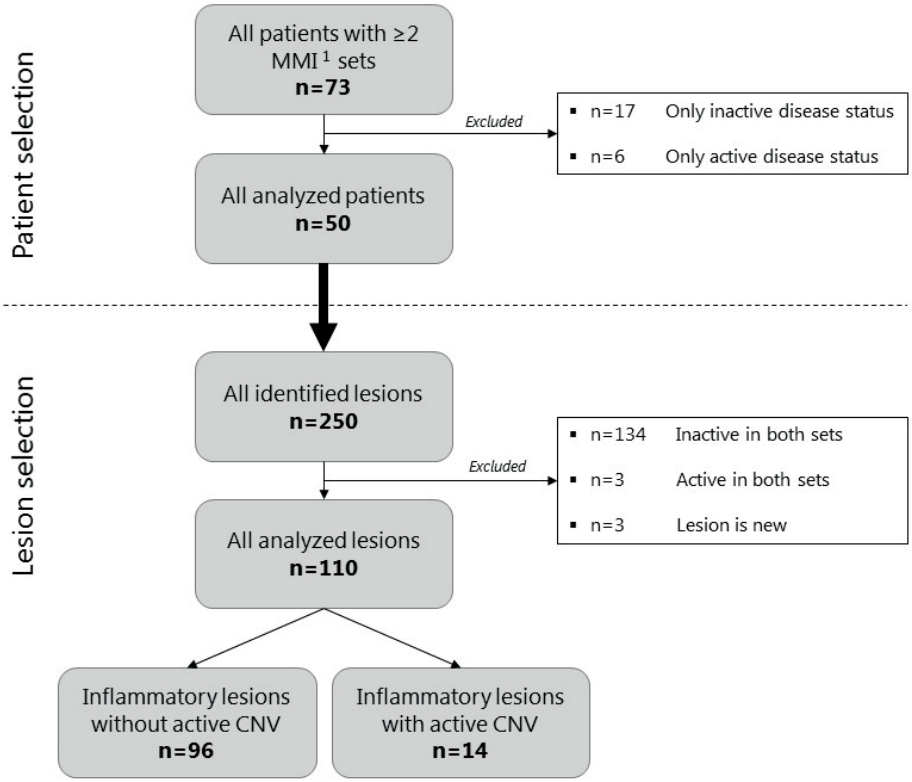

Figure 6.1. Flowchart visualizing patient and lesion selection. Patients were selected if MMI was available during the active and inactive stage of disease. In these patients, only the lesions were selected that were graded as active in one MMI set, and inactive in the other MMI set.
MMI, multimodal imaging; CNV, choroidal neovascularization.
[1] MMI included: fundus photography, fundus autofluorescence, near-infrared imaging, optical coherence tomography, optical coherence tomography angiography, fluorescein angiography, indocyanine green angiography.

Imaging characteristics of lesions with inflammatory activity

In total 96 lesions were analyzed that were graded as inflammatory lesions without CNV activity. Several imaging characteristics were identified that were associated with the presence of inflammatory activity (**Table 6.2 and 6.3; Figure 6.2-5**). The most important observations on SD-OCT during inflammatory activity were: 1. an increase in the focal choroidal thickness, 2. the presence of moderately reflective material located sub-RPE, in the outer retina or sub-RPE with outer retina infiltration, 3. disruption of the ellipsoid zone (EZ) and the RPE. When no inflammatory activity was present, the moderately reflective material was most likely to either disappear or become hyperreflective and fused with the RPE (**Figure 6.2**). The EZ was most likely to be absent and the RPE often remained disrupted (**Figure 6.2, Figure 6.3**). The majority of the lesions demonstrated hyperreflectivity of the choroid, independent of the presence of inflammatory activity (**Table 6.2**).

On FAF imaging, a hyperautofluorescent margin was more often observed on fundus autofluorescence imaging during the presence of inflammatory activity. However, note that this was only the case for 40% of the lesions and in the absence of inflammatory activity, still 20% of the lesions demonstrated a hyperautofluorescent margin (**Table 6.3; Figure 6.5**). The area of hypoautofluorescence on FAF was significantly lower during the presence of inflammatory activity. This most likely represents growth of the lesions over time, and suggests that multimodal imaging was first obtained during the presence of inflammatory activity in the majority of the cases (**Table 6.3; Figure 6.5**). All lesions were visible on ICGA imaging during the active stage of the disease and an increase in the area of hypofluorescence on ICGA imaging was observed compared to the inactive stage of the disease. This increase was especially apparent when this area was compared to the hypoautofluorescent area on FAF. During the active stage of the disease, the SD-OCTA demonstrated flow void in 96% of the lesions and again the area of flow void was increased (**Figure 6.4, Figure 6.5**). During the inactive stage of the disease, 96% of the lesions was visible on the ICGA image and 82% of the lesions on SD-OCTA. The hypofluorescent area on ICGA showed a high correlation with the flow void on SD-OCTA both during the presence (r=0.92) and absence (r=0.88) of inflammatory activity.

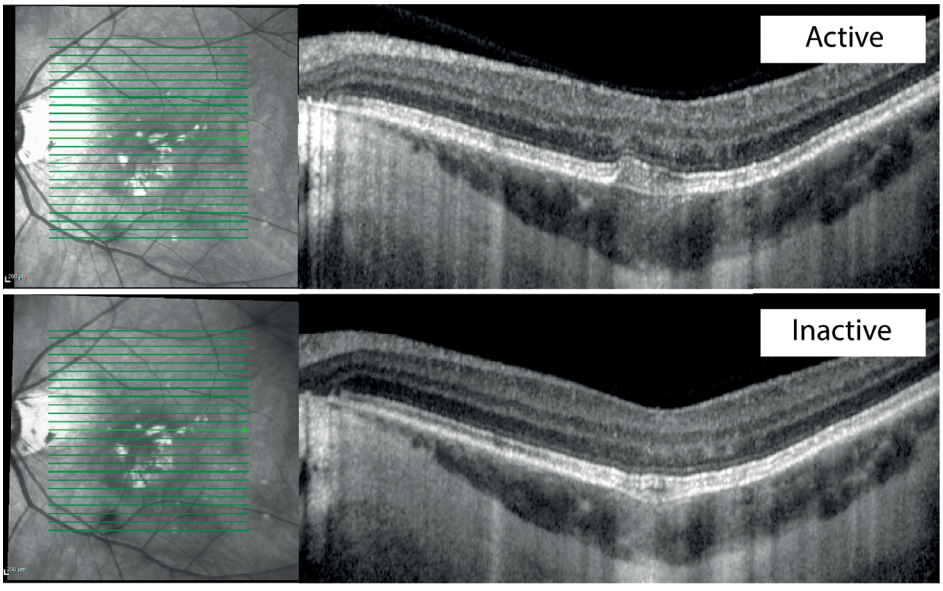

Figure 6.2. Disease activity in inflammatory lesions – Example 1. During the active stage of disease, moderately reflective sub-RPE material is observed with a disruption of the EZ and the RPE and subtle increase in the choroidal thickness below the lesion. In the inactive stage of the disease, the lesion demonstrates hyperreflective material at the level of the RPE, the EZ has mostly recovered and the RPE is still disrupted.
RPE, retinal pigment epithelium; EZ, ellipsoid zone.

Table 6.2. Imaging results of inflammatory lesions (n=96) – SD-OCT(A)

	Active inflammation	**Inactive inflammation**	***P-value*[a]**
SD-OCT	n=96 lesions	n=96 lesions	
Location of material[b], n (%)			<0.001[c]
No material	14 (15)	59 (61)	
Sub-RPE	24 (25)	6 (6)	
Material fused with the RPE	10 (10)	29 (30)	
Outer retina	20 (21)	0 (0)	
Sub-RPE with outer retinal infiltration	28 (29)	2 (2)	
Reflectivity of material[b], n (%)			<0.001[d]
No material	14 (15)	59 (61)	
Moderately reflective	64 (67)	6 (6)	
Hyperreflective	7 (7)	29 (30)	
Mixed	11 (11)	2 (2)	
EZ[b], n (%)			<0.001[e]
Continuous	3 (3)	19 (20)	
Disrupted	85 (89)	32 (33)	
Absent	8 (8)	45 (47)	
RPE[b], n (%)			<0.01[f]
Continuous	11 (11)	26 (27)	
Disrupted	83 (86)	61 (64)	
Absent	2 (2)	9 (9)	
Reflectivity of choroid[b], n (%)			0.72
Isoreflective	27 (28)	26 (27)	
Hyperreflective	65 (68)	68 (71)	
Hyporeflective	4 (4)	2 (2)	
Fluid, n (%)			1.0
None	88 (92)	88 (92)	
Atrophic cysts (>50µm)	7 (7)	7 (7)	
Subretinal fluid	1 (1)	1 (1)	
Intraretinal fluid (>50µm)	0 (0)	0 (0)	
Choroidal thickness underneath the lesion in µm, mean (SD)	205 (95)	180 (95)	<0.001
Choroidal thickness (distant from lesions) in µm, mean (SD)[g]	194 (70)	188 (68)	0.12
SD-OCTA[h]	n=84 lesions	n=84 lesions	
Flow void visible, n (%)	81 (96)	69 (82)	<0.01
Blurry borders of flow void, n (%)	75 (93)	60 (87)	0.57
Area of flow void in mm^2, median [IQR]	0.20 [0.10-0.43]	0.16 [0.05-0.44]	<0.001

SD-OCT, spectral-domain optical coherence tomography; RPE, retinal pigment epithelium; EZ, ellipsoid zone; SD, standard deviation; SD-OCTA, spectral-domain optical coherence tomography angiography.

[a] Imaging characteristics were tested with the McNemar test or the Wilcoxon signed-rank test. False discovery rate correction at 5% was applied to all the imaging characteristics in Table 2 and 3 combined.
[b] Every lesion was classified into one of the categories. If the EZ and RPE demonstrated disruption at some location in the lesion, it was graded as disrupted. The reflectivity in the choroid was graded according to the category that was predominantly present.
[c] The proportion of lesions with and without outer retina involvement were tested between the active and inactive disease.
[d] Both the proportion of lesions with moderately reflective material vs no material and moderately reflective material vs hyperreflective material was significantly different between the active and inactive disease.
[e] Both the proportion of lesions with absent EZ vs disrupted EZ and continuous EZ vs disrupted EZ was significantly different between the active and inactive disease.
[f] The proportion of lesions with disrupted RPE vs continuous RPE was significantly different between the active and inactive disease.
[g] The choroidal thickness was measured once per eye at 3mm extrafoveal (first or last line of the horizontal SD-OCT scan) at a single location distant from the lesions at an identical position in both imaging sets.
[h] Missing data for 12 lesions: 11 lesions due to poor imaging quality and 1 lesion was located outside the scan area.

Table 6.3. Imaging results of inflammatory lesions (n=96) – other imaging modalities

	Active inflammation	**Inactive inflammation**	**P-value[a]**
Lesion visible on			
Fundus picture (n=87[b]), n (%)	84 (97)	85 (98)	1.0
Hyperpigmentation, n (%)	45 (54)	48 (56)	0.59
Blurry borders, n (%)	67 (80)	61 (72)	0.12
Hemorrhage, n (%)	0 (0)	0 (0)	-
IR (n=96), n (%)	94 (98)	90 (94)	0.20
Hyperreflective lesion, n (%)	81 (86)	78 (87)	0.59
Hyporeflective margin, n (%)	53 (56)	38 (42)	0.05
Blurry borders, n (%)	73 (78)	57 (63)	0.04
FAF (n=91[b]), n (%)	86 (95)	89 (98)	0.49
Hyperautofluorescent margin, n (%)	34 (40)	18 (20)	<0.01
Lesion area mm^2, median [IQR]	0.27 [0.10-0.75]	0.32 [0.13-0.79]	<0.001
Patchy hyperautofluorescence of affected eyes (n=44), n (%)	5 (11)	2 (5)	0.35
FA (n=89[b]), n (%)	86 (97)	86 (97)	-
Leakage, n (%)	4 (4)	0 (0)	0.20
ICGA (n=96), n (%)	96 (100)	92 (96)	0.20
Hypofluorescence, n (%)	81 (84)	77 (84)	1.0
Blurry borders, n (%)	87 (91)	72 (78)	0.04
Lesion area mm^2, median [IQR]	0.49 [0.27-1.25]	0.38 [0.17-0.92]	<0.001
% difference in area FAF and ICGA, median [IQR]	74 [25-145]	9 [-10 – 49]	<0.001

IR, infra-red imaging; FAF, fundus autofluorescence imaging; IQR, interquartile range; FA, fluorescein angiography; ICGA, indocyanine green angiography.
[a] Imaging characteristics were tested with the McNemar test or the Wilcoxon signed-rank test. False discovery rate correction at 5% was applied to all the imaging characteristics in Table 2 and 3 combined.
[b] Missing data due to poor image quality/missing imaging: Fundus picture n=9 lesions, FAF imaging n=5 lesions, FA imaging n=7 lesions.

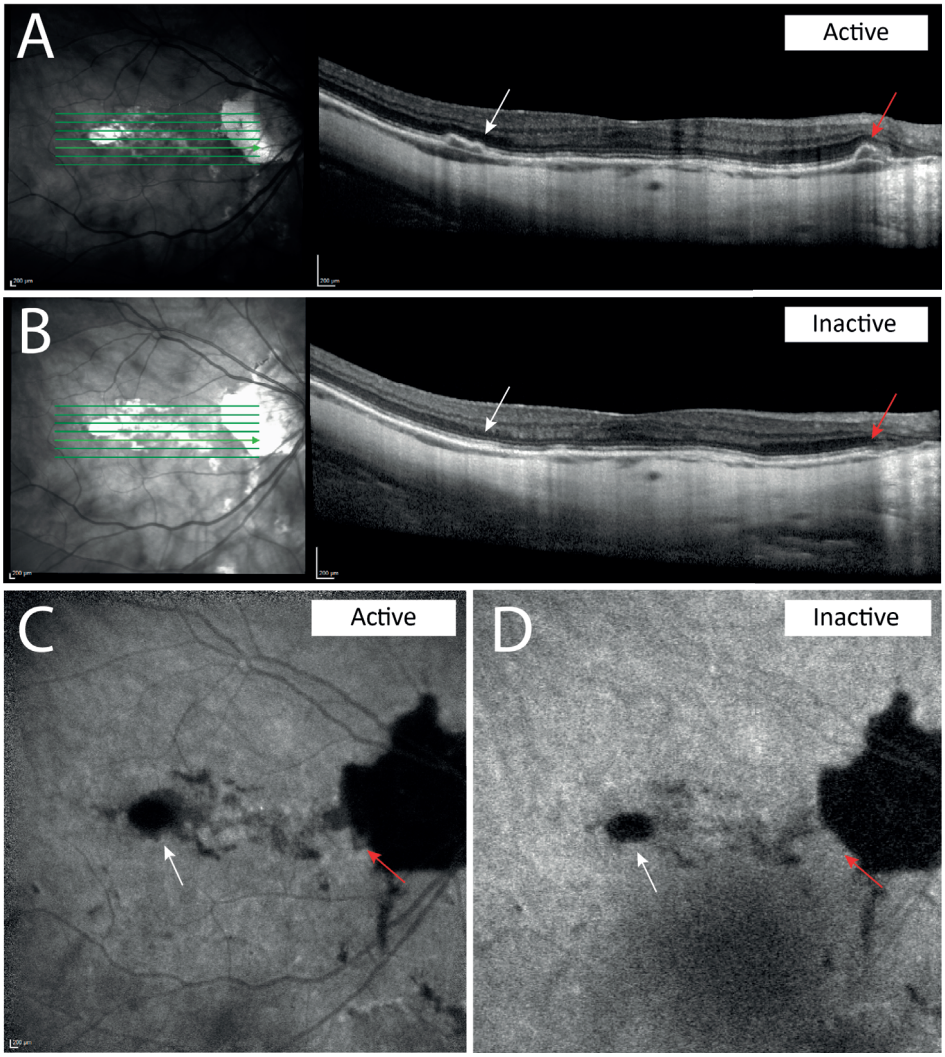

Figure 6.3. Disease activity in inflammatory lesions – Example 2. **A**. Two active lesions can be identified on this SD-OCT image indicated with the white and red arrow. Disease activity can be recognized by the increased choroidal thickness beneath the lesions, moderately reflective material located either sub-RPE (white arrow) or sub-RPE with outer retinal infiltration (red arrow). **B**. During the inactive stage normalization of the choroidal thickness can be observed with disappearance of the moderately reflective material. **C**. The ICGA image taken after 20 minutes during active disease shows blurry hypofluorescent areas at the location of both lesions. **D**. The ICGA image taken after 20 minutes during inactive disease shows disappearance of the blurry hypofluorescent areas (red arrow) or decrease in size of the areas (white arrow). SD-OCT, spectral-domain optical coherence tomography; RPE, retinal pigment epithelium; ICGA, indocyanine green angiography.

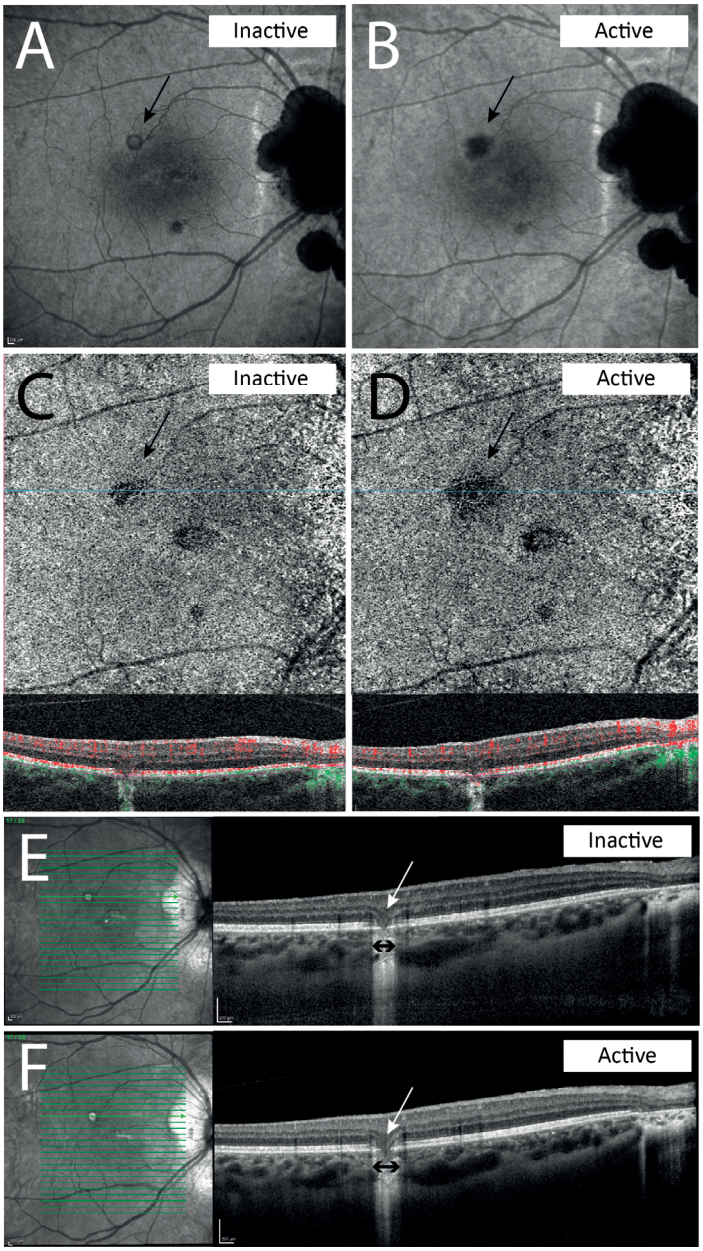

Figure 6.4. Disease activity in inflammatory lesion – Example 3. During the inactive stage of disease we observe a hypofluorescent area with sharp boundaries on the ICGA image **(A)**, a small area of flow void on the SD-OCTA image **(C),** absent EZ and absent RPE in a small area on the SD-OCT **(E)**. During the active stage of the disease we observe an increased hypofluorescent area with blurry boundaries on the ICGA image **(B)**, corresponding with an increased area of flow void in the choriocapillaris on SD-OCTA **(D)**. On the SD-OCT **(F),** no clear signs of disease activity can be identified. The choroidal thickness is not increased, there is no material visible, the EZ and RPE are still absent. The width of the area of EZ and RPE absence and hyperreflectivity in the choroid has slightly increased as indicated with the double black arrows.
ICGA, indocyanine green angiography; SD-OCTA, optical coherence tomography angiography; SD-OCT, spectral-domain optical coherence tomography; RPE, retinal pigment epithelium; EZ, ellipsoid zone.

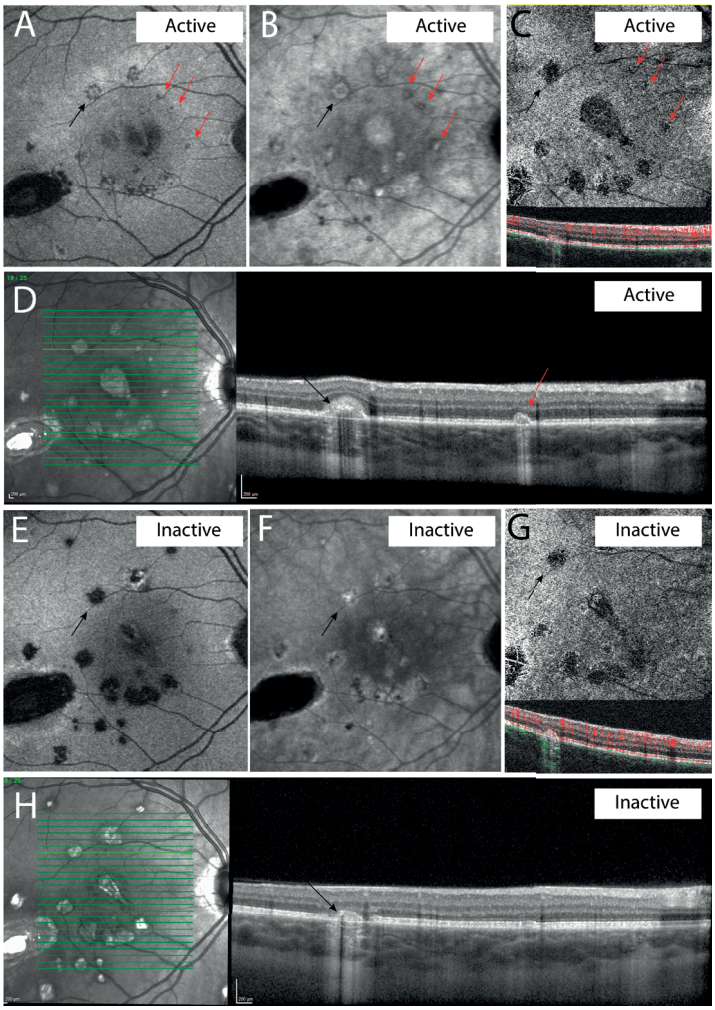

Figure 6.5. Inflammatory and CNV activity in multiple lesions – Example 4. Black arrow indicates an inflammatory lesion with an active CNV, the red arrows indicate inflammatory lesions without CNV. **A+E** FAF imaging demonstrating considerable growth of the hypoautofluorescent areas between the two sets. Hyperautofluorescent halo (black arrow) can be observed surrounding several lesions during active disease (**A**) which is absent for the majority of the lesions during the inactive disease (**E**). **B+F** ICGA imaging taken at 30 minutes after injection of dye. Large and blurry areas of hypofluorescence during active disease (**B**) mostly decreasing in size (black arrow) or resolving (red arrows) during inactive disease (**F**). **C+G** SD-OCTA images of the choriocapillaris slab demonstrating large areas of hypoperfusion during active disease (**C**). During the inactive disease (**G**) some of these areas on decrease (black arrow) or complete resolve (red arrows) and some have increased due to growth of the atrophic areas. **D+H** SD-OCT images. During the active disease (**D**) the lesion indicated with the black arrow demonstrates both subretinal and sub-RPE material with EZ and RPE disruption in the active phase with mixed reflectivity of the material. For the lesion indicated with the red arrow, during the active stage sub-RPE moderately reflective material arises with hyperreflective signal in the choroid. In the inactive phase (**H**), in the lesion with the black arrow the subretinal material disappears, the EZ is absent and the RPE remains disrupted. For the lesion with red arrow, the lesion has completely resolved with restoration of the RPE and EZ layers and the disappearance of the hyperreflectivity in the choroid.

CNV, choroidal neovascularization; FAF, fundus autofluorescence; ICGA, indocyanine green angiography; SD-OCTA, spectral-domain optical coherence tomography angiography; SD-OCT, spectral-domain optical coherence tomography; RPE, retinal pigment epithelium; EZ, ellipsoid zone.

Table 6.4. Imaging characteristics related to activity of choroidal neovascularization

	Inflammation with active CNV n=14 lesions	**Inflammation without active CNV n=96 lesions**	***P*-value[a]**
Location of material on SD-OCT, n (%)			<0.001
No material	0 (0)	14 (15)	
Sub-RPE	1 (7)	24 (25)	
Material fused with the RPE	2 (14)	10 (10)	
Subretinal*	5 (36)	0 (0)	
Outer retina	0 (0)	20 (21)	
Sub-RPE with outer retinal infiltration	0 (0)	28 (29)	
Sub-RPE and subretinal*	6 (43)	0 (0)	
Reflectivity of the material on SD-OCT, n (%)			<0.001
No material	0 (0)	14 (15)	
Moderately reflective*	1 (7)	64 (67)	
Hyperreflective	0 (0)	7 (7)	
Mixed*	13 (93)	11 (11)	
Reflectivity of the choroid on SD-OCT, n (%)			<0.05
Isoreflective	3 (21)	27 (28)	
Hyperreflective	6 (43)	65 (68)	
Hyporeflective*	5 (36)	4 (4)	
Fluid on SD-OCT, n (%)			<0.001[b]
No fluid	7 (50)	88 (92)	
Intraretinal fluid	5 (36)	0 (0)	
Subretinal fluid (>50µm)	5 (36)	1 (1)	
Atrophic cysts (>50µm)	2 (14)	7 (7)	
Leakage on FA[c], n (%)	6 (46)	4 (4)	<0.01
Hypofluorescent area on ICGA, median (IQR)	1.72 (1.21-1.87)	0.49 (0.27-1.23)	<0.01[d]
Vascular structure on SD-OCTA, n (%)	12[e] (100)	20[e] (24)	<0.001
Area of flow void on SD-OCTA, median (IQR)	0.54 (0.43-1.27)	0.22 (0.11-0.51)	<0.01[d]

CNV, choroidal neovascularization; SD-OCT, spectral-domain optical coherence tomography; RPE, retinal pigment epithelium; ICGA, indocyanine green angiography; SD-OCTA, spectral-domain optical coherence tomography angiography, FA, fluorescein angiography.

[a] Results of the chi-square test (or fisher exact test) for categorical variables and the Wilcoxon Rank-Sum Test for continuous variables. False discovery rate at 5% was applied for all tested imaging characteristics to correct for multiple testing. The categories that demonstrated significantly different proportions between inflammatory lesions with and without active CNV are indicated with an asterisk (*).

[b] The presence of fluid vs no fluid was tested (atrophic cysts were not included in the analyses).

[c] In one case with active CNV, no FA was performed due to a fluorescein allergy.

[d] When comparing the 14 lesions with active CNV with the 46 lesions with pre-existent and inactive CNV, these imaging characteristics were no longer significant.

[e] SD-OCTA was not available for some lesions due to poor image quality or severe artifacts (2 lesions with active CNV and 12 lesions without active CNV).

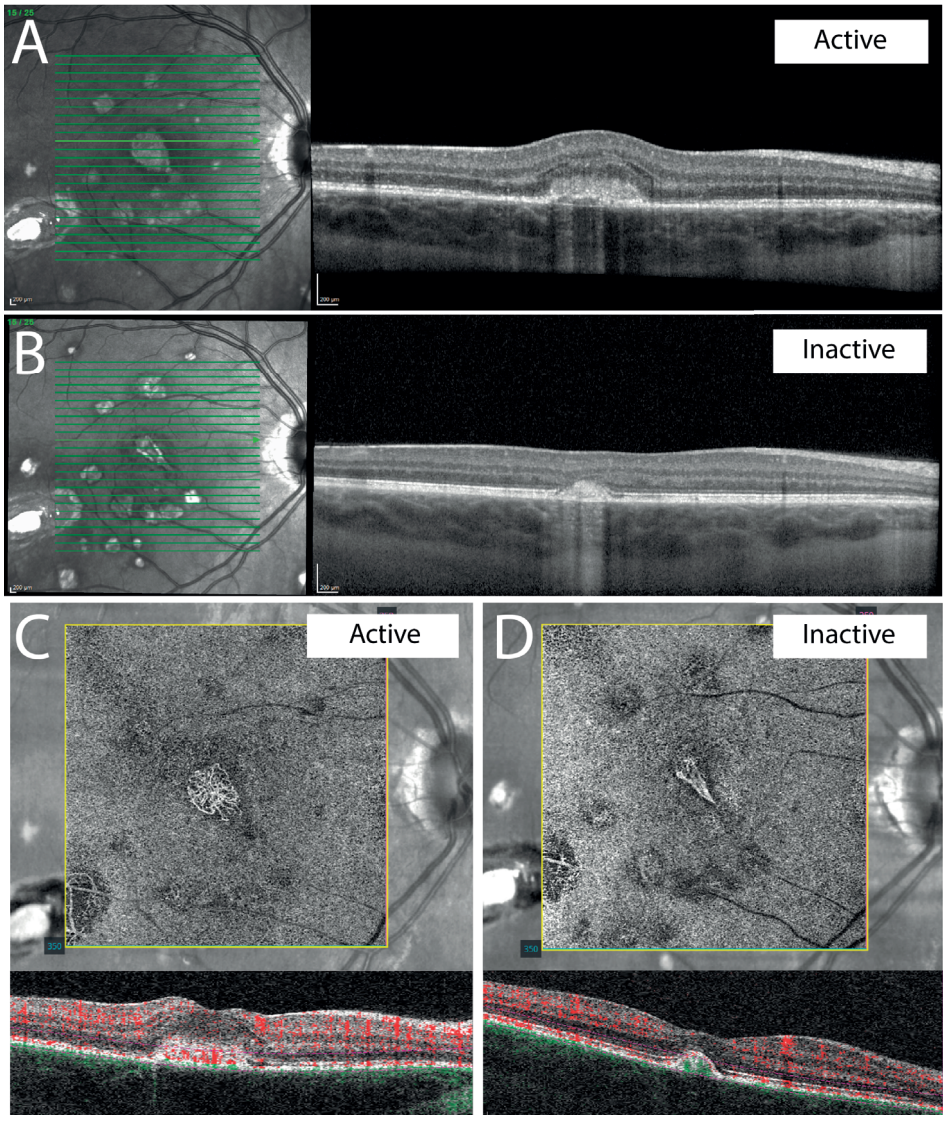

Figure 6.6. CNV activity – Example 5**. A+B** SD-OCT images. During the active phase (**A**) both moderately reflective and hyperreflective material in the subretinal space and sub-RPE can be observed with disruption of both the RPE and EZ with predominantly hyporeflectivity of the choroid. During the inactive phase (**B**) the subretinal moderately reflective material disappears and the choroid becomes predominantly hyperreflective. **C+D** SD-OCTA images of a slab between 80 micrometer above the RPE until 29 micrometer below the RPE. A vascular structure is visible both during the active and inactive disease. During the active disease both the area of the vascular network as the area of hypoperfusion or "halo" surrounding the vascular network are larger.
CNV, choroidal neovascularization; SD-OCT, spectral-domain optical coherence tomography; RPE, retinal pigment epithelium; EZ, ellipsoid zone; SD-OCTA, spectral-domain optical coherence tomography angiography, FA, fluorescein angiography.

Distinguishing CNV activity from inflammatory activity

To distinguish CNV activity from inflammatory activity, we compared the lesions graded as inflammation with active CNV (n=14) with lesions graded as inflammation without active CNV (n=96). We found that signs of active CNV on SD-OCT were: 1. material with a mixed reflectivity (both moderately and hyperreflective parts) in the subretinal space, 2. hyporeflectivity of the choroid and 3. the presence of fluid (**Figure 6.6**). Moreover, leakage on FA was more often observed in lesions with CNV activity. SD-OCTA identified vascular structures in 100% of the lesions with CNV activity (if the imaging quality of the SD-OCTA was sufficient). Also in 20 of the inflammatory lesions without CNV activity, a vascular structure was observed. Of these 20 lesions, 19 were known to have pre-existent and inactive CNV (**Table 6.4; Figure 6.6**). No differences in the morphology of the vascular structures were identified between the lesions with active and inactive CNV (**Supplemental Table 6.2**). The area of hypofluorescence on ICGA and flow void on SD-OCTA was larger in lesions with active CNV compared to all inflammatory lesions. When comparing the lesions with active CNV (n=14) with inflammatory lesions with pre-existent and inactive CNV (n=46), all imaging characteristics were still significantly different except for the area of hypofluorecence on ICGA and area of flow void on SD-OCTA. Results for all the imaging characteristics are summarized in **Supplemental Table 6.2 and 6.3**.

DISCUSSION

In lesions of idiopathic MFC patients, we identified imaging characteristics associated with inflammatory activity. These characteristics included an increased focal choroidal thickness, disruption of the EZ and the presence of moderately reflective material located sub-RPE and/or in the outer retina. Moreover, we observed an increase in the hypofluorescent area on ICGA and in the area of flow void on SD-OCTA. These imaging characteristics can help clinicians recognizing activity in inflammatory lesions on multimodal imaging in these patients.

We showed that inflammatory activity in a lesion was associated with an increase in the focal choroidal thickness. This phenomenon was previously described by Giuffre and colleagues as the “sponge sign” and they observed this phenomenon in lesions with inflammatory CNV and not in myopic CNV.[15] Zhang and colleagues also described an increase in the choroidal thickness in lesions with inflammatory activity.[11] Interestingly, in line with the report of Zhang and colleagues, we also found a trend of increased choroidal thickness in the posterior pole at a distant from the focal inflammatory activity (P=0.06; P_{adj}=0.1). This suggests that the choroid/choriocapillaris of a large area in the

posterior pole is affected by the focal inflammatory activity. In the current study, the choroidal thickness was compared within the same patient and not between patients. Therefore, our results were not influenced by the level of refractive error, age and gender.

On ICGA, the lesions showed hypofluorescent areas which were increased in size during inflammatory activity. The hypofluorescent areas on ICGA are suggested to represent hypoperfusion of the choroid/choriocapillaris.[3,11,22,23] When inflammatory activity is absent, the hypofluorescent areas represent hypoperfusion of the lesions due to atrophy. In this case, the area corresponds with the area of RPE loss (window defect on FA and hypoautofluorescence on FAF). However, lesions with inflammatory activity demonstrate hypofluorescent areas with blurry borders extending beyond the atrophic areas. This indicates that a larger area of the choriocapillaris endures hypo- or non-perfusion. In this study we demonstrate that the areas of hypofluorescence on ICGA correlate with the areas of flow void on SD-OCTA and that also the area of flow void on SD-OCTA increased during inflammatory activity. Since both imaging characteristics represent choriocapillaris hypoperfusion, this finding was expected but has not been confirmed before in idiopathic MFC. In line with other reports, lesions with inflammatory activity typically demonstrated moderately reflective sub-RPE material often infiltrating the outer retina with disruption of the EZ and RPE.[10,11,13,24] When inflammatory activity was not present, this material was most likely to disappear or become hyperreflective, the RPE often remains disrupted and the EZ was most likely to disappear. We suggest that this shift from moderately reflective to hyperreflective material or vice versa is the result of the development of fibrosis (hyperreflective) in the inactive stage which can again become moderately reflective after the infiltration of inflammatory cells. The EZ and RPE are most likely disrupted due to infiltration of inflammatory cells and local ischemia due to the hypoperfusion of the choriocapillaris.

In this study, no variables related to fundus photography were associated with inflammatory activity. Historically, fundus photography visualizes inflammatory activity in lesions as blurry and white-creamish colored regions in the posterior pole.[4,11] Perhaps this is only the case for new lesions and most lesions assessed in this study were pre-existing with reactivation of the inflammatory activity. We suggest that fundus photography is able to identify inflammatory activity in new lesions, but has a low sensitivity for the detection of inflammatory activity in pre-existing lesions.

Additionally, we found that CNV activity was associated with the presence of a vascular structure on SD-OCTA, leakage on FA, and mixed reflective subretinal material and choroidal hypo-reflectivity on SD-OCT. Choroidal hyporeflectivity has previously been associated with secondary CNV and is most likely the result of blockage of the

SD-OCT signal by the vascular structure.[12,16,25] In the current study, hyporeflectivity in the choroid was more often present in lesions with CNV activity compared to lesions with inflammatory activity. However, the majority of the lesions with CNV activity demonstrated predominantly choroidal hyperreflectivity. The choroidal hyporeflectivity is often transient and is only associated with active CNV and becomes less frequent when the CNV is inactive. Moreover, lesions with CNV activity often demonstrated mixed reflectivity within the lesion which could be used to distinguish CNV from inflammation. Though note that this is not pathognomic since also inflammatory lesions can demonstrate mixed reflectivity in the lesion.

Interestingly, Chen and colleagues reported that RPE disruption and choroidal hyperrreflectivity are early signs of secondary CNV.[17] We suggest that these imaging characteristics implicate inflammatory activity, which subsequently is able to trigger the development of secondary CNV explaining the association with secondary CNV. In line with other reports, we confirm that lesions with CNV activity demonstrated vascular structures on SD-OCTA imaging.[12,26-29] However, we suggest that OCTA imaging is particularly useful to detect CNV activity in new lesions or lesions without a history of CNV activity. As we also demonstrate in this study that the SD-OCTA seems less useful for detecting CNV activity in lesions with a history of CNV, since also these lesions often still demonstrate flow on the SD-OCTA.[26,28]

It is still subject of debate what the initially targeted structure is in idiopathic MFC. Some advocate the outer segments of the photoreceptors are first targeted in idiopathic MFC and subsequently the recruitment of inflammatory cells results in hypoperfusion of the choriocapillaris, increase in the choroidal thickness and the accumulation of material in the outer retina and under the RPE.[11] Others believe that the choriocapillaris is first targeted, resulting in hypoperfusion in the choriocapillaris with subsequent ischemia. In line with this theory, the local ischemia will result in the alterations observed in the EZ layer and recruitment of inflammatory cells.[30] Interestingly, in **Figure 6.4** we show a case with inflammatory activity in a lesion that only demonstrated increased hypoperfusion in the choriocapillaris without other signs of inflammatiory activity, including no increase in the choroidal thickness and no accumulation of material under the RPE or in the outer retina. Even though no direct conclusions can be drawn, this suggests that the initially targeted structure is indeed the choriocapillaris.

We believe our results can be used in future studies to further improve the monitoring of patients with idiopathic MFC. Automated quantification of choroidal parameters including choroidal thickness and total choroidal volume could perhaps be used for the early detection of disease activity.[31] Moreover, it would be interesting to explore the

choroidal thickness and visualization of flow voids using the additional swept-source technology. Furthermore, in this study not all lesions could be assessed on SD-OCTA imaging due to poor imaging quality and severe artifacts, especially in patients with very high myopia. The technology regarding OCTA imaging is continuously evolving and we believe this imaging modality will have a prominent position in the monitoring of idiopathic MFC patients in the future. In the current study, we measured the area of flow voids manually, making this a time-consuming measurement not suitable for the clinical practice. If this could be automatized using specific algorithms, this would probably improve the accuracy of this measurement and makes it suitable for clinical practice. Ideally, the OCTA would eventually replace the invasive imaging modality ICGA for the visualization of the hypoperfusion in the choriocapillaris. The areas of hypoperfusion are shown to respond to therapy in small case studies[32,33] and could perhaps be used in the future as endpoints for larger clinical trials concerning the treatment of idiopathic MFC.

Strengths of the current study were the relatively high number of included patients and the evaluation of the same lesions between the active and inactive stage of the disease. Limitations of this study were the low number of lesions with CNV activity resulting in limited power to detect imaging characteristics indicating CNV activity. Moreover, the image quality of the SD-OCTA was too poor for evaluation in a considerable proportion of the lesions. Lastly, both due to technical reasons and the COVID-19 pandemic not all imaging modalities were available in all cases.

In conclusion, inflammatory activity is associated with an increased focal choroidal thickness, moderately reflective material in the outer retina with disruption of the EZ and increased areas of hypoperfusion in the choriocapillaris. These characteristics can be used by clinicians to improve to monitoring of patients with idiopathic MFC.

REFERENCES

1. Papasavvas I, Herbort CPJ. Diagnosis and Treatment of Primary Inflammatory Choriocapillaropathies (PICCPs): A Comprehensive Overview. Medicina (B Aires). 2022;58(2):165.
2. Neri P, Herbort CP, Hedayatfar A, et al. “White dot syndromes”, an inappropriate and outdated misnomer. Int Ophthalmol. 2022;42(1):1-6.
3. Ahnood D, Madhusudhan S, Tsaloumas MD, Waheed NK, Keane PA, Denniston AK. Punctate inner choroidopathy: A review. Surv Ophthalmol. 2017;62(2):113-126.
4. Tavallali A, Yannuzzi LA. Idiopathic multifocal choroiditis. J Ophthalmic Vis Res. 2016;11(4):429-432.
5. Fung AT, Pal S, Yannuzzi NA, et al. Multifocal choroiditis without panuveitis; Clinical Characteristics and Progression. Retina. 2014;34(1):98-107.
6. Chen YC, Chen YL, Chen SN. Chorioretinal Atrophy in Punctate Inner Choroidopathy/multifocal Choroiditis: A Five-year Follow-up Study. Ocul Immunol Inflamm. 2021;00(00):1-6.
7. Erba S, Cozzi M, Xhepa A, Cereda M, Staurenghi G, Invernizzi A. Distribution and Progression of Inflammatory Chorioretinal Lesions Related to Multifocal Choroiditis and Their Correlations with Clinical Outcomes at 24 Months. Ocul Immunol Inflamm. 2022;30(2):409-416.
8. de Groot EL, de Boer J, Ossewaarde-van Norel J. Idiopathic multifocal choroiditis and punctate inner choroidopathy: evaluation of risk factors for increased relapse rate. A 2-year prospective observational cohort study. Ophthalmologica. Published online 2022.
9. Pohlmann D, Pleyer U, Joussen AM, Winterhalter S. Optical coherence tomography angiography in comparison with other multimodal imaging techniques in punctate inner choroidopathy. Br J Ophthalmol. 2019;103:60-66.
10. Li J, Li Y, Li H, Zhang L. Imageology features of different types of multifocal choroiditis. BMC Ophthalmol. 2019;19(1):1-7.
11. Zhang X, Zuo C, Li M, Chen H, Huang S, Wen F. Spectral-domain optical coherence tomographic findings at each stage of punctate inner choroidopathy. Ophthalmology. 2013;120(12):2678-2683.
12. Cheng L, Chen X, Weng S, et al. Spectral-Domain Optical Coherence Tomography Angiography Findings in Multifocal Choroiditis With Active Lesions. Am J Ophthalmol. 2016;169:145-161.
13. Channa R, Ibrahim M, Sepah Y, et al. Characterization of macular lesions in punctate inner choroidopathy with spectral domain optical coherence tomography. J Ophthalmic Inflamm Infect. 2012;2(3):113-120.
14. Zarranz-Ventura J, Sim DA, Keane PA, et al. Characterization of punctate inner choroidopathy using enhanced depth imaging optical coherence tomography. Ophthalmology. 2014;121(9):1790-1797.
15. Giuffrè C, Marchese A, Fogliato G, et al. The ‘Sponge sign’: A novel feature of inflammatory choroidal neovascularization. Eur J Ophthalmol. Published online 2020.
16. Shi X, Cai Y, Luo X, Liang S, Rosenfeld PJ, Li X. Presence or absence of choroidal hyper-transmission by SD-OCT imaging distinguishes inflammatory from neovascular lesions in myopic eyes. Graefe’s Arch Clin Exp Ophthalmol. 2020;258(4):751-758.
17. Chen Y, Chen Q, Li X, Li M. RPE disruption and hyper-transmission are early signs of secondary CNV with punctate inner choroidopathy in structure-OCT. BMC Ophthalmol. 2021;21(1):1-9.
18. Turkcuoglu P, Chang PY, Rentiya ZS, et al. Mycophenolate mofetil and fundus autofluorescence in the management of recurrent punctate inner choroidopathy. Ocul Immunol Inflamm. 2011;19(4):286-292.

19. Li M, Zhang X, Wen F. The fundus autofluorescence spectrum of punctate inner choroidopathy. J Ophthalmol. 2015;2015(stage III).
20. The Standardization of Uveitis Nomenclature (SUN) Working group. Classification Criteria for Punctate Inner Choroiditis. Am J Ophthalmol. 2021;228:275-280.
21. The Standardization of Uveitis Nomenclature (SUN) Working group. Classification criteria for multifocal choroiditis with panuveitis. Am J Ophthalmol. 2021;228:152-158.
22. Herbort CP. Fluorescein and Indocyanine Green Angiography for Uveitis. Middle East Afr J Ophthalmol. 2009;16(4):168-187.
23. Dingerkus VLS, Munk MR, Brinkmann MP, et al. Optical coherence tomography angiography (OCTA) as a new diagnostic tool in uveitis. J Ophthalmic Inflamm Infect. 2019;9(1).
24. Amer R, Priel E, Kramer M. Spectral-domain optical coherence tomographic features of choroidal neovascular membranes in multifocal choroiditis and punctate inner choroidopathy. Graefe's Arch Clin Exp Ophthalmol. 2015;253(6):949-957.
25. Agarwal A, Handa S, Marchese A, et al. Optical Coherence Tomography Findings of Underlying Choroidal Neovascularization in Punctate Inner Choroidopathy. Front Med. 2021;8(December):1-8.
26. Astroz P, Miere A, Mrejen S, et al. Optical Coherence Tomography Angiography to Distinguish Choroidal Neovascularization From Macular Inflammatory Lesions in Multifocal Choroiditis. Retina. 2018;38:299-309.
27. Levison AL, Baynes KM, Lowder CY, Kaiser PK, Srivastava SK. Choroidal neovascularisation on optical coherence tomography angiography in punctate inner choroidopathy and multifocal choroiditis. Br J Ophthalmol. 2017;101:616-622.
28. Dutheil C, Korobelnik JF, Delyfer MN, Rougier MB. Optical coherence tomography angiography and choroidal neovascularization in multifocal choroiditis: A descriptive study. Eur J Ophthalmol. 2018;28(5):614-621.
29. Zahid S, Chen KC, Jung JJ, et al. OPTICAL COHERENCE TOMOGRAPHY ANGIOGRAPHY of CHORIORETINAL LESIONS DUE to IDIOPATHIC MULTIFOCAL CHOROIDITIS. Retina. 2017;37(8):1451-1463.
30. Herbort CP, Tugal-Tutkun I, Mantovani A, Neri P, Khairallah M, Papasavvas I. Advances and potential new developments in imaging techniques for posterior uveitis Part 2: invasive imaging methods. Eye. 2021;35(1):52-73.
31. Khaing TT, Okamoto T, Ye C, et al. Automatic measurement of choroidal thickness and vasculature in optical coherence tomography images of eyes with retinitis pigmentosa. Artif Life Robot. 2022;27(1):70-79.
32. Agarwal A, Abhaypal K, Aggarwal K, et al. The use of optical coherence tomography angiography in comparing choriocapillaris recovery between two treatment strategies for multifocal choroiditis: a pilot clinical trial. J Ophthalmic Inflamm Infect. 2022;12(1).
33. Thompson IA, Caplash S, Akanda M, et al. Optical Coherence Tomography Angiography Changes in Choroidal Vasculature following Treatment in Punctate Inner Choroidopathy. Ocul Immunol Inflamm. 2020;00(00):1-7.
34. Essilfie J, Bacci T, Abdelhakim AH, et al. Are There Two Forms of Multiple Evanescent White Dot Syndrome? Retina. 2022;42(2):227-235.

SUPPLEMENTARY DATA

Supplemental Table 6.1. Explanation of imaging characteristics

SD-OCT imaging		
	Location of the material	The location was graded as sub-RPE if the RPE was visible above the material. The lesion was graded as material fused with the RPE, if the material was located at the level of the RPE, but the exact location of the RPE could not be determined. This was mainly the case when the material had identical reflectivity as the RPE (Supplemental Figure 1A+1B).
	EZ/RPE	The EZ was graded as continuous in the case no disruptions or absent parts of the EZ were present. If the lesion demonstrated parts of EZ that were disrupted and parts that were absent/continuous, it was graded as disrupted. If the EZ was fuzzy, this was also graded as disrupted (Supplemental Figure 1A+1B).
	Reflectivity of the material	The reflectivity of the material was graded hyperreflective if the intensity of the reflectivity was similar to the intensity of the RPE. If the intensity was less, it was graded as moderately reflective (Supplemental Figure 1A+1B).
	Choroidal reflectivity	The reflectivity of the choroid was graded isoreflective if no hyper- or hyporeflectivity of the choroid was present. If both hyporeflective and hyperreflective parts were present, it was graded according to the predominantly present characteristic (Supplemental Figure 1A+1B).
	Fluid	Lesions could demonstrate intraretinal fluid, subretinal fluid and atrophic cysts simultaneously and therefore the score was not defined to one category.
	Choroidal thickness beneath the lesions	This was measured perpendicularly to Bruch's membrane. If Bruch's membrane was absent or not visisble, we draw a line between the two points were the RPE was present and used this line the measure the choroidal thickness (Supplemental Figure 2). In case multiple scan lines captured the lesion, the choroidal thickness was measured at the scan line capturing the infiltrative material. The choroidal thickness was measured at the same location in the identical scan line in both sets.
	Choroidal thickness distant from the lesions	This was measured perpendicularly to the RPE. This was measured on either the most upper or lowest scan line (3mm outside the foveal area) dependent on the location of the lesions. The choroidal thickness was measured at the same location in the identical scan line in both sets.
IR		
	Reflectance of the lesion	The lesion was graded hyperreflective if the lesion was not hyporeflective. If the lesion was isoreflective, it was graded as not visible.
	Reflectance of the margin of the lesion	The reflectance of the margin was graded as 'hyporeflective margin', 'hyperreflective margin' or 'no margin' (Supplemental Figure 3).
FAF		
	Patchy hyperautofluorescence	This was graded as 'present' in case hyperautofluorescent patches were observed not adjacent to or near lesions. In the literature this is also referred to as EpiMEDWS (Supplemental Figure 3).[34] This was only graded once per eye and not per lesion.

Supplemental Table 6.2. Imaging characteristics related to activity of CNV – SD-OCT(A)

	Inflammation with active CNV	**Inflammation without active CNV**	***P-value*[a]**
SD-OCT	n=14	n=96	
Location of material, n (%)			<0.001
No material	0 (0)	14 (15)	
Sub-RPE	1 (7)	24 (25)	
Material fused with the RPE	2 (14)	10 (10)	
Subretinal*	5 (36)	0 (0)	
Outer retina	0 (0)	20 (21)	
Sub-RPE with outer retinal infiltration	0 (0)	28 (29)	
Sub-RPE and subretinal*	6 (43)	0 (0)	
Reflectivity of material[b], n (%)			<0.001
No material	0 (0)	14 (15)	
Moderately reflective*	1 (7)	64 (67)	
Hyperreflective	0 (0)	7 (7)	
Mixed*	13 (93)	11 (11)	
EZ[b], n (%)			0.85
Continuous	0 (0)	3 (3)	
Disrupted	12 (86)	85 (89)	
Absent	2 (14)	8 (8)	
RPE[b], n (%)			0.75
Continuous	0 (0)	11 (11)	
Disrupted	14 (100)	83 (87)	
vAbsent	0 (0)	2 (2)	
Reflectivity of choroid, n (%)			<0.05
Isoreflective	3 (21)	27 (28)	
Hyperreflective	6 (43)	65 (68)	
Hyporeflective*	5 (36)	4 (4)	
Fluid, n (%)			<0.001[b]
None	7 (50)	88 (92)	
Intraretinal fluid (>50µm)	5 (36)	0 (0)	
Subretinal fluid	5 (36)	1 (1)	
Atrophic cysts (>50µm)	2 (14)	7 (7)	
Choroidal thickness underneath the lesion in µm, mean (SD)	262 (117)	205 (95)	0.30
SD-OCTA	n=12[c]	n=84[c]	
Vascular structure visible, n (%)	12 (100)	20 (24)	<0.001
GLD in µm, median [IQR]	620 [315-872]	420 [295-658]	0.63
Area in mm^2, median [IQR]	0.25 [0.12-0.43]	0.10 [0.06-0.22]	0.19
Blurry borders	7 (58)	15 (75)	0.68

Supplemental Table 6.2. Imaging characteristics related to activity of CNV – SD-OCT(A) (*continued*)

	Inflammation with active CNV	**Inflammation without active CNV**	***P-value*[a]**
Not well-defined vessels	7 (58)	14 (70)	0.85
Halo surrounding the vascular structure	11 (92)	13 (65)	0.43
Flow void visible, n (%)	11 (92)	82 (98)	0.68
Blurry borders	9 (75)	76 (93)	0.45
Area, median [IQR]	0.54 [0.43-1.27]	0.22 [0.11-0.51]	<0.01[d]

CNV, choroidal neovascularization; SD-OCT, spectral-domain optical coherence tomography; SD-OCTA, spectral-domain optical coherence tomography angiography; RPE, retinal pigment epithelium; EZ, ellipsoid zone; SD, standard deviation; GLD, greatest linear dimension; IQR, interquartile range.

[a] Results of the chi-square test (or fisher exact test) for categorical variables and the Wilcoxon Rank-Sum Test for continuous variables. False discovery rate at 5% was applied for all tested imaging characteristics to correct for multiple testing. The categories that demonstrated significantly different proportions between inflammatory lesions with and without active CNV are indicated with an asterisk (*).

[b] The presence of fluid vs no fluid was tested (atrophic cysts were not included in the analyses).

[c] SD-OCTA was not available for some lesions due to poor image quality or severe artifacts (2 lesions with active CNV and 12 lesions without active CNV).

[d] When comparing the 14 lesions with active CNV with the 46 lesions with pre-existent and inactive CNV, this imaging characteristics were no longer significant.

Supplemental Table 6.3. Imaging characteristics related to activity of CNV – other imaging modalities

	Inflammation with active CNV n=14	**Inflammation without active CNV n=96**	***P.value*[a]**
Lesion visible on			
Fundus picture (n=13/89[b]), n (%)	13 (100)	86 (97)	1.0
Hyperpigmentation, n (%)	11 (85)	47 (55)	0.23
Blurry borders, n (%)	11 (85)	69 (80)	1.0
Hemorrhage, n (%)	1 (8)	0 (0)	0.29
IR (n=14/96), n (%)	14 (100)	94 (98)	1.0
Hyperreflective lesion, n (%)	11 (79)	81 (86)	0.68
Hyporeflective margin, n (%)	4 (29)	53 (56)	0.28
Blurry borders, n (%)	12 (86)	73 (78)	0.85
FAF (n=13/91[b]), n (%)	12 (92)	86 (95)	0.78
Hyperautofluorescent margin, n (%)	6 (50)	34 (40)	0.85
Lesion area mm^2, median [IQR]	0.61 [0.25-1.26]	0.29 [0.10-0.76]	0.25
FA (n=13/93[b]), n (%)	13 (100)	90 (97)	1.0
Leakage, n (%)	6 (46)	4 (4)	<0.01
ICGA (n=96), n (%)	13 (93)	96 (100)	0.30
Hypofluorescence, n (%)	9 (69)	81 (84)	0.45
Blurry borders, n (%)	13 (100)	87 (91)	0.78
Lesion area mm^2, median [IQR]	1.72 [1.21-1.87]	0.49 [0.27-1.25]	<0.01[c]
% difference in area FAF and ICGA, median [IQR]	140 [18-243]	74 [25-145]	0.76

CNV, choroidal neovascularization; IR, infrared imaging; FAF, fundus autofluorescence; FA, fluorescein angiography; ICGA, indocyanine green angiography; IQR, interquartile range.

[a] Results of the chi-square test (or fisher exact test) for categorical variables and the Wilcoxon Rank-Sum Test for continuous variables. False discovery rate at 5% was applied for all tested imaging characteristics to correct for multiple testing.

[b] Not all imaging modalities were available for all lesions. The number of lesions with available data is indicated for both the number of lesions with active CNV and without active CNV. In one case with active CNV, no FA was performed due to a fluorescein allergy.

[c] When comparing the 14 lesions with active CNV with the 46 lesions with pre-existent and inactive CNV, this imaging characteristics were no longer significant.

A

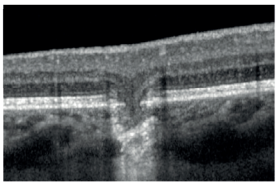

- No material
- Absent EZ
- Absent RPE
- Hyperreflectivity of the choroid

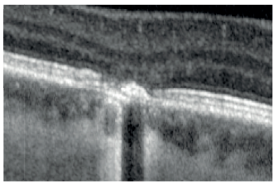

- Material fused with the RPE
- Absent EZ
- Disrupted RPE
- Hyperreflective material
- Hyporeflectivity of the choroid

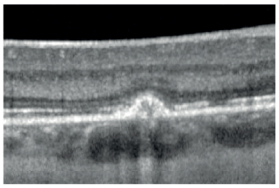

- Sub-RPE material
- Disrupted EZ
- Disrupted RPE
- Moderately reflective material
- Hyporeflectivity of the choroid

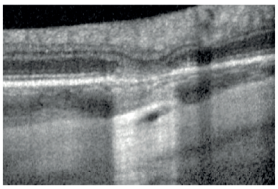

- Outer retinal infiltration
- Disrupted EZ
- Disrupted RPE
- Moderately reflective material
- Hyperreflectivity of the choroid

B

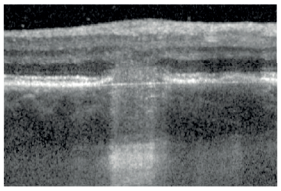

- Sub-RPE with outer retinal infiltration
- Disrupted EZ
- Disrupted RPE
- Moderately reflective material
- Hyperreflectivity of the choroid

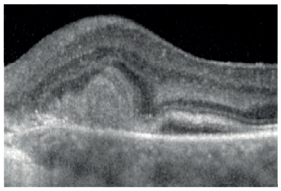

- Subretinal
- Disrupted EZ
- Continuous RPE
- Mixed reflective material
- Isoreflectivity of the choroid

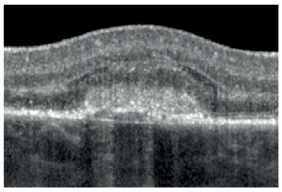

- Sub-RPE and subretinal
- Disrupted EZ
- Disrupted RPE
- Mixed reflective material
- Hyporeflectivity of the choroid

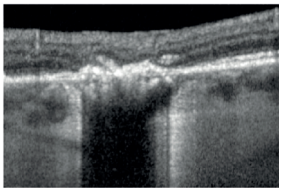

- Material fused with the RPE
- Absent EZ
- Disrupted RPE
- Hyperreflective material
- Hyporeflectivity of the choroid

Supplemental Figure 6.1. Examples of imaging characteristics on optical coherence tomography

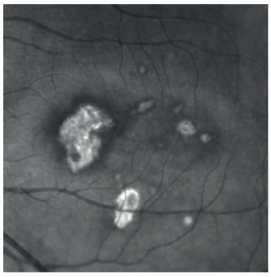

• Hyporeflective margin (NIR)

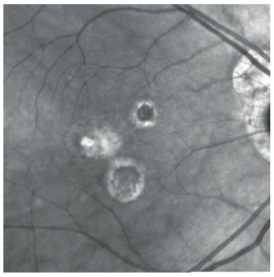

• No hyporeflective margin (NIR)

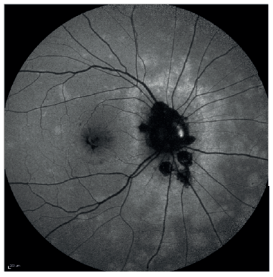

• Patchy hyperautofluorescence (EpiMEWDS) (FAF)

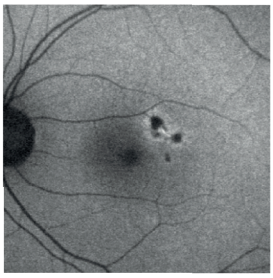

• Hyperautofluorent margin surrounding the lesions (FAF)

Supplemental Figure 6.2. Examples of imaging characteristics on fundus autofluorescence and near infrared imaging.

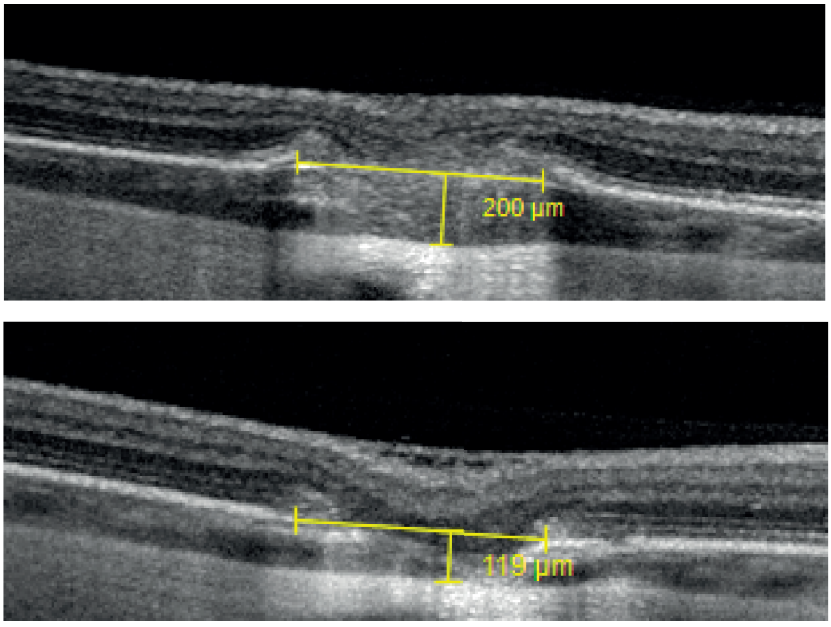

Supplemental Figure 6.3. Choroidal thickness measurement

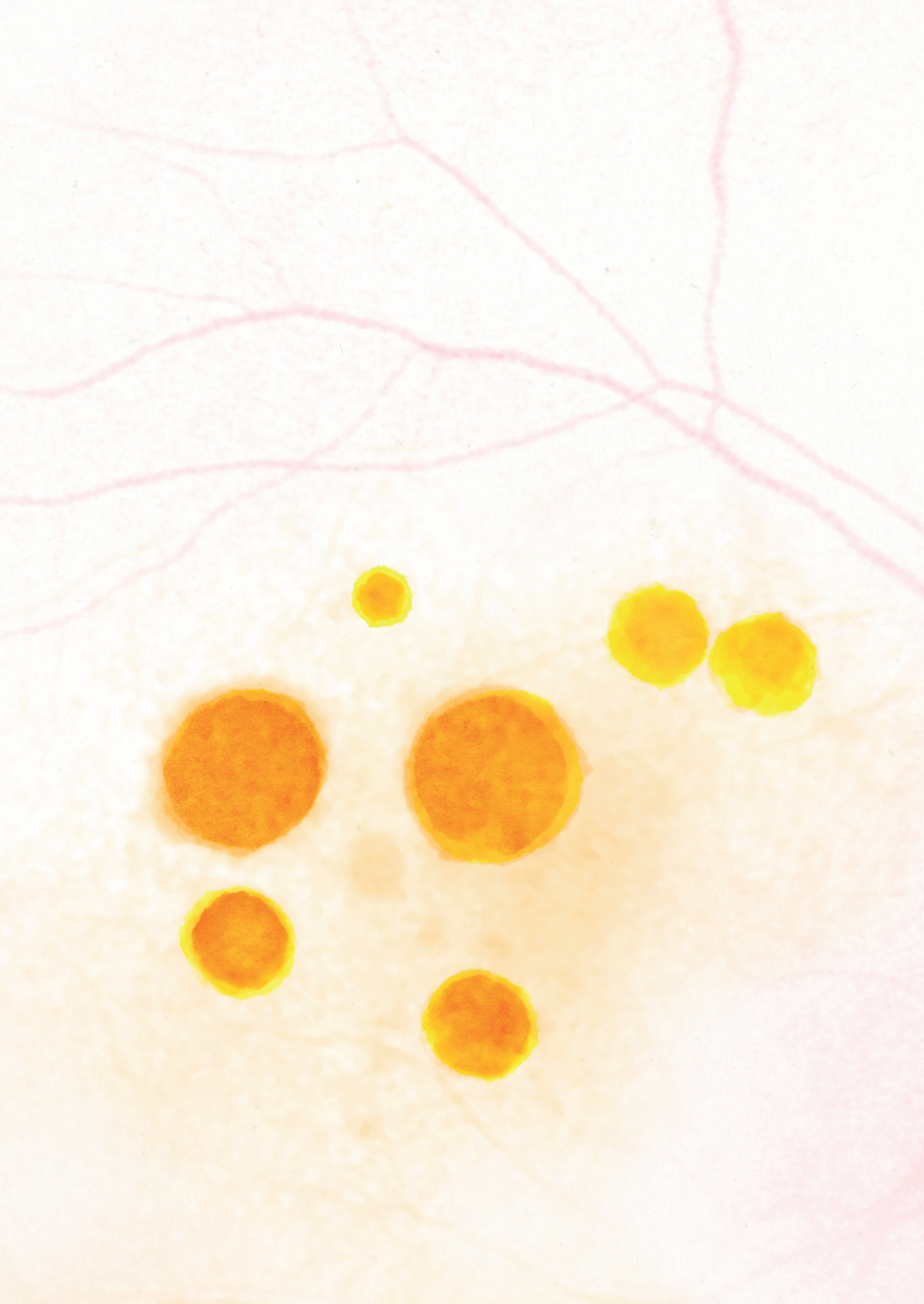

Chapter 7

Central Multifocal Choroiditis: Platelet Granularity as a Potential Marker for Treatment With Steroid-Sparing Immunomodulatory Therapy

Evianne L. de Groot
Jeannette Ossewaarde-van Norel
Imo E. Hoefer
Saskia Haitjema
Joke H. de Boer
Jonas J.W. Kuiper

Front. Ophthalmol. 2021; 784848. doi:10.3389/fopht.2021.784848

ABSTRACT

Purpose

We aimed to evaluate the blood cell composition in patients with central multifocal choroiditis (cMFC), a rare form of posterior uveitis predominantly affecting young myopic women.

Methods

In this retrospective observational case-control study, a 104-parameter automated hematocytometry was conducted by the Cell-Dyn Sapphire hematology analyzer for 122 cases and 364 age- and sex-matched controls. Cox proportional regression analysis was used to assess the relation between the blood cell composition and the time between disease onset (first visit) and the start of systemic corticosteroid-sparing immunomodulatory therapy (IMT).

Results

At a false discovery rate of 5% (P_{adj}), we identified a decrease of blood monocytes in cases with cMFC, which could be attributed to disease activity. Cox proportional hazard analysis including age and sex revealed that increased platelet granularity (measured by mean intermediate angle scatter) was an independent risk factor for treatment with IMT (hazard ratio = 2.3 [95% confidence interval = 1.28 - 4.14], P_{adj} = 0.049). The time between the first presentation and the start of IMT was 0.3 years in the group with an increased platelet granularity and 3.4 years in the group without increased platelet granularity.

Conclusions

Patients with cMFC demonstrated a decrease in blood monocytes. Moreover, platelet granularity could potentially be used as a marker for treatment with IMT.

INTRODUCTION

Central multifocal choroiditis (cMFC) is a group of inflammatory disorders of the choroid in the macular area of eyes. Predominantly young myopic Caucasian women are affected and the disease is often sight-threatening.[1,2] The clinical hallmark of white-yellowish lesions classifies these conditions among the white dot syndromes, and typically comprises several subtypes including *punctate inner choroidopathy (PIC)*,[3] *multifocal choroiditis (MFC)*,[4] *relentless placoid chorioretinitis (RPC)*,[5] *persistent placoid maculopathy (PPM)*[6] and *serpiginous choroiditis (SC)*.[7] CMFC is further characterized by hypofluorescent areas on indocyanine green angiography (ICGA) which in the active phase of the disease increase in size and have blurred margins. Moreover, it is typified by the absence of papillitis or vasculitis, which are often seen in other types of non-infectious uveitis. The etiology of cMFC is poorly understood, but the beneficial effect of systemic corticosteroids or corticosteroid-sparing immunomodulatory therapy (IMT) (e.g., methotrexate, adalimumab) on disease activity visualized with ICGA supports that inflammatory mechanisms drive the pathophysiology of cMFC.[8-11] In addition, small genetic studies indicated that susceptibility to cMFC is linked to immune genes including *IL10* and *TNF* loci, complement factor H (*CFH*) and increased prevalence of the Human Leukocyte Antigen DR2.[12-15] Immune profiling studies of cMFC are currently lacking. In this study, we aimed to compare the peripheral blood cell composition of patients with cMFC to control subjects. Secondly, we aimed to explore the relationship between the blood cell composition and disease severity using treatment with IMT as surrogate marker for disease severity.

MATERIALS AND METHODS

This observational case-control study was conducted in accordance with the Declaration of Helsinki including all its amendments. All patients were ≥18 years old and provided written informed consent to use their medical data for research purposes. The institutional review board of the University Medical Centre (UMC) of Utrecht approved this study.

Study Participants

Patients were diagnosed with cMFC in case they presented with chorioretinal scars in the posterior pole and without papillitis and vasculitis. Patients were subdivided in different subtypes based on the classification criteria of the Standardization of Uveitis Nomenclature working group for PIC, MFC and SC.[3,4,7] In case of overlapping criteria for different subtypes, this was resolved with discussion. Moreover, patients with RPC

and PPM were diagnosed based on typical appearance on multimodal imaging.[5,6] On indication, other causes of inflammatory eye diseases were ruled out by diagnostic work-up for uveitis, including soluble interleukine-2 receptor, angiotensin converting enzyme, QuantiFERON-TB, HLA-B27 and HLA-A29 typing and X-ray of the chest.

To enable comparison of cMFC blood cell composition with a reference, for every cMFC patient, three control subjects were extracted from the Utrecht Patient Oriented Database (UPOD). These control subjects were healthy individuals that underwent a periodic occupational health examination and were matched by sex and age with maximum age deviation of four years.

Blood Cell Composition Analysis

Automated blood cell composition analyses were performed with the Abbott Cell-Dyn Sapphire (Abbott Diagnostics, Santa Clara, CA, USA) hematology analyzer and data for 104 parameters were analyzed and stored by the UPOD of the University Medical Centre Utrecht. The Abbott Cell-Dyn Sapphire automated blood cell analyzer uses five optical scatter signals measuring cell size [0 degrees scatter, axial light loss (ALL)], cell complexity and granularity [7 degrees scatter, intermediate angle scatter (IAS)], nuclear lobularity [90 degrees scatter, polarized side scatter (PSS)], depolarization [90 degrees depolarized side scatter (DSS)] and viability [red fluorescence 90 degrees (FL3), 630 ± 30 nm]. The structure and content of UPOD have been described in more detail elsewhere.[16] The blood cell analyzer is equipped with an integrated 488-nm blue diode laser and uses spectrophotometry, electrical impedance, laser light scattering (multi angle polarized scatter separation), and 3-color fluorescent technologies to measure morphological parameters of leukocytes, red blood cells, and platelets for classification and enumeration.[17,18] Details on the blood cell parameters measured by the Cell-Dyn Sapphire analyzer is provided in **Supplementary Table 7.1**. UPOD stores blood cell data for >3 million samples from the University Medical Centre Utrecht. Data on disease activity and treatment were extracted from the electronic patient records. If blood cell composition data was available for multiple visits, preferably a sample collected during active disease without systemic immunomodulatory therapy (n=76) was used. If not available consecutively we used a sample collected during inactive disease without systemic immunomodulatory therapy (n=18), during active disease with systemic immunomodulatory therapy (n=23) and during inactive disease with systemic immunomodulatory therapy (n=5) (**Table 7.1**).

Statistical Framework

Data analyses were performed in RStudio version 1.2.5001 (RStudio Team, Boston, USA) and R version 4.0.0 (R Foundation for Statistical Computing, Austria). Principal

component analysis (PCA) was performed in 111 patients and 323 control subjects with complete data using the *factoextra* R package[19] after scaling of the data. Group differences were tested using a likelihood ratio test (LRT) with a false discovery rate (FDR) of 5% and corrected for disease activity and treatment with systemic corticosteroids respectively (added as a covariate to the linear models). For survival analysis, feature selection was conducted by filtering for parameters that were different (LRT, age and sex adjusted P_{LRT}<0.05) between cases with early start of corticosteroid-sparing immunomodulatory therapy (IMT within 6 months after the first presentation in the UMC Utrecht) and cases starting IMT after 6 months after the first presentation in the UMC Utrecht. An optimal cut off point was calculated based on the maximum log-rank statistic using the *surv_cutpoint()* function of the *survminer* R package[20] with a minimal proportion of observations per group of 0.3. This cut off point was used for a survival analysis and the hazard ratios of these parameters were explored using a cox proportional hazards model with age and sex as covariates using the R package *survival.*[21]

Table 7.1. Patient characteristics: disease activity and systemic immunomodulatory therapy

Total of 122 patients	Active disease	Inactive disease
Number of patients without systemic immunomodulatory therapy	76	18
Number of patients treated with systemic corticosteroids	13	3
Number of patients treated with IMT	4	1
Number of patients treated with systemic corticosteroids + IMT	6	1

In the patient group (n=122), blood samples for blood cell composition analysis were selected based on the presence of disease activity and treatment with systemic immunomodulatory therapy (systemic corticosteroids or IMT).
IMT, corticosteroid-sparing immunomodulatory therapy.

RESULTS

Study Population

Retrospective search by UPOD revealed available blood cell composition data for 122 cMFC patients measured between May 2005 and April 2020. The median age (range) at time of blood sampling of the 122 patients was 42 (16-80) years and 104 patients (85%) were female. The control group consisted of 364 individuals, of which 311 (85%) females, and with a median age (range) of 42 (17-83). Thirty-four (28%) patients were diagnosed with punctate inner choroidopathy (PIC), 71 (58%) patients with multifocal choroiditis (MFC), 2 (2%) patients with persistent placoid maculopathy (PPM), 4 (3%) patients with serpiginous choroiditis (SC) and 11 (9%) patients with relentless placoid chorioretinitis (RPC).

Decreased Blood Monocyte Count in Patients With cMFC

Principal component analysis revealed no global differences between the cMFC and reference population (**Figure 7.1A**), indicating that the blood profiles were largely comparable. At a false discovery rate (FDR) of 5%, we detected differences for 6 neutrophil and monocyte parameters (**Table 7.2**, and **Figures 7.1B–D**); specifically, the monocyte count and percentage of monocytes were decreased in cMFC patients (**Table 7.2**). Adjusting for disease activity (i.e., added as a covariate in the linear models) mitigated the signal for monocytes (P_{adj} > 0.05). Adjusting for treatment with systemic corticosteroids did not change the signal for monocytes, indicating that the decrease of monocytes could be primarily attributed to disease activity in patients.

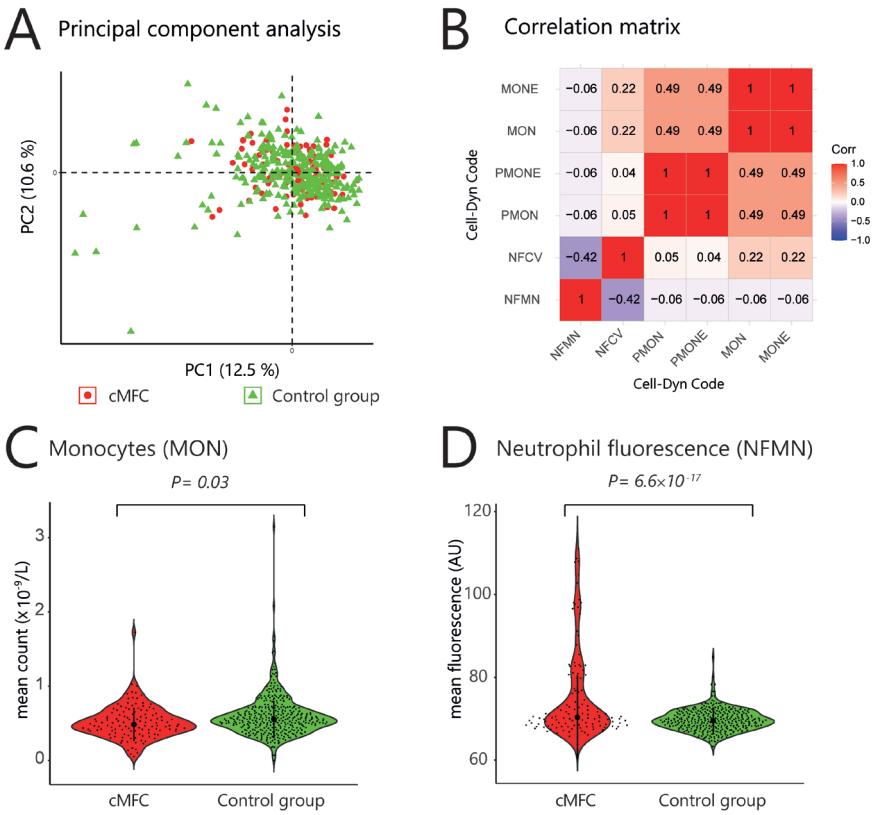

Figure 7.1 (**A**) Principal component analysis of blood cell count data from patients (red dots) and controls subjects (green triangles). (**B**) Correlation matrix of the six parameters associated with cMFC (Likelihood ratio test, P_{adj}<0.05) (**C, D**) Violin plots of the mean monocyte count (Cell-Dyn code MON) and the neutrophil fluorescence (NFMN) for cMFC cases and controls.

NFMN, mean FL3-fluorescence of neutrophil granulocytes; NFCV, the coefficient of variance as percentage of the mean of the FL3-fluorescence of neutrophil granulocytes; MON, number of monocytes; MONE, absolute number of monocytes without blasts; PMON, monocytes as percentage of all leukocytes; PMONE, the number of monocytes without blasts as percentage of all leukocytes; PC, principal component.

Table 7.2. Differences in blood cell composition parameters between patients with cMFC and healthy controls.

Description	Cell-Dyn Code	cMFC (n=122) median (IQR)	Controls (n=364) median (IQR)	P_{adj}	P_{adj} - corrected for disease activity	P_{adj} - corrected for systemic corticosteroids
Neutrophil fluorescence (AU)	NFMN	70.3 (68.4 - 77.9)	69.5 (68.0 - 71.3)	6.6×10^{-17}	0.04	3.5×10^{-16}
Neutrophil fluorescence (AU)	NFCV	7.6 (6.2 - 9.1)	8.2 (6.9 - 9.2)	0.030	0.86	5.9×10^{-3}
Blood monocyte count (x 10^9/L)	MON	0.48 (0.40 - 0.62)	0.56 (0.44 - 0.69)	0.026	0.87	5.9×10^{-3}
Blood monocyte count (without blasts) (x 10^9/L)	MONE	0.48 (0.39 - 0.62)	0.56 (0.44 - 0.69)	0.024	0.87	5.9×10^{-3}
Blood monocyte %	PMON	6.52 (5.35 - 7.88)	7.33 (6.08 - 8.95)	4.3×10^{-3}	0.87	0.06
Blood monocyte % (without blasts)	PMONE	6.52 (5.33 - 7.88)	7.33 (6.08 - 8.95)	4.1×10^{-3}	0.87	0.05

The adjusted *P*-values (false discovery rate of 5% from likelihood ratio test) (*Padj*) are indicated with and without including disease activity or systemic corticosteroids as covariate in the linear model.
cMFC, central multifocal choroiditis; IQR, interquartile range; AU, arbitrary units; NFMN, mean FL3-fluorescence of neutrophil granulocytes; NFCV, the coefficient of variance as percentage of the mean of the FL3-fluorescence of neutrophil granulocytes; MON, number of monocytes; MONE, absolute number of monocytes without blasts; PMON, monocytes as percentage of all leukocytes; PMONE, the number of monocytes without blasts as percentage of all leukocytes.

Table 7.3 Clinical characteristics associated with neutrophil fluorescence

	Low NFMN (n=85)	High NFMN (n=35)	*P*-value
Mean age[a]	42.7	41.0	0.49
Female/cases (%)[b]	70/85 (82.4%)	32/35 (91.4%)	0.33
FA-ICGA (%)[b,c]	7/85 (8.2%)	33/35 (94.3%)	6.9×10^{-19}

The patients with available data on neutrophil fluorescence (NFMN) (n=110) were divided in a group with a low NFMN (n=85) and high NFMN (n=35) using the mean of all patients of 75.1 arbitrary units as a cut-off point.
NFMN, mean FL3-fluorescence of neutrophil granulocytes; FA-ICGA, fluorescein and indocyanine green angiography.
[a] Student's t-test
[b] Chi-square ($\chi 2$) test
[c] The FA-ICGA was performed within 8 hours prior to blood sampling.

We also detected enhanced FL3 fluorescence of blood neutrophils (Cell-Dyn parameter; NFMN) in cMFC patients (**Table 7.2**). After correcting for disease activity, the increased fluorescence of neutrophils (NFMN) remained significant (P_{adj} = 0.04) (**Table 7.2**). Since enhanced fluorescence of neutrophils is unexpected [only reported in patients using certain anti-psychotic drugs[18]], we used available clinical parameters to infer possible confounders. To this end, we stratified cases according to the mean fluorescence of neutrophils of all patients (cut-off NFMN parameter = 75.1). Comparison of cases with relatively high and low fluorescence of neutrophils revealed comparable distributions for age and sex (**Table 7.3**). In contrast, 94% of cases with increased fluorescence

in neutrophils (NFMN>75.1) were subjected to fluorescein and indocyanine green angiography within 8 hours prior to blood sampling compared to 8% of cases without increased fluorescence of neutrophils (χ2; $P = 6.9 \times 10^{-19}$) (**Table 7.3**). This suggests that the increased fluorescence of blood neutrophils in cMFC was most likely directly related to exposure to fluorescent dyes for ocular imaging just prior to blood cell measurement.

Platelet Granularity Is Associated With Systemic Corticosteroid-Sparing Immunomodulatory Treatment

Next, we investigated if blood cell composition parameters could be used as a marker for treatment with systemic corticosteroid-sparing immunomodulatory therapy (IMT). For this analysis we included 69 patients with available blood cell composition data at time of the disease onset (first visit) and without systemic treatment. First, we filtered for parameters that were most associated with early start of IMT by comparing cases that started IMT within the first 6 months versus other cases using a likelihood ratio test. This analysis identified 9 parameters (P_{LRT}<0.05) considered for further investigation, including several parameters related to blood platelets. Cox proportional hazards analysis for these 9 parameters (adjusting for age and sex) identified increased platelet granularity (≧148.7 units, Cell-Dyn code PIMN) as a risk factor for treatment with IMT in cMFC patients (hazard ratio = 2.3, 95% confidence interval = 1.28-4.14, P_{adj} = 0.049) (**Table 7.4**). Correcting for disease activity (added as a covariate in addition to age and sex in the model) moderately affected the association between platelet granularity and treatment with IMT ($P_{adj:\ age+sex+activity}$= 0.13). The median time between the first presentation in the UMC Utrecht and the start of IMT was 98 days (0.3 years) for cases with increased platelet granularity (≧148.7 units), and 1236 days (3.4 years) in cases without

Table 7.4. The results for the cox proportional hazards model for the probability for treatment with IMT in cMFC cases stratified by the degree of platelet granularity.

Description	Cell-Dyn code	Median (IQR)	Cut-off	N (high/ low)		HR (95% CI)	*P*-value	P_{adj}-value
Platelet granularity	*PIMN*	148.4 (144.4-152.6)	148.7	32/36	Univariate	2.19 (1.23-3.90)	0.008	0.038
					Multivariate (age + sex)	2.30 (1.28-4.14)	0.005	0.049
					Multivariate (age + sex + disease activity)	1.98 (1.11-3.56)	0.02	0.13

The results for both the univariate model and the multivariate model including the covariates age and sex are demonstrated both without (*P*-value) and with (P_{adj}-value) false discovery rate correction at 5%.
IMT, corticosteroid-sparing immunomodulatory therapy; cMFC, central multifocal choroiditis; IQR, interquartile range; HR, hazard ratio; CI, confidence interval; PIMN, platelet count measured at intermediate angle scatter of 7 degrees.

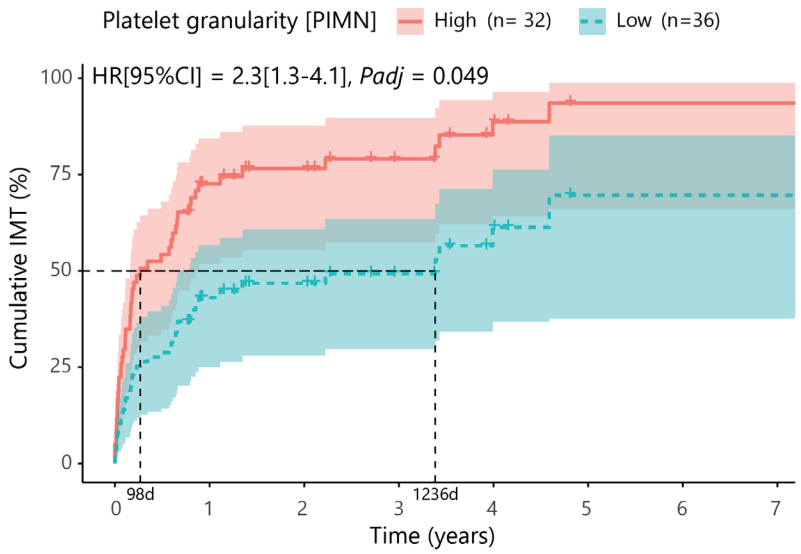

Figure 7.2 Cumulative incidence curve (Cox proportional hazards model corrected for age and sex with false discovery rate correction at 5%) for the probability for IMT in cMFC cases stratified by the degree of platelet granularity. The horizontal axis (x-axis) represents time in years, and the vertical axis (y-axis) shows the cumulative proportion of patients that are treated with IMT. The red line indicates the cases with high granularity (≧148.7 units for Cell-Dyn code PIMN) and the blue line indicates the curve for cases with low granularity (<148.7 units). The 95% confidence interval for each curve is also shown. The dotted lines represent the median time to start treatment with IMT in the group with a high and a low PIMN, which were 98 days and 1236 days, respectively.
HR, hazard ratio; CI, confidence interval; PIMN, platelet count measured at intermediate angle scatter of 7 degrees; IMT; corticosteroid-sparing immunomodulatory therapy; d, days.

increased granularity (<148.7 units) (**Figure 7.2**). Note that the platelet granularity was not significantly different between the subtypes of cMFC.

DISCUSSION

In this study, we investigated differences in blood cell composition parameters between patients with cMFC and control subjects. Although overall the differences were moderate, we identified a decrease in monocytes linked to disease activity in cMFC. We further revealed that an increased platelet granularity is a risk factor for treatment with IMT.

Although none of our cMFC cases exhibited a monocyte count below $0.2x10^9$/L (i.e., monocytopenia), the number and percentage of blood monocytes were decreased as compared to healthy controls. Monocytes are inflammatory cells central to immune pathology in a wide variety of chronic inflammatory conditions and our data support that these cells are related to disease activity in cMFC.[22] Decreased monocyte counts have been reported in chronic inflammatory conditions, such as systemic lupus

erythematosus,[23] and eye inflammation, including in Fuchs uveitis syndrome.[22,24] Since treatment with systemic corticosteroids tends to influence the monocyte count we adjusted for corticosteroids use (**Table 7.2**). Adjusting for concomitant corticosteroid use further strengthened the observation of decreased monocytes in cMFC. This makes it tempting to speculate that in the active stage of cMFC, monocytes become activated, and migrate into tissue to differentiate into macrophages as is observed in other forms of vasculitis.[25-27] This may possibly result in a relatively low monocyte count. Although a routine hematology analyzer does not differentiate monocyte subsets, the monocyte population is heterogeneous and single cell technology could quickly reveal novel subsets that play a role in ocular inflammation.[22,28] Application of single-cell transcriptomics to leukocytes from cMFC patients will be required to dissect the precise changes in composition of subsets of leukocytes in this condition.

We detected that a subset of patients exhibited enhanced FL3 neutrophil granulocyte fluorescence. Although autofluorescence of neutrophils can drop after bacterial infection,[29] an increase in fluorescence of blood neutrophils is only reported after clozapine use,[18] which made us consider to evaluate the exposure to fluorescent agents commonly used for ocular imaging. Although our evidence remains circumstantial, fluorescein and indocyanine green angiography within 8 hours prior to sampling was able to explain nearly all cases with enhanced neutrophil FL3 signals. The most simple explanation is that neutrophils take up the fluorescein dye which subsequently is measured in the FL3 channel of the automated hematology analyzer as an increased fluorescence of the neutrophils.[30-32]

Patients with cMFC show great heterogeneity in disease course, considering relapse rate and in line with this whether or not they require systemic treatment with IMT.[1] Postponing treatment with IMT may result in irreversible retinal damage and deterioration of visual functioning. On the other hand, overtreatment is a burden for the patient and increases the risk for considerable side-effects, which may compromise future therapy compliance.[33] Approaches that aid in patient stratification to predict at an early stage whether or not the patient will require systemic treatment with IMT will help alleviate the raised concerns on adequate application of IMT in the treatment of cMFC. The use of IMT in this patient group is also challenging considering that patients are often young and in the fertile stage of life, which warrant accurate predictive tools to help guide shared decision making by uveitis experts and patients. In this study, treatment with IMT is considered a surrogate marker for disease severity since patients with more severe disease are more likely to start treatment with IMT. Though one should keep in mind that the decision to start with treatment with IMT is dependent on more factors

such as bilateral ocular involvement, macular involvement, development of choroidal neovascularization and the preference of the patient.

In an attempt to provide a framework for patient risk stratification in the context of IMT, we deliberately used data from a routine hematology analyzer that is widely available and thus may allow prompt adaptation of its results in a clinical setting. We discovered that patients with a relatively high granularity (i.e., cell "complexity") of platelets were at higher risk for starting IMT with a median time to start with IMT that was approximately 10-fold shorter compared to cases with relatively low granularity. The Cell-Dyn Sapphire hematology analyzer has high sensitivity and fully automatically assesses the whole blood composition using optical light scatter and fluorescent signals, of which the platelet complexity is detected under a 7° angle light scatter[34] which is very similar to SSC from flow cytometer.[35] Although not exceeding the threshold for statistical significance in the Cox regression, other platelets parameters were also linked to IMT in cMFC, including the "platelet distribution width" (cases that started IMT within the first 6 months versus other cases, P_{LRT}= 0.01) and "mean polarized platelets" (P_{LRT} =0.008), suggesting that besides platelets complexity also the size of platelets is linked to the risk for IMT.

The disease mechanisms driving cMFC are poorly understood, but immune pathology is considered central to its pathogenesis. Previous studies have linked variants in complement genes (i.e., *CFH* and *CFB* genes) to susceptibility to cMFC.[13] This is of interest, because increasing evidence supports a close relationship between complement and platelets.[36] Therefore, platelets are increasingly recognized as key contributors to immune responses and are involved in disease mechanisms of several chronic inflammatory diseases.[37-39] This relation is thought to be mediated by the observation that platelets can secrete proinflammatory cytokines and chemokines stored in granules which can activate the complement cascade. Moreover, on the other hand complement activation can also lead to platelet activation.[36,40] Immature platelets are generally larger in size, contain higher dense granules content and are thought to be more hyper-reactive than the mature platelets.[41] Possibly, the increased platelet granularity observed in cMFC patients may reflect an increased proportion of immature platelets. This concept is supported by the suggestive association of the increased size of the platelets (parameter platelet distribution width) since this is also associated with immaturity of platelets. Interestingly, in the literature a positive correlation was found between the proportion of immature platelets, the size of platelets and the disease activity score in patients with systemic lupus erythematosus (SLE).[42] SLE is an autoimmune disease primarily affecting women, similar to cMFC. Moreover, the inflammatory choriocapillaropathy observed in cMFC is in fact a form of choroidal vasculitis.[43] In systemic vasculitis including giant cell

arthritis and Behcet disease, markers of platelet activation are observed to be higher during active disease.[44] Moreover, Von Willebrand Factor, a marker for endothelial cell activation and a mediator for platelet activation, is observed to be increased in Behcet disease and ischemic retinal vasculitis.[45] The data used in this study reports on morphology and enumeration of cells and not on functionality. Therefore we are unable to determine the relationship between platelet activity and the start of treatment with IMT.

It is tempting to speculate that in cMFC, platelets play a role in the pathophysiology of cMFC. We suggest that the association between platelet granularity and the start of IMT we observed in this study could be explained by the fact that both the platelet granularity and the start of IMT are related to the severity of the inflammation in the choriocapillaris. A proposed disease mechanism is that inappropriate complement regulation leads to endothelial activation which on its turn mediates platelet activation. Activated platelets can form platelet aggregates in the choriocapillaris, a phenomenon known to occur in cutaneous small vessel vasculitis.[46] Hypothetically, these platelet aggregates form microthrombi in the choriocapillaris resulting in capillary dropout as observed as hypofluorescent areas on indocyanine green angiography imaging. Nevertheless more research is needed, particularly regarding the functionality of platelets, in patients with cMFC to confirm our findings and to further unravel the pathophysiological mechanism of cMFC. Possibly, detailed analysis of platelets function, using analysis of surface receptors can help dissect the platelet subsets affected in cMFC and help improve patient stratification approaches.[47] Moreover, is would be interesting to explore the presence of markers of endothelial activation, including Von Willebrand Factor, or antibodies against platelets, for example antiphospholipid antibodies, to attempt to further unravel the pathophysiology of cMFC.

The results of this study should be interpreted with the knowledge of possible limitations of this study. The number of cases we used for this study is based on available data in the UPOD database rather than determined by a power calculation. Moreover, the control subjects used in this study were relatively young individuals that underwent blood sampling in the context of a periodic occupational health examination. These subjects were not checked for comorbidities, though considering the young age it is unlikely, but cannot be ruled out, that these subjects have underlying comorbidities.

To our knowledge, this is the first study reporting on readily available blood cell composition parameters in patients with cMFC. We evaluated these parameters in a large group of patients, especially considering the rarity of the disease. In our study population most patients were diagnosed with MFC and only a minority with the other

subtypes PIC, PPM, RPC or SC. It will be interesting to compare changes in platelets in subgroup analysis using larger cohorts in future studies.

In conclusion, we found a decreased level of monocytes in patients compared to control subjects. Moreover, increased platelet granularity could potentially be used as a marker for treatment with IMT.

ACKNOWLEDGMENTS

For this study data from the Utrecht Patient Oriented Database (UPOD) were used. UPOD is an infrastructure of relational databases comprising data on patient characteristics, hospital discharge diagnoses, medical procedures, medication orders and laboratory tests for all patients treated at the University Medical Centre Utrecht (UMC Utrecht) since 2004. The UMC Utrecht is a 1,042-bed academic teaching hospital in the center of the Netherlands, with annually about 28,000 clinical and 15,000 day-care hospitalizations and 334,000 outpatient visits. UPOD data acquisition and management is in accordance with current regulations concerning privacy and ethics. The structure and content of UPOD have been described in more detail elsewhere.[16]

REFERENCES

1. Ahnood D, Madhusudhan S, Tsaloumas MD, Waheed NK, Keane PA, Denniston AK. Punctate inner choroidopathy: A review. Surv Ophthalmol. 2017;62(2):113-126.
2. Fung AT, Pal S, Yannuzzi NA, et al. Multifocal choroiditis without panuveitis; Clinical Characteristics and Progression. Retina. 2014;34(1):98-107.
3. The Standardization of Uveitis Nomenclature (SUN) Working group. Classification Criteria for Punctate Inner Choroiditis. Am J Ophthalmol. 2021;228:275-280.
4. The Standardization of Uveitis Nomenclature (SUN) Working group. Classification criteria for multifocal choroiditis with panuveitis. Am J Ophthalmol. 2021;228:152-158.
5. Jones EB, Jampol LM, Yannuzzi LA, et al. Relentless placoid chorioretinitis. Arch Ophthalmol. 2000;118:931-938.
6. Kolomeyer AM, Brucker AJ. Persistent Placoid Maculopathy: A Systematic Review. Retina. 2018;38(10):1881-1895.
7. The Standardization of Uveitis Nomenclature (SUN) Working group. Classification Criteria for Serpiginous Choroiditis. Am J Ophthalmol. 2021;228:126-133.
8. de Groot EL, ten Dam-van Loon NH, de Boer JH, Ossewaarde-van Norel J. The efficacy of corticosteroid-sparing immunomodulatory therapy in treating patients with central multifocal choroiditis. Acta Ophthalmol. 2020;98(8):816-821.
9. Spaide RF, Goldberg N, Freund KB. Redefining multifocal choroiditis and panuveitis and punctate inner choroidopathy through multimodal imaging. Retina. 2013;33(7):1315-1324.
10. Turkcuoglu P, Chang PY, Rentiya ZS, et al. Mycophenolate mofetil and fundus autofluorescence in the management of recurrent punctate inner choroidopathy. Ocul Immunol Inflamm. 2011;19(4):286-292.
11. de Groot EL, Ossewaarde - van Norel J, Ho L, ten Dam - van Loon NH, de Boer JH. The efficacy of adalimumab in treating patients with central multifocal choroiditis. Am J Ophthalmol Case Reports. 2020;20:100921.
12. Atan D, Fraser-Bell S, Plskova J, et al. Punctate Inner choroidopathy and multifocal choroiditis with panuveitis share haplotypic associations with IL10 and TNF loci. Investig Ophthalmol Vis Sci. 2011;52(6):3573-3581.
13. Ferrara DC, Takahashi BS, Yannuzzi LA, et al. Analysis of major alleles associated with age-related macular degeneration in patients with multifocal choroiditis: Strong association with complement factor H. Arch Ophthalmol. 2008;126(11):1562-1566.
14. Moshfeghi DM, Blumenkranz MS. Role of genetic factors and inflammation in age-related macular degeneration. Retina. 2007;27(3):269-275.
15. Spaide RF, Skerry JE, Yannuzzi LA, Derosa JT. Lack of the HLA-DR2 specificity in multifocal choroiditis and panuveitis. Br J Ophthalmol. 1990;74(9):536-537.
16. Ten Berg MJ, Huisman A, Van Den Bemt PMLA, Schobben AFAM, Egberts ACG, Van Solinge WW. Linking laboratory and medication data: New opportunities for pharmacoepidemiological research. Clin Chem Lab Med. 2007;45(1):13-19.
17. Gijsberts CM, Den Ruijter HM, De Kleijn DPV, et al. Hematological Parameters Improve Prediction of Mortality and Secondary Adverse Events in Coronary Angiography Patients. Med (United States). 2015;94(45):e1992.
18. Man WH, ten Berg M, Wilting I, et al. Fluorescence of neutrophil granulocytes as a biomarker for clozapine use. Eur Neuropsychopharmacol. 2013;23(11):1408-1413.

19. Kassambara A, Mundt F. factoextra: Extract and Visualize the Results of Multivariate Data Analyses. R package version 1.0.7. Published online 2020.
20. Kassambara A, Kosinski M, Biecek P. survminer: Drawing Survival Curves using “ggplot2”. R package version 0.4.9. Published online 2021.
21. Therneau TM. A Package for Survival Analysis in R. R package version 3.2-11. Published online 2021.
22. Ma WT, Gao F, Gu K, Chen DK. The role of monocytes and macrophages in autoimmune diseases: A comprehensive review. Front Immunol. 2019;10(MAY):1-24.
23. Li Y, Lee PY, Sobel ES, et al. Increased expression of FcγRI/CD64 on circulating monocytes parallels ongoing inflammation and nephritis in lupus. Arthritis Res Ther. 2009;11(1):1-13.
24. Simsek M, Ozdal PC. Inflammatory markers of complete blood count in Fuchs uveitis syndrome. Can J Ophthalmol. 2021;56(3):197-2020.
25. Vegting Y, Vogt L, Anders HJ, de Winther MPJ, Bemelman FJ, Hilhorst ML. Monocytes and macrophages in ANCA-associated vasculitis. Autoimmun Rev. 2021;20(10):102911.
26. Şahin Ş, Lawrence R, Direskeneli H, Hamuryudan V, Yazici H, Akoğlu T. Monocyte activity in Behcet’s disease. Br J Rheumatol. 1996;35(5):424-429.
27. Muller Kobold AC, Kallenberg CGM, Cohen Tervaert JW. Monocyte activation in patients with Wegener’s granulomatosis. Ann Rheum Dis. 1999;58(4):237-245.
28. Hu Y, Hu Y, Xiao Y, et al. Genetic landscape and autoimmunity of monocytes in developing Vogt-Koyanagi-Harada disease. Proc Natl Acad Sci U S A. 2020;117(41):25712-25721.
29. Monsel A, Lécart S, Roquilly A, et al. Analysis of autofluorescence in polymorphonuclear neutrophils: A new tool for early infection diagnosis. PLoS One. 2014;9(3):1-10.
30. Bürgisser P, Vaudaux J, Bart PA. Severe interference between retinal angiography and automated four-color flow cytometry analysis of blood mononuclear cells. Cytom Part A. 2007;71(8):632-636.
31. Meisingset KK, Steen HB. Intracellular binding of fluorescein in lymphocytes. Cytometry. 1981;1(4):272-278.
32. Felberg NT, Haimowitz AJ. Flow cytometry of leukocytes after intravenous fluorescein angiography. Cytometry. 1985;6(1):74-76.
33. Spierings J, Sloeserwij A, Vianen ME, et al. Health-related quality of life in patients with immune mediated inflammatory diseases: A cross-sectional, multidisciplinary study. Clin Immunol. 2020;214:108392.
34. Grimaldi E, Del Vecchio L, Scopacasa F, et al. Evaluation of the platelet counting by Abbott CELL-DYN® SAPPHIRETM haematology analyser compared with flow cytometry. Int J Lab Hematol. 2009;31(2):151-160.
35. Groeneveld KM, Heeres M, Leenen LPH, Huisman A, Koenderman L. Immunophenotyping of posttraumatic neutrophils on a routine haematology analyser. Mediators Inflamm. 2012;2012.
36. Eriksson O, Mohlin C, Nilsson B, Ekdahl KN. The human platelet as an innate immune cell: Interactions between activated platelets and the complement system. Front Immunol. 2019;10:1590.
37. Habets KLL, Huizinga TWJ, Toes REM. Platelets and autoimmunity. Eur J Clin Invest. 2013;43(7):746-757.
38. Liu X, Gorzelanny C, Schneider SW. Platelets in skin autoimmune diseases. Front Immunol. 2019;10:1453.
39. Łukasik ZM, Makowski M, Makowska JS. From blood coagulation to innate and adaptive immunity: the role of platelets in the physiology and pathology of autoimmune disorders. Rheumatol Int. 2018;38(6):959-974.

40. Blair P, Flaumenhaft R. Platelet α-granules: Basic biology and clinical correlates. Blood Rev. 2009;23(4):177-189.
41. Perelshtein Brezinov O, Sevylia Z, Rahkovich M, et al. Measurements of immature platelet fraction and inflammatory markers in atrial fibrillation patients - Does persistency or ablation affect results? Int J Lab Hematol. 2021;43(4):602-608.
42. Hanata N, Shoda H, Kono M, et al. Immature platelet levels correlate with disease activity and predict treatment response of thrombocytopenia in lupus patients. Lupus. Published online 2021.
43. Bouchenaki N, Cimino L, Auer C, Tran VT, Herbort CP. Assessment and classification of choroidal vasculitis in posterior uveitis using indocyanine green angiography. Klin Monbl Augenheilkd. 2002;219(4):243-249.
44. Misra DP, Agarwal V. Innate immune cells in the pathogenesis of primary systemic vasculitis. Rheumatol Int. 2016;36(2):169-182.
45. Probst K, Fijnheer R, Rothova A. Endothelial cell activation and hypercoagulability in ocular Behçet?s disease. Am J Ophthalmol. 2004;137(5):850-857.
46. Meijer-Jorna LB, Mekkes JR, Van Der Wal AC. Platelet involvement in cutaneous small vessel vasculitis. J Cutan Pathol. 2002;29(3):176-180.
47. Blair TA, Michelson AD, Frelinger AL. Mass Cytometry Reveals Distinct Platelet Subtypes in Healthy Subjects and Novel Alterations in Surface Glycoproteins in Glanzmann Thrombasthenia. Sci Rep. 2018;8(1):1-13.

SUPPLEMENTARY DATA

Supplementary Table 7.1. Cell-Dyn Codes blood cell composition parameters measured within the UPOD database

Leukocytes			
WBC	White blood cell count (x 10^9/L)	WVF	White blood cell viability fraction
Neutrophil granulocytes			
NEU	Neutrophil count (x 10^9/L)	PNEU	% neutrophils of leukocyte count
SEG	Segmented neutrophil count (x 10^9/L)	PSEG	% segmented neutrophils of leukocyte count
BND	Banded neutrophil count (x 10^9/L)	PBND	% banded neutrophils of leukocyte count
IG	Immature granulocyte count (x 10^9/L)	PIG	% immature granulocytes of leukocyte count
NAMN	Mean neutrophil 0 degrees (ALL)	NACV	CV% neutrophil 0 degrees (ALL)
NIMN	Mean neutrophil 7 degrees (IAS)	NICV	CV% neutrophil 7 degrees (IAS)
NPMN	Mean neutrophil 90 degrees polarized (PSS)	NPCV	CV% neutrophil 90 degrees polarized (PSS)
NDMN	Mean neutrophil 90 degrees depolarized (DSS)	NDCV	CV% neutrophil 90 degrees depolarized (DSS)
NFMN	Mean fluorescence neutrophil (FL3)	NFCV	CV% fluorescence neutrophil (FL3)
Lymphocytes			
LYM	Lymphocyte count (x 10^9/L)	PLYM	% lymphocytes of leukocyte count
LYME	Lymphocyte count without atypical lymphocytes (x 10^9/L)	PLYME	% lymphocytes without atypical lymphocytes of leukocyte count
VLYM	Atypical lymphocyte count (x 10^9/L)	PVLYM	% atypical lymphocytes of leukocyte count
LAMN	Mean lymphocyte 0 degrees (ALL)	LACV	CV% lymphocyte 0 degrees (ALL)
LIMN	Mean lymphocyte 7 degrees (IAS)	LICV	CV% lymphocyte 7 degrees (IAS)
Monocytes			
MON	Monocyte count (x 10^9/L)	PMON	% monocytes of leukocyte count
MONE	Monocyte count without blasts (x 10^9/L)	PMONE	% monocytes without blasts of leukocyte count
BLST	Blast count without monocytes (x 10^9/L)	PBLST	% blasts without monocytes of leukocyte count
Eosinophils + Basophils			
EOS	Eosinophil count (x 10^9/L)	PEOS	% eosinophils of leukocyte count
BAS	Basophil count (x 10^9/L)	PBAS	% basophils of leukocyte count
Platelets			
PLT	Platelet count (x 10^9/L)	PCT	Platelet crit (ml/L)
PLTO	Platelet count (x 10^9/L) optical measurement	PLTI	Platelet count (x 10^9/L) impedance measurement
PDW	Platelet distribution width	prP	Enumeration of reticulated platelets

Supplementary Table 7.1. (*continued*)

Leukocytes			
WBC	White blood cell count (x 10^9/L)	WVF	White blood cell viability fraction
PIMN	Mean platelet 7 degrees (IAS)	PICV	CV% platelet 7 degrees (IAS)
PPMN	Mean platelet 90 degrees polarized (PSS)	PPCV	CV% platelet 90 degrees polarized (PSS)
MPV	Mean platelet volume (fL)		
Erythrocytes			
RBCO	Rbc count (x 10^9/L) optical measurement	RBCI	Rbc count (x 10^9/L) impedance measurement
RBCIMN	Mean rbc 7 degrees (IAS)	RBCICV	CV% rbc 7 degrees (IAS)
RBCFMN	Mean fluorescence rbc (FL3)	RBCFCV	CV% fluorescence rbc (FL3)
MCV	Mean corpuscular volume rbc fL	MCH	Mean corpuscular hemoglobin rbc fmol
MCHC	Mean corpuscular hemoglobin concentration rbc mmol/L	MCH USA	Mean corpuscular hemoglobin rbc (USA unit)
MCHC USA	Mean corpuscular hemoglobin concentration rbc (USA unit)	RDW	Red blood cell distribution width
PMIC	% rbc with volume of less than 60 fL	PMAC	% rbc with volume greater than 120 fL
HB	Hemoglobin (mmol/L)	HB USA	Hemoglobin USA units
HT	Hematocrit (L/L)	PHPO	% rbc with a hemoglobin concentration < 28 g/dL
PHPR	% rbc with a hemoglobin concentration > 41 g/dL	HDW	CV% hemoglobin concentration
RETC	Reticulocyte count (x 10^9/L)	PRETC	% reticulocytes of rbc count
MCVR	Mean corpuscular volume reticulocyte fL	MCHR	Mean corpuscular hemoglobin reticulocyte fmol
MCHCR	Mean corpuscular hemoglobin concentration reticulocyte mmol/L	IRF	Immature reticulocyte fraction
RTCFMN	Mean fluorescence reticulocyte (FL3)	RTCFCV	CV% fluorescence reticulocyte (FL3)
NRBC	Erythroblast count (x 10^9/L)	PNRBC	% erythroblasts per 100 white blood cells

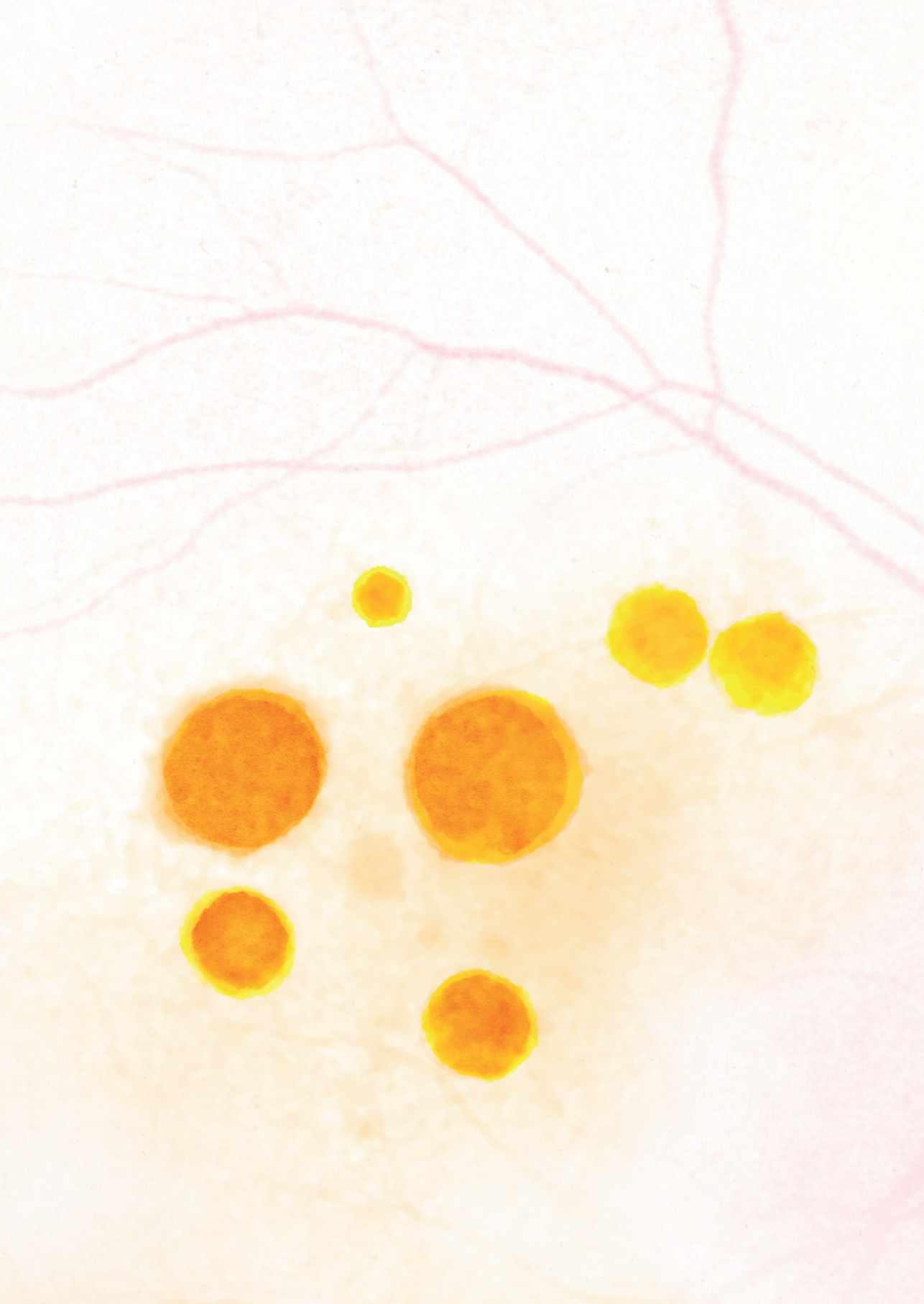

Chapter 8

Fluorescein angiography leads to increased fluorescence of blood cells and may hamper routine haematology analysis of ophthalmology patients

Evianne L. de Groot
Albert Huisman
Wouter W. van Solinge
Jeannette Ossewaarde-van Norel
Saskia Haitjema

Int J Lab Hematol. 2022 Jun;44(3):e91-e94. doi: 10.1111/ijlh.13741

Dear Editors,

Haematology analysers are routinely applied in healthcare, using the complete blood count (CBC) as a common screening parameter. Haematology analysers adopt a variety of techniques to classify blood cells, including optical light scattering and blood cell fluorescence (with and without added reagents).[1] Interference in the measurement can lead to abnormal CBC results and thus to incorrect diagnoses and unnecessary treatments. In this study, we describe an unexpected CBC interference that occurs after a routine ophthalmic examination. Fluorescein angiography (FA) and indocyanine green angiography (ICGA) are imaging modalities frequently used for the diagnosis and monitoring of several eye diseases involving the retina and choroid.[2] Sodium fluorescein is a small molecule that extravasates in the choroid and, in case of damaged retinal vessels or neovascular lesions, leaks out of these vessels. FA is mainly suitable to visualize (sub)retinal structures, since the blue excitation light and the green fluorescence are partially absorbed by the retinal pigment epithelium. The near-infrared wavelength for excitation and emission of indocyanine green (ICG) molecules is relatively long. Therefore, is it possible to penetrate the retinal pigment epithelium and visualize the underlying choroidal structures.[3] Central multifocal choroiditis (cMFC) is a rare form of non-infectious uveitis predominantly affecting young myopic women. In this disease, FA and ICGA are frequently performed to monitor the choroidal inflammation and the complication of choroidal neovascularization.[2] Patients are often treated with immunomodulatory agents, requiring regular blood analysis for the monitoring of side effects. Question is to what extent the outcome of routine CBC analysis in ophthalmology patients is affected by FA and ICGA.

In this study, we included patients diagnosed with cMFC who were incorporated in the Utrecht Patient Oriented Database (UPOD) in the UMC Utrecht, Utrecht, the Netherlands. The study followed the tenets of the Declaration of Helsinki and all subjects provided a written informed consent. UPOD collects and stores the results from the Abbott Cell-Dyn Sapphire automated blood cell analysers. The blood cell analyser is equipped with an integrated 488-nm blue diode laser and uses spectrophotometry, electrical impedance, laser light scattering (multi angle polarized scatter separation) and 3-colour fluorescent technologies to measure morphological parameters of leukocytes, red blood cells and platelets for classification and enumeration.[4] Data were collected from the electronic patient record system concerning demographic information and information about FA and ICGA including the time between the intravenous administration of fluorescein and ICG dye and CBC analysis by the haematology analyser. Standard dye dose consisted of 4 mL of 100 mg/mL sodium fluorescein and either 4 mL of 5 mg/mL indocyanine green or 6.5 mL of 2.5 mg/mL infracyanine green. The patients were stratified in three groups:

a group without FA and ICGA within 8 hours prior to the analysis of CBC (FA−/ICGA−), a group with exclusively ICGA prior to CBC analysis (FA−/ICGA+) and a group with both FA and ICGA prior to CBC analysis (FA+/ICGA+). The raw CBC data from UPOD, including research only parameters, were used as an outcome. Data analyses were performed in RStudio version 1.2.5001 (RStudio Team) and R version 3.6.1 (R Foundation for Statistical Computing). A likelihood ratio test (LRT) with a false discovery rate of 5% was applied for all the raw CBC parameters to perform differential abundance analysis for the 3 groups including the covariates age and sex. Linear regression analysis was performed in FA+/ICGA+ and FA−/ICGA+ patients to evaluate the gradient of the associated CBC parameters over time. All fluorescence-related CBC parameters were measured in arbitrary units (AU).

A total of 122 patients with cMFC were included in this study with a median (range) age of 42 (16-80) years and 104/122 (85%) were female. The FA−/ICGA− group consisted of 82 patients, FA−/ICGA+ of 4 patients and finally the FA+/ICGA+ comprised 36 patients. Differential abundant analysis revealed several fluorescence-related parameters that were significantly different between the three groups: mean neutrophil fluorescence (NFMN), mean lymphocyte fluorescence (LFMN), mean monocyte fluorescence (MFMN) and mean erythrocyte fluorescence (RBCFMN) (**Table 8.1**). Note that the time between the administration of fluorescein and/or indocyanine green dye and CBC analysis was not significantly different between the FA+/ICGA+ and FA−/ICGA+ groups (P =0.56) (**Table 8.1**).

All fluorescence-related parameters were exclusively increased in patients in the FA+/ICGA+ group. The difference for NFMN between the 3 groups is visualized in **Figure 8.1A**. In patients who underwent ICGA (either with or without FA), linear regression analysis was performed for the time between the intravenous injection of ICG and (if applicable) fluorescein dye and CBC analysis and NFMN. This analysis revealed a significant negative association (beta −0.11 AU/minute (95% CI −0.15 to −0.07), intercept=107.0, $P = 3.9 \times 10^{-6}$, Adj. $R^2 = 0.42$). The decline of NFMN over time is exclusively present in the FA+/ICGA+ group and was not observed in the FA−/ICGA+ group (**Figure 8.1B**). Similar results were found for the monocytes, lymphocytes and erythrocytes (data not shown).

In this study, we found that after intravenous injection of fluorescein dye for ocular angiography, patients demonstrated altered fluorescence-related parameters explored with a routine haematology analyser. The most predominant alterations were an elevated mean fluorescence of neutrophils, monocytes and lymphocytes. On the contrary, in patients who received solely ICG dye, these alterations were not observed. This is probably due to the fact that the excitation and emission peaks of ICG are 789 nm

Table 8.1. Fluorescence-related parameters that were increased after the performance of FA and ICGA

	FA+/ICGA+		FA-/ICGA+		FA-/ICGA-		
	Median	(IQR)	Median	(IQR)	Median	(IQR)	*P*-value[a]
NFMN	83.0	(17.3)	68.7	(1.7)	69.3	(2.5)	3.13×10^{-43}
LFMN	58.9	(23.6)	37.9	(6.1)	38.5	(8.3)	5.75×10^{-34}
MFMN	77.3	(24.1)	54.1	(7.6)	52.9	(6.6)	2.77×10^{-49}
RBCFMN	86.8	(5.4)	85.3	(3.1)	84.9	(4.5)	2.25×10^{-2}
Time (hours)[b]	2.8	(1.3)	3.3	(2.1)	NA	NA	0.56[c]

Fluorescence-related parameters that were significantly different between patients undergoing FA and ICGA (FA+/ICGA+) within 8 hours prior to CBC analysis, patients undergoing exclusively ICGA (FA-/ICGA+) and patients who did not undergo FA or ICGA prior to CBC analysis (FA-/ICGA-). All fluorescence-related parameters are quantified in arbitrary units. The time between the administration of fluorescein and/or indocyanine green dye was not significantly different for the FA-/ICGA+ and FA+/ICGA+ group.

FA, fluorescein angiography, ICGA, indocyanine green angiography; IQR, interquartile range; NFMN, mean neutrophil fluorescence; LFMN, mean lymphocyte fluorescence; MFMN, mean monocyte fluorescence; RBCFMN, mean erythrocyte fluorescence; CBC, complete blood count.

[a] Results of the likelihood-ratio test after false discovery rate correction of 5% and with the covariates age and gender incorporated in the model.

[b] The time between the injection of indocyanine green dye (and if applicable fluorescein dye) and the CBC analysis by the haematology analyser.

[c] The results of the t-test for the FA+/ICGA+ and FA-/ICGA+ group.

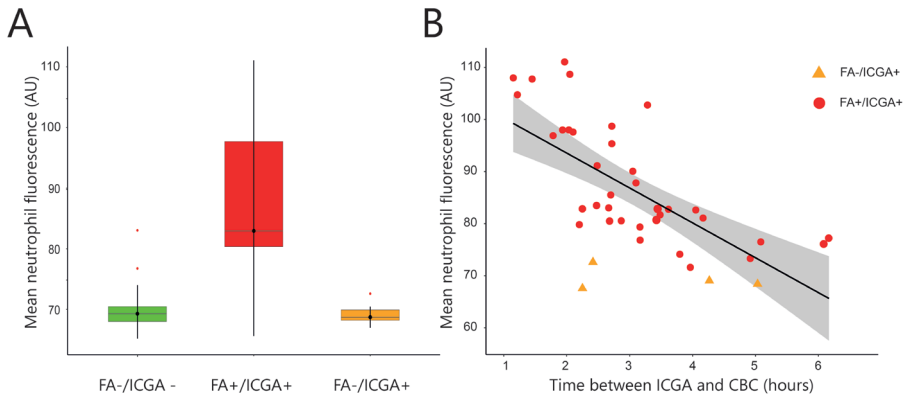

Figure 8.1 (**A**) The difference in NFMN between patients undergoing FA and ICGA (FA+/ICGA+) within 8 hr prior to CBC analysis, patients who underwent exclusively ICGA (FA−/ICGA+) and patients who did not undergo FA or ICGA prior to CBC analysis (FA−/ICGA−) including the group median, interquartile range and outliers (red dots). (**B**) The relationship between NFMN and the time between ICGA (and if applicable FA) and CBC analysis. The black line represents the linear model including the 95% confidence interval (grey area). The red points represent patients in the FA+/ICGA+ group (n = 36), and the orange triangles represent patients in the FA-ICGA+ group (n = 4).

AU, arbitrary units; FA, fluorescein angiography; ICGA, indocyanine green angiography; CBC, complete blood count; NFMN, mean neutrophil fluorescence

and 814 nm, respectively, which are out of range of the Cell-Dyn Sapphire fluorescence detectors. The fluorescence of the blood cells is measured using a fluorescence detector (FL3 channel) with a wavelength of 615-648 nm and the excitation and emission peaks of fluorescein are 494 nm and 521 nm, respectively. We suggest that particularly the

monocytes, neutrophils and lymphocytes take up the fluorescein dye following fluorescein angiography. The fluorescein molecules are strongly polar and diffuse only slowly through the cell membrane.[5] Therefore, the mechanism of entry probably involves facilitated diffusion or active transport across the cell membrane.[6] Previously, Meisingset and Steen[5] estimated that the fraction of intracellular fluorescein bound to proteins or associated with cell structures was 70%, the rest of the fluorescein being dissolved in the cellular water. Subsequently, caused by the strong fluorescence intensity of fluorescein, fluorescein in these cells is measured in the FL3 channel as an increased mean fluorescence of these cells. Our study demonstrates that this alteration in fluorescence measurement in these cells is present at least up until 6 hours after fluorescein angiography. This is the first study in a large group of patients that confirms the disturbance of fluorescence-related parameters with a routine haematology analyser. Similar results were described in a case report.[7] In this case report, the increased fluorescence in the lymphocytes, monocytes, and granulocytes was seen as long as 20 hours after fluorescein injection. The interference of fluorescent dyes has also been reported in the context of analytical flow cytometry impairing a proper discrimination of lymphocyte subsets labelled with fluorochrome-conjugated antibodies.[6,8] Fluorescence-related measurements are only performed in the context of medical research, and consequently, we think FA will not have great impact on the relevant clinical laboratory results. However, current generation haematology analysers used in routine analysis of the CBC use fluorescent techniques for the classification of bloods cells. Moreover, it cannot be ruled out that fluorescein dye influences other biochemical processes and alters additional laboratory results. Thus, if possible, we would advise to perform CBC analysis prior to the intravenous injection of fluorescein dye. Moreover, if CBC analysis demonstrates unexpected results, ophthalmologists should always consider interference with fluorescein dye as a possible explanatory factor and could repeat the CBC analysis on a day fluorescein dye is not administered to the patient. In the future, it would be interesting to compare CBC data prior to and shortly after the administration of fluorescein dye within the same patient to explore which parameters are most severely influenced by fluorescein dye in a prospective design.

REFERENCES

1. Vis JY, Huisman A. Verification and quality control of routine hematology analyzers. Int J Lab Hematol. 2016;38:100-109.
2. Tavallali A, Yannuzzi LA. Idiopathic multifocal choroiditis. J Ophthalmic Vis Res. 2016;11(4):429-432.
3. Herbort CP. Fluorescein and Indocyanine Green Angiography for Uveitis. Middle East Afr J Ophthalmol. 2009;16(4):168-187.
4. Gijsberts CM, Den Ruijter HM, De Kleijn DPV, et al. Hematological Parameters Improve Prediction of Mortality and Secondary Adverse Events in Coronary Angiography Patients. Med (United States). 2015;94(45):e1992.
5. Meisingset KK, Steen HB. Intracellular binding of fluorescein in lymphocytes. Cytometry. 1981;1(4):272-278.
6. Bürgisser P, Vaudaux J, Bart PA. Severe interference between retinal angiography and automated four-color flow cytometry analysis of blood mononuclear cells. Cytom Part A. 2007;71(8):632-636.
7. Felberg NT, Haimowitz AJ. Flow cytometry of leukocytes after intravenous fluorescein angiography. Cytometry. 1985;6(1):74-76.
8. Kaur H, Hainsworth DP, Caldwell CW, Hamm CW, Madsen RW. Interpretation of flow cytometric measurement of lymphocytes after fluorescein angiography. Retina. 2002;22(1):44-47.

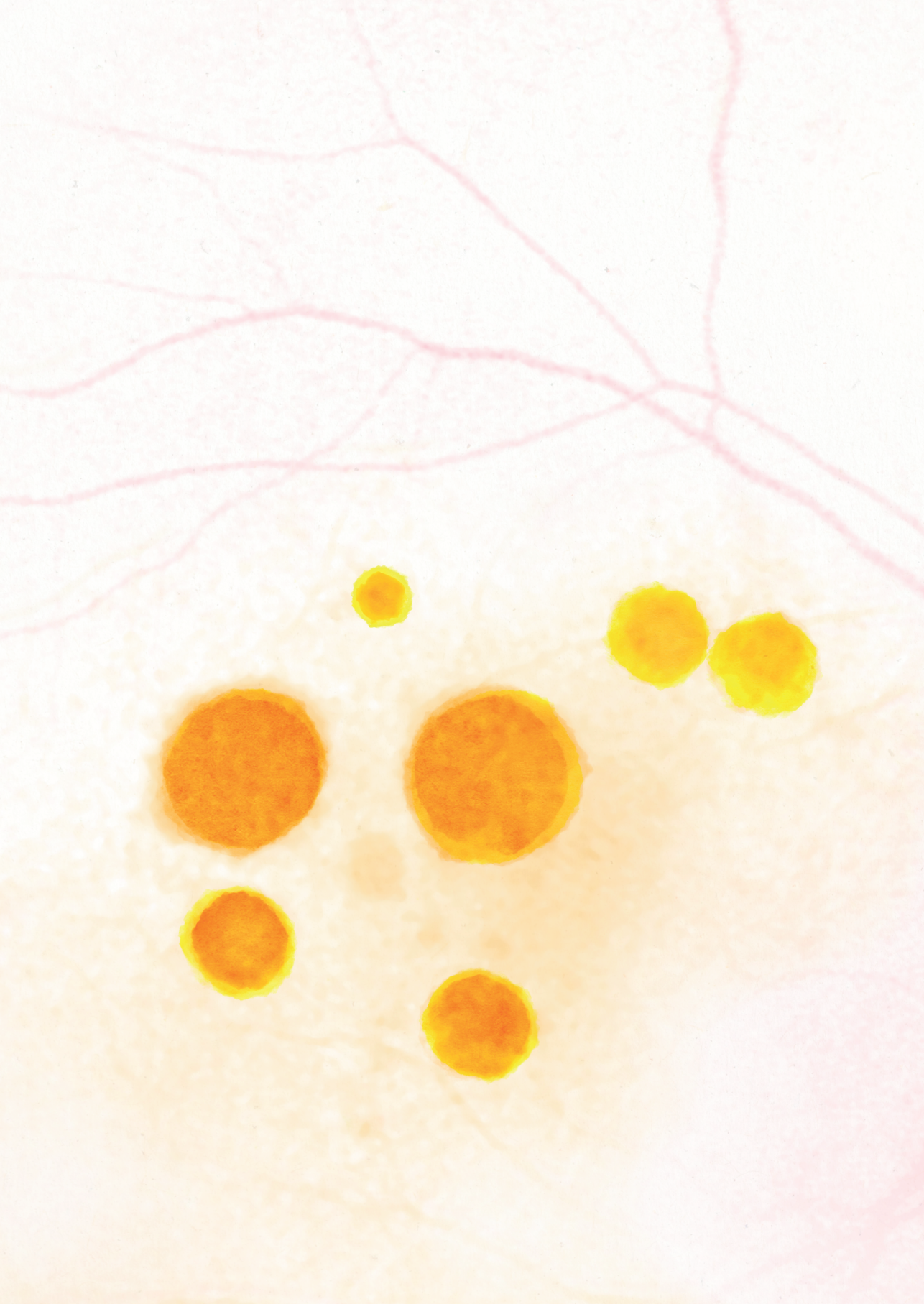

Chapter 9

Risk variants in the *CFH* gene associate with elevated levels of coagulation and complement factors in idiopathic multifocal choroiditis

Evianne L. de Groot
Jeannette Ossewaarde-van Norel
Joke H. de Boer
Sanne Hiddingh
Bjorn Bakker
Ramon A.C. van Huet
Ninette H. ten Dam-van Loon
Alberta A.H.J. Thiadens
Magda A. Meester-Smoor
Yvonne de Jong-Hesse
Leonoor I. Los
Anneke I. den Hollander
Camiel J.F. Boon
Lambertus A. Kiemeney
Kristel R. van Eijk
Mark K. Bakker
Carel B. Hoyng
Jonas J.W. Kuiper

Adapted version accepted for publication in JAMA Ophthalmology

ABSTRACT

Importance

Idiopathic multifocal choroiditis (MFC) is poorly understood, hindering optimal treatment and monitoring of patients.

Objective

To identify genes and pathways involved in idiopathic MFC.

Design

Genome-wide association study (GWAS) in case controls, and proteomics of blood plasma samples.

Setting

A multicenter study involving six Dutch universities.

Participants

170 Dutch idiopathic MFC cases and 4267 controls (cohort 1), and 52 cases and 1292 controls (cohort 2). Plasma samples from 87 treatment-free idiopathic MFC cases were subjected to targeted proteomics. Idiopathic MFC was diagnosed according to the SUN working group guidelines for punctate inner choroidopathy and multifocal choroiditis with panuveitis.

Main outcomes and measures

Genetic variants associated with idiopathic MFC and risk variants associated with plasma protein concentrations in patients.

Results

The primary GWAS association mapped to the *complement factor H* (*CFH*) gene with genome-wide significance (lead variant the A allele of rs7535263; odds ratio (OR) [95% confidence interval (95%CI)] = 0.52 [0.41-0.64]; $P = 9.3 \times 10^{-9}$). There was no significant association with classical HLA alleles (lead classical allele; *HLA-A*31:01*, $P = 0.002$). The association with rs7535263 showed consistent direction of effect in an independent cohort of 52 cases and 1292 control samples (combined meta-analysis OR [95%CI] = 0.58 [0.38-0.77], $P = 3.0 \times 10^{-8}$). In proteomic analysis of 87 patients, the risk allele G of rs7535263 in the *CFH* gene was strongly associated with increased plasma concentrations of Factor H-related (FHR) proteins (e.g., FHR-2, *likelihood ratio test*, $P_{adj} = 1.1 \times 10^{-3}$) and proteins involved in platelet activation and the complement cascade.

Conclusions and relevance

CFH gene variants increase systemic concentrations of key factors of the complement and coagulation cascades, thereby conferring susceptibility to idiopathic MFC. In conclusion, these results indicate that the complement and coagulation pathways are key targets for the treatment of idiopathic MFC.

INTRODUCTION

Idiopathic multifocal choroiditis (MFC) is a rare idiopathic inflammatory choroidopathy in the absence of a systemic disease. The disease is characterized by inflammation of the choriocapillaris, loss of retinal pigment epithelium, outer retinal ischemia and the frequent development of choroidal neovascularization.[1-3] Patients with idiopathic MFC are predominantly young myopic women that appear otherwise healthy, who experience vision loss, metamorphopsia, scotomas and photopsias.[2,4] Idiopathic MFC may manifest with or without panuveitis and shows a variable degree of involvement of the peripheral retina. Idiopathic MFC without involvement of the peripheral retina and without cells in the anterior or vitreous cavity is often referred to as punctate inner choroidopathy (PIC) (**Figure 9.1**).[4-7] However, definite standardization of disease definitions lack and whether MFC and PIC are indeed separate disease entities remains a subject of debate.[5,8-10]

Molecular profiling studies of idiopathic MFC remain sparse. Previous studies revealed changes in platelet granularity,[11] while candidate gene association studies have linked complement and interleukin encoding genes to idiopathic MFC.[12,13] This supports an inflammatory basis for this disease in combination with coagulation dysfunction. This is also evident from the efficacy of immunosuppressive agents - including disease-modifying antirheumatic drugs (DMARDs) – used as treatment for idiopathic MFC.[14-16] However, how these inflammatory factors contribute to disease remains uncertain. Better understanding of the key disease pathways driving idiopathic MFC and a molecular basis in support of the clinical categories are needed to improve disease management. To allow unbiased identification of genetic variants that confer susceptibility to idiopathic MFC, we conducted a genome-wide association study and targeted proteomic profiling in a Dutch cohort.

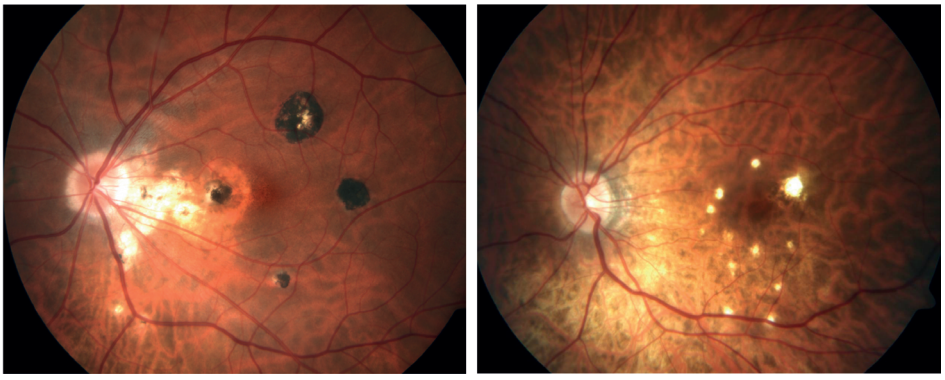

Figure 9.1. Subtypes of idiopathic MFC. A patient diagnosed with multifocal choroiditis (L) and a patient diagnosed with punctate inner choroidopathy (R).

METHODS

Study population

This study was performed following the tenets of the Declaration of Helsinki and its further amendments. Institutional Review Board (IRB) approval was obtained from all participating centers. In total, 283 patients were recruited at the University Medical Center Utrecht (UMCU) (MEC-12-514/20-307), the Radboud University Medical Center (Radboudumc)(MEC-2017-3535), Nijmegen, the Netherlands, the Amsterdam University Medical Center (AUMC) (MEC-12-514/2020.356), Amsterdam, the Netherlands, the Leiden University Medical Center (LUMC)(B14.003/B21.021), Leiden, the Netherlands, the Erasmus Medical Center (EMC)(MEC-2012-031/2020-0756), Rotterdam, the Netherlands, and the University Medical Center Groningen (UMCG) (MEC12-514/20200083), Groningen, the Netherlands. All patients provided written informed consent. Each case was evaluated according to the SUN guidelines[8,9] and evaluation included standard diagnostic work-up for uveitis, comprising routine laboratory testing, chest X-ray, and when indicated positron emission tomography–computed tomography, anterior chamber paracentesis with PCR and/or Goldmann-Witmer index and cytokine analysis. The diagnosis idiopathic MFC was established for cases that presented with chorioretinal lesions in the posterior pole in the absence of papillitis and retinal vasculitis, nor evidence for an ocular infection, sarcoidosis, tuberculosis, inflammatory bowel disease, Birdshot chorioretinopathy, or vitreoretinal lymphoma. Idiopathic MFC patients were subdivided into the two subtypes MFC and PIC. Subtype classification was in accordance with the SUN working group criteria with minor adjustments based on consensus recommendation by an expert panel (i.e., uveitis- and/or retina-specialists of all participating Centers) (**Figure 9.1**).[8,9] Patients were diagnosed with PIC if: 1) chorioretinal lesions were located within the posterior pole with or without involvement of the mid-peripheral retina but without involvement of the peripheral retina, 2) no cells in the anterior chamber or vitreous were observed (grade 0) and 3) predominant lesions size was <250 µm with a punctate appearance. MFC diagnosis was established if 1) chorioretinal lesions were located both in the posterior pole and extending to the peripheral retina, and/or 2) cells were observed in the anterior chamber or vitreous (>1+ cells) and/or 3) predominant lesion size was >125 µm with a round appearance. We introduced the group of MFC/PIC comprising cases with insufficient clinical data to be classified as either MFC or PIC. For cohort 1, 231 patients were recruited and were subjected to genotyping. In total 35 cases were removed after quality control of genotyping, because after inclusion the patients were diagnosed with an alternative diagnosis (**Figure 9.2**). For the purpose of replication, we recruited an independent Dutch cohort of 52 cases with idiopathic MFC (cohort 2) (**Figure 9.2**).

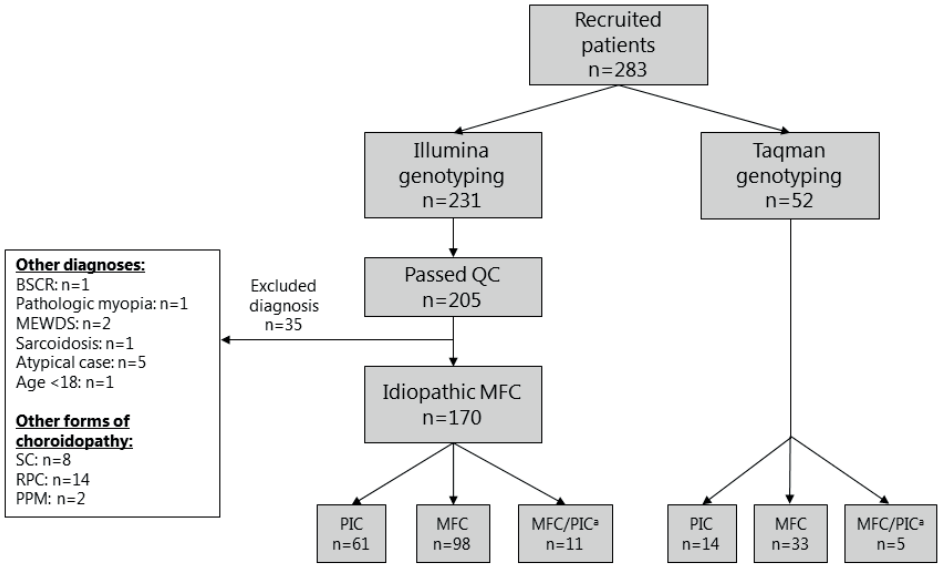

Figure 9.2. Overview of all recruited patients in cohort 1 and 2. For cohort 1, after quality control (QC) and case selection, 170 idiopathic MFC cases were analyzed.
QC, quality control; BSCR, Birdshot chorioretinopathy; MEWDS, Multiple Evanescent White Dot Syndrome; SC, serpiginous choroiditis; RPC, relentless placoid chorioretinitis; PPM, persistent placoid maculopathy; PIC, punctate inner choroidopathy; MFC, multifocal choroiditis.
[a] Insufficient data for accurate subtype classification between MFC or PIC.

SNP array genotyping

For a detailed description of the genomic DNA extraction see **Supplemental Methods**. Cases of cohort 1 were genotyped with the Illumina Infinium OmniExpress-24 bead chip at the Genome Analysis Center, Helmholtz Zentrum München, Germany in August 2021. Data from 5,363 Dutch population controls from the Nijmegen Biomedical Study (NBS) that were genotyped with either the Illumina Infinium OmniExpress-12 bead chip or the Illumina Infinium OmniExpress-24 bead chip were used as reference for cohort 1.[17] For the purpose of replication, we genotyped the rs7535263 variant in an independent Dutch cohort (cohort 2) by TaqMan® SNP genotyping technology (ThermoFisher Scientific Inc. Waltham, MA, USA) and compared these to genotype data from 1292 Dutch control subjects from the ALS study (cohort 23/NL4).[18] The genotyping results from both cohorts were combined for meta-analysis.

Quality control and Imputation

Quality control was performed in PLINK (v1.90b3z 64-bit) for samples (i.e., sample call rate, sex mis-match, population outliers and duplicates/relatedness) and single nucleotide polymorphisms (SNPs) (SNP call rate, multiallelic SNPs, minor allele frequency (MAF), deviation from the Hardy-Weinberg equilibrium (HWE)). For the

complete overview of the quality steps see **Supplemental Figures 9.1-3**. After quality control, samples from 205 cases and 4267 control subjects were retained. Data were phased using Eagle 2.4 and was imputed using the HRC reference panel (1.1) on the Michigan Imputation Server.[19] All monomorphic and multi-allelic SNPs were removed. For all imputed SNPs we calculated INFO scores and SNPs with an INFO-score (Rsquare) <0.6 were removed and additionally post-imputation QC was performed (**Supplemental Figure 9.3**). After imputation 8,653,120 SNPs passed the quality control check and were used for analysis. The Major histocompatibility complex (MHC) region was imputed with the Michigan Imputation Server pipeline including the script for Imputation preparation and checking provided by the Michigan server (v4.2.7) using the Haplotype Reference Consortium v1.1. This pipeline results in the imputation of classical Human Leukocyte Antigens (HLA) alleles, amino acids positions, SNPs in the MHC region and insertions/deletions in the MHC region.

Association testing

The single variant association tests were performed with the *Scalable and Accurate Implementation of GEneralized mixed model* (SAIGE) v0.29.3 and were performed in R v4.2.8.[20] To determine the appropriate number of Principal Components (PC's) to correct for population stratification, we performed a general linear model with the first 10 PC's, sex and phenotype and identified the largest PC that was significantly associated ($p<0.05$) with the phenotype and selected all PC's up to that last significant PC. This resulted in a final model with the covariates age, sex and the first 6 principal components. Association testing was performed for all cases in cohort 1 and for the subtypes MFC and PIC separately.

Olink targeted proteomics of blood plasma

Available plasma samples from treatment-free idiopathic MFC patients from cohort 1 (n=87) at the time of the blood withdrawal were centrifuged at 2000 × g for 10 minutes at room temperature and stored directly at −80°C. Samples from patients were thawed and randomized over plates before the samples were shipped on dry ice to Olink Proteomics (Erasmus Medical Center, Rotterdam, the Netherlands). The Olink Explore 384 inflammation II panel was used to measure 370 proteins associated with inflammatory responses. Olink uses proximity extension assay (PEA) technology to measure protein concentrations by next-generation sequencing. The protein expression data is expressed in arbitrary units (Normalized Protein eXpression (NPX)) and represents the relative protein concentration in the serum of the sample on a log2 scale.[21,22] The full list of measured proteins in the inflammation II panel is in **Supplemental Table 9.4**. The relation between the genotype of the lead variant rs7535263 and plasma protein

concentrations were assessed using a likelihood ratio test (LRT) adjusted for age and sex.

RESULTS

Variants at 1q31 associate with idiopathic multifocal choroiditis

To identify idiopathic MFC susceptibility genes, we conducted genome-wide and *MHC*-region association analysis for cases in cohort 1. After quality control, imputation and exclusion of patients with alternative diagnoses, 170 patients and 4267 controls and 8,653,120 autosomal SNPs remained for subsequent analysis (**Figure 9.2**). The mean age (standard deviation (SD)) was 43 (13) and 93% of the participants in cohort 1 was female. The patient characteristics for both cohort 1 and 2 are shown in **Supplemental Table 9.1**. We used an additive logistic mixed model, adjusted for age, sex and the top six principal components from ancestry analysis for genome-wide association testing. We identified a genome-wide significant association on chromosome 1 with the A allele of rs7535263 in *Complement Factor H* (*CFH*) (odds ratio (OR) = 0.52 [95%CI 0.41-0.64]; $P = 9.3 \times 10^{-9}$; **Figure 9.3, Figure 9.4**). Both subtypes PIC and MFC demonstrated nearly identical allele frequency in cases (**Figure 9.4**). The risk allele, G, of rs7535263 had an allele frequency of 73% in cohort 1 compared to 57% in Dutch controls.

Due to strong linkage disequilibrium (LD), in total 20 SNPs across the *CFH* locus showed genome wide significant association ($P < 5.0 \times 10^{-8}$)(**Supplemental Table 9.2**). After conditioning for the SNP rs7535263 in *CFH* the association signal of the remaining variants in *CFH* was mitigated (**Figure 9.3**). The risk allele G of rs7535263 was also more frequent in cohort 2 compared to 1292 control samples with moderate effect size (G allele of rs7535263 in cases and controls, 62% and 56%, respectively, OR [95%CI] = 0.81 [0.54-1.21], $P = 0.30$). The association did not reach statistical significance, most likely representing an underpowered comparison (combined meta-analysis (OR [95%CI] = 0.58 [0.38-0.77], $P = 3.0 \times 10^{-8}$) (**Figure 9.4**).

We also imputed and tested polymorphisms and classical alleles in the MHC region in cohort 1, but no genome-wide association in the *MHC* region was detected (lead variant in intron 5 of *HLA-DRB1*, $P = 3.7 \times 10^{-4}$) nor was any classical HLA allele markedly associated (lead classic HLA allele: *HLA-A*31*, $P = 0.002$ **Supplemental Table 9.3** and **Supplemental Figure 9.4**).

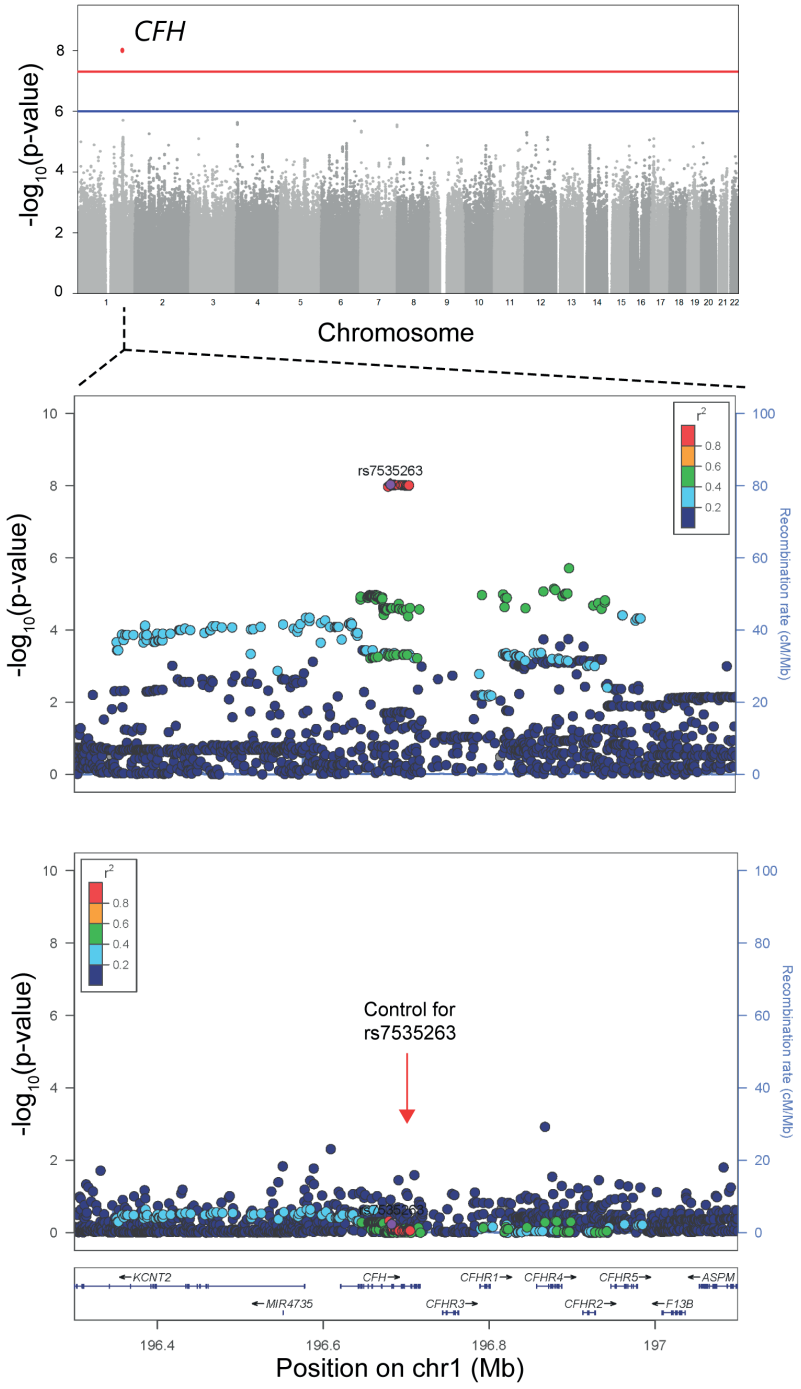

Figure 9.3. Manhattan and regional plot of genome-wide association analysis of idiopathic multifocal choroiditis or punctate inner choroidopathy.

Figure 9.3. Manhattan and regional plot of genome-wide association analysis of idiopathic multifocal choroiditis or punctate inner choroidopathy. The top figure shows the Manhattan Plot of the results of a genome-wide association study in 170 patients with idiopathic multifocal choroiditis or punctate inner choroidopathy and 4266 Dutch control participants. Each dot represents the result of the association test for a SNP. On the x-axis the chromosomes are displayed, the y-axis represents the -$\log_{10}$ of the *P*-value from a *Scalable and Accurate Implementation of GEneralized* mixed model (SAIGE) including the covariates age, sex, and the first 6 principal components from ancestry analysis. The blue line indicates the threshold for suggestive association ($P < 1.0 \times 10^{-6}$), the red line indicates the threshold for genome-wide significance ($P < 5 \times 10^{-8}$). One genome-wide significant signal was observed in the *CFH* gene (20 SNPs); lead variant the A allele of rs7535263). The middle and bottom figures show the regional association plot generated in LocusZoom of the *CFH* region before (middle) and after (bottom) conditioning on rs7535263. On the x-axis the position on the chromosome is displayed including the position of the genes in this region. The left y-axis represents the -$\log_{10}$(*P*-value) of the results of the association tests and the right y-axis represents the recombination rate. The lead SNP is plotted as a purple diamond; other data points are colored according to their r2 with the lead SNP.
SNP, single nucleotide polymorphism; CFH, complement factor H. *(continued)*

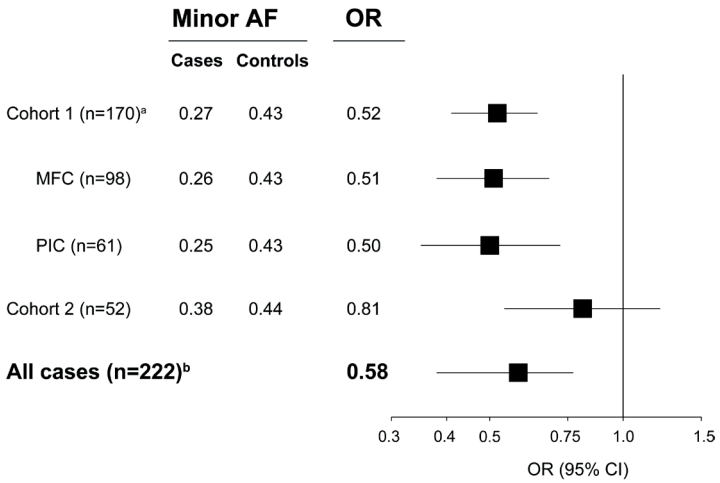

Figure 9.4. Forrest plot visualizing the summary statistics for association analysis for different disease groups for the A allele of rs7535263 in *CFH* gene. Controls for cohort 1 include the 4266 population control participants used in GWAS analysis, controls for cohort 2 include 1292 population control participants.
AF, allele frequency; OR, odds ratio; MFC, multifocal choroiditis; PIC, punctate inner choroidopathy; CI, confidence interval.
[a] Insufficient data for accurate subtype classification between MFC or PIC for 11 cases.
[b] Results of a meta-analysis of cohort 1 (n=170) and cohort 2 (n=52).

Idiopathic MFC risk variant associates with plasma coagulation and complement protein levels

The *CFH* gene and *CFH related* genes (*CFHR1-5*) cluster together on chromosome *1q31*. The variants (in LD with rs7535263) at *1q31* identified in this study were recently shown to be associated with circulating Factor H related [FHR] protein concentrations.[23,24] To assess the relation between the genetic signal at *1q31* and the plasma proteome, we used a 370-plex proximity extension assay for targeted proteomics of 87 treatment-free patients from this study. We performed an association analysis of the top idiopathic MFC variant rs7535263 in *CFH* gene with plasma protein concentrations. Adjusting for sex and age, the risk allele G of rs7535263 was associated with differential plasma levels of 27 proteins (**Figure 9.5A**), including Factor H related (FHR) protein 2, FHR-4,

FHR-5, complement C5, coagulation factors such as prothrombin (F2) and fibrinogen alpha chain (FGA), and in proteins involved in lipid metabolism (*e.g.*, apolipoprotein F (APOF), apolipoprotein C-I (APOC1) and Gastric inhibitory polypeptide receptor (GIPR) (**Supplemental Table 9.4**). No association with Factor H (FH) protein (encoded by the *CFH* gene) concentrations were observed with rs7535263 (**Figure 9.5B**). The strongest association was found with FHR-2 (P_{adj} = 1.1 × 10^{-3}) and APOF (P_{adj} =6.6 × 10^{-5}); which were increased in plasma of cases carrying the risk allele G of rs7535263 (**Figure 9.5B**). Pathway enrichment analysis of the 27 proteins associated with the rs7535263 genotype

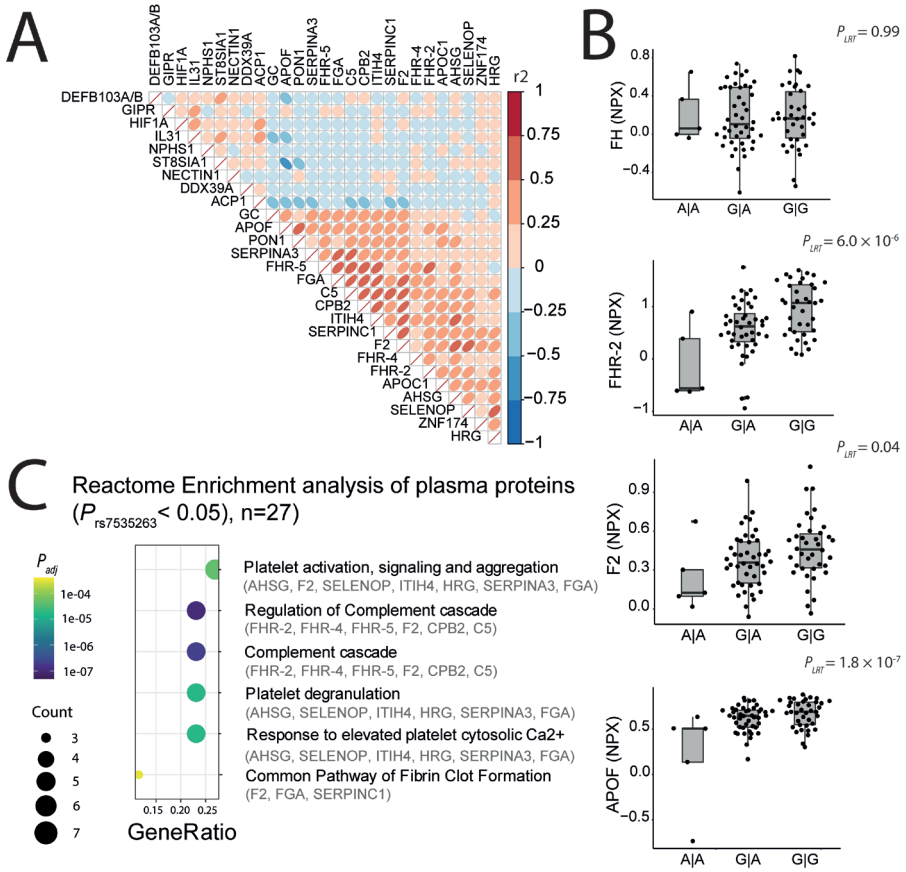

Figure 9.5. Association between the rs7535263 in *CFH* and plasma concentrations of immune mediators in multifocal choroiditis. EDTA plasma was subjected to targeted 370-plex proteomics Olink array in 87 treatment naive patients with idiopathic multifocal choroiditis or punctate inner choroidopathy **(A)** Heatmap of the correlation (color-coded from blue to red) between 27 plasma proteins associated (likelihood ratio test *P*<0.05) with the genotype of rs7535263 in *CFH*. **(B)** The plasma levels for complement factor H (FH), complement factor H-related protein 2 (FHR-2), prothrombin (F2) and apolipoprotein F (APOF) across the genotype of rs7535263 in patients. Protein concentrations are expressed as *normalized protein expression* from Olink (NPX). **(C)** The results of the reactome enrichment analysis of the 27 identified proteins (likelihood ratio test *P*<0.05). The top 6 pathways are shown and the adjusted *P*-value from enrichment analysis is color-coded. Plasma proteins that were annotated in each of the pathways are indicated in gray.

revealed strong enrichment for complement (e.g., Regulation of Complement cascade [R-HSA-977606], P_{adj} = 1.1 × 10^{-7}) and coagulation cascades (e.g., Platelet activation, signaling and aggregation [R-HSA-76002], P_{adj} = 4.4 × 10^{-5})(**Figure 9.5C**). Considered collectively, we identified rs7535263 in the *CFH* locus as a novel risk variant for idiopathic MFC that associates with increased circulating levels of key factors of complement and coagulation cascades.

DISCUSSION

We identified genetic variants at *1q31* at the extended *CFH* locus that were associated with idiopathic MFC with nearly identical allele frequencies for the subtypes MFC and PIC. We further demonstrated that patients that carry the risk alleles exhibited increased plasma levels of complement factor H related proteins and other proteins related to the complement cascade and platelet degranulation pathways. This supports the hypothesis that coagulation and inflammatory processes contribute to the disease biology of idiopathic MFC.

Recently, classification criteria for MFC with panuveitis and PIC have been proposed. These include differentiating criteria for PIC and MFC, such as the location and size of the chorioretinal lesions and the presence of inflammation in the vitreous or anterior chamber.[8,9] The close clinical similarities of MFC and PIC subtypes suggest that they may actually represent the same disease entity with MFC representing cases with more profound inflammation.[25,26] Using an approach with idiopathic MFC clinical phenotypes only distinguished by differential peripheral retinal involvement, lesion size and the presence of intraocular inflammation, revealed that both phenotypically related subtypes share genetic association with the *CFH* locus on chromosome *1q31* with almost identical allele frequency of the lead variant in both subtypes. Our results support that both subtypes have a similar molecular basis. However, comprehensive assessment of the genetic correlation between PIC and MFC requires a much larger sample size in subsequent genome-wide association studies.

This study includes the largest reported genetic analysis of idiopathic MFC thus far. However, owing to the rarity of the condition, we performed a GWAS in a relatively small number of cases. This influenced the power and limited the ability to detect association to variants with relatively large effect size and hampered efforts to replicate statistically the signal in the *CFH* gene in an independent cohort. However, the *CFH* risk locus demonstrated consistent direction of effect in cohort 2 and we demonstrated functional

implications of the GWAS signal on plasma protein concentrations in patients with idiopathic MFC.

This study identified a variant in the *CFH* locus that associates with idiopathic MFC. This risk variant is in full LD with rs10922109, a variant that is associated with age-related macular degeneration (AMD).[23,24,27] Among the established genetic loci associated with AMD,[28] we detected only a suggestive association for another variant in the *CFH* gene (rs570618 [Y402H], P=1.1×10^{-5}) (**Supplemental Table 9.5**). On the contrary, while being a risk factor for AMD and idiopathic MFC, the G allele of rs7535263 is protective for central serous chorioretinopathy (CSC), another disease affecting the retinal pigment epithelium (RPE) and choroid.[29,30] Interestingly, patients with all these conditions are prone to develop choroidal neovascularization. The shared association with a locus in the *CFH* gene suggests that choroid/RPE homeostasis is strongly influenced by genetic variation at *1q31*. Despite the fact that 75% of the affected eyes in the current study were myopic, we did not find an association with risk loci observed in myopia.[31-35]

Using plasma proteomics of treatment-free patients with idiopathic MFC, we demonstrated that the risk genotype of rs7535263 in *CFH* was not accompanied by changes in the levels of its encoding protein FH, but instead strongly associated with increased plasma concentration of FHR proteins, such as FHR-2, FHR-4, and FHR-5. These findings are in line with recent studies in AMD patients that also showed that the G allele of rs7535263 (and variants in strong LD with it) is associated with increased FHR-2,-4,-5 levels.[23,24,36,37] FHR-2, -4 and -5 have been shown to accumulate in the intercapillary septa of the choriocapillaris in AMD and to interrupt regulation of the complement cascade by competing with FH-binding sites.[23] These observations are of interest for the understanding of the disease biology of idiopathic MFC. Potentially, the genetic predisposition to higher systemic levels of FHRs in idiopathic MFC results in the accumulation of FHR proteins in the choriocapillaris and subsequently, to local increased complement activation.

Our proteomic analysis revealed that the *CFH* risk variant also associates with increased levels of proteins involved in lipid metabolism (e.g., apolipoproteins), and key components of the coagulation pathway (e.g., prothrombin). The association of risk variants in *CFH* with circulating coagulation factors has also previously been reported in plasma proteomic analysis in 4998 healthy blood donors, indicating that the here described genetic predisposition in the extended *CFH* locus with altered levels of coagulation pathway factors is robust.[38] The association between variants in *CFH* and coagulation pathway factors, such as prothrombin (F2) is not yet reported in large

proteomic studies of AMD. An explanation could be that these studies measured protein concentrations in serum, which could influence quantification of coagulation factors.

The association of the *CFH* risk locus with plasma coagulation factors is of interest because there is increasing evidence for a cross-talk between coagulation factors and the complement cascade.[39,40] In idiopathic MFC, hypoperfusion of the choriocapillaris is observed on imaging modalities which is hypothesized to be the result of microthrombi in the choriocapillaris.[11] Elevated plasma FHR proteins have been linked to prothrombotic events,[41] while genetic disruption of FH-binding leads to complement component 3 (C3)-mediated ischemic retinopathy and cotton wool spots in mice.[42] Since FH and FHR-2, FHR-4, FHR-5 compete for C3,[23,43] it is tempting to speculate that elevated systemic levels of FHR-2, FHR-4 or FHR-5 may contribute to C3 accumulation and ischemia in the choriocapillaris in idiopathic MFC. Treatment with immunomodulatory therapy including DMARDs and biologicals positively influences the disease course in idiopathic MFC.[14-16,44] Interestingly, we previously reported that idiopathic MFC cases who demonstrate increased platelet granularity characteristics in blood require more often immunomodulatory therapy to control the disease activity.[11]

Taken together, we hypothesize that an increased activity of the complement system and coagulation cascade leads to a local inflammatory response and the development of microthrombi/ischemia in the choriocapillaris. This supports the use of immunomodulatory treatment (DMARD/biologicals) in these patients. Given the shared genetic predisposition at the extended *CFH* locus with AMD, it is tempting to speculate that emerging treatments that target *CFH* downstream C3 and C5 for treatment of AMD may be repurposed for management of idiopathic MFC.[45,46] However, future research should determine the involvement of C3 and C5 in idiopathic MFC disease mechanisms.

In conclusion, we discovered a locus in the *CFH* gene that predisposes individuals to idiopathic MFC. Furthermore, we found that this locus affects the concentration of circulating proteins with key functions in coagulation and complement cascades in patients with idiopathic MFC. This may indicate a key role of the complement and coagulation cascades in the underlying disease mechanism of idiopathic MFC.

REFERENCES

1. Spaide RF, Goldberg N, Freund KB. Redefining multifocal choroiditis and panuveitis and punctate inner choroidopathy through multimodal imaging. Retina. 2013;33(7):1315-1324.
2. Tavallali A, Yannuzzi LA. Idiopathic multifocal choroiditis. J Ophthalmic Vis Res. 2016;11(4):429-432.
3. Ahnood D, Madhusudhan S, Tsaloumas MD, Waheed NK, Keane PA, Denniston AK. Punctate inner choroidopathy: A review. Surv Ophthalmol. 2017;62(2):113-126.
4. Leung TG, Moradi A, Liu D, et al. Clinical features and incidence rate of ocular complications in punctate inner choroidopathy. Retina. 2014;34(8):1666-1674.
5. Gilbert RM, Niederer RL, Kramer M, et al. Differentiating Multifocal Choroiditis and Punctate Inner Choroidopathy: A Cluster Analysis Approach. Am J Ophthalmol. 2020;213:244-251.
6. Kedhar SR, Thorne JE, Wittenberg S, Jabs DA. Multifocal choroiditis with Panuveitis and Punctate Inner Choroidopathy: Comparison of Clinical Characteristics at Presentation. Retina. 2007;27(9):1174-1179.
7. Thorne JE, Wittenberg S, Jabs DA, et al. Multifocal Choroiditis with Panuveitis. Incidence of Ocular Complications and of Loss of Visual Acuity. Ophthalmology. 2006;113(12):2310-2316.
8. The Standardization of Uveitis Nomenclature (SUN) Working group. Classification Criteria for Punctate Inner Choroiditis. Am J Ophthalmol. 2021;228:275-280.
9. The Standardization of Uveitis Nomenclature (SUN) Working group. Classification criteria for multifocal choroiditis with panuveitis. Am J Ophthalmol. 2021;228:152-158.
10. Park JG, Halim MS, Uludag G, et al. Distinct Patterns of Choroidal Lesions in Punctate Inner Choroidopathy and Multifocal Choroiditis Determined by Heatmap Analysis. Ocul Immunol Inflamm. 2022;30(2):276-281.
11. de Groot EL, Ossewaarde-van Norel J, Hoefer IE, Haitjema S, de Boer JH, Kuiper JJW. Central Multifocal Choroiditis: Platelet Granularity as a Potential Marker for Treatment With Steroid-Sparing Immunomodulatory Therapy. Front Ophthalmol. 2021;1:784848.
12. Atan D, Fraser-Bell S, Plskova J, et al. Punctate Inner choroidopathy and multifocal choroiditis with panuveitis share haplotypic associations with IL10 and TNF loci. Investig Ophthalmol Vis Sci. 2011;52(6):3573-3581.
13. Ferrara DC, Takahashi BS, Yannuzzi LA, et al. Analysis of major alleles associated with age-related macular degeneration in patients with multifocal choroiditis: Strong association with complement factor H. Arch Ophthalmol. 2008;126(11):1562-1566.
14. de Groot EL, ten Dam-van Loon NH, de Boer JH, Ossewaarde-van Norel J. The efficacy of corticosteroid-sparing immunomodulatory therapy in treating patients with central multifocal choroiditis. Acta Ophthalmol. 2020;98(8):816-821.
15. Goldberg NR, Lyu T, Moshier E, Godbold J, Jabs DA. Success with single-agent immunosuppression for multifocal choroidopathies. Am J Ophthalmol. 2014;158(6):1310-1317.
16. Turkcuoglu P, Chang PY, Rentiya ZS, et al. Mycophenolate mofetil and fundus autofluorescence in the management of recurrent punctate inner choroidopathy. Ocul Immunol Inflamm. 2011;19(4):286-292.
17. Galesloot TE, Vermeulen SH, Swinkels DW, et al. Cohort Profile: The Nijmegen Biomedical Study (NBS). Int J Epidemiol. 2017;46(4):1099-1100j.
18. van Rheenen W, van der Spek RAA, Bakker MK, van Vugt JJFA. Common and rare variant association analyses in amyotrophic lateral sclerosis identify 15 risk loci with distinct genetic architectures and neuron-specific biology. Nat Genet. 2021;53(12):1636-1648.

19. Das S, Forer L, Schönherr S, et al. Next-generation genotype imputation service and methods. Nat Genet. 2016;48(10):1284-1287.
20. Zhou W, Nielsen JB, Fritsche LG, et al. Efficiently controlling for case-control imbalance and sample relatedness in large-scale genetic association studies. Nat Genet. 2018;50(9):1335-1341.
21. Olink proteomics AB. Data Normalization and Standardization.
22. Olink proteomics AB. PEA – a high-multiplex immunoassay technology with qPCR or NGS readout.
23. Cipriani V, Lorés-Motta L, He F, et al. Increased circulating levels of Factor H-Related Protein 4 are strongly associated with age-related macular degeneration. Nat Commun. 2020;11(1):178.
24. Lorés-Motta L, van Beek AE, Willems E, et al. Common haplotypes at the CFH locus and low-frequency variants in CFHR2 and CFHR5 associate with systemic FHR concentrations and age-related macular degeneration. Am J Hum Genet. 2021;108(8):1367-1384.
25. Essex RW, Wong J, Jampol LM, Bird AC. Editorial Idiopathic Multifocal Choroiditis : A Comment on Present and Past Nomenclature. Retina. 2013;33(1):1-4.
26. Fung AT, Pal S, Yannuzzi NA, et al. Multifocal choroiditis without panuveitis; Clinical Characteristics and Progression. Retina. 2014;34(1):98-107.
27. Den Hollander AI, Mullins RF, Orozco LD, et al. Systems genomics in age-related macular degeneration. Exp Eye Res. 2022;225:109248.
28. Fritsche Lars G., Wilmar I, Jessica N, et al. A large genome-wide association study of age-related macular degeneration highlights contributions of rare and common variants. Nat Genet. 2016;48(2):134–143.
29. Kaye R, Chandra S, Sheth J, Boon CJF, Sivaprasad S, Lotery A. Central serous chorioretinopathy: An update on risk factors, pathophysiology and imaging modalities. Prog Retin Eye Res. 2020;79:100865.
30. Schellevis RL, Van Dijk EHC, Breukink MB, et al. Role of the Complement System in Chronic Central Serous Chorioretinopathy: A Genome-Wide Association Study. JAMA Ophthalmol. 2018;136(10):1128-1136.
31. Tedja MS, Haarman AEG, Meester-Smoor MA, et al. IMI – Myopia genetics report. Investig Ophthalmol Vis Sci. 2019;60(3):M89-M105.
32. Liao X, Tan QQ, Lan CJ. Myopia genetics in genome-wide association and postgenome- wide association study era. Int J Ophthalmol. 2019;12(9):1487-1492.
33. Hysi PG, Young TL, Mackey DA, et al. A genome-wide association study for myopia and refractive error identifies a susceptibility locus at 15q25. Nat Genet. 2010;42(10):902-905.
34. Solouki AM, Verhoeven VJM, van Duijn CM, et al. A genome-wide association study identifies a susceptibility locus for refractive errors and myopia at 15q14. Nat Genet. 2010;42(10):897-901.
35. Verhoeven VJM, Hysi PG, Saw SM, et al. Large scale international replication and meta-analysis study confirms association of the 15q14 locus with myopia. The CREAM consortium. Hum Genet. 2012;131(9):1467-1480.
36. Cipriani V, Tierney A, Griffiths JR, et al. Beyond factor H: The impact of genetic-risk variants for age-related macular degeneration on circulating factor-H-like 1 and factor-H-related protein concentrations. Am J Hum Genet. 2021;108(8):1385-1400.
37. Emilsson V, Gudmundsson EF, Jonmundsson T, et al. A proteogenomic signature of age-related macular degeneration in blood. Nat Commun. 2022;13(1):3401.
38. Sun BB, Maranville JC, Peters JE, et al. Genomic atlas of the human plasma proteome. Nature. 2018;558(7708):73-79.

39. Puy C, Pang J, Reitsma SE, et al. Crosstalk between the complement pathway and the contact activation system of coagulation: activated factor XI neutralizes complement factor H. J Immunol. 2021;206(8):1784-1792.
40. Eriksson O, Mohlin C, Nilsson B, Ekdahl KN. The human platelet as an innate immune cell: Interactions between activated platelets and the complement system. Front Immunol. 2019;10:1590.
41. Sanchez-Rivera L, Iglesias MJ, Ibrahim-Kosta M, et al. Elevated plasma Complement Factor H Regulating Protein 5 is associated with venous thromboembolism and COVID-19 severity. Preprint.
42. Ueda Y, Mohammed I, Song D, et al. Murine systemic thrombophilia and hemolytic uremic syndrome from a factor H point mutation. Blood. 2017;129(9):1184-1196.
43. Eberhardt HU, Buhlmann D, Hortschansky P, et al. Human factor H-related protein 2 (CFHR2) regulates complement activation. PLoS One. 2013;8(11):e78617.
44. de Groot EL, Ossewaarde - van Norel J, Ho L, ten Dam - van Loon NH, de Boer JH. The efficacy of adalimumab in treating patients with central multifocal choroiditis. Am J Ophthalmol Case Reports. 2020;20:100921.
45. Liao DS, Grossi F V., El Mehdi D, et al. Complement C3 Inhibitor Pegcetacoplan for Geographic Atrophy Secondary to Age-Related Macular Degeneration: A Randomized Phase 2 Trial. Ophthalmology. 2020;127(2):186-195.
46. Jaffe GJ, Westby K, Csaky KG, et al. C5 Inhibitor Avacincaptad Pegol for Geographic Atrophy Due to Age-Related Macular Degeneration: A Randomized Pivotal Phase 2/3 Trial. Ophthalmology. 2021;128(4):576-586.

SUPPLEMENTARY DATA

Supplemental Methods

Genomic DNA extraction

The samples for genetic analysis were collected in two cohorts. Cohort 1 (n=231) consisted of samples obtained between 2006 and 2021 in the EMC, UMCU, Radboudumc and LUMC. Cohort 2 (n=52) consisted of samples obtained between 2021 and 2022 in the Radboudumc, UMCU, AUMC and UMCG. For cohort 1, genomic DNA isolation was performed at the Radboudumc, UMCU and the EMC. In the UMCU and Radboudumc DNA isolation was performed using the Hamilton Microlab STAR autoload system with an integrated Chemagen MSM I separation module (Hamilton Robotics GmbH, Martinsried, Germany) and the DNA was isolated with the Chemagic DNA blood kit special (PerkinElmer). In the EMC the DNA isolation was performed with the Tecan Freedom EVO®-HSM Workstation using the ReliaPrep™ Large Volume HT gDNA Isolation System chemistry. Following DNA isolation, all samples were sent to the Radboudumc where the concentrations of DNA fractions were determined (Hamilton Microlab Starlet robot with integrated Tecan Infinite 200 Pro reader) and the samples were checked for degradation by 1% agarose gel electrophoresis before the samples were genotyped. For cohort 2, genomic DNA isolation was performed either with the Hamilton Microlab STAR or manually with the AllPrep DNA/RNA/miRNA Universal Kit (Qiagen, Hilden, Germany) following standard protocol.

Supplemental Tables

Supplemental Table 9.1. Patient characteristics

	Cohort 1 n=170 patients n=250 eyes	**Cohort 1** n=170 patients n=250 eyes
Female gender, n(%) of all patients	158 (93)	42 (81)
Mean (SD) age of all patients	43 (13)	45 (13)
Subtype, n (%) of all patients		
PIC	61 (36)	14 (27)
MFC	98 (58)	33 (63)
MFC/PIC	11 (6)	5 (10)
Bilateral disease, n (%) of all patients	80 (47)	34 (65)
History of CNV, n (%) of all patients	126 (74)	36 (69)
Median LogMAR BCVA [IQR] of all affected eyes	0.09 [-0.04 – 0.40]	0.03 [0.07 – 0.41]
Median myopia [IQR] of all affected eyes	-4.5 [-7.75 - -0.75]	-3.0 [-7.6 – 0.0]

MFC, multifocal choroiditis; PIC, punctate inner choroidopathy; CNV, choroidal neovascularization; LogMAR, Logarithm of the Minimum Angle of Resolution; BCVA, best-corrected visual acuity. Missing data consisted of: bilateral disease 1 patient, history of CNV 2 patients, BCVA 2 eyes, myopia 19 eyes

Supplemental Table 9.2. All genome-wide significant hits in cohort 1 comprising patients diagnosed with the subtypes idiopathic multifocal choroiditis and punctate inner choroidopathy

SNP	CHR	Gene	bp (Hg19)	Major/minor allele	Minor AF		OR (95% CI)	*P*-value
					Controls	Cases		
rs7535263	1	*CFH*	196682346	G/A	0.430	0.270	0.52 (0.41-0.64)	9.30×10^{-9}
rs6677089	1	*CFH*	196684313	A/C	0.430	0.270	0.52 (0.41-0.64)	9.35×10^{-9}
rs3753395	1	*CFH*	196686652	A/T	0.430	0.270	0.52 (0.41-0.64)	9.35×10^{-9}
rs2274700	1	*CFH*	196682947	G/A	0.430	0.270	0.52 (0.41-0.64)	9.48×10^{-9}
rs10922105	1	*CFH*	196690250	A/C	0.430	0.269	0.52 (0.41-0.64)	9.50×10^{-9}
rs10922106	1	*CFH*	196691464	A/G	0.430	0.269	0.52 (0.41-0.64)	9.50×10^{-9}
rs3766405	1	*CFH*	196695161	C/T	0.431	0.269	0.52 (0.41-0.64)	9.56×10^{-9}
rs6688272	1	*CFH*	196684392	G/T	0.430	0.270	0.52 (0.41-0.64)	9.57×10^{-9}
rs10465586	1	*CFH*	196687329	A/T	0.430	0.270	0.52 (0.41-0.64)	9.57×10^{-9}
rs10922104	1	*CFH*	196687730	A/G	0.430	0.270	0.52 (0.41-0.64)	9.57×10^{-9}
rs1410996	1	*CFH*	196696933	G/A	0.432	0.271	0.52 (0.41-0.64)	9.60×10^{-9}
rs10801558	1	*CFH*	196699044	T/G	0.431	0.269	0.52 (0.41-0.64)	9.69×10^{-9}
rs10922109	1	*CFH*	196704632	C/A	0.430	0.269	0.52 (0.41-0.64)	9.72×10^{-9}
rs10922108	1	*CFH*	196701473	A/T	0.430	0.269	0.52 (0.41-0.64)	9.72×10^{-9}
rs7540032	1	*CFH*	196701284	C/T	0.432	0.271	0.52 (0.41-0.64)	9.87×10^{-9}
rs1329428	1	*CFH*	196702810	C/T	0.432	0.271	0.52 (0.41-0.64)	9.87×10^{-9}
rs1329427	1	*CFH*	196704559	C/T	0.430	0.269	0.52 (0.41-0.64)	9.95×10^{-9}
rs10801559	1	*CFH*	196704204	G/A	0.430	0.269	0.52 (0.41-0.64)	9.96×10^{-9}
rs7514261	1	*CFH*	196700914	G/A	0.430	0.269	0.52 (0.41-0.64)	9.98×10^{-9}
rs10737680	1	*CFH*	196679455	A/C	0.430	0.270	0.52 (0.41-0.64)	1.05×10^{-8}

SNP, single nucleotide polymorphism; CHR, chromosome; bp, basepair; CFH, complement factor H; AF, allele frequency; OR, odds ratio; CI, confidence interval.

Supplemental Table 9.3A. Association results for classical HLA alleles with frequency >0.01 in cases versus a reference population with four digits imputation. For each classical HLA allele, the frequency in the cases and controls are displayed including the odds ratios, confidence intervals and P-values. The reference data was derived from the Haplotype Reference Consortium.

OR, odds ratio; CI, confidence interval; HLA, Human Leukocyte Antigen

Classical HLA allele	Allele frequency		OR	95% CI	*P*-value
	Cases	Controls			
*HLA_A*01*	0.14	0.17	1.62	0.96-2.74	0.072
*HLA_A*01:01*	0.14	0.17	1.63	0.96-2.77	0.069
*HLA_A*01:01:01:01*	0.14	0.17	1.63	0.96-2.77	0.070
*HLA_A*02*	0.34	0.30	0.88	0.63-1.23	0.470
*HLA_A*02:01*	0.34	0.29	0.90	0.64-1.25	0.526
*HLA_A*02:01:01:01*	0.33	0.29	0.90	0.64-1.26	0.546
*HLA_A*03*	0.16	0.16	0.76	0.53-1.09	0.137
*HLA_A*03:01*	0.16	0.16	0.75	0.52-1.08	0.123
*HLA_A*03:01:01:01*	0.16	0.16	0.75	0.52-1.08	0.123
*HLA_A*11*	0.05	0.05	1.26	0.73-2.17	0.412
*HLA_A*11:01*	0.05	0.05	1.28	0.73-2.24	0.399
*HLA_A*11:01:01:01*	0.05	0.05	1.28	0.73-2.24	0.399
*HLA_A*23*	0.02	0.02	2.54	0.94-6.88	0.067
*HLA_A*23:01*	0.02	0.02	2.56	0.94-6.94	0.066
*HLA_A*23:01:01:01*	0.02	0.02	2.56	0.94-6.94	0.066
*HLA_A*24*	0.07	0.09	0.78	0.52-1.17	0.229
*HLA_A*24:02*	0.07	0.09	0.78	0.52-1.18	0.252
*HLA_A*24:02:01:01*	0.07	0.09	0.79	0.52-1.18	0.252
*HLA_A*26*	0.01	0.02	0.79	0.32-1.95	0.622
*HLA_A*26:01*	0.01	0.02	0.82	0.33-2.04	0.683
*HLA_A*26:01:01:01*	0.01	0.02	0.82	0.33-2.04	0.683
*HLA_A*29*	0.02	0.03	0.83	0.41-1.65	0.602
*HLA_A*29:02*	0.02	0.03	0.77	0.37-1.59	0.488
*HLA_A*29:02:01:01*	0.02	0.03	0.77	0.37-1.59	0.490
*HLA_A*30*	0.01	0.02	0.68	0.29-1.56	0.369
*HLA_A*31*	0.06	0.03	3.08	1.52-6.23	0.002
*HLA_A*31:01*	0.06	0.03	3.01	1.49-6.09	0.002
*HLA_A*31:01:02:01*	0.06	0.03	3.01	1.49-6.09	0.002
*HLA_A*32*	0.04	0.04	0.97	0.57-1.65	0.918
*HLA_A*32:01*	0.04	0.04	0.97	0.57-1.65	0.924
*HLA_A*32:01:01:01*	0.04	0.04	0.97	0.57-1.65	0.924
*HLA_A*68*	0.05	0.05	1.08	0.65-1.79	0.788
*HLA_A*68:01*	0.04	0.04	1.05	0.62-1.78	0.862
*HLA_A*68:01:01:01*	0.01	0.01	1.76	0.57-5.42	0.327

Supplemental Table 9.3A. (*continued*)

Classical HLA allele	Allele frequency		OR	95% CI	*P*-value
	Cases	Controls			
*HLA_A*68:01:02:01*	0.03	0.03	0.88	0.47-1.65	0.715
*HLA_C*01*	0.03	0.03	1.10	0.55-2.19	0.803
*HLA_C*01:02*	0.03	0.03	1.10	0.55-2.19	0.802
*HLA_C*01:02:01:01*	0.03	0.03	1.10	0.55-2.19	0.802
*HLA_C*02*	0.04	0.06	0.84	0.51-1.39	0.512
*HLA_C*02:02*	0.04	0.06	0.84	0.51-1.39	0.516
*HLA_C*02:02:02:01*	0.04	0.06	0.85	0.52-1.41	0.545
*HLA_C*03*	0.21	0.18	0.93	0.69-1.27	0.673
*HLA_C*03:03*	0.07	0.07	0.89	0.59-1.35	0.596
*HLA_C*03:03:01:01*	0.07	0.07	0.90	0.59-1.36	0.618
*HLA_C*03:04*	0.13	0.10	1.02	0.70-1.49	0.909
*HLA_C*03:04:01:01*	0.13	0.10	1.03	0.70-1.50	0.897
*HLA_C*04*	0.12	0.11	1.07	0.72-1.60	0.743
*HLA_C*04:01*	0.12	0.11	1.07	0.72-1.60	0.745
*HLA_C*04:01:01:01*	0.12	0.11	1.07	0.72-1.60	0.745
*HLA_C*05*	0.06	0.07	0.92	0.60-1.43	0.735
*HLA_C*05:01*	0.06	0.07	0.92	0.59-1.43	0.708
*HLA_C*05:01:01:01*	0.06	0.07	0.92	0.59-1.43	0.709
*HLA_C*06*	0.08	0.09	1.08	0.71-1.64	0.739
*HLA_C*06:02*	0.08	0.09	1.08	0.71-1.64	0.739
*HLA_C*06:02:01:01*	0.08	0.09	1.08	0.71-1.65	0.738
*HLA_C*07*	0.34	0.33	0.96	0.69-1.32	0.792
*HLA_C*07:01*	0.14	0.16	1.29	0.80-2.08	0.304
*HLA_C*07:01:01:01*	0.14	0.16	1.29	0.80-2.08	0.304
*HLA_C*07:02*	0.19	0.15	0.78	0.48-1.24	0.295
*HLA_C*07:02:01:01*	0.19	0.15	0.78	0.48-1.24	0.294
*HLA_C*07:04*	0.01	0.02	0.80	0.35-1.81	0.600
*HLA_C*07:04:01:01*	0.01	0.02	0.80	0.35-1.81	0.600
*HLA_C*08*	0.02	0.02	1.50	0.61-3.71	0.384
*HLA_C*08:02*	0.02	0.02	1.50	0.61-3.71	0.383
*HLA_C*08:02:01:01*	0.02	0.02	1.50	0.61-3.71	0.384
*HLA_C*12*	0.02	0.04	0.64	0.34-1.20	0.166
*HLA_C*12:03*	0.02	0.04	0.70	0.36-1.37	0.302
*HLA_C*12:03:01:01*	0.02	0.04	0.70	0.36-1.37	0.303
*HLA_C*14*	0.01	0.01	0.90	0.36-2.30	0.845
*HLA_C*14:02*	0.01	0.01	0.91	0.36-2.32	0.860
*HLA_C*14:02:01:01*	0.01	0.01	0.91	0.36-2.32	0.860
*HLA_C*15*	0.04	0.02	2.85	1.30-6.23	0.009

Supplemental Table 9.3A. (*continued*)

Classical HLA allele	Allele frequency		OR	95% CI	*P*-value
	Cases	Controls			
*HLA_C*15:02*	0.03	0.02	2.49	1.09-5.70	0.031
*HLA_C*15:02:01:01*	0.03	0.02	2.49	1.09-5.70	0.031
*HLA_C*16*	0.02	0.03	0.70	0.35-1.40	0.314
*HLA_C*16:01*	0.01	0.03	0.52	0.24-1.11	0.091
*HLA_C*16:01:01:01*	0.01	0.03	0.52	0.24-1.11	0.091
*HLA_B*07*	0.18	0.14	0.90	0.55-1.47	0.677
*HLA_B*07:02*	0.17	0.14	0.81	0.49-1.35	0.431
*HLA_B*07:02:01:01*	0.17	0.14	0.81	0.49-1.35	0.430
*HLA_B*08*	0.10	0.12	1.80	0.88-3.71	0.108
*HLA_B*08:01*	0.10	0.12	1.76	0.85-3.61	0.126
*HLA_B*08:01:01:01*	0.10	0.12	1.79	0.87-3.69	0.112
*HLA_B*13*	0.02	0.02	1.11	0.51-2.42	0.798
*HLA_B*13:02*	0.02	0.02	1.11	0.51-2.43	0.797
*HLA_B*13:02:01:01*	0.02	0.02	1.11	0.51-2.43	0.797
*HLA_B*14*	0.02	0.02	1.43	0.59-3.48	0.437
*HLA_B*14:02*	0.01	0.01	0.94	0.37-2.39	0.905
*HLA_B*14:02:01:01*	0.01	0.01	0.94	0.37-2.39	0.905
*HLA_B*15*	0.14	0.10	1.23	0.85-1.78	0.286
*HLA_B*15:01*	0.14	0.09	1.33	0.90-1.97	0.147
*HLA_B*15:01:01:01*	0.14	0.09	1.33	0.90-1.97	0.147
*HLA_B*18*	0.02	0.04	0.65	0.35-1.21	0.177
*HLA_B*18:01*	0.02	0.04	0.68	0.36-1.29	0.238
*HLA_B*18:01:01:01*	0.02	0.04	0.68	0.36-1.29	0.238
*HLA_B*27*	0.04	0.04	1.21	0.68-2.14	0.524
*HLA_B*27:05*	0.04	0.04	1.29	0.70-2.37	0.423
*HLA_B*27:05:02:01*	0.04	0.03	1.29	0.70-2.37	0.422
*HLA_B*35*	0.09	0.09	0.97	0.63-1.49	0.894
*HLA_B*35:01*	0.07	0.07	0.90	0.55-1.47	0.686
*HLA_B*35:01:01:01*	0.07	0.07	0.90	0.55-1.47	0.686
*HLA_B*35:02*	0.01	0.01	2.86	0.62-13.12	0.176
*HLA_B*35:02:01:01*	0.01	0.01	2.86	0.62-13.12	0.176
*HLA_B*37*	0.02	0.01	1.28	0.51-3.24	0.607
*HLA_B*37:01*	0.02	0.01	1.29	0.51-3.24	0.607
*HLA_B*37:01:01:01*	0.02	0.01	1.29	0.51-3.24	0.607
*HLA_B*39*	0.02	0.02	0.89	0.40-1.97	0.787
*HLA_B*40*	0.07	0.08	0.80	0.52-1.22	0.304
*HLA_B*40:01*	0.06	0.06	0.81	0.51-1.28	0.365
*HLA_B*40:01:01*	0.06	0.06	0.81	0.51-1.28	0.365

Supplemental Table 9.3A. (*continued*)

Classical HLA allele	Allele frequency		OR	95% CI	*P*-value
	Cases	Controls			
*HLA_B*40:02*	0.01	0.01	0.81	0.32-2.04	0.666
*HLA_B*40:02:01:01*	0.01	0.01	0.81	0.32-2.04	0.666
*HLA_B*41*	0.02	0.00	18.93	2.94-121.89	0.002
*HLA_B*44*	0.11	0.13	0.93	0.65-1.32	0.688
*HLA_B*44:02*	0.07	0.08	0.97	0.65-1.47	0.909
*HLA_B*44:02:01:01*	0.07	0.08	0.97	0.65-1.47	0.909
*HLA_B*44:03*	0.03	0.04	0.92	0.49-1.73	0.799
*HLA_B*44:03:01:01*	0.03	0.04	0.93	0.50-1.75	0.840
*HLA_B*51*	0.06	0.06	1.10	0.67-1.83	0.710
*HLA_B*51:01*	0.05	0.06	1.01	0.62-1.64	0.977
*HLA_B*51:01:01:01*	0.05	0.06	1.01	0.62-1.64	0.977
*HLA_B*55*	0.01	0.02	0.64	0.28-1.46	0.289
*HLA_B*55:01*	0.01	0.02	0.64	0.28-1.47	0.298
*HLA_B*55:01:01*	0.01	0.02	0.64	0.28-1.47	0.298
*HLA_B*57*	0.03	0.03	1.30	0.65-2.62	0.470
*HLA_B*57:01*	0.03	0.03	1.35	0.67-2.75	0.409
*HLA_B*57:01:01:01*	0.03	0.03	1.35	0.67-2.75	0.409
*HLA_DRB1*01*	0.12	0.11	0.88	0.60-1.29	0.518
*HLA_DRB1*01:01*	0.11	0.10	0.86	0.58-1.29	0.487
*HLA_DRB1*01:01:01*	0.11	0.10	0.86	0.58-1.29	0.488
*HLA_DRB1*03*	0.10	0.13	1.03	0.60-1.76	0.931
*HLA_DRB1*03:01*	0.10	0.13	1.05	0.61-1.82	0.865
*HLA_DRB1*03:01:01:01*	0.10	0.13	1.05	0.61-1.82	0.866
*HLA_DRB1*04*	0.17	0.14	1.24	0.87-1.76	0.241
*HLA_DRB1*04:01*	0.12	0.09	1.39	0.90-2.16	0.140
*HLA_DRB1*04:01:01:01*	0.12	0.09	1.39	0.90-2.16	0.140
*HLA_DRB1*04:04*	0.04	0.03	1.24	0.64-2.39	0.533
*HLA_DRB1*04:04:01*	0.04	0.03	1.24	0.64-2.39	0.533
*HLA_DRB1*07*	0.08	0.11	0.85	0.55-1.32	0.484
*HLA_DRB1*07:01*	0.07	0.10	0.85	0.55-1.32	0.481
*HLA_DRB1*07:01:01:01*	0.07	0.10	0.85	0.55-1.32	0.481
*HLA_DRB1*08*	0.02	0.03	0.67	0.33-1.35	0.263
*HLA_DRB1*08:01*	0.01	0.02	0.58	0.27-1.25	0.165
*HLA_DRB1*08:01:01*	0.01	0.02	0.58	0.27-1.25	0.165
*HLA_DRB1*09*	0.02	0.01	2.11	0.76-5.82	0.151
*HLA_DRB1*09:01*	0.02	0.01	2.11	0.77-5.84	0.149
*HLA_DRB1*09:01:02:01*	0.02	0.01	2.11	0.77-5.84	0.149
*HLA_DRB1*10*	0.02	0.01	4.28	1.29-14.13	0.017

Supplemental Table 9.3A. (*continued*)

Classical HLA allele	Allele frequency		OR	95% CI	*P*-value
	Cases	Controls			
*HLA_DRB1*10:01*	0.02	0.01	4.28	1.29-14.13	0.017
*HLA_DRB1*10:01:01:01*	0.02	0.01	4.28	1.29-14.13	0.017
*HLA_DRB1*11*	0.05	0.09	0.63	0.40-0.99	0.047
*HLA_DRB1*11:01*	0.04	0.06	0.64	0.37-1.11	0.114
*HLA_DRB1*11:01:01:01*	0.04	0.06	0.64	0.37-1.12	0.120
*HLA_DRB1*13*	0.12	0.13	0.90	0.64-1.26	0.533
*HLA_DRB1*13:01*	0.05	0.07	0.74	0.46-1.20	0.225
*HLA_DRB1*13:01:01:01*	0.05	0.07	0.74	0.46-1.20	0.225
*HLA_DRB1*13:02*	0.05	0.05	0.98	0.61-1.59	0.953
*HLA_DRB1*13:02:01:01*	0.05	0.05	0.98	0.61-1.59	0.953
*HLA_DRB1*13:03*	0.01	0.01	1.75	0.49-6.31	0.397
*HLA_DRB1*13:03:01*	0.01	0.01	1.75	0.49-6.31	0.397
*HLA_DRB1*14*	0.03	0.04	0.95	0.52-1.73	0.868
*HLA_DRB1*14:01*	0.03	0.04	0.97	0.53-1.78	0.921
*HLA_DRB1*14:01:01*	0.03	0.04	0.97	0.53-1.78	0.921
*HLA_DRB1*15*	0.22	0.15	1.53	0.99-2.37	0.055
*HLA_DRB1*15:01*	0.20	0.13	1.62	1.03-2.55	0.036
*HLA_DRB1*15:01:01:01*	0.20	0.13	1.65	1.05-2.60	0.031
*HLA_DRB1*16*	0.02	0.01	1.96	0.69-5.54	0.206
*HLA_DRB1*16:01*	0.02	0.01	1.59	0.56-4.53	0.396
*HLA_DRB1*16:01:01*	0.02	0.01	1.59	0.56-4.53	0.395
*HLA_DQA1*01*	0.51	0.44	1.12	0.87-1.45	0.383
*HLA_DQA1*01:01*	0.17	0.16	1.00	0.73-1.35	0.976
*HLA_DQA1*01:01:01:01*	0.17	0.16	1.00	0.73-1.35	0.976
*HLA_DQA1*01:02*	0.28	0.21	1.50	1.05-2.14	0.026
*HLA_DQA1*01:02:01:01*	0.28	0.21	1.50	1.05-2.14	0.026
*HLA_DQA1*01:03*	0.06	0.07	0.79	0.51-1.22	0.287
*HLA_DQA1*01:03:01:01*	0.06	0.07	0.79	0.51-1.22	0.287
*HLA_DQA1*02*	0.08	0.12	0.78	0.52-1.18	0.238
*HLA_DQA1*02:01*	0.08	0.12	0.78	0.52-1.18	0.238
*HLA_DQA1*02:01:01:01*	0.08	0.12	0.78	0.52-1.18	0.238
*HLA_DQA1*03*	0.22	0.17	1.36	0.99-1.86	0.055
*HLA_DQA1*03:01*	0.22	0.17	1.36	0.99-1.86	0.055
*HLA_DQA1*03:01:01*	0.22	0.17	1.36	0.99-1.86	0.055
*HLA_DQA1*04*	0.02	0.03	0.56	0.29-1.07	0.078
*HLA_DQA1*04:01*	0.02	0.03	0.56	0.29-1.07	0.078
*HLA_DQA1*04:01:01:01*	0.02	0.03	0.56	0.29-1.07	0.078
*HLA_DQA1*05*	0.16	0.22	0.77	0.52-1.13	0.176

Supplemental Table 9.3A. (*continued*)

Classical HLA allele	Allele frequency		OR	95% CI	*P*-value
	Cases	Controls			
*HLA_DQA1*05:01*	0.16	0.22	0.77	0.52-1.13	0.176
*HLA_DQA1*05:01:01:01*	0.16	0.22	0.77	0.52-1.13	0.176
*HLA_DQB1*02*	0.15	0.21	0.85	0.59-1.23	0.403
*HLA_DQB1*02:01*	0.15	0.21	0.85	0.58-1.23	0.393
*HLA_DQB1*02:01:01*	0.15	0.21	0.85	0.58-1.23	0.394
*HLA_DQB1*03*	0.32	0.32	1.03	0.80-1.32	0.831
*HLA_DQB1*03:01*	0.12	0.17	0.76	0.54-1.08	0.123
*HLA_DQB1*03:01:01:01*	0.12	0.17	0.76	0.54-1.08	0.123
*HLA_DQB1*03:02*	0.14	0.10	1.35	0.93-1.97	0.114
*HLA_DQB1*03:02:01:01*	0.14	0.10	1.36	0.93-1.98	0.114
*HLA_DQB1*03:03*	0.05	0.04	1.24	0.69-2.22	0.476
*HLA_DQB1*03:03:02:01*	0.05	0.04	1.24	0.69-2.23	0.476
*HLA_DQB1*04*	0.02	0.03	0.58	0.30-1.12	0.107
*HLA_DQB1*04:02*	0.02	0.03	0.58	0.30-1.13	0.111
*HLA_DQB1*04:02:01:01*	0.02	0.03	0.58	0.30-1.13	0.108
*HLA_DQB1*05*	0.20	0.17	1.09	0.79-1.49	0.616
*HLA_DQB1*05:01*	0.14	0.12	0.99	0.70-1.39	0.951
*HLA_DQB1*05:01:01:01*	0.14	0.12	0.99	0.70-1.39	0.951
*HLA_DQB1*05:02*	0.02	0.02	1.43	0.59-3.47	0.442
*HLA_DQB1*05:02:01:01*	0.02	0.02	1.43	0.59-3.47	0.442
*HLA_DQB1*05:03*	0.04	0.04	1.10	0.60-2.00	0.772
*HLA_DQB1*05:03:01:01*	0.04	0.04	1.10	0.60-2.00	0.772
*HLA_DQB1*06*	0.31	0.26	1.13	0.83-1.53	0.443
*HLA_DQB1*06:02*	0.19	0.13	1.57	0.99-2.48	0.055
*HLA_DQB1*06:02:01:01*	0.19	0.13	1.58	1.00-2.51	0.050
*HLA_DQB1*06:03*	0.06	0.07	0.85	0.55-1.32	0.481
*HLA_DQB1*06:03:01:01*	0.06	0.07	0.85	0.55-1.32	0.482
*HLA_DQB1*06:04*	0.04	0.05	0.88	0.52-1.50	0.650
*HLA_DQB1*06:04:01*	0.04	0.05	0.88	0.52-1.50	0.651
*HLA_DPA1*01*	0.81	0.81	0.87	0.64-1.18	0.378
*HLA_DPA1*01:03*	0.81	0.81	0.90	0.66-1.22	0.497
*HLA_DPA1*01:03:01:01*	0.81	0.81	0.90	0.66-1.22	0.513
*HLA_DPA1*02*	0.18	0.18	1.14	0.84-1.56	0.401
*HLA_DPA1*02:01*	0.16	0.14	1.35	0.96-1.91	0.086
*HLA_DPA1*02:01:01:01*	0.08	0.07	1.28	0.81-2.04	0.297
*HLA_DPA1*02:01:02:01*	0.06	0.06	1.26	0.73-2.19	0.409
*HLA_DPA1*02:02*	0.02	0.04	0.65	0.35-1.19	0.159
*HLA_DPA1*02:02:02:01*	0.02	0.04	0.64	0.35-1.19	0.162

Supplemental Table 9.3A. (*continued*)

Classical HLA allele	Allele frequency		OR	95% CI	*P*-value
	Cases	Controls			
*HLA_DPB1*01*	0.06	0.07	1.12	0.69-1.83	0.663
*HLA_DPB1*01:01*	0.06	0.07	1.12	0.69-1.83	0.663
*HLA_DPB1*01:01:01:01*	0.06	0.07	1.12	0.69-1.84	0.652
*HLA_DPB1*02*	0.13	0.14	0.94	0.69-1.30	0.735
*HLA_DPB1*02:01*	0.12	0.14	0.94	0.68-1.29	0.717
*HLA_DPB1*02:01:02:01*	0.12	0.14	0.94	0.68-1.30	0.721
*HLA_DPB1*03*	0.12	0.12	0.96	0.69-1.33	0.807
*HLA_DPB1*03:01*	0.12	0.12	0.96	0.69-1.33	0.807
*HLA_DPB1*03:01:01:01*	0.12	0.12	0.96	0.69-1.33	0.807
*HLA_DPB1*04*	0.53	0.52	0.98	0.79-1.22	0.874
*HLA_DPB1*04:01*	0.40	0.41	0.94	0.74-1.18	0.589
*HLA_DPB1*04:01:01:01*	0.40	0.41	0.94	0.74-1.18	0.588
*HLA_DPB1*04:02*	0.12	0.11	1.12	0.78-1.60	0.556
*HLA_DPB1*04:02:01:01*	0.12	0.11	1.12	0.78-1.60	0.556
*HLA_DPB1*05*	0.01	0.02	0.67	0.30-1.49	0.332
*HLA_DPB1*05:01*	0.01	0.02	0.67	0.30-1.49	0.332
*HLA_DPB1*05:01:01:01*	0.01	0.02	0.67	0.30-1.49	0.332
*HLA_DPB1*06*	0.03	0.02	1.97	0.8-04.85	0.142
*HLA_DPB1*06:01*	0.03	0.02	1.97	0.80-4.84	0.142
*HLA_DPB1*06:01:01:01*	0.03	0.02	1.97	0.80-4.84	0.142
*HLA_DPB1*09*	0.01	0.01	1.35	0.48-3.80	0.579
*HLA_DPB1*09:01*	0.01	0.01	1.35	0.48-3.80	0.579
*HLA_DPB1*09:01:01*	0.01	0.01	1.35	0.48-3.80	0.579
*HLA_DPB1*10*	0.01	0.01	1.52	0.53-4.35	0.444
*HLA_DPB1*10:01*	0.01	0.01	1.52	0.53-4.35	0.444
*HLA_DPB1*10:01:01:01*	0.01	0.01	1.52	0.53-4.35	0.444
*HLA_DPB1*11*	0.01	0.02	0.85	0.37-1.97	0.715
*HLA_DPB1*11:01*	0.01	0.02	0.85	0.37-1.97	0.715
*HLA_DPB1*11:01:01*	0.01	0.02	0.85	0.37-1.97	0.715
*HLA_DPB1*13*	0.01	0.01	1.33	0.46-3.84	0.608
*HLA_DPB1*13:01*	0.01	0.01	1.33	0.46-3.84	0.608
*HLA_DPB1*13:01:01:01*	0.01	0.01	1.33	0.46-3.84	0.608
*HLA_DPB1*14*	0.03	0.02	3.58	1.32-9.65	0.012
*HLA_DPB1*14:01*	0.03	0.02	3.58	1.32-9.65	0.012
*HLA_DPB1*16*	0.01	0.01	1.08	0.40-2.94	0.893
*HLA_DPB1*16:01*	0.01	0.01	1.08	0.40-2.94	0.893

Supplemental Table 9.3B. Association results for classical HLA alleles with frequency >0.01 in cases versus a reference population with g group imputation. For each classical HLA allele, the frequency in the cases and controls are displayed including the odds ratios, confidence intervals and P-values. The reference data was derived from the Haplotype Reference Consortium.

OR, odds ratio; CI, confidence interval; HLA, Human Leukocyte Antigen.

Classical HLA allele	Allele frequency		OR	95% CI	*P*-value
	Cases	Controls			
*HLA_A*01*	0.14	0.17	1.61	0.95-2.73	0.074
*HLA_A*01:01:01:01*	0.14	0.17	1.62	0.95-2.75	0.074
*HLA_A*02*	0.34	0.30	0.88	0.63-1.23	0.464
*HLA_A*02:01:01:01*	0.34	0.29	0.90	0.64-1.25	0.538
*HLA_A*03*	0.16	0.16	0.76	0.53-1.09	0.137
*HLA_A*03:01:01:01*	0.16	0.16	0.74	0.52-1.07	0.114
*HLA_A*11*	0.05	0.05	1.26	0.73-2.17	0.409
*HLA_A*11:01:01:01*	0.05	0.05	1.27	0.73-2.22	0.406
*HLA_A*23*	0.02	0.02	2.52	0.93-6.82	0.069
*HLA_A*23:01:01:01*	0.02	0.02	2.52	0.93-6.83	0.069
*HLA_A*24*	0.07	0.09	0.78	0.52-1.17	0.229
*HLA_A*24:02:01:01*	0.07	0.09	0.78	0.52-1.18	0.249
*HLA_A*26*	0.01	0.02	0.78	0.32-1.92	0.606
*HLA_A*26:01:01:01*	0.01	0.02	0.81	0.33-2.01	0.664
*HLA_A*29*	0.02	0.03	0.83	0.41-1.66	0.611
*HLA_A*29:02:01:01*	0.02	0.03	0.77	0.37-1.60	0.497
*HLA_A*30*	0.01	0.02	0.68	0.30-1.57	0.372
*HLA_A*31*	0.06	0.03	3.08	1.53-6.21	0.002
*HLA_A*31:01:02:01*	0.06	0.03	3.02	1.50-6.09	0.002
*HLA_A*32*	0.04	0.04	0.97	0.57-1.64	0.911
*HLA_A*32:01:01:01*	0.04	0.04	0.97	0.57-1.65	0.920
*HLA_A*68*	0.05	0.05	1.07	0.65-1.78	0.793
*HLA_A*68:01:01:01*	0.01	0.01	1.74	0.56-5.43	0.343
*HLA_A*68:01:02:01*	0.03	0.03	0.88	0.47-1.65	0.704
*HLA_C*01*	0.03	0.03	1.10	0.55-2.19	0.803
*HLA_C*01:02:01:01*	0.03	0.03	1.10	0.55-2.19	0.802
*HLA_C*02*	0.04	0.06	0.84	0.51-1.39	0.513
*HLA_C*02:02:02:01*	0.04	0.06	0.85	0.51-1.41	0.546
*HLA_C*03*	0.21	0.18	0.93	0.69-1.27	0.673
*HLA_C*03:03:01:01*	0.07	0.07	0.89	0.59-1.35	0.602
*HLA_C*03:04:01:01*	0.14	0.10	1.03	0.71-1.51	0.877
*HLA_C*04*	0.12	0.11	1.07	0.72-1.60	0.749
*HLA_C*04:01:01:01*	0.12	0.11	1.07	0.72-1.60	0.751

Supplemental Table 9.3B. (*continued*)

Classical HLA allele	Allele frequency		OR	95% CI	*P*-value
	Cases	Controls			
*HLA_C*05*	0.06	0.07	0.92	0.60-1.43	0.737
*HLA_C*05:01:01:01*	0.06	0.07	0.92	0.59-1.43	0.722
*HLA_C*06*	0.08	0.09	1.08	0.71-1.64	0.738
*HLA_C*06:02:01:01*	0.08	0.09	1.08	0.71-1.65	0.735
*HLA_C*07*	0.34	0.33	0.96	0.69-1.32	0.790
*HLA_C*07:01:01:01*	0.14	0.16	1.29	0.80-2.08	0.303
*HLA_C*07:02:01:01*	0.19	0.15	0.78	0.48-1.24	0.294
*HLA_C*07:04:01:01*	0.01	0.02	0.80	0.35-1.81	0.599
*HLA_C*08*	0.02	0.02	1.50	0.61-3.69	0.389
*HLA_C*08:02:01:01*	0.02	0.02	1.50	0.61-3.69	0.388
*HLA_C*12*	0.02	0.04	0.64	0.34-1.20	0.166
*HLA_C*12:03:01:01*	0.02	0.04	0.70	0.36-1.37	0.303
*HLA_C*14*	0.01	0.01	0.90	0.36-2.30	0.845
*HLA_C*14:02:01:01*	0.01	0.01	0.91	0.36-2.32	0.860
*HLA_C*15*	0.04	0.02	2.81	1.28-6.13	0.010
*HLA_C*15:02:01:01*	0.03	0.02	2.41	1.05-5.52	0.037
*HLA_C*16*	0.02	0.03	0.70	0.35-1.41	0.322
*HLA_C*16:01:01:01*	0.01	0.03	0.52	0.24-1.12	0.095
*HLA_B*07*	0.18	0.14	0.89	0.55-1.46	0.670
*HLA_B*07:02:01:01*	0.17	0.14	0.80	0.48-1.33	0.395
*HLA_B*08*	0.10	0.12	1.82	0.88-3.74	0.105
*HLA_B*08:01:01:01*	0.10	0.12	1.85	0.89-3.81	0.097
*HLA_B*13*	0.02	0.02	1.12	0.52-2.45	0.779
*HLA_B*13:02:01:01*	0.02	0.02	1.13	0.52-2.45	0.778
*HLA_B*14*	0.02	0.02	1.43	0.59-3.45	0.442
*HLA_B*14:02:01:01*	0.01	0.01	0.93	0.37-2.37	0.894
*HLA_B*15*	0.14	0.10	1.23	0.85-1.78	0.282
*HLA_B*15:01:01:01*	0.14	0.09	1.34	0.91-1.97	0.140
*HLA_B*18*	0.02	0.04	0.68	0.36-1.28	0.237
*HLA_B*18:01:01:01*	0.02	0.04	0.68	0.36-1.29	0.242
*HLA_B*27*	0.05	0.04	1.30	0.73-2.31	0.380
*HLA_B*27:05:02:01*	0.04	0.03	1.40	0.76-2.59	0.289
*HLA_B*35*	0.09	0.09	0.97	0.63-1.49	0.902
*HLA_B*35:01:01:01*	0.07	0.07	0.89	0.54-1.46	0.664
*HLA_B*35:02:01:01*	0.01	0.01	2.85	0.63-12.83	0.174
*HLA_B*37*	0.02	0.01	1.28	0.51-3.21	0.612
*HLA_B*37:01:01:01*	0.02	0.01	1.28	0.51-3.21	0.612

Supplemental Table 9.3B. (*continued*)

Classical HLA allele	Allele frequency		OR	95% CI	*P*-value
	Cases	Controls			
*HLA_B*39*	0.02	0.02	0.90	0.41-2.00	0.816
*HLA_B*40*	0.07	0.08	0.75	0.49-1.15	0.188
*HLA_B*40:01:01*	0.06	0.06	0.79	0.50-1.25	0.314
*HLA_B*41*	0.02	0.00	19.2	2.98-123.79	0.002
*HLA_B*44*	0.11	0.13	0.93	0.65-1.32	0.680
*HLA_B*44:02:01:01*	0.07	0.08	0.97	0.64-1.46	0.891
*HLA_B*44:03:01:01*	0.03	0.04	0.93	0.50-1.75	0.839
*HLA_B*51*	0.06	0.06	1.10	0.67-1.81	0.726
*HLA_B*51:01:01:01*	0.05	0.06	1.00	0.61-1.63	0.999
*HLA_B*55*	0.01	0.02	0.64	0.28-1.46	0.290
*HLA_B*55:01:01*	0.01	0.02	0.64	0.28-1.47	0.299
*HLA_B*57*	0.03	0.03	1.29	0.64-2.60	0.478
*HLA_B*57:01:01:01*	0.03	0.03	1.34	0.66-2.72	0.418
*HLA_DRB1*01*	0.12	0.12	0.88	0.60-1.28	0.512
*HLA_DRB1*01:01:01*	0.11	0.10	0.85	0.56-1.27	0.428
*HLA_DRB1*03*	0.10	0.13	1.05	0.61-1.80	0.875
*HLA_DRB1*03:01:01:01*	0.10	0.13	1.07	0.62-1.85	0.812
*HLA_DRB1*04*	0.18	0.14	1.26	0.89-1.79	0.197
*HLA_DRB1*04:01:01:01*	0.12	0.09	1.46	0.94-2.24	0.089
*HLA_DRB1*04:04:01*	0.04	0.03	1.22	0.62-2.38	0.582
*HLA_DRB1*07*	0.07	0.11	0.82	0.53-1.27	0.382
*HLA_DRB1*07:01:01:01*	0.07	0.10	0.84	0.54-1.31	0.451
*HLA_DRB1*08*	0.02	0.03	0.68	0.35-1.34	0.269
*HLA_DRB1*08:01:01*	0.01	0.03	0.61	0.29-1.26	0.180
*HLA_DRB1*09*	0.02	0.01	2.17	0.78-6.08	0.139
*HLA_DRB1*09:01:02:01*	0.02	0.01	2.16	0.77-6.05	0.142
*HLA_DRB1*10*	0.02	0.01	4.15	1.27-13.61	0.019
*HLA_DRB1*10:01:01:01*	0.02	0.01	4.15	1.27-13.61	0.019
*HLA_DRB1*11*	0.05	0.09	0.62	0.40-0.98	0.039
*HLA_DRB1*11:01:01:01*	0.04	0.06	0.63	0.36-1.10	0.103
*HLA_DRB1*13*	0.11	0.13	0.90	0.64-1.26	0.548
*HLA_DRB1*13:01:01:01*	0.05	0.07	0.75	0.47-1.21	0.240
*HLA_DRB1*13:02:01:01*	0.05	0.05	0.98	0.61-1.58	0.939
*HLA_DRB1*13:03:01*	0.01	0.01	1.81	0.50-6.58	0.371
*HLA_DRB1*14*	0.04	0.04	1.07	0.58-1.96	0.847
*HLA_DRB1*14:01:01*	0.03	0.03	1.11	0.59-2.08	0.767
*HLA_DRB1*15*	0.21	0.15	1.45	0.94-2.24	0.093

Supplemental Table 9.3B. (*continued*)

Classical HLA allele	Allele frequency		OR	95% CI	*P*-value
	Cases	Controls			
*HLA_DRB1*15:01:01:01*	0.20	0.13	1.64	1.04-2.57	0.033
*HLA_DRB1*16*	0.02	0.01	2.10	0.74-5.94	0.163
*HLA_DRB1*16:01:01*	0.02	0.01	1.60	0.56-4.57	0.385
*HLA_DQA1*01*	0.52	0.44	1.12	0.87-1.45	0.383
*HLA_DQA1*01:01:01:01*	0.17	0.16	1.00	0.74-1.36	0.995
*HLA_DQA1*01:02:01:01*	0.28	0.21	1.48	1.04-2.11	0.030
*HLA_DQA1*01:03:01:01*	0.06	0.07	0.79	0.51-1.22	0.292
*HLA_DQA1*02*	0.08	0.12	0.79	0.52-1.19	0.255
*HLA_DQA1*02:01:01:01*	0.08	0.12	0.79	0.52-1.19	0.255
*HLA_DQA1*03*	0.22	0.17	1.36	0.99-1.86	0.056
*HLA_DQA1*03:01:01*	0.22	0.17	1.36	0.99-1.86	0.056
*HLA_DQA1*04*	0.02	0.03	0.58	0.30-1.10	0.096
*HLA_DQA1*04:01:01:01*	0.02	0.03	0.58	0.30-1.10	0.096
*HLA_DQB1*02*	0.15	0.21	0.86	0.59-1.24	0.414
*HLA_DQB1*02:01:01*	0.15	0.21	0.86	0.59-1.24	0.420
*HLA_DQB1*03*	0.32	0.32	1.02	0.80-1.31	0.891
*HLA_DQB1*03:01:01:01*	0.12	0.17	0.75	0.54-1.06	0.104
*HLA_DQB1*03:02:01:01*	0.14	0.10	1.33	0.91-1.93	0.141
*HLA_DQB1*03:03:02:01*	0.05	0.04	1.26	0.70-2.25	0.452
*HLA_DQB1*04*	0.02	0.03	0.60	0.31-1.16	0.127
*HLA_DQB1*04:02:01:01*	0.02	0.03	0.60	0.31-1.16	0.126
*HLA_DQB1*05*	0.20	0.17	1.09	0.79-1.49	0.618
*HLA_DQB1*05:01:01:01*	0.14	0.12	0.99	0.70-1.39	0.941
*HLA_DQB1*05:02:01:01*	0.02	0.02	1.47	0.60-3.60	0.404
*HLA_DQB1*05:03:01:01*	0.04	0.04	1.09	0.60-2.00	0.778
*HLA_DQB1*06*	0.31	0.26	1.13	0.83-1.54	0.437
*HLA_DQB1*06:02:01:01*	0.20	0.13	1.59	1.01-2.52	0.046
*HLA_DQB1*06:03:01:01*	0.06	0.07	0.85	0.55-1.31	0.479
*HLA_DQB1*06:04:01*	0.04	0.05	0.88	0.51-1.50	0.644
*HLA_DPA1*01*	0.81	0.81	0.87	0.64-1.19	0.395
*HLA_DPA1*01:03:01:01*	0.81	0.81	0.91	0.67-1.23	0.545
*HLA_DPA1*02*	0.18	0.18	1.14	0.84-1.55	0.415
*HLA_DPA1*02:01:01:01*	0.08	0.07	1.32	0.83-2.10	0.250
*HLA_DPA1*02:01:02:01*	0.07	0.06	1.31	0.76-2.26	0.340
*HLA_DPA1*02:02:02:01*	0.02	0.04	0.66	0.36-1.20	0.170
*HLA_DPB1*01*	0.06	0.07	1.12	0.69-1.83	0.660
*HLA_DPB1*01:01:01:01*	0.06	0.07	1.13	0.69-1.84	0.649

Supplemental Table 9.3B. (*continued*)

Classical HLA allele	Allele frequency		OR	95% CI	*P*-value
	Cases	Controls			
*HLA_DPB1*02*	0.13	0.14	0.94	0.69-1.30	0.740
*HLA_DPB1*02:01:02:01*	0.12	0.14	0.94	0.68-1.30	0.722
*HLA_DPB1*03*	0.12	0.12	0.95	0.68-1.32	0.755
*HLA_DPB1*03:01:01:01*	0.12	0.12	0.95	0.68-1.32	0.755
*HLA_DPB1*04*	0.53	0.52	0.98	0.80-1.22	0.899
*HLA_DPB1*04:01:01:01*	0.41	0.41	0.94	0.75-1.19	0.639
*HLA_DPB1*04:02:01:01*	0.12	0.11	1.10	0.77-1.58	0.598
*HLA_DPB1*05*	0.01	0.02	0.69	0.32-1.52	0.369
*HLA_DPB1*05:01:01:01*	0.01	0.02	0.69	0.32-1.52	0.369
*HLA_DPB1*06*	0.03	0.02	2.02	0.81-5.04	0.131
*HLA_DPB1*06:01:01:01*	0.03	0.02	2.02	0.81-5.03	0.131
*HLA_DPB1*09*	0.01	0.01	1.37	0.49-3.84	0.559
*HLA_DPB1*09:01:01*	0.01	0.01	1.37	0.49-3.84	0.559
*HLA_DPB1*10*	0.01	0.01	1.48	0.52-4.20	0.468
*HLA_DPB1*10:01:01:01*	0.01	0.01	1.48	0.52-4.21	0.468
*HLA_DPB1*11*	0.01	0.02	0.85	0.37-1.97	0.716
*HLA_DPB1*11:01:01*	0.01	0.02	0.85	0.37-1.97	0.716
*HLA_DPB1*13*	0.01	0.01	1.31	0.46-3.73	0.626
*HLA_DPB1*13:01:01:01*	0.01	0.01	1.31	0.46-3.73	0.626
*HLA_DPB1*14*	0.03	0.02	3.76	1.37-10.27	0.010
*HLA_DPB1*14:01:01:01*	0.03	0.02	3.76	1.37-10.27	0.010
*HLA_DPB1*16*	0.01	0.01	1.07	0.39-2.93	0.896
*HLA_DPB1*16:01:01*	0.01	0.01	1.07	0.39-2.93	0.896

Supplemental Table 9.4. Full list of proteins measured in the Olink Explore 384 inflammation II panel including the mean and standard deviation in normalized protein expression (NPX) stratified per genotype of the lead variant rs7535263. The proteins were measured in 87 treatment-naive patients with multifocal choroiditis or punctate inner choroidopathy. The proteins were tested for differential expression between the genotypes with a likelihood-ratio test before (*P*-LRT) and after (*Padj*-LRT) correction for multiple testing (FDR 5%).

Gene	Protein	AA Mean (sd)	GA Mean (sd)	GG Mean (sd)	*P*-LRT	*Padj*-LRT
A1BG	Alpha-1B-glycoprotein	0.18 (0.25)	0.19 (0.19)	0.26 (0.24)	0.214	0.941
ABO	Histo-blood group ABO system transferase	0.73 (1.41)	-0.01 (1.72)	-0.01 (1.83)	0.594	0.941
ACE	Angiotensin-converting enzyme	0.44 (0.26)	0.48 (0.45)	0.3 (0.41)	0.149	0.941
ACHE	Acetylcholinesterase	0.26 (0.55)	0.22 (0.37)	0.24 (0.44)	0.979	0.999
ACP1	Low molecular weight phosphotyrosine protein phosphatase	1.87 (0.69)	1.12 (0.58)	1.17 (0.53)	0.0228	0.454
ACRV1	Acrosomal protein SP-10	-0.95 (0.49)	-0.54 (0.92)	-0.58 (0.7)	0.74	0.951
ACYP1	Acylphosphatase-1	3.35 (0.22)	2.9 (0.83)	3.04 (0.61)	0.415	0.941
ADAM12	Disintegrin and metalloproteinase domain-containing protein 12	0.59 (0.52)	0.44 (0.71)	0.58 (1.16)	0.809	0.961
ADAMTS1	A disintegrin and metalloproteinase with thrombospondin motifs 1	0.28 (0.47)	0.39 (0.38)	0.36 (0.37)	0.495	0.941
ADAMTS4	A disintegrin and metalloproteinase with thrombospondin motifs 4	1.44 (0.37)	1.13 (0.65)	1.15 (0.59)	0.799	0.961
ADD1	Alpha-adducin	3.65 (0.54)	3.14 (0.91)	3.4 (0.82)	0.281	0.941
ADGRD1	Adhesion G-protein coupled receptor D1	0.48 (0.45)	0.13 (0.33)	0.17 (0.41)	0.142	0.941
ADH1B	All-trans-retinol dehydrogenase	1.54 (1.2)	0.91 (0.73)	0.89 (0.75)	0.338	0.941
ADIPOQ	Adiponectin	1.11 (0.63)	1.08 (0.94)	1.08 (0.85)	0.983	0.999
AFAP1	Actin filament-associated protein 1	3.02 (1.33)	2.08 (1.91)	2.41 (1.93)	0.431	0.941
AFM	Afamin	0.29 (0.38)	0.27 (0.25)	0.27 (0.29)	0.998	0.999
AGT	Angiotensinogen	-0.29 (0.23)	-0.22 (0.21)	-0.17 (0.26)	0.412	0.941
AHSG	Alpha-2-HS-glycoprotein	-0.1 (0.32)	0.23 (0.31)	0.37 (0.4)	0.00834	0.25
AKAP12	A-kinase anchor protein 12	0.1 (0.43)	0.18 (0.65)	0.14 (0.35)	0.924	0.984
AKR7L	Aflatoxin B1 aldehyde reductase member 4	0.84 (0.59)	0.59 (0.67)	0.51 (0.8)	0.687	0.941

Supplemental Table 9.4. (*continued*)

Gene	Protein	AA Mean (sd)	GA Mean (sd)	GG Mean (sd)	*P*-LRT	*Padj*-LRT
ALPI	Intestinal-type alkaline phosphatase	-0.96 (0.62)	-0.49 (1.43)	-1 (1.58)	0.232	0.941
AMOT	Angiomotin	0.81 (0.55)	0.82 (0.61)	0.99 (0.86)	0.479	0.941
AMY1A_ AMY1B_ AMY1C	Alpha-amylase 1A_Alpha-amylase 1B_Alpha-amylase 1C	-0.07 (0.44)	-0.02 (0.4)	0.01 (0.43)	0.909	0.984
ANKMY2	Ankyrin repeat and MYND domain-containing protein 2	3.33 (0.37)	3.06 (1)	3.19 (0.75)	0.708	0.945
ANXA1	Annexin A1	-1.25 (0.21)	-1.39 (0.31)	-1.25 (0.67)	0.434	0.941
APCS	Serum amyloid P-component	-0.28 (0.37)	-0.08 (0.59)	0.01 (0.5)	0.456	0.941
APOA2	Apolipoprotein A-II	-0.28 (0.53)	-0.5 (0.61)	-0.3 (0.55)	0.308	0.941
APOA4	Apolipoprotein A-IV	0.11 (0.6)	0.31 (0.53)	0.36 (0.41)	0.469	0.941
APOB	Apolipoprotein B-100	0.13 (0.33)	0.37 (0.4)	0.36 (0.38)	0.333	0.941
APOC1	Apolipoprotein C-I	0.27 (0.24)	0.48 (0.32)	0.58 (0.32)	0.035	0.506
APOD	Apolipoprotein D	0.25 (0.32)	0.36 (0.37)	0.38 (0.27)	0.653	0.941
APOE	Apolipoprotein E	-0.04 (0.29)	0.1 (0.75)	0.22 (0.54)	0.466	0.941
APOF	Apolipoprotein F	0.21 (0.56)	0.62 (0.14)	0.67 (0.15)	1.84e-07	6.59e-05
APOL1	Apolipoprotein L1	-2.24 (0.58)	-2.22 (0.48)	-2.23 (0.54)	0.986	0.999
APPL2	DCC-interacting protein 13-beta	5.73 (0.35)	5.26 (1.33)	5.55 (0.76)	0.389	0.941
ARHGAP45	Rho GTPase-activating protein 45	4 (0.39)	3.79 (1.06)	3.99 (0.7)	0.566	0.941
ASGR2	Asialoglycoprotein receptor 2	0.17 (0.27)	0.53 (0.41)	0.63 (0.54)	0.0542	0.675
ATRN	Attractin, Isoform 2	0.2 (0.26)	0.2 (0.17)	0.23 (0.18)	0.611	0.941
B2M	Beta-2-microglobulin	0.32 (0.22)	0.31 (0.38)	0.41 (0.5)	0.559	0.941
BABAM1	BRISC and BRCA1-A complex member 1	0.88 (0.47)	0.51 (0.42)	0.63 (0.61)	0.235	0.941
BAG4	BAG family molecular chaperone regulator 4	1.82 (0.26)	1.43 (0.59)	1.54 (0.48)	0.311	0.941
BCHE	Cholinesterase	0.19 (0.29)	0.21 (0.35)	0.15 (0.36)	0.625	0.941
BCL2L15	Bcl-2-like protein 15	-1.6 (0.45)	-1.64 (0.53)	-1.62 (0.67)	0.99	0.999
BLNK	B-cell linker protein	1.11 (0.87)	0.59 (0.42)	0.72 (0.42)	0.0691	0.764
BMP10	Bone morphogenetic protein 10	0.28 (0.39)	0.25 (0.37)	0.26 (0.34)	0.991	0.999
BMPER	BMP-binding endothelial regulator protein	0.06 (0.46)	0.1 (0.28)	0.1 (0.3)	0.918	0.984

Supplemental Table 9.4. (*continued*)

Gene	Protein	AA Mean (sd)	GA Mean (sd)	GG Mean (sd)	*P*-LRT	*Padj*-LRT
BNIP3L	BCL2/adenovirus E1B 19 kDa protein-interacting protein 3-like	2.5 (0.32)	2.21 (0.79)	2.22 (0.59)	0.73	0.951
BTD	Biotinidase	0.12 (0.24)	0.15 (0.24)	0.2 (0.2)	0.47	0.941
C1QL2	Complement C1q-like protein 2	1.11 (0.5)	1.35 (0.7)	1.23 (0.46)	0.608	0.941
C1QTNF5	Complement C1q tumor necrosis factor-related protein 5	-0.15 (0.51)	0.07 (0.53)	0.16 (0.39)	0.381	0.941
C1QTNF9	Complement C1q and tumor necrosis factor-related protein 9A	0.91 (1.04)	1.12 (0.56)	1.15 (0.57)	0.756	0.953
C1R	Complement C1r subcomponent	0.73 (0.17)	0.76 (0.2)	0.82 (0.23)	0.335	0.941
C1RL	Complement C1r subcomponent-like protein	0.26 (0.17)	0.3 (0.23)	0.33 (0.29)	0.626	0.941
C1S	Complement C1s subcomponent	0.52 (0.23)	0.49 (0.21)	0.54 (0.23)	0.665	0.941
C3	Complement C3	-2.32 (0.39)	-2.35 (0.35)	-2.31 (0.39)	0.889	0.97
C5	Complement C5	-0.05 (0.23)	0.12 (0.19)	0.18 (0.23)	0.0379	0.523
C8B	Complement component C8 beta chain	0.15 (0.31)	0.4 (0.32)	0.37 (0.32)	0.135	0.941
C9	Complement component C9	-0.02 (0.43)	0.28 (0.53)	0.27 (0.58)	0.353	0.941
CA8	Carbonic anhydrase-related protein	0.32 (0.27)	0.33 (0.48)	0.19 (0.29)	0.27	0.941
CACYBP	Calcyclin-binding protein	3.86 (0.32)	3.56 (1.2)	3.78 (0.72)	0.527	0.941
CASP9	Caspase-9	1.13 (0.44)	0.9 (1.05)	0.97 (0.79)	0.851	0.961
CAT	Catalase	1.79 (0.57)	1.45 (0.55)	1.43 (0.6)	0.493	0.941
CCNE1	G1/S-specific cyclin-E1	-0.26 (0.11)	-0.09 (0.49)	0.03 (0.71)	0.506	0.941
CD226	CD226 antigen	1.11 (0.32)	0.86 (0.53)	0.97 (0.45)	0.403	0.941
CD300A	CMRF35-like molecule 8	0.4 (0.45)	0.36 (0.31)	0.43 (0.33)	0.583	0.941
CD3G	T-cell surface glycoprotein CD3 gamma chain	0.3 (0.67)	0.23 (0.77)	0.1 (1.2)	0.815	0.961
CD5L	CD5 antigen-like	0.31 (0.2)	0.39 (0.52)	0.48 (0.43)	0.596	0.941
CD7	T-cell antigen CD7	0.49 (0.57)	0.41 (0.37)	0.37 (0.46)	0.834	0.961
CD72	B-cell differentiation antigen CD72	0.58 (0.67)	0.39 (0.55)	0.54 (0.5)	0.425	0.941
CEBPA	CCAAT/enhancer-binding protein alpha	0.43 (0.31)	0.3 (0.33)	0.27 (0.37)	0.683	0.941

Supplemental Table 9.4. (*continued*)

Gene	Protein	AA Mean (sd)	GA Mean (sd)	GG Mean (sd)	*P*-LRT	*Padj*-LRT
CELSR2	Cadherin EGF LAG seven-pass G-type receptor 2	0.74 (0.22)	0.98 (0.33)	1.01 (0.36)	0.317	0.941
CEMIP2	Cell surface hyaluronidase	0.55 (0.77)	0.24 (0.27)	0.22 (0.33)	0.187	0.941
CFD	Complement factor D	0.2 (0.2)	0.15 (0.24)	0.21 (0.25)	0.584	0.941
CFH	Complement factor H	0.21 (0.3)	0.17 (0.32)	0.18 (0.31)	0.994	0.999
CFHR2	Complement factor H-related protein 2	-0.1 (0.71)	0.57 (0.54)	0.95 (0.5)	5.99e-06	0.00108
CFHR4	Complement factor H-related protein 4	-0.46 (0.42)	0.27 (0.58)	0.49 (0.62)	0.00225	0.135
CFHR5	Complement factor H-related protein 5	-0.17 (0.18)	0.31 (0.45)	0.46 (0.42)	0.0068	0.235
CFI	Complement factor I	0.1 (0.17)	0.18 (0.29)	0.24 (0.25)	0.206	0.941
CFP	Properdin	0.08 (0.37)	0.13 (0.26)	0.11 (0.22)	0.798	0.961
CGB3_ CGB5_CGB8	Choriogonadotropin subunit beta 3	0.32 (0.51)	0.46 (0.55)	0.86 (1.95)	0.34	0.941
CHAD	Chondroadherin	-0.08 (0.76)	0.1 (0.52)	-0.03 (0.54)	0.555	0.941
CLEC12A	C-type lectin domain family 12 member A	0.28 (0.43)	0.42 (0.32)	0.38 (0.27)	0.566	0.941
CLEC3B	Tetranectin	0.18 (0.15)	0.25 (0.21)	0.3 (0.24)	0.342	0.941
CLU	Clusterin	0.13 (0.26)	0.17 (0.21)	0.22 (0.22)	0.32	0.941
COL5A1	Collagen alpha-1(V) chain	0.48 (0.39)	0.4 (0.49)	0.22 (0.45)	0.162	0.941
CPA4	Carboxypeptidase A4	0 (0.37)	0.21 (0.37)	0.18 (0.6)	0.853	0.961
CPB2	Carboxypeptidase B2	0.16 (0.19)	0.35 (0.28)	0.45 (0.29)	0.0296	0.506
CPOX	Oxygen-dependent coproporphyrinogen-III oxidase, mitochondrial	0.54 (0.23)	0.6 (0.45)	0.54 (0.26)	0.737	0.951
CR1	Complement receptor type 1	0.29 (0.41)	0.34 (0.34)	0.47 (0.41)	0.198	0.941
CRELD1	Protein disulfide isomerase CRELD1	0.36 (0.46)	0.41 (0.41)	0.48 (0.45)	0.643	0.941
CRISP3	Cysteine-rich secretory protein 3	0.17 (0.23)	0.43 (0.3)	0.41 (0.25)	0.193	0.941
CSF1R	Macrophage colony-stimulating factor 1 receptor	0.36 (0.74)	0.33 (0.46)	0.47 (0.48)	0.426	0.941
CSF2RB	Cytokine receptor common subunit beta	0.69 (0.35)	0.26 (0.61)	0.56 (0.66)	0.0545	0.675
CSF3R	Granulocyte colony-stimulating factor receptor	0.88 (0.17)	0.65 (0.47)	0.84 (0.81)	0.373	0.941

Supplemental Table 9.4. (*continued*)

Gene	Protein	AA Mean (sd)	GA Mean (sd)	GG Mean (sd)	*P*-LRT	*Padj*-LRT
CSH1	Chorionic somatomammotropin hormone 1	0.01 (0.32)	0.13 (0.29)	0.28 (1.81)	0.801	0.961
CSNK1D	Casein kinase I isoform delta	1.89 (0.51)	1.36 (0.73)	1.45 (0.69)	0.295	0.941
CST1	Cystatin-SN	0.85 (1.32)	0.35 (0.9)	0.69 (0.89)	0.176	0.941
CTBS	Di-N-acetylchitobiase	0.23 (0.19)	0.29 (0.3)	0.29 (0.44)	0.932	0.987
CTSE	Cathepsin E	0.88 (1.01)	0.75 (0.69)	0.62 (0.59)	0.59	0.941
DAAM1	Disheveled-associated activator of morphogenesis 1	4.64 (0.49)	4.41 (1.07)	4.63 (0.7)	0.501	0.941
DAND5	DAN domain family member 5	0.12 (0.74)	-0.18 (1.53)	0.16 (1.17)	0.557	0.941
DAPK2	Death-associated protein kinase 2	-0.79 (0.5)	-0.87 (0.66)	-0.72 (0.63)	0.562	0.941
DBH	Dopamine beta-hydroxylase	0.04 (2.01)	0.49 (1.39)	0.6 (0.92)	0.55	0.941
DBN1	Drebrin	1.98 (0.37)	1.85 (0.55)	1.88 (0.37)	0.857	0.961
DCTD	Deoxycytidylate deaminase	3.89 (0.26)	3.73 (1.04)	3.91 (0.69)	0.603	0.941
DDI2	Protein DDI1 homolog 2	4.16 (0.73)	3.52 (0.94)	3.6 (0.95)	0.431	0.941
DDX39A	ATP-dependent RNA helicase DDX39A	0.61 (0.76)	0.08 (0.19)	0.04 (0.22)	6.98e-05	0.00836
DDX4	Probable ATP-dependent RNA helicase DDX4	0.35 (0.21)	0.61 (0.54)	0.41 (0.35)	0.13	0.941
DEFB103A DEFB103B	Beta-defensin 103	0.53 (0.76)	0.15 (0.49)	-0.03 (0.35)	0.0166	0.373
DENR	Density-regulated protein	2.34 (0.37)	2.14 (0.82)	2.28 (0.5)	0.595	0.941
DGKA	Diacylglycerol kinase alpha	2.73 (0.24)	2.58 (0.71)	2.69 (0.55)	0.701	0.943
DIPK2B	Divergent protein kinase domain 2B	0.4 (0.17)	0.56 (0.27)	0.62 (0.29)	0.144	0.941
DNAJB2	DnaJ homolog subfamily B member 2	3.51 (0.3)	2.99 (0.77)	3.15 (0.57)	0.25	0.941
DNAJB6	DnaJ homolog subfamily B member 6	3.68 (0.41)	3.52 (1.12)	3.69 (0.69)	0.686	0.941
DTD1	D-aminoacyl-tRNA deacylase 1	4.26 (0.65)	4.18 (1.19)	4.46 (0.89)	0.467	0.941
ECM1	Extracellular matrix protein 1	0.41 (0.2)	0.42 (0.43)	0.48 (0.38)	0.821	0.961
EDNRB	Endothelin receptor type B	0.7 (0.69)	0.59 (0.94)	0.41 (0.57)	0.516	0.941

Supplemental Table 9.4. (*continued*)

Gene	Protein	AA Mean (sd)	GA Mean (sd)	GG Mean (sd)	*P*-LRT	*Padj*-LRT
EIF4E	Eukaryotic translation initiation factor 4E	4.57 (0.55)	4.49 (1.26)	4.6 (0.83)	0.835	0.961
EP300	Histone acetyltransferase p300	0.34 (0.39)	0.37 (0.39)	0.45 (0.31)	0.581	0.941
EPHA4	Ephrin type-A receptor 4	0.15 (0.36)	0.3 (0.41)	0.33 (0.43)	0.668	0.941
ERMAP	Erythroid membrane-associated protein	0.62 (0.38)	0.82 (0.52)	0.76 (0.46)	0.682	0.941
ERP29	Endoplasmic reticulum resident protein 29	5.06 (0.34)	4.74 (1.21)	4.98 (0.73)	0.478	0.941
ESR1	Estrogen receptor	0.4 (0.55)	0.03 (0.44)	0.17 (0.62)	0.202	0.941
EVI5	Ecotropic viral integration site 5 protein homolog	3.62 (0.46)	4.06 (1.12)	4.07 (0.81)	0.667	0.941
F10	Coagulation factor X	-0.03 (0.29)	0.15 (0.36)	0.22 (0.3)	0.226	0.941
F11	Coagulation factor XI	0.32 (0.34)	0.32 (0.29)	0.42 (0.28)	0.215	0.941
F12	Coagulation factor XII	0.57 (0.82)	0.51 (0.47)	0.62 (0.57)	0.687	0.941
F13B	Coagulation factor XIII B chain	0.59 (0.14)	0.67 (0.24)	0.77 (0.3)	0.0784	0.804
F2	Prothrombin	0.24 (0.26)	0.37 (0.21)	0.47 (0.24)	0.0352	0.506
FCN1	Ficolin-1	0.27 (0.5)	0.41 (0.45)	0.55 (0.58)	0.256	0.941
FGA	Fibrinogen alpha chain	0.22 (0.34)	0.58 (0.39)	0.66 (0.46)	0.0254	0.457
FGF12	Fibroblast growth factor 12	0.47 (0.25)	0.77 (0.94)	0.61 (0.7)	0.68	0.941
FGF16	Fibroblast growth factor 16	-1.34 (0.26)	-1.3 (0.74)	-1.63 (0.5)	0.0609	0.729
FGF20	Fibroblast growth factor 20	-0.59 (0.31)	-0.44 (1.02)	-0.55 (0.43)	0.718	0.95
FGF3	Fibroblast growth factor 3	0.22 (1.4)	-0.27 (0.35)	-0.26 (0.33)	0.0776	0.804
FGF6	Fibroblast growth factor 6	0.7 (0.65)	0.28 (0.64)	0.41 (0.92)	0.531	0.941
FGFR4	Fibroblast growth factor receptor 4	-0.28 (0.5)	0.17 (0.51)	0.24 (0.52)	0.0838	0.836
FGL1	Fibrinogen-like protein 1	0.32 (0.71)	0.53 (0.81)	0.64 (0.82)	0.449	0.941
FN1	Fibronectin	0.92 (0.24)	1.03 (0.34)	1.02 (0.32)	0.604	0.941
FOLH1	Glutamate carboxypeptidase 2	0.26 (0.15)	0.44 (0.95)	0.18 (0.89)	0.461	0.941
FOXJ3	Forkhead box protein J3	1.65 (0.21)	1.21 (0.59)	1.28 (0.46)	0.211	0.941
FUOM	Fucose mutarotase	0.32 (1.03)	-0.11 (0.67)	-0.14 (0.67)	0.509	0.941
GAD2	Glutamate decarboxylase 2	0.24 (0.28)	0.34 (0.8)	0.44 (0.86)	0.74	0.951
GAPDH	Glyceraldehyde-3-phosphate dehydrogenase	1.82 (0.25)	1.75 (0.24)	1.8 (0.12)	0.319	0.941

Supplemental Table 9.4. (*continued*)

Gene	Protein	AA Mean (sd)	GA Mean (sd)	GG Mean (sd)	*P*-LRT	*Padj*-LRT
GC	Vitamin D-binding protein	-0.14 (0.14)	0.09 (0.32)	0.26 (0.36)	0.00995	0.255
GCHFR	GTP cyclohydrolase 1 feedback regulatory protein	0.76 (0.42)	0.39 (0.49)	0.43 (0.53)	0.467	0.941
GHR	Growth hormone receptor	0.07 (0.34)	0.15 (0.37)	0.17 (0.34)	0.848	0.961
GIMAP7	GTPase IMAP family member 7	0.48 (0.28)	0.44 (0.31)	0.48 (0.4)	0.856	0.961
GIPR	Gastric inhibitory polypeptide receptor	-0.57 (1)	0.4 (0.8)	-0.01 (0.46)	0.00159	0.13
GIT1	ARF GTPase-activating protein GIT1	3.84 (0.38)	3.82 (1.02)	3.96 (0.54)	0.706	0.945
GLA	Alpha-galactosidase A	0.66 (0.11)	0.75 (0.39)	0.79 (0.37)	0.75	0.951
GLI2	Zinc finger protein GLI2	0.58 (0.27)	0.52 (0.68)	0.45 (0.35)	0.783	0.961
GLRX5	Glutaredoxin-related protein 5, mitochondrial	3.2 (0.5)	2.9 (1.09)	3.07 (0.81)	0.68	0.941
GMPR2	GMP reductase 2	3.67 (0.65)	3.46 (0.91)	3.68 (0.61)	0.405	0.941
GNPDA2	Glucosamine-6-phosphate isomerase 2	0.92 (0.31)	0.71 (0.43)	0.8 (0.49)	0.526	0.941
GP5	Platelet glycoprotein V	1.02 (0.17)	0.9 (0.35)	0.96 (0.19)	0.422	0.941
GPI	Glucose-6-phosphate isomerase	1.16 (0.34)	1.09 (0.61)	1.17 (0.51)	0.783	0.961
GSN	Gelsolin	0.16 (0.16)	0.22 (0.17)	0.2 (0.27)	0.849	0.961
GSR	Glutathione reductase, mitochondrial	0.81 (0.22)	0.8 (0.28)	0.89 (0.24)	0.309	0.941
HDAC8	Histone deacetylase 8	0.34 (0.61)	0.12 (0.42)	0.26 (0.76)	0.451	0.941
HEG1	Protein HEG homolog 1	0.26 (0.32)	0.28 (0.33)	0.22 (0.27)	0.659	0.941
HGFAC	Hepatocyte growth factor activator	0.06 (0.28)	0.07 (0.36)	0.14 (0.33)	0.539	0.941
HIF1A	Hypoxia-inducible factor 1-alpha	0.91 (1.45)	-0.11 (0.66)	-0.18 (0.61)	0.00491	0.218
HMCN2	Hemicentin-2	-0.91 (0.43)	-1.31 (0.56)	-1.46 (0.72)	0.16	0.941
HRG	Histidine-rich glycoprotein	0.67 (0.52)	0.52 (0.38)	0.79 (0.34)	0.00374	0.192
HS6ST2	Heparan-sulfate 6-O-sulfotransferase 2	0.72 (0.48)	0.71 (0.39)	0.8 (0.41)	0.582	0.941
IDO1	Indoleamine 2,3-dioxygenase 1	-0.19 (0.37)	-0.65 (0.61)	-0.59 (0.53)	0.356	0.941
IGFL4	Insulin growth factor-like family member 4	-0.49 (0.58)	-0.55 (0.77)	-0.17 (1.56)	0.29	0.941
IGLC2	Immunoglobulin lambda constant 2	0.23 (0.24)	0.15 (0.19)	0.17 (0.22)	0.821	0.961

Supplemental Table 9.4. (*continued*)

Gene	Protein	AA Mean (sd)	GA Mean (sd)	GG Mean (sd)	*P*-LRT	*Padj*-LRT
IL12RB2	Interleukin-12 receptor subunit beta-2	-0.08 (0.47)	-0.25 (0.44)	-0.19 (0.48)	0.804	0.961
IL20RB	Interleukin-20 receptor subunit beta	0.09 (0.47)	0.05 (0.47)	-0.06 (0.37)	0.454	0.941
IL21R	Interleukin-21 receptor	0.63 (0.89)	0.16 (0.79)	0 (0.45)	0.16	0.941
IL31	Interleukin-31	0.48 (1.13)	-0.19 (0.77)	-0.34 (0.44)	0.0414	0.551
IL31RA	Interleukin-31 receptor subunit alpha	-0.1 (0.15)	0.38 (0.53)	0.28 (0.6)	0.213	0.941
IL36A	Interleukin-36 alpha	0.31 (0.74)	0.14 (0.62)	0.14 (0.62)	0.817	0.961
IL36G	Interleukin-36 gamma	-1.22 (0.43)	-0.81 (0.59)	-0.81 (0.6)	0.419	0.941
INHBB	Inhibin beta B chain	0.16 (0.68)	0.24 (0.63)	0.36 (0.68)	0.543	0.941
INSR	Insulin receptor	0.24 (0.15)	0.26 (0.23)	0.25 (0.19)	0.832	0.961
ITGA2	Integrin alpha-2	0.81 (0.23)	0.76 (0.52)	0.71 (0.47)	0.879	0.965
ITGAL	Integrin alpha-L	-1.31 (0.81)	-1.72 (0.56)	-1.63 (0.5)	0.426	0.941
ITIH1	Inter-alpha-trypsin inhibitor heavy chain H1	0.1 (0.18)	0.18 (0.14)	0.22 (0.18)	0.213	0.941
ITIH4	Inter-alpha-trypsin inhibitor heavy chain H4	0.13 (0.28)	0.3 (0.27)	0.41 (0.31)	0.02	0.423
JAM3	Junctional adhesion molecule C	1.8 (0.51)	1.76 (0.85)	1.84 (0.56)	0.867	0.962
KDM3A	Lysine-specific demethylase 3A	-0.21 (0.19)	0.25 (1.24)	-0.02 (0.64)	0.455	0.941
KLK7	Kallikrein-7	-0.19 (0.6)	0 (0.47)	-0.05 (0.74)	0.917	0.984
KLRF1	Killer cell lectin-like receptor subfamily F member 1	0.53 (0.28)	0.49 (0.39)	0.5 (0.31)	0.999	0.999
LATS1	Serine/threonine-protein kinase LATS1	2.69 (0.89)	2.33 (0.96)	2.38 (0.67)	0.5	0.941
LCAT	Phosphatidylcholine-sterol acyltransferase	0.03 (0.3)	0.14 (0.3)	0.22 (0.25)	0.188	0.941
LEG1	Protein LEG1 homolog	0.04 (0.63)	0.02 (0.66)	0.04 (0.57)	0.865	0.962
LGALS3BP	Galectin-3-binding protein	-0.18 (0.39)	-0.16 (0.52)	-0.2 (0.55)	0.949	0.996
LMOD1	Leiomodin-1	0.96 (0.3)	0.64 (0.5)	0.72 (0.47)	0.562	0.941
LPA	Apolipoprotein(a)	-2.09 (1.65)	-1.5 (1.94)	-1.94 (2)	0.559	0.941
LRG1	Leucine-rich alpha-2-glycoprotein	0.32 (0.27)	0.26 (0.31)	0.35 (0.35)	0.467	0.941
LRIG3	Leucine-rich repeats and immunoglobulin-like domains protein 3	0.4 (0.33)	0.1 (0.29)	0.13 (0.31)	0.213	0.941

Supplemental Table 9.4. (*continued*)

Gene	Protein	AA Mean (sd)	GA Mean (sd)	GG Mean (sd)	*P*-LRT	*Padj*-LRT
LYVE1	Lymphatic vessel endothelial hyaluronic acid receptor 1	0.26 (0.35)	0.3 (0.24)	0.38 (0.26)	0.232	0.941
LZTFL1	Leucine zipper transcription factor-like protein 1	1.78 (0.31)	1.58 (0.71)	1.69 (0.66)	0.726	0.951
MARS1	Methionine--tRNA ligase, cytoplasmic	3.13 (0.28)	2.83 (1)	3.02 (0.68)	0.513	0.941
MBL2	Mannose-binding protein C	-0.56 (0.57)	0.35 (1.04)	0.18 (1.17)	0.261	0.941
MCEMP1	Mast cell-expressed membrane protein 1	4.28 (1.23)	4.33 (1.27)	4.31 (1.14)	0.998	0.999
MDH1	Malate dehydrogenase, cytoplasmic	1.27 (0.24)	1.16 (0.45)	1.22 (0.41)	0.795	0.961
MENT	Protein MENT	0.38 (0.24)	0.49 (0.24)	0.53 (0.22)	0.316	0.941
MFAP4	Microfibril-associated glycoprotein 4	0.17 (0.44)	0.23 (0.35)	0.2 (0.43)	0.701	0.943
MKI67	Proliferation marker protein Ki-67	0.12 (0.26)	0.12 (0.46)	0.03 (0.36)	0.6	0.941
MOCS2	Molybdopterin synthase catalytic subunit	1.84 (0.48)	1.7 (0.8)	1.72 (0.7)	0.966	0.999
MRC1	Macrophage mannose receptor 1	0.39 (0.34)	0.32 (0.32)	0.42 (0.38)	0.406	0.941
MRPS16	28S ribosomal protein S16, mitochondrial	0.09 (0.21)	0.24 (0.39)	0.28 (0.47)	0.62	0.941
MST1	Hepatocyte growth factor-like protein	0.3 (0.35)	0.22 (0.55)	0.35 (0.44)	0.458	0.941
MTDH	Protein LYRIC	2.51 (0.42)	2.38 (1.13)	2.55 (0.79)	0.667	0.941
MXRA8	Matrix remodeling-associated protein 8	0.5 (0.33)	0.53 (0.41)	0.56 (0.37)	0.752	0.951
MYOM3	Myomesin-3	-1.01 (0.48)	-0.88 (1.15)	-0.57 (1.06)	0.329	0.941
NAGA	Alpha-N-acetylgalactosaminidase	0.9 (0.44)	1.02 (0.42)	1.12 (0.41)	0.408	0.941
NAGPA	N-acetylglucosamine-1-phosphodiester alpha-N-acetylglucosaminidase	0.17 (0.33)	0.17 (0.25)	0.18 (0.36)	0.972	0.999
NDUFA5	NADH dehydrogenase [ubiquinone] 1 alpha subcomplex subunit 5	0.42 (0.15)	0.64 (0.6)	0.56 (0.38)	0.634	0.941
NECTIN1	Nectin-1	-0.16 (0.67)	0.3 (0.37)	0.25 (0.26)	0.0242	0.457
NEDD4L	E3 ubiquitin-protein ligase NEDD4-like	1.84 (0.46)	1.58 (0.53)	1.52 (0.5)	0.518	0.941

Supplemental Table 9.4. (*continued*)

Gene	Protein	AA Mean (sd)	GA Mean (sd)	GG Mean (sd)	*P*-LRT	*Padj*-LRT
NEDD9	Enhancer of filamentation 1	-0.88 (0.22)	-1.19 (0.38)	-1.12 (0.28)	0.139	0.941
NEXN	Nexilin	2.18 (0.33)	1.97 (0.83)	2.14 (0.85)	0.623	0.941
NFAT5	Nuclear factor of activated T-cells 5	4.9 (0.47)	4.64 (1.19)	4.68 (0.74)	0.85	0.961
NHLRC3	NHL repeat-containing protein 3	1.09 (0.37)	1.07 (0.36)	1.13 (0.51)	0.838	0.961
NME1	Nucleoside diphosphate kinase A	0.29 (0.23)	0.36 (0.35)	0.3 (0.23)	0.638	0.941
NPHS1	Nephrin	0.27 (0.31)	-0.1 (0.28)	-0.03 (0.31)	0.0332	0.506
NPHS2	Podocin	0.36 (0.69)	0.29 (1.23)	0.31 (1.06)	0.999	0.999
NRGN	Neurogranin	3.49 (0.64)	3.24 (1.03)	3.51 (0.91)	0.41	0.941
NUMB	Protein numb homolog	2.49 (0.3)	2.28 (0.82)	2.31 (0.53)	0.746	0.951
NXPH3	Neurexophilin-3	0.86 (0.4)	0.62 (0.41)	0.61 (0.4)	0.562	0.941
ORM1	Alpha-1-acid glycoprotein 1	0.02 (0.18)	0.08 (0.24)	0.06 (0.26)	0.558	0.941
PALLD	Palladin	0.73 (0.87)	0.41 (0.66)	0.42 (0.49)	0.69	0.941
PAXX	Protein PAXX	1.19 (0.28)	1.13 (0.48)	1.16 (0.49)	0.968	0.999
PCBD1	Pterin-4-alpha-carbinolamine dehydratase	0.77 (0.55)	0.34 (0.41)	0.33 (0.47)	0.187	0.941
PDE5A	cGMP-specific 3',5'-cyclic phosphodiesterase	4.36 (0.31)	3.97 (1.08)	4.09 (0.65)	0.616	0.941
PDIA3	Protein disulfide-isomerase A3	0.38 (0.21)	0.36 (0.39)	0.48 (0.62)	0.504	0.941
PDZK1	Na(+)/H(+) exchange regulatory cofactor NHE-RF3	0.32 (0.69)	-0.1 (0.46)	-0.12 (0.46)	0.211	0.941
PENK	Proenkephalin-A	0.01 (0.21)	0.08 (0.36)	0.08 (0.39)	0.879	0.965
PEPD	Xaa-Pro dipeptidase	0.13 (0.13)	0.42 (0.36)	0.48 (0.41)	0.116	0.941
PER3	Period circadian protein homolog 3	1.8 (1.88)	2.36 (1.56)	2.47 (1.4)	0.695	0.942
PF4	Platelet factor 4	1.58 (0.43)	1.13 (1.01)	1.21 (0.95)	0.662	0.941
PGA4	Pepsin A-4	0.52 (1.04)	0.3 (0.48)	0.15 (0.55)	0.254	0.941
PGLYRP2	N-acetylmuramoyl-L-alanine amidase	0.31 (0.17)	0.31 (0.39)	0.33 (0.46)	0.869	0.962
PGR	Progesterone receptor	1.08 (2.08)	0.38 (0.99)	0.15 (0.66)	0.0998	0.918
PHYKPL	5-phosphohydroxy-L-lysine phospho-lyase	0.82 (0.32)	0.62 (0.46)	0.67 (0.57)	0.696	0.942
PI16	Peptidase inhibitor 16	0.19 (0.13)	0.37 (0.34)	0.38 (0.35)	0.472	0.941
PIKFYVE	1-phosphatidylinositol 3-phosphate 5-kinase	1.92 (0.35)	1.85 (0.67)	1.82 (0.51)	0.921	0.984

Supplemental Table 9.4. (*continued*)

Gene	Protein	AA Mean (sd)	GA Mean (sd)	GG Mean (sd)	*P*-LRT	*Padj*-LRT
PINLYP	phospholipase A2 inhibitor and Ly6/PLAUR domain-containing protein	-0.01 (0.47)	-0.08 (0.61)	-0.05 (0.53)	0.839	0.961
PLCB1	1-phosphatidylinositol 4,5-bisphosphate phosphodiesterase beta-1	0.26 (0.13)	0.37 (0.42)	0.31 (0.26)	0.68	0.941
PLG	Plasminogen	0.14 (0.31)	0.29 (0.25)	0.39 (0.32)	0.0634	0.734
PNLIP	Pancreatic triacylglycerol lipase	0.36 (0.65)	0.12 (0.57)	0.34 (0.78)	0.332	0.941
POF1B	Protein POF1B	0.57 (0.39)	0.64 (0.52)	0.7 (0.52)	0.725	0.951
POLR2A	DNA-directed RNA polymerase II subunit RPB1	0.23 (0.28)	0.26 (0.39)	0.26 (0.38)	0.935	0.987
PON1	Serum paraoxonase/ arylesterase 1	0.3 (0.54)	0.57 (0.25)	0.69 (0.22)	0.00181	0.13
PPBP	Platelet basic protein	2.04 (0.31)	1.69 (0.91)	1.75 (0.76)	0.737	0.951
PPL	Periplakin	0.76 (0.45)	0.63 (0.41)	0.65 (0.29)	0.915	0.984
PPM1B	Protein phosphatase 1B	0.25 (0.3)	0.36 (0.48)	0.32 (0.44)	0.808	0.961
PRKG1	cGMP-dependent protein kinase 1	6.03 (0.44)	5.53 (1.46)	5.7 (0.94)	0.658	0.941
PROS1	Vitamin K-dependent protein S	0.78 (0.39)	0.88 (0.33)	0.94 (0.31)	0.425	0.941
PRR4	Proline-rich protein 4	-0.26 (0.56)	-0.21 (0.79)	-0.17 (0.82)	0.957	0.999
PRR5	Proline-rich protein 5	0.32 (0.52)	-0.06 (0.74)	-0.11 (0.59)	0.438	0.941
PRSS22	Brain-specific serine protease 4	0.96 (0.28)	0.79 (0.4)	0.76 (0.69)	0.72	0.95
PSMG4	Proteasome assembly chaperone 4	1.86 (0.66)	1.35 (0.65)	1.38 (0.6)	0.291	0.941
PSTPIP2	Proline-serine-threonine phosphatase-interacting protein 2	4.65 (0.47)	4.31 (1.21)	4.64 (0.73)	0.31	0.941
PTGES2	Prostaglandin E synthase 2	1.6 (0.37)	1.68 (0.79)	1.7 (0.68)	0.976	0.999
PTP4A3	Protein tyrosine phosphatase type IVA 3	0.52 (0.37)	0.39 (0.48)	0.33 (0.51)	0.76	0.954
PTPN9	Tyrosine-protein phosphatase non-receptor type 9	0.33 (0.35)	0.49 (0.35)	0.41 (0.46)	0.399	0.941
PTRHD1	Putative peptidyl-tRNA hydrolase PTRHD1	4.02 (0.26)	3.65 (0.86)	3.83 (0.54)	0.359	0.941
PZP	Pregnancy zone protein	0.14 (0.72)	0.35 (1.22)	0.41 (1.36)	0.812	0.961
QSOX1	Sulfhydryl oxidase 1	0.25 (0.2)	0.19 (0.33)	0.23 (0.2)	0.837	0.961

Supplemental Table 9.4. (*continued*)

Gene	Protein	AA Mean (sd)	GA Mean (sd)	GG Mean (sd)	*P*-LRT	*Padj*-LRT
RABEP1	Rab GTPase-binding effector protein 1	3.51 (0.17)	3.02 (0.95)	3.22 (0.75)	0.362	0.941
RALB	Ras-related protein Ral-B	0.56 (0.39)	0.34 (0.41)	0.38 (0.32)	0.524	0.941
RAP1A	Ras-related protein Rap-1A	0.15 (0.38)	0.12 (0.58)	0.37 (0.84)	0.251	0.941
RBPMS	RNA-binding protein with multiple splicing	2.7 (1)	2.13 (1.47)	2.12 (1.22)	0.641	0.941
RELB	Transcription factor RelB	-0.33 (1.78)	-0.92 (0.67)	-0.86 (0.64)	0.315	0.941
REPS1	RalBP1-associated Eps domain-containing protein 1	1.04 (0.65)	0.96 (0.52)	1.2 (0.68)	0.198	0.941
RICTOR	Rapamycin-insensitive companion of mTOR	0.29 (0.29)	0.44 (0.69)	0.61 (0.93)	0.518	0.941
RIDA	2-iminobutanoate/2-iminopropanoate deaminase	0.73 (0.87)	0.28 (0.51)	0.3 (0.61)	0.447	0.941
RLN2	Prorelaxin H2	-3.27 (0.32)	-2.91 (1.88)	-2.92 (2.01)	0.921	0.984
RNASE1	Ribonuclease pancreatic	0.26 (0.15)	0.2 (0.37)	0.25 (0.39)	0.838	0.961
RNASE4	Ribonuclease 4	0.29 (0.14)	0.44 (0.31)	0.45 (0.44)	0.426	0.941
RNASE6	Ribonuclease K6	0.25 (0.12)	0.3 (0.27)	0.29 (0.36)	0.743	0.951
RNF168	E3 ubiquitin-protein ligase RNF168	0.09 (0.15)	0.45 (0.75)	0.47 (0.5)	0.436	0.941
RNF31	E3 ubiquitin-protein ligase RNF31	0.06 (1.03)	-0.32 (0.44)	-0.3 (0.63)	0.52	0.941
RPA2	Replication protein A 32 kDa subunit	0.34 (0.36)	0.31 (0.61)	0.16 (0.38)	0.392	0.941
S100A13	Protein S100-A13	1.44 (0.44)	1.22 (0.32)	1.15 (0.38)	0.265	0.941
SAA4	Serum amyloid A-4 protein	-0.04 (0.18)	0.03 (0.2)	0.04 (0.24)	0.571	0.941
SCGB3A1	Secretoglobin family 3A member 1	0.27 (0.37)	0.23 (0.41)	0.22 (0.35)	0.981	0.999
SCRIB	Protein scribble homolog	1.84 (0.24)	1.8 (0.7)	1.73 (0.53)	0.851	0.961
SDK2	Protein sidekick-2	0.68 (0.32)	0.3 (0.55)	0.31 (0.42)	0.141	0.941
SELENOP	Selenoprotein P	0.41 (0.31)	0.58 (0.37)	0.79 (0.37)	0.00547	0.218
SELL	L-selectin	0.25 (0.12)	0.35 (0.3)	0.44 (0.28)	0.145	0.941
SEMA3G	Semaphorin-3G	0.16 (0.56)	-0.05 (0.38)	0.02 (0.39)	0.482	0.941
SEMA6C	Semaphorin-6C	0.22 (0.23)	0.31 (0.51)	0.19 (0.27)	0.393	0.941
SERPINA3	Alpha-1-antichymotrypsin	-0.16 (0.2)	0.04 (0.19)	0.09 (0.24)	0.0165	0.373
SERPINA4	Kallistatin	0.3 (0.32)	0.32 (0.27)	0.41 (0.25)	0.208	0.941
SERPINA5	Plasma serine protease inhibitor	-0.43 (0.4)	-0.39 (0.25)	-0.33 (0.26)	0.407	0.941

Supplemental Table 9.4. (*continued*)

Gene	Protein	AA Mean (sd)	GA Mean (sd)	GG Mean (sd)	*P*-LRT	*Padj*-LRT
SERPINA6	Corticosteroid-binding globulin	0.59 (0.18)	0.62 (0.34)	0.76 (0.43)	0.188	0.941
SERPINA7	Thyroxine-binding globulin	0.26 (0.18)	0.3 (0.37)	0.46 (0.37)	0.106	0.924
SERPINC1	Antithrombin-III	0.1 (0.23)	0.26 (0.17)	0.33 (0.16)	0.00721	0.235
SERPIND1	Heparin cofactor 2	0.21 (0.32)	0.4 (0.36)	0.53 (0.43)	0.0945	0.917
SERPINF2	Alpha-2-antiplasmin	0.14 (0.23)	0.16 (0.13)	0.19 (0.13)	0.42	0.941
SERPING1	Plasma protease C1 inhibitor	0.09 (0.15)	0.2 (0.2)	0.24 (0.22)	0.104	0.924
SERPINI1	Neuroserpin	-0.28 (0.36)	-0.32 (0.32)	-0.29 (0.36)	0.932	0.987
SFRP4	Secreted frizzled-related protein 4	0.37 (0.44)	0.34 (0.37)	0.28 (0.44)	0.63	0.941
SHH	Sonic hedgehog protein	-0.19 (0.51)	0.03 (0.76)	-0.01 (0.62)	0.682	0.941
SIRT1	NAD-dependent protein deacetylase sirtuin-1	0.7 (0.44)	0.52 (0.36)	0.53 (0.61)	0.557	0.941
SLC9A3R1	Na(+)/H(+) exchange regulatory cofactor NHE-RF1	2.23 (0.29)	2.1 (0.96)	2.24 (0.77)	0.75	0.951
SLITRK1	SLIT and NTRK-like protein 1	0.47 (0.31)	0.63 (0.56)	0.76 (0.49)	0.313	0.941
SMPD3	Sphingomyelin phosphodiesterase 3	0.18 (0.34)	0.47 (0.4)	0.59 (0.52)	0.173	0.941
SNCA	Alpha-synuclein	6.6 (0.79)	6.02 (1.6)	6.51 (1.15)	0.248	0.941
SNX15	Sorting nexin-15	2.5 (0.32)	2 (0.72)	2.11 (0.58)	0.318	0.941
SOD3	Extracellular superoxide dismutase	0.73 (0.38)	1.02 (1.14)	0.82 (0.92)	0.517	0.941
SPART	Spartin	3.65 (0.25)	3.32 (1.03)	3.49 (0.69)	0.594	0.941
SPINK2	Serine protease inhibitor Kazal-type 2	-0.03 (0.46)	0.16 (0.5)	0.07 (0.42)	0.462	0.941
SPRED2	Sprouty-related, EVH1 domain-containing protein 2	2.35 (0.29)	2.09 (0.69)	2.21 (0.59)	0.658	0.941
SSBP1	Single-stranded DNA-binding protein, mitochondrial	0.51 (0.21)	0.44 (0.55)	0.48 (0.46)	0.837	0.961
ST13	Hsc70-interacting protein	3.62 (0.37)	3.11 (0.65)	3.27 (0.54)	0.189	0.941
ST8SIA1	Alpha-N-acetylneuraminide alpha-2,8-sialyltransferase	1.01 (2.18)	0.19 (0.39)	0.2 (0.34)	0.00971	0.255
STAT2	Signal transducer and activator of transcription 2	2.33 (0.36)	2.17 (0.85)	2.23 (0.6)	0.822	0.961
STX5	Syntaxin-5	1.02 (1.03)	0.44 (0.48)	0.43 (0.45)	0.0702	0.764

Supplemental Table 9.4. (*continued*)

Gene	Protein	AA Mean (sd)	GA Mean (sd)	GG Mean (sd)	*P*-LRT	*Padj*-LRT
STX7	Syntaxin-7	1.32 (0.38)	0.72 (0.64)	0.88 (0.57)	0.133	0.941
SUMF1	Formylglycine-generating enzyme	-0.02 (0.64)	0.41 (1.32)	0.15 (0.78)	0.491	0.941
SUSD5	Sushi domain-containing protein 5	0.14 (0.48)	0.47 (0.45)	0.51 (0.36)	0.115	0.941
SYAP1	Synapse-associated protein 1	1.97 (0.43)	1.85 (0.8)	2.13 (0.76)	0.207	0.941
TBCA	Tubulin-specific chaperone A	3.53 (0.48)	3.2 (1.17)	3.51 (0.95)	0.388	0.941
TCN1	Transcobalamin-1	0.29 (0.3)	0.4 (0.32)	0.33 (0.31)	0.459	0.941
TERF1	Telomeric repeat-binding factor 1	0.19 (0.34)	0.26 (0.61)	0.23 (0.39)	0.878	0.965
TF	Serotransferrin	0.06 (0.19)	0.1 (0.29)	0.21 (0.35)	0.252	0.941
TGFBR1	TGF-beta receptor type-1	0.41 (0.23)	0.22 (0.35)	0.25 (0.24)	0.508	0.941
TGOLN2	Trans-Golgi network integral membrane protein 2	0.3 (0.2)	0.57 (0.33)	0.57 (0.35)	0.153	0.941
THSD1	Thrombospondin type-1 domain-containing protein 1	-0.06 (0.47)	0.14 (0.44)	0.1 (0.53)	0.763	0.954
TLR1	Toll-like receptor 1	0.1 (0.47)	0.38 (0.35)	0.32 (0.26)	0.152	0.941
TLR4	Toll-like receptor 4	0.56 (0.2)	0.49 (0.51)	0.46 (0.42)	0.939	0.988
TNFAIP8L2	Tumor necrosis factor alpha-induced protein 8-like protein 2	2.02 (0.45)	1.92 (0.92)	2.11 (0.68)	0.546	0.941
TNFRSF17	Tumor necrosis factor receptor superfamily member 17	0.35 (0.32)	0.17 (0.49)	0.12 (0.5)	0.639	0.941
TNFSF9	Tumor necrosis factor ligand superfamily member 9	-0.26 (0.45)	0.04 (0.39)	0.03 (0.47)	0.441	0.941
TOP2B	DNA topoisomerase 2B	2.41 (0.65)	2.57 (1.07)	2.69 (0.8)	0.781	0.961
TP53BP1	TP53-binding protein 1	-0.78 (0.48)	-0.91 (0.56)	-0.67 (0.71)	0.223	0.941
TP53I3	Quinone oxidoreductase PIG3	1.75 (0.35)	1.54 (0.58)	1.59 (0.52)	0.767	0.956
TPD52L2	Tumor protein D54	3.43 (0.3)	3.09 (1.04)	3.34 (0.71)	0.401	0.941
TPSG1	Tryptase gamma	0.43 (0.39)	0.4 (0.53)	0.23 (0.35)	0.214	0.941
TRAF3	TNF receptor-associated factor 3, Isoform 2	0.96 (0.42)	0.62 (0.36)	0.63 (0.35)	0.168	0.941
TREML1	Trem-like transcript 1	2.5 (0.3)	2.17 (0.89)	2.24 (0.69)	0.712	0.947
TSC1	Hamartin	2.06 (0.32)	1.63 (0.96)	1.43 (0.66)	0.214	0.941

Supplemental Table 9.4. (*continued*)

Gene	Protein	AA Mean (sd)	GA Mean (sd)	GG Mean (sd)	*P*-LRT	*Padj*-LRT
TSPYL1	Testis-specific Y-encoded-like protein 1	1.39 (0.19)	1.13 (0.53)	1.21 (0.38)	0.469	0.941
TTR	Transthyretin	0.26 (0.3)	0.2 (0.38)	0.27 (0.31)	0.62	0.941
TXN	Thioredoxin	1.05 (0.18)	0.89 (0.51)	1.08 (0.58)	0.283	0.941
TYRP1	5,6-dihydroxyindole-2-carboxylic acid oxidase	2.28 (0.68)	1.33 (0.89)	1.63 (0.96)	0.0975	0.918
UBE2Z	Ubiquitin-conjugating enzyme E2 Z	1.68 (0.29)	1.6 (0.72)	1.55 (0.49)	0.86	0.961
UBXN1	UBX domain-containing protein 1	2.25 (0.3)	1.97 (0.74)	2.12 (0.69)	0.554	0.941
UNC5D	Netrin receptor UNC5D	0.35 (0.42)	0.33 (0.4)	0.3 (0.31)	0.922	0.984
UROD	Uroporphyrinogen decarboxylase	3.67 (0.55)	3.32 (0.91)	3.46 (0.74)	0.59	0.941
VAMP8	Vesicle-associated membrane protein 8	3.99 (0.26)	3.76 (0.99)	3.89 (0.68)	0.668	0.941
VASP	Vasodilator-stimulated phosphoprotein	2.1 (0.45)	2.08 (0.75)	2.26 (0.7)	0.465	0.941
VEGFB	Vascular endothelial growth factor B	0.29 (0.36)	0.45 (0.47)	0.38 (0.44)	0.436	0.941
VNN1	Pantetheinase	-0.48 (1.61)	-0.04 (0.87)	-0.18 (0.94)	0.508	0.941
VTI1A	Vesicle transport through interaction with t-SNAREs homolog 1A	2.82 (0.33)	2.46 (0.98)	2.69 (0.74)	0.387	0.941
WASL	Neural Wiskott-Aldrich syndrome protein	0.05 (0.66)	-0.01 (1.29)	-0.07 (0.66)	0.962	0.999
XIAP	E3 ubiquitin-protein ligase XIAP	1.89 (0.33)	1.76 (0.66)	1.79 (0.49)	0.887	0.97
YWHAQ	14-3-3 protein theta	3.38 (0.44)	3.05 (1.02)	3.23 (0.81)	0.598	0.941
YY1	Transcriptional repressor protein YY1	1.18 (0.11)	0.97 (0.57)	1.04 (0.47)	0.675	0.941
ZBP1	Z-DNA-binding protein 1	-0.44 (0.43)	-0.72 (0.33)	-0.71 (0.33)	0.185	0.941
ZNF174	Zinc finger protein 174	-0.01 (0.44)	0.19 (0.31)	0.46 (0.73)	0.0338	0.506

Supplemental Table 9.5. Summary statistics of the 52 risk loci for age-related macular degeneration (AMD).[28] Both the results for the association of the loci with AMD and idiopathic MFC are displayed. Association results were available for 43 loci.

Chr	Locus name	SNP ID	Bp (Hg19)	Major / minor allele	AMD				Idiopathic MFC			
					MAF		OR	*P*-value	MAF		OR	*P*-value
					Cases	Controls			Cases	Controls		
1	*CFH*	rs10922109	196704632	C/A	.223	.426	0.38	9.6×10^{-618}	.269	.430	0.516	9.7×10^{-9}
1	*CFH*	rs570618	196657064	G/T	.580	.364	2.38	2.0×10^{-590}	.495	.372	1.69	1.1×10^{-5}
1	*CFH*	rs121913059	196716375	C/T	.003	.00014	20.28	8.9×10^{-24}	NA	NA	NA	NA
1	*CFH*	rs148553336	196613173	T/C	.003	.009	0.29	8.6×10^{-26}	.004	.011	0.516	0.316
1	*CFH*	rs187328863	196380158	C/T	.054	.028	2.27	1.1×10^{-68}	NA	NA	NA	NA
1	*CFH (CFHR3/CFHR1)*	rs61818925	196815450	G/T	.284	.385	0.60	6.0×10^{-165}	NA	NA	NA	NA
1	*CFH*	rs35292876	196706642	C/T	.021	.009	2.42	8.2×10^{-37}	.012	.01	1.001	0.998
1	*CFH*	rs191281603	196958651	C/G	.007	.006	1.07	0.68	.003	.007	0.724	0.736
2	*COL4A3*	rs11884770	228086920	C/T	.258	.278	0.90	2.9×10^{-8}	.276	0.271	1.018	0.891
3	*ADAMTS9-AS2*	rs62247658	64715155	T/C	.466	.433	1.14	1.8×10^{-14}	.558	0.587	0.922	0.484
3	*COL8A1*	rs140647181	99180668	T/C	.023	.016	1.59	1.4×10^{-11}	.014	0.02	0.752	0.571
3	*COL8A1*	rs55975637	99419853	G/A	.132	.117	1.15	1.3×10^{-8}	.135	0.118	1.255	0.212
4	*CFI*	rs10033900	110659067	C/T	.511	.477	1.15	5.4×10^{-17}	.512	0.508	0.986	0.899
4	*CFI*	rs141853578	110685820	C/T	.003	.0008	3.64	6.3×10^{-10}	NA	NA	NA	NA
5	*C9*	rs62358361	39327888	G/T	.016	.009	1.80	1.3×10^{-14}	.003	0.012	0.446	0.168
5	*PRLR/SPEF2*	rs114092250	35494448	G/A	.016	.021	0.70	2.1×10^{-8}	.028	0.031	1.033	0.933
6	*C2/CFB/SKIV2L*	rs116503776	31930462	G/A	.090	.148	0.57	1.2×10^{-103}	.106	0.142	0.73	0.067
6	*C2/CFB/SKIV2L*	rs144629244	31946792	G/A	.016	.012	1.39	2.6×10^{-6}	.000	0.007	0.326	0.129
6	*C2/CFB/SKIV2L (PBX2)*	rs114254831	32155581	A/G	.284	.260	1.13	9.4×10^{-12}	.203	0.257	0.943	0.727
6	*C2/CFB/SKIV2L*	rs181705462	31947027	G/T	.018	.012	1.55	3.1×10^{-10}	.012	0.009	1.894	0.333

Supplemental Table 9.5. (*continued*)

Chr	Locus name	SNP ID	Bp (Hg19)	Major / minor allele	AMD				Idiopathic MFC			
					MAF		OR	*P*-value	MAF		OR	*P*-value
					Cases	Controls			Cases	Controls		
6	*VEGFA*	rs943080	43826627	T/C	.465	.497	0.88	1.1×10^{-14}	.476	0.494	0.886	0.292
7	*KMT2E/SRPK2*	rs1142	104756326	C/T	.370	.346	1.11	1.4×10^{-9}	.387	0.345	1.215	0.111
7	*PILRB/PILRA*	rs7803454	99991548	C/T	.209	.190	1.13	4.8×10^{-9}	.202	0.186	1.121	0.435
8	*TNFRSF10A*	rs79037040	23082971	T/G	.451	.479	0.90	4.5×10^{-11}	.491	0.518	0.906	0.402
9	*MIR6130/RORB*	rs10781182	76617720	G/T	.328	.306	1.11	2.6×10^{-9}	.282	0.316	0.51	0.16
9	*TRPM3*	rs71507014	73438605	GC/G	.427	.405	1.10	3.0×10^{-8}	NA	NA	NA	NA
9	*TGFBR1*	rs1626340	101923372	G/A	.189	.209	0.88	3.8×10^{-10}	0.197	0.202	0.982	0.899
9	*ABCA1*	rs2740488	107661742	A/C	.255	.275	0.90	1.2×10^{-8}	0.252	0.26	0.968	0.807
10	*ARHGAP21*	rs12357257	24999593	G/A	.243	.223	1.11	4.4×10^{-8}	0.244	0.242	0.988	0.93
10	*ARMS2/HTRA1*	rs3750846	124215565	T/C	.436	.208	2.81	6.5×10^{-735}	0.185	0.198	0.905	0.479
12	*RDH5/CD63*	rs3138141	56115778	C/A	.222	.207	1.16	4.3×10^{-9}	0.181	0.221	0.756	0.053
12	*ACAD10*	rs61941274	112132610	G/A	.024	.018	1.51	1.1×10^{-9}	0.009	0.014	0.724	0.559
13	*B3GALTL*	rs9564692	31821240	C/T	.277	.299	0.89	3.3×10^{-10}	0.317	0.294	1.118	0.376
14	*RAD51B*	rs61985136	68769199	T/C	.360	.384	0.90	1.6×10^{-10}	NA	NA	NA	NA
14	*RAD51B*	rs2842339	68986999	A/G	.107	.094	1.14	1.4×10^{-6}	0.105	0.09	1.230	0.321
15	*LIPC*	rs2043085	58680954	T/C	.350	.381	0.87	4.3×10^{-15}	0.353	0.397	0.811	0.079
15	*LIPC*	rs2070895	58723939	G/A	.195	.217	0.87	2.4×10^{-11}	0.192	0.203	0.947	0.699
16	*CETP*	rs5817082	56997349	C/CA	.232	.264	0.84	3.6×10^{-19}	NA	NA	NA	NA
16	*CETP*	rs17231506	56994528	C/T	.348	.315	1.16	2.2×10^{-18}	0.305	0.322	0.918	0.485
16	*CTRB2/CTRB1*	rs72802342	75234872	C/A	.067	.080	0.79	5.0×10^{-12}	0.068	0.066	1.058	0.812
17	*TMEM97/VTN*	rs11080055	26649724	C/A	.463	.486	0.91	1.0×10^{-8}	0.509	0.522	0.948	0.637

Supplemental Table 9.5. (*continued*)

Chr	Locus name	SNP ID	Bp (Hg19)	Major / minor allele	AMD				Idiopathic MFC			
					MAF		OR	*P*-value	MAF		OR	*P*-value
					Cases	Controls			Cases	Controls		
17	*NPLOC4/TSPAN10*	rs6565597	79526821	C/T	.400	.381	1.13	1.5×10^{-11}	0.341	0.356	0.937	0.609
19	*C3*	rs2230199	6718387	C/G	.266	.208	1.43	3.8×10^{-69}	0.231	0.213	1.179	0.259
19	*C3*	rs147859257	6718146	T/G	.012	.004	2.86	3.1×10^{-28}	0.003	0.006	1.017	0.988
19	*C3 (NRTN/FUT6)*	rs12019136	5835677	G/A	.036	.048	0.71	2.4×10^{-15}	0.047	0.041	1.133	0.662
19	*CNN2*	rs67538026	1031438	C/T	.460	.498	0.90	2.6×10^{-8}	NA	NA	NA	NA
19	*APOE*	rs429358	45411941	T/C	.099	.135	0.70	2.4×10^{-42}	0.133	0.149	0.816	0.205
19	*APOE(EXOC3L2/MARK4)*	rs73036519	45748362	G/C	.284	.302	0.91	3.1×10^{-7}	0.31	0.297	1.036	0.783
20	*MMP9*	rs142450006	44614991	TTTTC/T	.124	.141	0.85	2.4×10^{-10}	0.049	0.053	0.859	0.615
20	*C20orf85*	rs201459901	56653724	T/TA	.054	.070	0.76	3.1×10^{-16}	NA	NA	NA	NA
22	*SYN3/TIMP3*	rs5754227	33105817	T/C	.109	.137	0.77	1.1×10^{-24}	0.152	0.131	1.24	0.203
22	*SLC16A8*	rs8135665	38476276	C/T	.217	.195	1.14	5.5×10^{-11}	0.198	0.197	1.003	0.985

Chr, chromosome; SNP, single nucleotide polymorphism; BP, basepair; MFC, multifocal choroiditis; MAF, minor allele frequency; OR, odds ratio; NA, not available.

Supplemental Figures

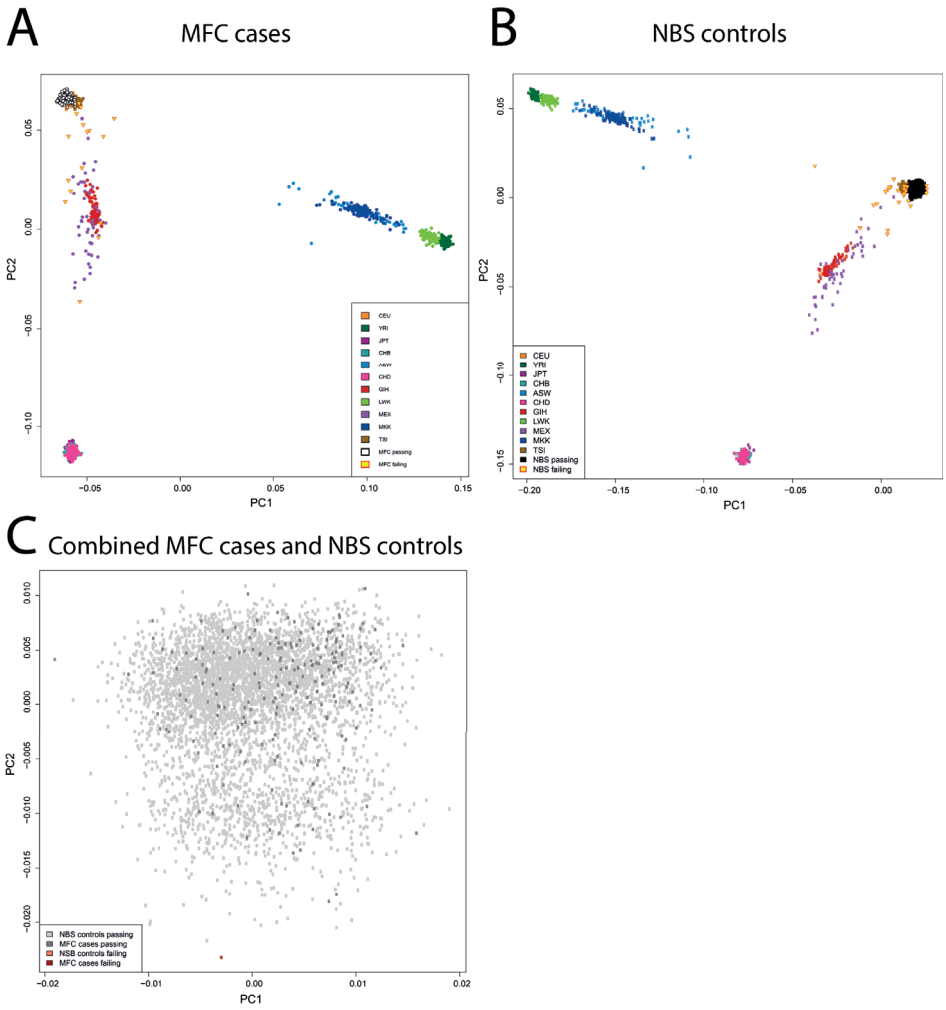

Supplemental figure 9.1. Principal component analysis. The visualization of the first 2 principal components in cases (**A**), NBS controls (**B**) and the combined cohort (**C**). The colors in A and B indicate the Hapmap3 samples as stated in the legend and the yellow triangles with red lining indicate the samples that were considered outliers (>4SD) and excluded from further analyses. Subsequently the analysis was repeated in the combined cohort (remaining NBS controls and cases) and 1 outlier (>4SD) was excluded.

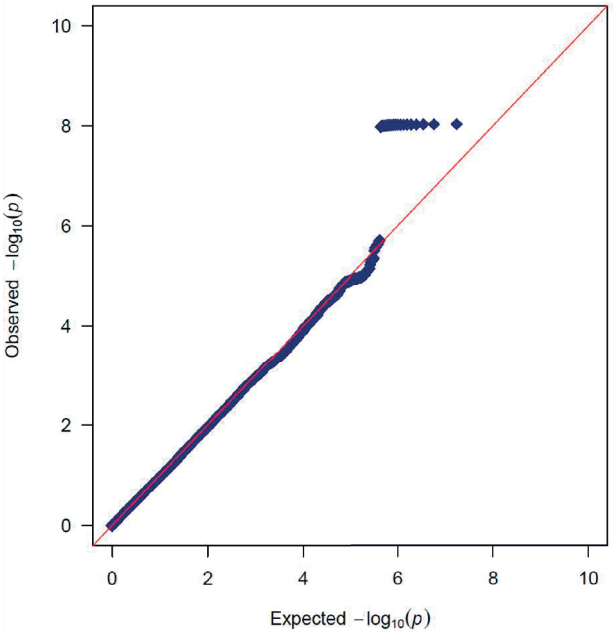

Supplemental figure 9.2. Quantile-quantile plot. In a quantile-quantile plot every dot represents a single nucleotide polymorphism with its expected and observed chi-square statistics. The associations were tested with a Scalable and Accurate Implementation of GEneralized mixed model including the covariates age, sex and the first 6 principal components. The red line indicates the normal distribution (labda (λ) = 1.000).

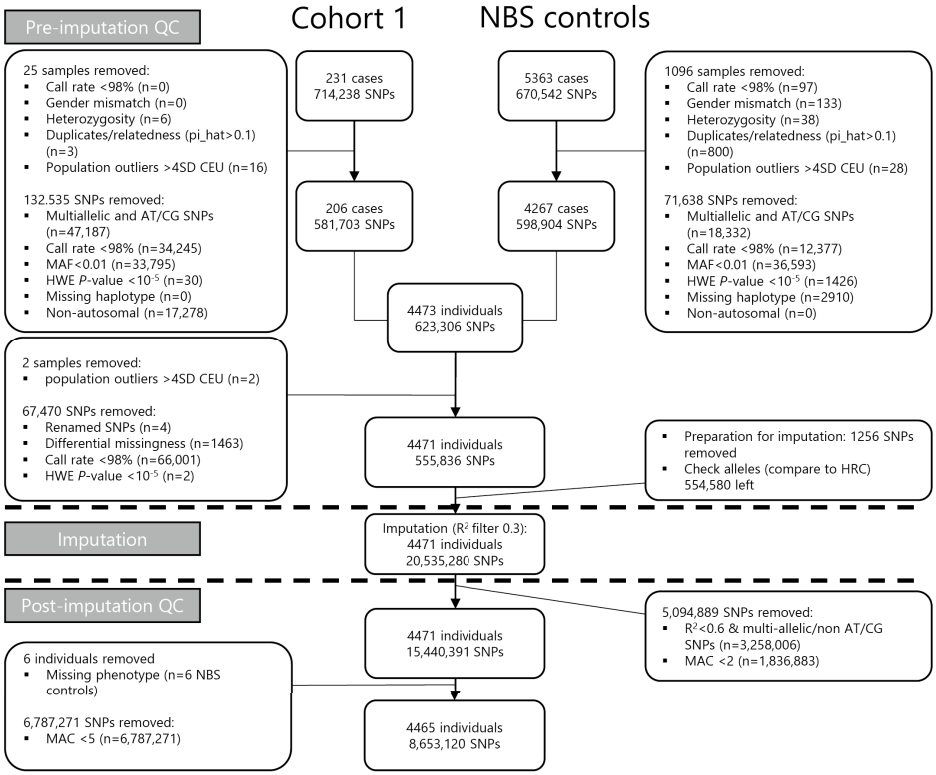

Supplemental figure 9.3. Overview of the quality control steps. First we performed quality control for both datasets separately (Cohort 1 and NBS controls). Next the datasets were merged and again subjected to stringent quality control. After imputation SNPs with an allele count of less than 5 were removed. In total 4465 cases and 8,653,120 SNPs were analyzed.

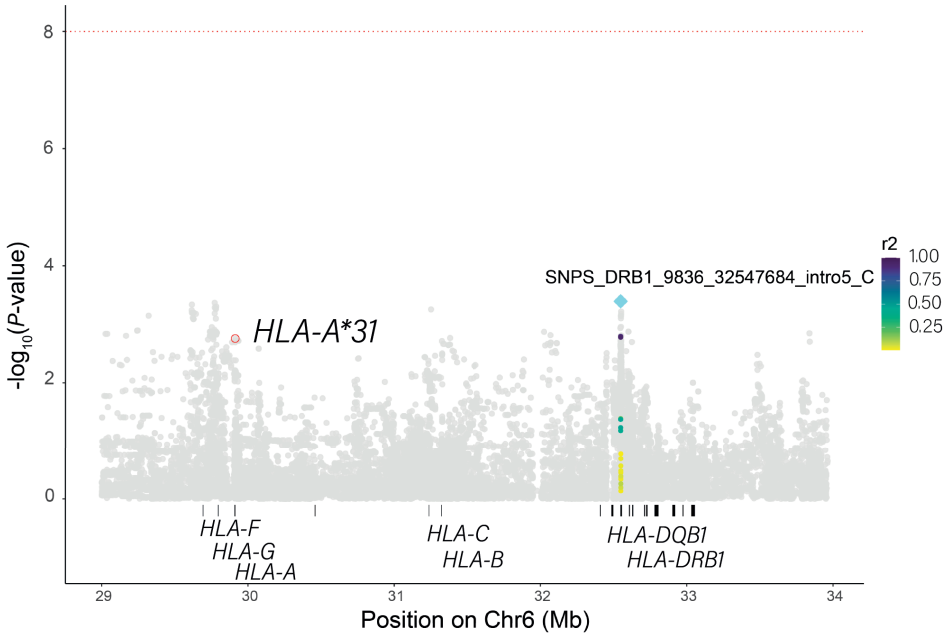

Supplemental figure 9.4. Association results of the Major histocompatibility complex (MHC) region. This plot visualizes the association results of the MHC region on chromosome 6 after imputation (g group) of the MHC region including the imputation of classical *Human Leukocyte Antigens* (*HLA*) alleles, amino acids positions, single nucleotide polymorphisms (SNPs) in the MHC region and insertions/deletions in the MHC region. The x-axis represents the location on chromosome 6 including the annotation of the *HLA* genes and the y-axis represents the $-\log_{10}$ of the *P*-value. The associations were tested with a *Scalable and Accurate Implementation of GEneralized* (SAIGE) mixed model including the covariates age, gender and the first 6 principal components and association results are visualized as gray dots. The red dotted line indicates the threshold for genome-wide significant signals ($P < 5.0 \times 10^{-8}$). The most associated locus in the MHC region was a SNP at position 9836 of the gene body, genomic position 32547684 in intron 5 ($P = 3.7 \times 10^{-4}$) (blue triangle). This SNP showed very little linkage disequilibrium in the region as indicated by the r2 (see legend). From the classical *HLA* alleles, *HLA-A*31* was most associated (*P*=0.002) (red circle).

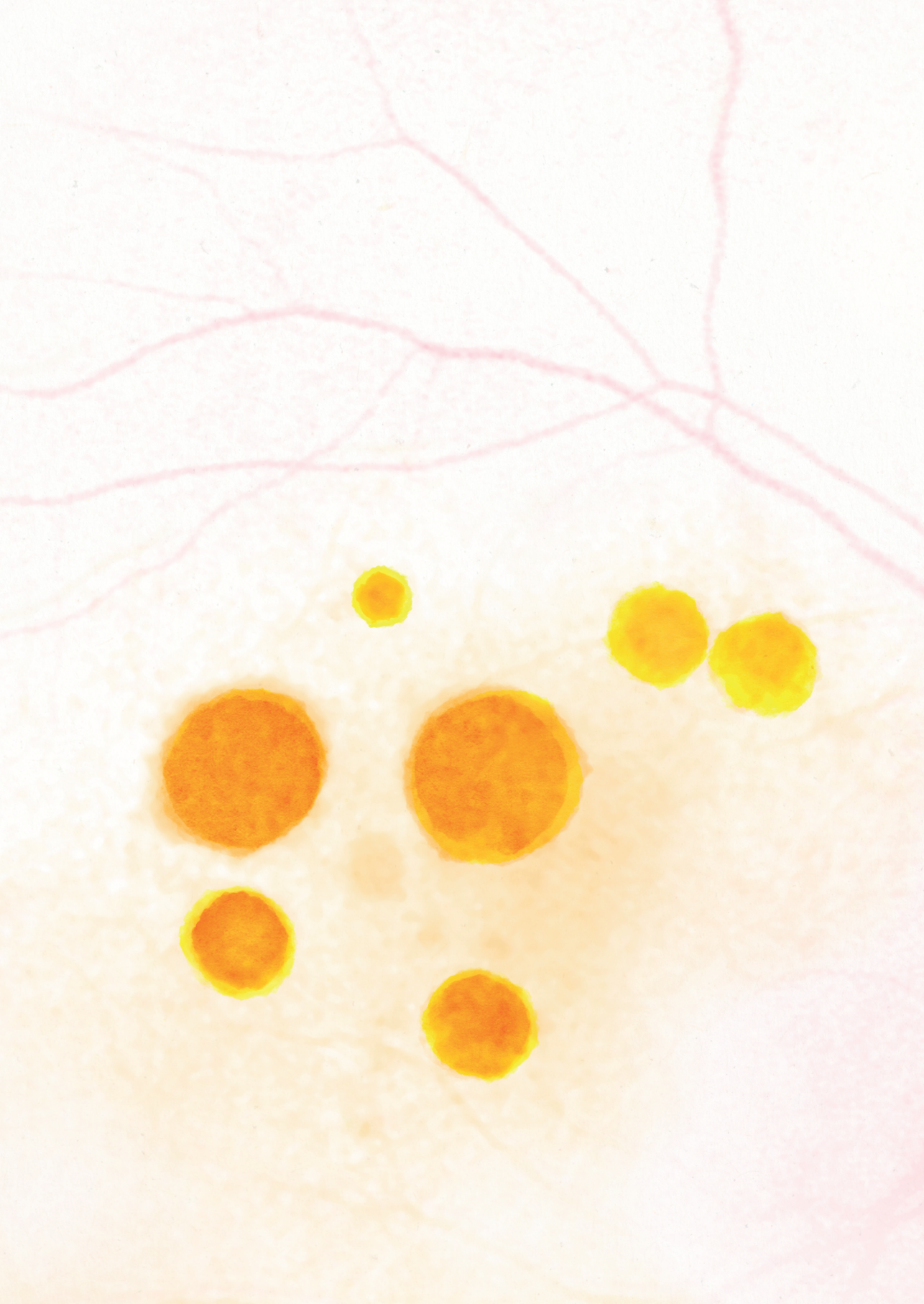

Chapter 10

The risk variant for idiopathic multifocal choroiditis in the *CFH* gene is not associated with serpiginous choroiditis and relentless placoid chorioretinitis

Evianne L. de Groot
Jeannette Ossewaarde-van Norel
Joke H. de Boer
Sanne Hiddingh
Bjorn Bakker
Ramon A.C. van Huet
Ninette H. ten Dam-van Loon
Alberta A.H.J. Thiadens
Magda A. Meester-Smoor
Yvonne de Jong-Hesse
Leonoor I. Los
Anneke I. den Hollander
Camiel J.F. Boon
Lambertus A. Kiemeney
Kristel R. van Eijk
Mark K. Bakker
Carel B. Hoyng
Jonas J.W. Kuiper

Manuscript in preparation

Editor,

Primary inflammatory choriocapillaropathies (PICCPs) refer to a group of conditions including *idiopathic multifocal chorioditis* (MFC), and the more rare *serpiginous choroiditis* (SC), *relentless placoid chorioretinitis* (RPC) and *persistent placoid maculopathy* (PPM) subtypes.[1]

We have recently discovered that common variants in the *complement factor H* (*CFH*) gene confer risk for idiopathic MFC (Chapter 9). Since SC, RPC and PPM fall within the same disease spectrum, we wondered whether this association could also be observed in patients with these subtypes. The frequency of the risk genotype in the *CFH* gene was therefore assessed in 11 SC, 17 RPC and 3 PPM cases. The criteria of the Sun Working Group were used for diagnosis of SC.[2] RPC was established in cases with both clinical characteristics of serpiginous choroiditis and acute posterior multifocal placoid pigment epitheliopathy (**Figure 10.1**).[3] The mean (SD) age was 48 (20) years and 52% of patients were male. The prevalence of secondary choroidal neovascularization was 23% and 25 patients (81%) were bilaterally affected.

The risk variant rs7535263 was genotyped in genomic DNA from blood leukocytes from 31 cases using the Illumina Infinium OmniExpress-24 bead chip or TaqMan® SNP genotyping technology (ThermoFisher Scientific Inc. Waltham, MA, USA), as previously described in chapter 9. We compared the frequency of rs7535263 with genotype data from Dutch population controls[4] using a logistic regression model adjusted for age and sex.

The allele frequency (AF) of the risk allele, G, of rs7535263 was 48% in cases and 57% in controls. We observed no significant association with the risk variant rs7535263 in the *CFH* gene in patients with SC, PPM and RPC (odds ratio (OR) = 0.89 [95%CI 0.45-1.74]; *P* = 0.73). Separate analyses of the subtypes SC and RPC revealed similar results (SC; AF G-allele 41%, OR=0.64 [95%CI 0.28-1.46]; *P* = 0.29; RPC: AF G-allele 50%, OR= 0.89 [95%CI 0.45-1.75]; *P* = 0.74).

The variant rs7535263 in the *CFH* gene was not associated with SC and RPC in this study. No conclusions can be drawn regarding the subtype PPM considering only 3 patients were included. Despite being underpowered, the G allele frequency in SC, RPC and PPM cases was 48% (57% in controls), which is considerably different from the 73% observed in our GWAS of idiopathic MFC. PICCPs have been considered to have similar pathophysiological mechanisms since they belong to the same clinical spectrum. Our analysis showed, however, that SC and RPC cases were less likely to carry the *CFH* risk

variant for idiopathic MFC compared to controls. Therefore, SC and RPC may have different disease mechanisms that do not involve the *CFH* gene. In order to compare genetic susceptibility of idiopathic MFC with SC, RPC and PPM, follow-up studies in larger cohorts are required, but this is challenging due to the rare nature of these diseases.

In conclusion, the idiopathic MFC risk variant in the *CFH* gene was not associated with SC or RPC.

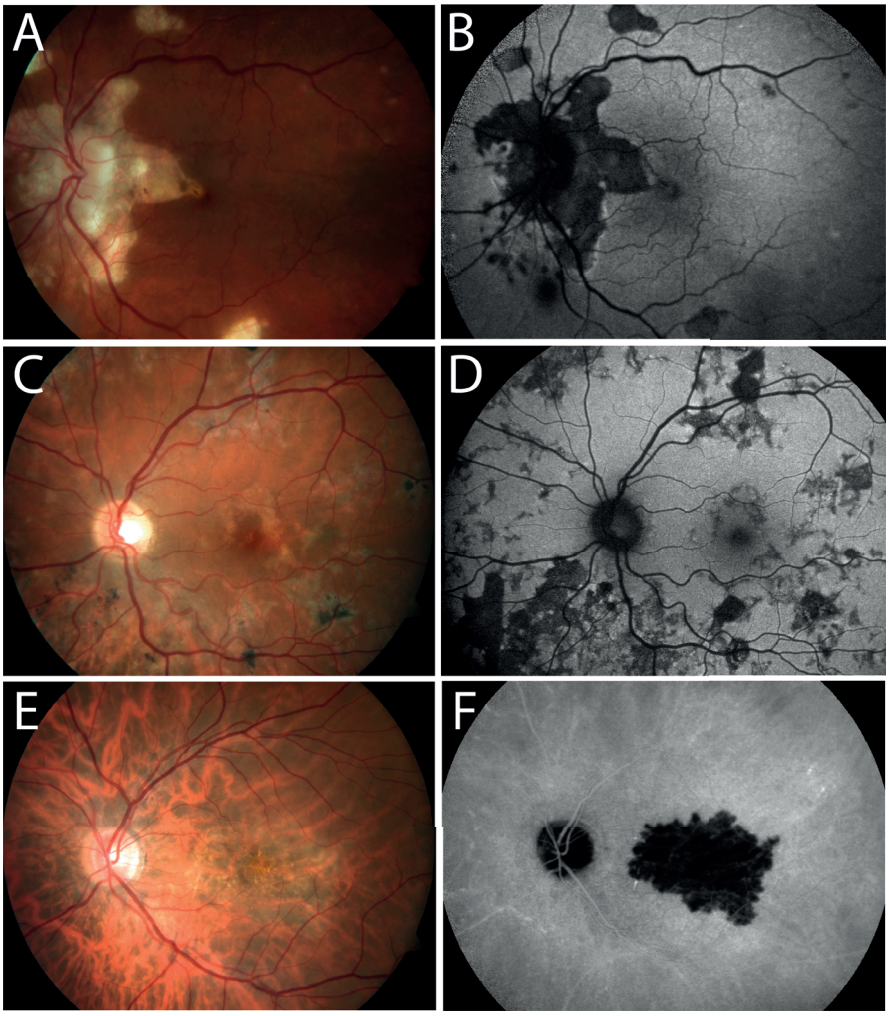

Figure 10.1. Serpiginous choroiditis, relentless placoid chorioretinitis and persistent placoid maculopathy. Top: Fundus picture (**A**) and fundus autofluorescence picture (**B**) of a case diagnosed with serpiginous choroiditis demonstrating the classical serpentine growth pattern. Middle: Fundus picture (**C**) and fundus autofluorescence picture (**D**) of a case diagnosed with relentless placoid chorioretinitis demonstrating both features of serpiginous choroiditis and acute posterior multifocal placoid pigment epitheliopathy. Bottom: Fundus picture (**E**) and indocyanine green angiography image taken 20 minutes after dye injection (**F**) of a case diagnosed with persistent placoid maculopathy.

REFERENCES

1. Papasavvas I, Herbort CPJ. Diagnosis and Treatment of Primary Inflammatory Choriocapillaropathies (PICCPs): A Comprehensive Overview. Medicina (B Aires). 2022;58(2):165.
2. The Standardization of Uveitis Nomenclature (SUN) Working group. Classification Criteria for Serpiginous Choroiditis. Am J Ophthalmol. 2021;228:126-133.
3. Jones EB, Jampol LM, Yannuzzi LA, et al. Relentless placoid chorioretinitis. Arch Ophthalmol. 2000;118:931-938.
4. Galesloot TE, Vermeulen SH, Swinkels DW, et al. Cohort Profile: The Nijmegen Biomedical Study (NBS). Int J Epidemiol. 2017;46(4):1099-1100j.

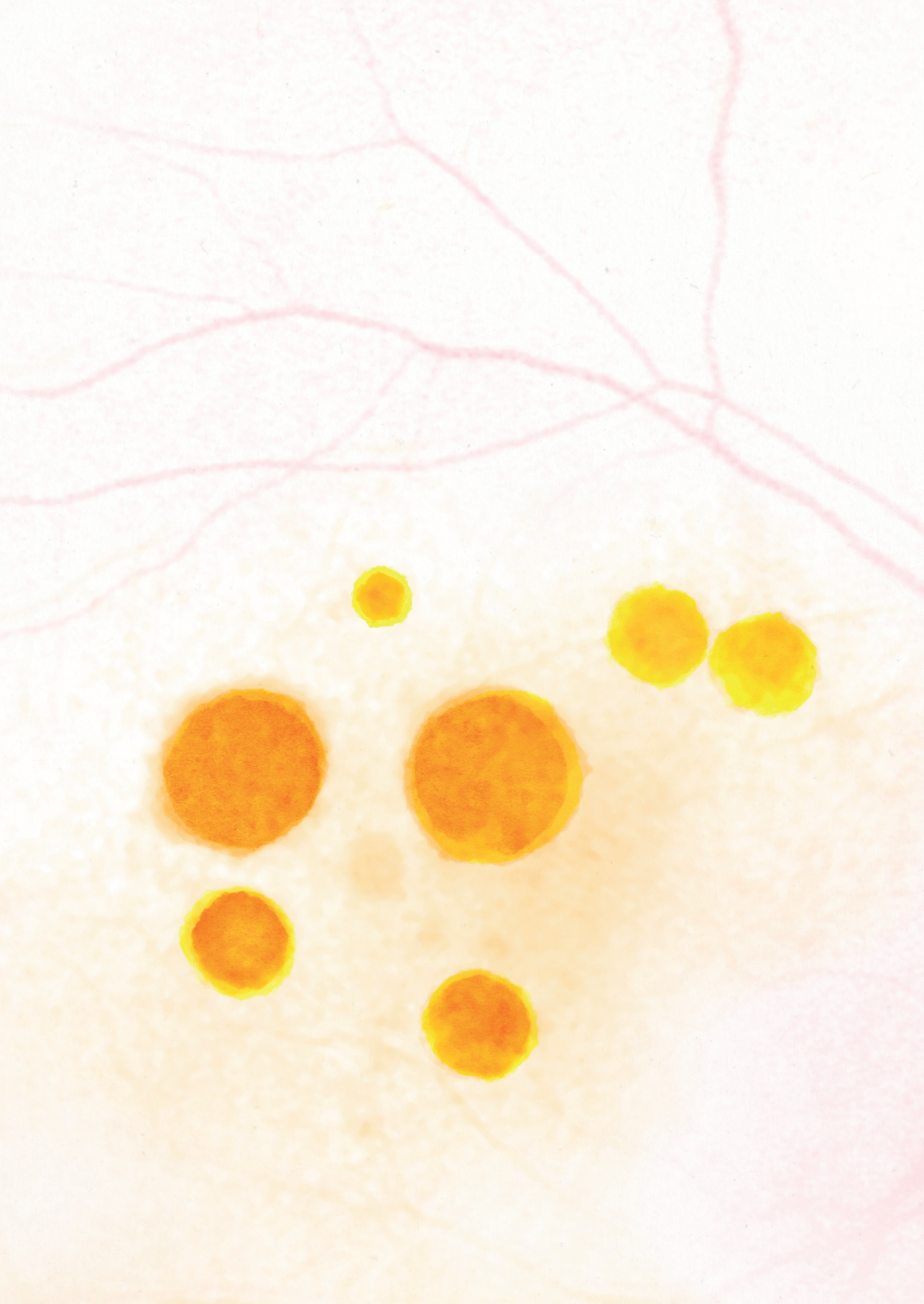

Chapter 11

Summary, general discussion and future perspectives

Central multifocal choroiditis (cMFC) is a group of rare idiopathic forms of primary choriocapillaritis and includes the entities "multifocal choroiditis (MFC)", "punctate inner choroidopathy (PIC)", "relentless placoid chorioretinitis (RPC)", "serpiginous choroiditis (SC)" and "persistent placoid maculopathy (PPM)". These entities have in common that the choriocapillaris is affected in the posterior pole of the eye and the pathophysiology is widely unknown. The disease entities MFC and PIC show very similar characteristics and are often considered a single disease entity. In here, we use the term idiopathic MFC to address both these subtypes.

In this thesis, we study several aspects of cMFC with the overarching aim to identify clinical and genetic risk factors for this disease. Identifying these risk factors will increase our understanding of the pathophysiological mechanism underlying cMFC. Moreover, the risk factors can be used to improve treatment strategies for patients with cMFC with the ultimate goal to preserve visual function in these patients. In this thesis we address three aims for three different aspects of this disease:

1. To improve the clinical outcomes of cMFC by investigating the efficacy of current therapies and explore clinical risk factors for increased relapse rate.
2. To explore imaging characteristics that can aid in early recognition of disease activity and can help to distinguish inflammation from secondary choroidal neovascularization (CNV).
3. To determine genetic and immunologic risk factors to gain insight into the pathophysiology underlying this disease.

In this chapter, we will summarize the main findings, place the results in a broader perspective and propose future research opportunities.

SUMMARY OF THE MAIN FINDINGS

Clinical outcomes in patients with idiopathic MFC

In **chapter 2**, we describe a large cohort of idiopathic MFC patients where we confirm the typical clinical characteristics of this patient group. In this cohort 93% was female, the median age at the time of the first complaints was 37 years and the median refractive error of all affected eyes was -5.5 diopters. The reported prevalence of secondary CNV was exceptionally high in this idiopathic MFC and was 66% in this cohort.

In **chapter 3** and **chapter 4**, we explored the efficacy of disease-modifying antirheumatic drugs (DMARDs) and/or biologicals in patients with idiopathic MFC. In **chapter 3**, we report that after treatment with a DMARD, the number of relapses of disease activity per

year significantly decreased in 32 patients. This was specifically the case for relapses of disease activity with active secondary CNV but also resulted in a reduction of 50% of the number of relapses without active CNV. Remission and steroid-free remission was achieved after a median of 21 and 83 weeks, respectively. In **chapter 4**, we describe the course of disease in 12 patients before and after the start of treatment with the biological adalimumab. In this study, we show that the majority of patients with refractory disease to conventional DMARDs responded well to treatment with adalimumab. Twelve months after the start of adalimumab, 9 out of 12 patients achieved steroid-free remission. Unfortunately, multiple clinical relapses still occurred in 2 patients who were diagnosed with serpiginous choroiditis and persistent placoid maculopathy. Our results demonstrate that adalimumab is very effective in patients with idiopathic MFC but might be less effective in patients with serpiginous choroiditis and persistent placoid maculopathy.

In **chapter 2**, we performed an observational cohort study of 2 years including 82 patients with idiopathic MFC. In this study, we observed a total of 135 relapses of inflammation (median (interquartile range) 1.0 (0.25-3)) in 61 patients of which the majority of the relapses (75%) was diagnosed before the patient experienced symptoms. The affected area of the posterior pole significantly increased during the 2 years of follow-up and this increase was significantly higher in patients who did not receive treatment with DMARDs and/or biologicals. Almost two-third of the patients were treated with oral cycles of prednisolone during the 2 years of follow-up. In addition, 21% of the patients started treatment with a DMARD and 26% of the patients started treatment with a biological agent in addition to a DMARD during follow-up.

Self-reported quality of life in patients with idiopathic MFC

Despite being a very important clinical factor in the monitoring and treatment of patients, the quality of life in patients with idiopathic MFC was never investigated before. To gain more insight into the psychological burden of this disease and to explore clinical factors influencing the quality of life, we investigated the general health quality of life (GH-QoL) and vision-related quality of life (VR-QoL) scores in this patient group (**chapter 2**). We found that at baseline patients had lower VR-QoL scores for almost all domains but also for several domains regarding the GH-QoL. We did not find an association between the QoL-scores and the relapse rate or treatment with DMARDs/biologicals or prednisolone.

Idiopathic MFC and pregnancy

Patients with idiopathic MFC are mostly females in their fertile stage of life and therefore more information is warranted regarding the natural course of disease during pregnancy and the efficacy and safety of the various treatment options. **Chapter 5** reports on

the results of sixteen pregnancies of patients with idiopathic MFC. In this study, we observed a relapse of disease activity in almost half of the pregnancies, especially in patients without immunomodulatory therapy (azathioprine and/or prednisolone). Most relapses occurred in the second and third trimester of pregnancy. Overall, the treatment with both azathioprine, prednisolone and intravitreal anti-vascular endothelial growth factor (VEGF) injections was safe and no major maternal or fetal complications occurred. If treatment is initiated during pregnancy, we advise to do this in the context of shared-decision making and we encourage pre-conception counseling by both the ophthalmologist as the gynecologist.

Multimodal imaging characteristics for monitoring disease activity in idiopathic MFC

In **chapter 6**, we investigated if we could identify imaging characteristics that indicate inflammatory disease activity. In this study, we included 50 idiopathic MFC patients with 110 lesions and we evaluated the lesions during the active and inactive stage. On the spectral-domain optical coherence tomography (SD-OCT), lesions with inflammatory activity (n=96) typically demonstrated an increase in the focal choroidal thickness, moderately reflective material located sub-retinal pigment epithelium (RPE) and/or in the outer retina with disruption of the ellipsoid zone (EZ). Moreover, an increase in the area of hypoperfusion in the choriocapillaris was observed, visualized as an increase in the hypofluorescent areas on indocyanine green angiography (ICGA) and an increase in the areas of flow void on spectral-domain optical coherence tomography angiography (SD-OCTA). To distinguish CNV activity from inflammation, we compared the imaging characteristics of active lesions with CNV activity (n=14) with active lesions without CNV activity (n=96). We found that active CNV was associated with leakage on fluorescein angiography (FA) and the observation of a vascular structure on SD-OCTA. Moreover, the imaging characteristics that were more often visible on SD-OCT were the presence of fluid, hyporeflectivity of the choroid and the presence of mixed reflective subretinal material.

Moving towards personalized medicine

The natural course of disease shows great variability in patients with idiopathic MFC. In this thesis, we aimed to identify determinants predicting the disease severity in individual patients. In **chapter 2** we discovered that the relapse rate during follow-up was influenced by two clinical characteristics: the level of myopia and the complication of secondary CNV. The majority of patients who will develop secondary CNV, have already developed this complication at first presentation. Therefore, both risk factors can help clinicians to predict the disease severity at an early stage and might be of assistance in selecting the appropriate treatment strategy. In **chapter 7**, we used a different

approach to identify determinants associated with disease severity. In this study, we used available data concerning morphological characteristics of blood cells including size, lobularity and complexity of cells. We discovered that patients who demonstrate a relatively high granularity of the platelets, were not only more likely to start treatment with immunomodulatory therapy (IMT) but also started the treatment faster after first presentation.

Pathophysiology – what have we learned

The genes and biological pathways involved in idiopathic MFC are poorly understood, which hinders the adequate monitoring and treatment of this patient group. In this thesis, we aimed to unravel the pathophysiology of this rare disease by exploring the association with blood cell characteristics, single nucleotide polymorphisms (SNPs), and protein concentrations.

In **chapter 7**, we compared morphological characteristics of blood cells between 122 cMFC cases and 364 age and sex-matched control subjects. In this study, we observed a decreased blood monocyte count and a decreased percentage in circulating monocytes in patients compared to controls. Additionally, in **chapter 8**, we describe the incidental observation of altered blood cell characteristics after the patients underwent FA. We observed increased fluorescence of neutrophils, lymphocytes, monocytes and erythrocytes at least up until eight hours after the injection of the fluorescein dye.

In **chapter 9**, we describe the results of a *genome-wide association study* including 222 patients diagnosed with idiopathic MFC. We discovered a genetic variation in the *complement factor H* (*CFH*) gene (lead variant the A allele of rs7535263; odds ratio (OR) [95% confidence interval (95%CI)] = 0.52 [0.41-0.64]; $P = 9.3 \times 10^{-9}$) that was significantly associated with idiopathic MFC. Additionally, we measured 370 proteins linked to inflammation in 87 treatment-naïve idiopathic MFC patients, using the Olink targeted proteomics platform. In this study, we showed that the risk genotype (GG) of this specific rs7535263 variant resulted in increased concentrations of 27 proteins in idiopathic MFC patients. We identified that these proteins are involved in the platelet degranulation pathway and the complement regulation, using pathway-enrichment analysis.

In **chapter 10**, the allele frequency (AF) of lead variant (rs7535263) was also determined in patients with the more rare subtypes serpiginous choroiditis (SC) (n=11), persistent placoid chorioretinopathy (PPM) (n=3) and relentless placoid chorioretinitis (RPC) (n=17). The AF of the risk allele, G, of rs7535263 was 48% in cases and 57% in controls and did not demonstrate a significant association with these subtypes (odds ratio (OR) = 0.89 [95%CI 0.45-1.74]; $P = 0.73$). Separate analyses of both the subtypes RPC and SC

revealed similar results (SC; AF G-allele 41%, OR=0.64 [95%CI 0.28-1.46]; *P* = 0.29; RPC: AF G-allele 50%, OR= 0.89 [95%CI 0.45-1.75]; *P* = 0.74).

GENERAL DISCUSSION AND FUTURE PERSPECTIVES

Idiopathic MFC: MFC and PIC as a single disease entity

In this thesis, we present genetic evidence that the pathophysiology of the subtypes MFC and PIC is similar or even identical. The variants in the *CFH* gene that were significantly associated with idiopathic MFC showed almost identical allele frequencies in both subtypes (MFC and PIC) indicating that both subtypes have a similar genetic basis. Moreover, in line with the literature, we did not find clinical characteristics, e.g. the prevalence of CNV, age at presentation, sex distribution and best-corrected visual acuity, that were different between the subtypes (**Supplemental Table 11.1**).[1] However, it must be noted that patients with severe ocular inflammation (presenting with papillitis or retinal vasculitis) were not included. Moreover, the proportion of patients presenting with cells in the anterior chamber or the vitreous was low in our patient cohort. Therefore, we cannot rule out that patients with severe intraocular inflammation do demonstrate clinical and genetic differences. It is not surprising that no clinical or genetic differences are observed when considering the initial description of both subtypes is almost identical.[2,3] Even though the SUN working group has developed separate disease criteria for each proposed entity, many patients present with manifestations that overlap with criteria deemed specific for these "subtypes". This makes classification of patients into one of the two subtypes in practice rather challenging.[4-6]

The use of the nomenclature in clinical practice and the literature should be uniformed by adopting a single term for this idiopathic disease. We prefer the term "idiopathic multifocal choroiditis" as more comprehensive disease name because it captures the inflammatory involvement but also emphasizes its idiopathic nature, which distinguishes it from other causes of multifocal choroiditis. We will refer to "idiopathic MFC" for the remainder of this thesis and not differentiate between PIC and MFC

For future studies, it would be interesting to perform a GWAS exploring genetic differences throughout the genome between the subtypes PIC and MFC. However, this will require larger patient groups, which is challenging considering the rarity of the disease. We suggest to also include patients presenting with severe ocular inflammation (papillitis and retinal vasculitis) for this GWAS, since this subgroup of patients is not studied in the current thesis.

New insights into the pathophysiology of idiopathic MFC

Based on the results of this thesis, we propose that the process of complement-mediated thrombotic microangiopathy, resulting in hypoperfusion in the choriocapillaris, is central to the pathophysiology of idiopathic MFC. Myopia acts as an extra stressor on the choriocapillaris and could amplify the disease mechanisms underlying idiopathic MFC, which is supported by the observation that more 75% of the cases are myopic. Uncertainty exists regarding the mechanism behind this association.

Several studies have shown that the severity of myopia is associated with a progressive decline in choroidal thickness, choriocapillary blood perfusion, and diminished vascularity of the choroid and the choriocapillaris.[7-11] Interestingly, a recent study in patients with diabetic retinopathy (another disease affecting the choroidal vasculature) and myopia demonstrated that the blood flow in the choriocapillaris was lowest in patients suffering from both conditions.[12] This indicates that the combination of multiple diseases of the choriocapillaris amplifies the negative effects of each disease. As a consequence, patients with myopia and idiopathic multifocal choroiditis may be at higher risk of developing severe hypoperfusion of the choriocapillaris. In case of additional pathology in the choriocapillaris, the choriocapillaris is no longer able to compensate for the hypoperfusion and consequently ischemia of the retina and choriocapillaris develops. This may also explain the relationship we found between the relapse rate and the severity of the myopia. As the myopia increases, the choriocapillaris has less capacity to compensate for the hypoperfusion.

As a side note, Herbort and colleagues mentioned that if the disease is unilateral, it tends to affect the more myopic of fellow eyes.[13] Although it is outside the scope of this thesis, 74% of the patients in our study population (including those with unilateral disease and a refractive error difference greater than one diopter) developed MFC in their more myopic eye (data not shown).

When idiopathic MFC is active, the first sign of disease activity is the local increase of the areas of hypoperfusion in the choriocapillaris visible on multiple imaging modalities. During the active stage of the disease, an increase in the hypofluorescent areas on ICGA is observed, as well as an increase in the areas of flow void on SD-OCTA.[14] Also signs of ischemia in the retina will appear as a result of hypoperfusion. Especially the outer segments of the photoreceptors will be affected by the hypoperfusion, due to their high energy consumption.[14] This hypoperfusion might be reversible when patients demonstrating signs of disease activity are treated promptly. However, when the hypoperfusion is not treated or not treated adequately, irreversible damage to the

choriocapillaris without reperfusion is observed and the choriocapillaris will become atrophic at the location of hypoperfusion.

Another question is; why do idiopathic MFC patients develop hypoperfusion in the choriocapillaris? We showed a relation between treatment with IMT, as a proxy for disease severity, and the morphological characteristic platelet granularity. We suggest that the increased granularity of the platelets represents platelet activity, which is supported by the fact that we also found an association, albeit not statistically significant, with the morphological characteristic "platelet distribution width" (known to be associated with platelet activity).[15-17] The activated platelets release chemokines, growth factors and other molecules, promoting a prothrombotic state in the choriocapillaris.[18] Moreover, the activated platelets will form aggregates in the choriocapillaris and will thus result in the development of microthrombi in the choriocapillaris. These microthrombi will consequently cause hypoperfusion of the choriocapillaris.

Nevertheless, what causes the local activation of platelets in the choriocapillaris is unclear. This thesis identified a key role for the complement system. The complement system maintains a close relationship with platelets and both are able to activate one another.[19] The platelets have alpha-granules containing many growth factors, coagulation and complement components including factor H (FH) and complement protein 1. Moreover, platelets express many surface receptors and are able to bind complement components including FH and C3.[19-21]

In this thesis, we discovered an association between idiopathic MFC and common variants in the *CFH* gene. Interestingly, these genetic variants are also associated with age-related macular degeneration (AMD), as will be discussed in depth later. Moreover, we show that the risk allele of the lead variant is associated with altered concentrations of proteins involved in the regulation of the complement cascade but also with proteins involved in platelet degranulation and platelet activation. These results support that the complement system plays a major role in idiopathic MFC susceptibility. FH is a regulator of the alternative pathway of the complement system and has several regulating functions ultimately resulting in the inhibition of the complement system and the prevention of damage to self-cells.[22] Although the lead variant identified in our study is physically located within an intron of the *CFH* gene, we showed that the risk allele stronger correlates with proteins encoded by directly adjacent genes and not significantly with plasma levels of the FH protein itself. The *CFH* locus has a complex structure of linkage disequilibrium and encodes a variety of extended haplotypes. Variants in strong linkage disequilibrium at this locus correlate with expression levels from the adjacent and functionally related *CFHR 1-5* genes.[23] It is proposed that the FHR

proteins compete or alter the function of FH and affect the inhibitory effect of FH on the complement system, subsequently leading to unrestricted complement activation.[23,24] Lorres-Motta and colleagues showed with immunohistochemistry that FHR-2 and FHR-5 proteins are located in the intercapillary septa of the choriocapillaris, but not in the choroid or RPE.[23,25] Together this suggests that the FHR proteins are derived from the systemic circulation, enter the eye through the fenestrations of the choriocapillaris and consequently affect the complement system in the choriocapillaris.

Eventually, both the activated complement system and the proinflammatory cytokines released by platelets, including interleukin 6, interleukin 8 and tumor necrosis factor-α, will further enhance an inflammatory response including the recruitment of monocytes and lymphocytes and the activation of the adaptive immune system.[18] This local inflammatory response explains the increase in the choroidal thickness beneath a lesion and the development of moderate reflective material in the sub-RPE and the outer retina. Furthermore, the prevalence of secondary CNV in idiopathic MFC patients is relatively high (over 70% in cases in our studies) and substantially higher compared to other forms of non-infectious posterior uveitis or the prevalence of myopic CNV.[26-28] Because hypoxic and inflammatory conditions promote pro-angiogenic factors, CNV may be caused by both hypoperfusion and localized complement activation.

Finally, we haven't addressed the subject of female predominance. Idiopathic MFC's pathophysiology may also involve the hormonal system, as we will shortly discuss. This may explain why the age of disease onset is nearly exclusively during the reproductive stage of life and may explain why the disease course tends to become less severe after menopause. In pregnancy, platelets are activated and the complement cascade is activated, promoting thrombogenesis.[16,29,30] This phenomenon may be associated with the observation that idiopathic MFC tends to relapse during the second and third trimesters and does not become quiescent after the first trimester, like most other forms of uveitis.[31-33] Another argument in support of a role of sex hormone dysregulation comes from observations in central serious chorioretinopathy (CSC), another disease of the choroid that affects primarily males and is characterized by elevated steroid hormone levels during disease activity. Strikingly, CSC is also associated with the *CFH* gene but the risk allele for MFC is protective against CSC.[34,35]

As mentioned, the genetic variants in the *CFH* gene we found to be associated with idiopathic MFC, are also associated with AMD. However, considering the differences in patient characteristics and the natural course of disease, we believe that the pathophysiology is most likely not identical. Patients with AMD are generally older and there is no evidence for female predominance or association with myopia.[36,37] Moreover,

patients with AMD do not demonstrate signs of intraocular inflammation, while patients with idiopathic MFC do not have drusen, the clinical hallmark of AMD.[38,39] We suggest that the dysregulation of the complement system plays a role in the pathophysiology of both diseases, but other factors modifying these pathways differ, including for example myopia in idiopathic MFC and oxidative stress in AMD.

The involvement of platelets and the coagulation system in AMD remains sparsely studied, most likely because reported proteomic studies are typically performed in serum and not in plasma hindering the quantification of coagulation factors.[40] However, increased protein concentrations involved in the platelet degranulation pathway in the aqueous humor of AMD patients has been reported.[41]

To further unravel the pathophysiology of idiopathic MFC and confirm our hypothesis, it would be interesting to investigate platelet functionality and activity in patients with idiopathic MFC and the relation with disease activity. Coagulation assays, for example clot-based tests, could be used to screen for alterations in the clotting times further dissecting the specific parts of the coagulation cascade involved in idiopathic MFC. Furthermore, specific receptors on platelets indicating platelet activity, for example the GP IIb/IIIa receptor, could be assessed to explore the relation between platelet activity and disease activity in idiopathic MFC patients.

More research is warranted to dissect the mechanisms by which the complement system drives disease in idiopathic MFC patients. Whole-genome or exome-sequencing would be particularly useful for identifying rare variants in additional susceptibility genes, as well as further elucidating the functional changes in complement genes in idiopathic MFC pathophysiology. In order to detect loci with intermediate and moderate effect sizes, these studies should be conducted in much larger sample sizes.

Improving the treatment of idiopathic MFC patients

In this thesis, we found compelling evidence supporting the beneficial effect of the treatment of immunomodulatory therapy in patients with idiopathic MFC. Not only did the number of relapses decrease after therapy with a DMARD and/or biological, also the reported outcomes are favorable compared with the literature. In our cohort, the best-corrected visual acuity was better, we report limited growth of the chorioretinal lesions over time and the complication rate was low.[1,42-45] We believe that this is the result of close monitoring of these patients in combination with prompt and adequate treatment with immunomodulatory therapy. This is supported by the observation of significantly less growth of chorioretinal lesions in the group of patients that were treated with DMARDs and/or biologicals compared to patients that did not receive treatment with

these agents. Even though the treatment of patients with idiopathic MFC is still subject of debate, we believe that treatment with DMARDs and/or biologicals has a beneficial effect on the course of disease in idiopathic MFC patients. We would therefore advise to add these agents to the treatment regime in patients with a severe course of disease.

However, we also report in this thesis that despite adequate monitoring and treatment, still many patients experience relapses of disease activity indicating that the management of idiopathic MFC is not yet optimal and the introduction of new therapeutic agents have to be considered. As described, we found compelling evidence for the involvement of complement dysregulation in the pathophysiology of idiopathic MFC. Therefore, we believe that it would be interesting to explore the efficacy of therapeutic agents targeting this specific biological pathway for the treatment of idiopathic MFC patients. Currently, therapeutic agents that target the components C3 and C5 in the complement system are being developed for treatment of AMD with promising results.[36,45] Future studies should explore the efficacy of these agents in the treatment of patients with idiopathic MFC.

Moreover, we found evidence that platelet activation plays a key role in the pathophysiology of idiopathic MFC which opens doors for new treatment strategies. We suggest that especially the group of antiplatelet drugs such as acetylsalicylic acid and clopidogrel could have a beneficial effect on the disease activity in patients with idiopathic MFC. These agents are safe, inexpensive and widely used and could be added to the treatment regime of patients with idiopathic MFC. Future studies should explore the beneficial effect of these agents on the course of disease in patients with idiopathic MFC.

Idiopathic MFC as part of the white dot syndromes

Historically, idiopathic MFC is a syndrome described within the group of white dot syndromes.[47] At the beginning of this thesis, we introduced the term central MFC for 4 diagnoses which were all considered a form of non-infectious uveitis affecting the choriocapillaris namely; multifocal choroiditis, punctate inner choroidopathy, relentless placoid chorioretinitis (RPC) and serpiginous choroiditis (SC). Even though the targeted structures are similar in these diseases, we suggest that RPC and SC should not be considered in the same disease spectrum as idiopathic MFC. The clinical characteristics for SC and RPC are different from idiopathic MFC. Moreover, the genetic association detected in patients with idiopathic MFC is less evident in patients with RPC and SC, indicating that the genetic and molecular basis for RPC and SC may differ from idiopathic MFC.[48-50] We therefore believe that the pathophysiological mechanism of these subtypes is different from idiopathic MFC, and further research is needed to expose which biological pathways are involved in the pathophysiology of these subtypes.

The impact of idiopathic MFC: from a patients perspective

In this thesis, we showed that patients with idiopathic MFC report lower quality of life (QoL) scores for both vision-related items and general health-related items. This finding was unexpected since the visual function is preserved in most patients and pain is not a common symptom.[38,39,51,52] Moreover, the disease only affects the eye and no association with a systemic disease is reported.[39,53] We hypothesize that these relatively low QoL scores are the result of the young age of disease manifestation in combination with the stress and the uncertainty caused by any relapsing and chronic (eye)disease. Even though we did not find an association between QoL scores and treatment with prednisone or DMARDs, it is plausible that these medical agents will negatively influence the QoL due to side-effects. In conclusion, these results emphasize the importance of future research to improve the QoL in this patient group. Research should especially focus on the pathophysiology of the disease and the development of prediction tools for disease severity in individual patients. Gaining insight into the pathophysiology will possibly lead to new therapeutic agents with higher effectivity and less side-effects. Moreover, we believe that individual prediction tools will decrease stress and anxiety in patients by providing more certainty about the course of the disease and can aid ophthalmologists and patients in selecting the appropriate treatment regime.

REFERENCES

1. Essex RW, Wong J, Fraser-Bell S, et al. Punctate inner choroidopathy: Clinical Features and Outcomes. Arch Ophthalmol. 2010;128(8):982-987.
2. Watzke RC, Packer AJ, Folk JC, Benson WE, Burgess D, Ober RR. Punctate Inner Choroidopathy. Am J Ophthalmol. 1984;98(5):572-584.
3. Essex RW, Wong J, Jampol LM, Bird AC. Editorial Idiopathic Multifocal Choroiditis : A Comment on Present and Past Nomenclature. Retina. 2013;33(1):1-4.
4. Gilbert RM, Niederer RL, Kramer M, et al. Differentiating Multifocal Choroiditis and Punctate Inner Choroidopathy: A Cluster Analysis Approach. Am J Ophthalmol. 2020;213:244-251.
5. The Standardization of Uveitis Nomenclature (SUN) Working group. Classification Criteria for Punctate Inner Choroiditis. Am J Ophthalmol. 2021;228:275-280.
6. The Standardization of Uveitis Nomenclature (SUN) Working group. Classification criteria for multifocal choroiditis with panuveitis. Am J Ophthalmol. 2021;228:152-158.
7. Wu H, Zhang G, Shen M, et al. Assessment of choroidal vascularity and choriocapillaris blood perfusion in anisomyopic adults by SS-OCT/OCTA. Investig Ophthalmol Vis Sci. 2021;62(1):1-4.
8. Xu A, Sun G, Duan C, Chen Z, Chen C. Quantitative assessment of three-dimensional choroidal vascularity and choriocapillaris flow signal voids in myopic patients using ss-octa. Diagnostics. 2021;11(11).
9. Al-Sheikh M, Phasukkijwatana N, Dolz-Marco R, et al. Quantitative OCT angiography of the retinal microvasculature and the choriocapillaris in myopic eyes. Investig Ophthalmol Vis Sci. 2017;58(4):2063-2069.
10. Liu Y, Wang L, Xu Y, Pang Z, Mu G. The influence of the choroid on the onset and development of myopia: from perspectives of choroidal thickness and blood flow. Acta Ophthalmol. 2021;99(7):730-738.
11. Gupta P, Thakku SG, Saw SM, et al. Characterization of Choroidal Morphologic and Vascular Features in Young Men With High Myopia Using Spectral-Domain Optical Coherence Tomography. Am J Ophthalmol. 2017;177:27-33.
12. Xiong K, Wang W, Gong X, et al. Influence of High Myopia on Choriocapillaris Perfusion and Choroidal Thickness in Diabetic Patients Without Diabetic Retinopathy. Retina. 2022;42(6):1077-1084.
13. Herbort CP, Papadia M, Neri P. Myopia and inflammation. J Ophthalmic Vis Res. 2011;6(4):270-283.
14. Herbort CP, Neri P, Papasavvas I. Clinicopathology of non-infectious choroiditis: evolution of its appraisal during the last 2–3 decades from “white dot syndromes” to precise classification. J Ophthalmic Inflamm Infect. 2021;11(1).
15. Chai D, Yang X, Wang A, Lu S, Dai Y, Zhou J. Usefulness of Platelet Distribution Width and Fibrinogen in Predicting In-stent Restenosis With Stable Angina and Type 2 Patients With Diabetes Mellitus. Front Cardiovasc Med. 2022;9(March):1-8.
16. Vagdatli E, Gounari E, Lazaridou E, Katsibourlia E, Tsikopoulou F, Labrianou I. Platelet distribution width: A simple, practical and specific marker of activation of coagulation. Hippokratia. 2010;14(1):28-32.
17. Grimaldi E, Del Vecchio L, Scopacasa F, et al. Evaluation of the platelet counting by Abbott CELL-DYN® SAPPHIRETM haematology analyser compared with flow cytometry. Int J Lab Hematol. 2009;31(2):151-160.

18. Chen Y, Zhong H, Zhao Y, Luo X, Gao W. Role of platelet biomarkers in inflammatory response. Biomark Res. 2020;8(1):2-8.
19. Eriksson O, Mohlin C, Nilsson B, Ekdahl KN. The human platelet as an innate immune cell: Interactions between activated platelets and the complement system. Front Immunol. 2019;10:1590.
20. Blair P, Flaumenhaft R. Platelet α-granules: Basic biology and clinical correlates. Blood Rev. 2009;23(4):177-189.
21. Peerschke EI, Yin W, Ghebrehiwet B. Complement Activation on Platelets: Implications for Vascular Inflammation and Thrombosis. Mol Immunol. 2010;47(13):2170-2175.
22. Kavanagh D, Sheerin N. Thrombotic Microangiopathies. In: Brenner and Rector's The Kidney. ; 2020:1178-1195.
23. Lorés-Motta L, van Beek AE, Willems E, et al. Common haplotypes at the CFH locus and low-frequency variants in CFHR2 and CFHR5 associate with systemic FHR concentrations and age-related macular degeneration. Am J Hum Genet. 2021;108(8):1367-1384.
24. Cipriani V, Lorés-Motta L, He F, et al. Increased circulating levels of Factor H-Related Protein 4 are strongly associated with age-related macular degeneration. Nat Commun. 2020;11(1):178.
25. Clark SJ, Bishop PN. The eye as a complement dysregulation hotspot. Semin Immunopathol. 2018;40(1):65-74.
26. Baxter SL, Pistilli M, Pujari SS, et al. Risk of choroidal neovascularization among the uveitides. Am J Ophthalmol. 2013;156:468-477.
27. Wu K, Zhang X, Su Y, et al. Clinical Characteristics of Inflammatory Choroidal Neovascularization in a Chinese Population. Ocul Immunol Inflamm. 2016;24(3):261-267.
28. Fang Y, Yokoi T, Nagaoka N, et al. Progression of Myopic Maculopathy during 18-Year Follow-up. Ophthalmology. 2018;125(6):863-877.
29. Szklanna PB, Parsons ME, Wynne K, et al. The Platelet Releasate is Altered in Human Pregnancy. Proteomics - Clin Appl. 2019;13(3):1-5.
30. Thornton P, Douglas J. Coagulation in pregnancy. Best Pract Res Clin Obstet Gynaecol. 2010;24(3):339-352.
31. Rabiah PK, Vitale AT. Noninfectious uveitis and pregnancy. Am J Ophthalmol. 2003;136(1):91-98.
32. Chiam NPY, Hall AJH, Stawell RJ, Busija L, Lim LLP. The course of uveitis in pregnancy and postpartum. Br J Ophthalmol. 2013;97(10):1284-1288.
33. Verhagen FH, Braakenburg AM, Kremer T, Drylewicz J, Rothova A, de Boer JH. Reduced number of relapses of human leucocyte antigen-B27-associated uveitis during pregnancy. Acta Ophthalmol. 2017;95(8):e798-e799.
34. Schellevis RL, Altay L, Kalisingh A, et al. Elevated steroid hormone levels in active chronic central serous chorioretinopathy. Investig Ophthalmol Vis Sci. 2019;60(10):3407-3413.
35. Çiloğlu E, Unal F, Dogan NC. The relationship between the central serous chorioretinopathy, choroidal thickness, and serum hormone levels. Graefe's Arch Clin Exp Ophthalmol. 2018;256:1111-1116.
36. Jaffe GJ, Westby K, Csaky KG, et al. C5 Inhibitor Avacincaptad Pegol for Geographic Atrophy Due to Age-Related Macular Degeneration: A Randomized Pivotal Phase 2/3 Trial. Ophthalmology. 2021;128(4):576-586.
37. Yurtseven ÖG, Aksoy S, Arsan AK, Özkurt YB, Kökçen HK. Evaluation of the relationship between age-related macular degeneration and refractive error, socio-demographic features, and biochemical variables in a Turkish population. Turkish J Ophthalmol. 2018;48(5):238-244.

38. Ahnood D, Madhusudhan S, Tsaloumas MD, Waheed NK, Keane PA, Denniston AK. Punctate inner choroidopathy: A review. Surv Ophthalmol. 2017;62(2):113-126.
39. Tavallali A, Yannuzzi LA. Idiopathic multifocal choroiditis. J Ophthalmic Vis Res. 2016;11(4):429-432.
40. Emilsson V, Gudmundsson EF, Jonmundsson T, et al. A proteogenomic signature of age-related macular degeneration in blood. Nat Commun. 2022;13(1):3401.
41. Rinsky B, Beykin G, Grunin M, et al. Analysis of the aqueous humor proteome in patients with age-related macular degeneration. Investig Ophthalmol Vis Sci. 2021;62(10).
42. Leung TG, Moradi A, Liu D, et al. Clinical features and incidence rate of ocular complications in punctate inner choroidopathy. Retina. 2014;34(8):1666-1674.
43. Kedhar SR, Thorne JE, Wittenberg S, Jabs DA. Multifocal choroiditis with Panuveitis and Punctate Inner Choroidopathy: Comparison of Clinical Characteristics at Presentation. Retina. 2007;27(9):1174-1179.
44. Thorne JE, Wittenberg S, Jabs DA, et al. Multifocal Choroiditis with Panuveitis. Incidence of Ocular Complications and of Loss of Visual Acuity. Ophthalmology. 2006;113(12):2310-2316.
45. Chen YC, Chen YL, Chen SN. Chorioretinal Atrophy in Punctate Inner Choroidopathy/multifocal Choroiditis: A Five-year Follow-up Study. Ocul Immunol Inflamm. 2021;00(00):1-6.
46. Liao DS, Grossi F V., El Mehdi D, et al. Complement C3 Inhibitor Pegcetacoplan for Geographic Atrophy Secondary to Age-Related Macular Degeneration: A Randomized Phase 2 Trial. Ophthalmology. 2020;127(2):186-195.
47. Neri P, Herbort CP, Hedayatfar A, et al. “White dot syndromes”, an inappropriate and outdated misnomer. Int Ophthalmol. 2022;42(1):1-6.
48. Jones EB, Jampol LM, Yannuzzi LA, et al. Relentless placoid chorioretinitis. Arch Ophthalmol. 2000;118:931-938.
49. The Standardization of Uveitis Nomenclature (SUN) Working group. Classification Criteria for Serpiginous Choroiditis. Am J Ophthalmol. 2021;228:126-133.
50. Dutta Majumder P, Biswas J, Gupta. Enigma of serpiginous choroiditis. Indian J Ophthalmol. 2019;67:325-333.
51. Fung AT, Pal S, Yannuzzi NA, et al. Multifocal choroiditis without panuveitis; Clinical Characteristics and Progression. Retina. 2014;34(1):98-107.
52. Amer R, Lois N. Punctate inner choroidopathy. Surv Ophthalmol. 2011;56(1):36-53.
53. Gerstenblith AT, Thorne JE, Sobrin L, et al. Punctate Inner Choroidopathy. A Survey Analysis of 77 Persons. Ophthalmology. 2007;114(6).

SUPPLEMENTAL DATA

Table 11.1. Patient characteristics for the different subtypes PIC and MFC

	MFC n=159 n=242 eyes	**PIC n=87 cases n=131 eyes**	***P*-value**
Female gender, n(%) of all patients	140 (88)	80 (92)	0.54
Mean (SD) age of all patients	44 (12)	42 (13)	0.12
Bilateral disease, n (%) of all patients	83 (52)	44 (51)	0.91
History of CNV[a], n (%) of all patients	110 (70)	63 (72)	0.75
Median LogMAR BCVA[a] [IQR] of all affected eyes	0.09 [-0.04-0.38]	0.04 [-0.04 – 0.34]	0.98

PIC, punctate inner choroidopathy; MFC, multifocal choroiditis; SD, standard deviation; CNV, choroidal neovascularization; LogMAR, Logarithm of the Minimum Angle of Resolution; BCVA, best-corrected visual acuity; IQR, interquartile range.
[a] Data was not available regarding the presence of CNV in 1 MFC case. BCVA was not available for 5 eyes of patients with PIC and 2 eyes of patients with MFC.

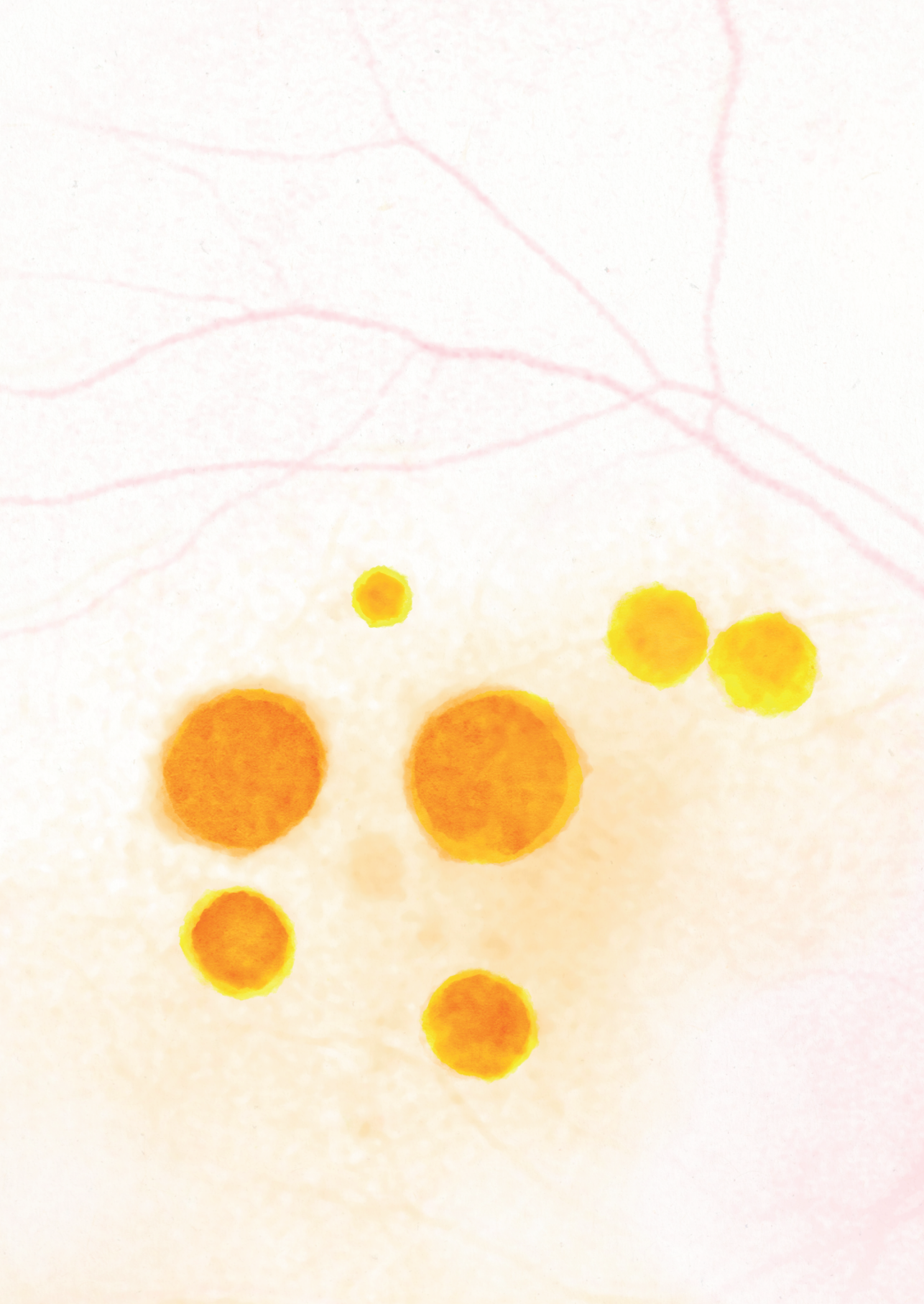

Chapter 12

Nederlandse samenvatting

Centrale multifocale choroïditis (cMFC) is een groep van zeldzame aandoeningen die vallen onder de primaire ontstekingen van de choriocapillaris. CMFC bestaat uit de entiteiten “multifocale choroïditis (MFC)”, “punctate inner choroidopathie (PIC)”, relentless placoïde chorioretinitis (RPC)”, “serpigineuze choroïditis (SC)” en “persistente placoïde maculopathie (PPM)”. Deze entiteiten hebben met elkaar gemeen dat de choriocapillaris van de achterpool van het oog is aangedaan en de pathofysiologie grotendeels onbekend is. De entiteiten MFC en PIC laten sterke klinische overeenkomsten zien en worden daarom vaak beschouwd als een enkele ziekte. De term idiopathische MFC zal worden gebruikt om deze twee subtypen aan te duiden.

In deze thesis hebben we verschillende aspecten van cMFC onderzocht met als overkoepeld doel om klinische en genetische risicofactoren vast te stellen. Het vaststellen van deze risicofactoren zal leiden tot meer inzicht in de pathofysiologie van dit ziektebeeld. Daarnaast kunnen deze risicofactoren gebruikt worden om de behandeling van cMFC te verbeteren met het uiteindelijk doel om de visuele functie van deze patiëntengroep te behouden. In deze thesis bespreken we de drie doelen voor de drie verschillende aspecten van deze ziekte:

1. Het verbeteren van de klinische uitkomsten van cMFC patiënten door de effectiviteit van de huidige behandelopties te onderzoeken en risicofactoren vast te stellen die het aantal recidieven bij patiënten verhoogd.
2. Het identificeren van karakteristieken op beeldvormende technieken die kunnen helpen bij het vroegtijdig herkennen van ziekteactiviteit en die kunnen differentiëren tussen actieve inflammatie en actieve secundaire choroidale neovascularisatie (CNV).
3. Het identificeren van genetische en immunologische risicofactoren met als doel om meer inzicht te krijgen in de onderliggende pathofysiologie van deze ziekte.

In dit hoofdstuk zullen we de belangrijkste bevindingen van deze thesis samenvatten.

Klinische uitkomsten bij patiënten met idiopathische MFC

In **hoofdstuk 2** beschrijven wij een groot cohort van idiopathische MFC patiënten waarin we de typische klinische karakteristieken van deze patiëntengroep bevestigen. In dit cohort was 93% vrouw, de gemiddelde leeftijd ten tijde van de eerste klachten was 37 jaar en de gemiddelde refractieafwijking van alle aangedane ogen was -5.5 dioptrieën. De prevalentie van secundaire CNV is uitzonderlijk hoog in dit ziektebeeld en was 66% in dit cohort.

In **hoofdstuk 3** en **hoofdstuk 4** hebben we de effectiviteit onderzocht van disease-modifying antirheumatic drugs (DMARDs) en/of biologicals bij patiënten met cMFC.

In **hoofdstuk 3** rapporteren we dat het aantal recidieven van ziekteactiviteit per jaar significant verminderde bij 32 patiënten nadat er gestart was met de behandeling met een DMARD. Met name het aantal recidieven van ziekteactiviteit waarbij ook de secundaire CNV actief was nam af, maar ook het aantal recidieven van ziekteactiviteit zonder actieve CNV reduceerde met 50%. Remmissie en steroïd-vrije remissie werd behaald respectievelijk gemiddeld 21 en 83 weken na de start van een DMARD. In het geval dat de behandeling met een DMARD onvoldoende effectief is, is de volgende stap het toevoegen van een biological aan de behandelstrategie. In **hoofdstuk 4** beschrijven we het ziektebeloop van twaalf patiënten voor en na het starten van de behandeling met de biological adalimumab. In deze studie laten we zien dat de meerderheid van de patiënten die onvoldoende reageren op de behandeling met een DMARD, goed reageren op de behandeling met adalimumab. Twaalf maanden na het starten van adalimumab werd bij negen van de twaalf patiënten steroïd-vrij remissie bereikt. Bij twee patiënten, gediagnosticeerd met serpigineuze choroïditis en persistente placoïde maculopathie, vonden desondanks meerdere klinische recidieven plaats. Onze resultaten laten zien dat adalimumab effectief is voor het behandelen van patiënten met idiopathische MFC, maar mogelijk minder effectief is voor het behandelen van patiënten met serpigineuze choroïditis en persistente placoïde maculopathie.

In **hoofdstuk 2** beschrijven we de resultaten van een observationele cohortstudie waarin we het ziektebeloop van 82 patiënten hebben vervolgd gedurende twee jaar. In deze studie werden 135 recidieven van ziekteactiviteit (mediaan (interkwartielafstand) 1.0 (0.25-3)) gediagnosticeerd bij 61 patiënten waarvan de meeste recidieven (75%) werden gediagnosticeerd voordat de patiënt symptomen ontwikkelde. Het aangedane gebied in de achterpool nam significant toe tijdens de twee jaar van follow-up en deze toename was significant groter bij patiënten die niet werden behandeld met DMARDs en/of biologicals. Bijna tweederde van de patiënten werd behandeld met stootkuren prednison gedurende de twee jaar follow-up, 21% startte met de behandeling met een DMARD en 26% van de patiënten startte met de behandeling met een biological in combinatie met een DMARD.

Zelf-gerapporteerde kwaliteit van leven

De kwaliteit van leven (QoL) van patiënten met idiopathische MFC is nog niet eerder onderzocht, ondanks dat het een erg belangrijke factor is voor de monitoring en behandeling van patiënten. Om meer inzicht te krijgen in de psychologische last van deze ziekte en om te onderzoeken welke factoren de kwaliteit van leven beïnvloeden, hebben we de kwaliteit van leven ten aanzien van de algemene gezondheid (GH-QoL) en visueel-gerelateerde (VR-QoL) kwaliteit van leven onderzocht in **hoofdstuk 2**. We vonden dat bij de start van follow-up patiënten lager scoorden voor bijna alle domeinen

van de VR-QoL, maar ook voor enkele domeinen van de GH-QoL. We hebben geen associatie gevonden tussen de QoL scores en het aantal recidieven of behandeling met DMARDs/biologicals of prednison.

Idiopathische MFC en zwangerschap

Voornamelijk vrouwen in de fertiele fase van het leven ontwikkelen idiopathische MFC. Om deze reden is meer informatie nodig over het natuurlijk beloop van deze ziekte tijdens de zwangerschap en de effectiviteit en veiligheid van verschillende behandelopties. **Hoofdstuk 5** beschrijft de resultaten van zestien zwangerschappen bij patiënten met idiopathische MFC. In deze studie vonden we dat bijna de helft van de patiënten een recidief ontwikkelde tijdens de zwangerschap. Recidieven ontstonden vooral bij vrouwen die niet behandeld werden met immunomodulerende therapie (azathioprine en/of prednison). De meeste recidieven ontstonden in het tweede en derde trimester van de zwangerschap. De behandeling met azathioprine, prednison en intravitreale anti-vascular endothelial growth factor (VEGF) injecties was over het algemeen veilig en er zijn geen ernstige complicaties geobserveerd bij de moeder of het kind. Wij adviseren om de behandeling van een zwangere patiënt altijd in de context van shared-decision making te laten plaatsvinden en moedigen preconceptioneel advies door zowel de oogarts als de gynaecoloog aan.

Multimodal imaging karakteristieken voor het monitoren van ziekteactiviteit

In **hoofdstuk 6** hebben we onderzocht of we imaging karakteristieken konden identificeren die duiden op inflammatoire ziekteactiviteit. Voor deze studie hebben we 50 patiënten geïncludeerd met idiopathische MFC met in totaal 110 laesies die we zowel tijdens de actieve fase en de inactieve fase hebben geëvalueerd. We vonden dat laesies met actieve inflammatie zonder actieve CNV (n=96) werden gekarakteriseerd door toename van de dikte van het vaatvlies onder de laesie, de aanwezigheid van materiaal met gematigde reflectiviteit in de sub-retinaal pigment epitheel (RPE) ruimte en/of het buitenste deel van het netvlies en disruptie van de ellipsoïde zone, allen te zien op spectral-domain optical coherence tomography (SD-OCT) scans. Daarnaast werd een toename van het gebied van hypoperfusie in de choriocapillaris gezien. Dit gebied van hypoperfusie was zichtbaar als een toename van het gebied van hypofluorescentie op indocyanine groen angiografie (ICGA) en een toename van het gebied van flow void op spectral-domain optical coherence tomography angiography (SD-OCTA). Om imaging karakteristieken te identificeren die actieve CNV kunnen onderscheiden van inflammatie, hebben we 14 laesies die waren gescoord als actieve inflammatie met actieve CNV vergeleken met 96 laesies die waren gescoord als actieve inflammatie zonder actieve CNV. We vonden dat actieve CNV geassocieerd was met lekkage van kleurstof op het

fluoresceïne angiogram en de observatie van een vasculaire structuur op de SD-OCTA. Daarnaast waren op de SD-OCT scan de aanwezigheid van vocht, hyporeflectiviteit van het choroïd en heterogeen hyperreflectief subretinaal materiaal geassocieerd met actieve CNV.

Bewegen richting gepersonaliseerde behandeling

Het natuurlijk beloop van de ziekte laat grote variabiliteit zien tussen patiënten. Daarom was een van de doelen om determinanten te identificeren die de ziekte-ernst van individuele patiënten kan voorspellen. In **hoofdstuk 2** vonden we dat het aantal recidieven bij patiënten werd beïnvloed door twee klinische factoren namelijk de refractieafwijking en de aanwezigheid van secundaire CNV. Het merendeel van de patiënten die secundaire CNV ontwikkelen, hebben dit al ontwikkeld bij de eerste presentatie. Hierdoor kunnen beide klinische factoren gebruikt worden om in een vroeg stadium de ziekte-ernst in te schatten en kunnen deze factoren assisteren bij het selecteren van de juiste behandelstrategie. In **hoofdstuk 7** hebben we een andere benadering gebruikt om determinanten te bepalen die geassocieerd zijn met de ziekte-ernst. In deze studie hebben we gebruik gemaakt van data ten aanzien van morfologische kenmerken van bloedcellen zoals de grootte, lobulariteit en complexiteit van deze cellen. In deze studie vonden we dat patiënten die een relatief hoge granulariteit hadden van de bloedplaatjes bij eerste presentatie, een grotere kans hadden om te starten met een DMARD en daarnaast ook sneller na eerste presentatie startten met een DMARD.

Pathofysiologie – wat hebben we geleerd

De genen en biologische systemen die betrokken zijn bij het ontstaan van idiopathische MFC zijn grotendeels onbekend, wat de ontwikkeling van adequate monitoring en behandeling van deze patiëntengroep hindert. We hebben geprobeerd de pathofysiologie van dit zeldzame ziektebeeld verder te ontrafelen door associaties met bloedcel karakteristieken, single nucleotide polymorfismen (SNPs), en eiwit concentraties te onderzoeken.

In **hoofdstuk 7** hebben we de morfologische bloedcel karakteristieken vergeleken tussen 122 patiënten met cMFC en 364 leeftijd en geslacht gekoppelde controles. In deze studie vonden we dat cMFC patiënten een verlaagd aantal monocyten in het bloed hadden en daarnaast het percentage van de monocyten lager was ten opzichte van de controles. In **hoofdstuk 8** beschrijven we een toevalsbevinding waarbij we ontdekten dat in een subset van patiënten een verhoogde fluorescentie werd gemeten van neutrofielen, lymfocyten, monocyten en erytrocyten. Het bleek dat deze subset van patiënten binnen 8 uur voor de bloedafname een fluoresceïne angiogram hadden ondergaan.

In **hoofdstuk 9** beschrijven we de resultaten van een genoom-wijde associatie studie waarin 222 idiopathische MFC patiënten werden geïncludeerd. In deze studie ontdekten we een associatie met een genetische variant in het *complement factor H* (*CFH*) gen (sterkst geassocieerde variant was het A allel van de rs7535263 SNP; odds ratio (OR) [95% confidence interval (95%CI)] = 0.52 [0.41-0.64]; $P = 9.3 \times 10^{-9}$). Daarnaast hebben we in 87 patiënten zonder systemische behandeling, de concentraties van 370 inflammatie-gerelateerde eiwitten gemeten middels het Olink platform. In deze studie laten we zien dat het risico genotype (GG) van deze specifieke SNP (rs7535263) geassocieerd is met een verhoogde concentratie van 27 eiwitten bij patiënten met idiopathische MFC. Middels reactome pathway enrichment analyse hebben we 2 biologische systemen geïdentificeerd waar deze eiwitten bij betrokken zijn namelijk de degranulatie van bloedplaatjes en de regulatie van het complement systeem.

In **hoofdstuk 10** hebben we de allelfrequentie (AF) van de sterkst geassocieerde SNP (rs7535263) met idiopathische MFC onderzocht bij patiënten met de overige subtypes van cMFC. Voor deze studie hebben we 31 patiënten geïncludeerd waarvan 11 patiënten met serpigineuze choroïditis (SC), 3 patiënten met persistente placoïde chorioretinopathie (PPM) en 17 patiënten met relentless placoïde chorioretinitis (RPC). De allelfrequentie van het risico allel G van rs7535263 was 48% in de patiënten en 57% in de controles en liet geen significante associatie zien met deze subtypen (odds ratio (OR) = 0.89 [95%CI 0.45-1.74]; $P = 0.73$). Wanneer de subtypen apart werden geanalyseerd, werden vergelijkbare resultaten gevonden (SC; AF G-allel 41%, OR=0.64 [95%CI 0.28-1.46]; $P = 0.29$; RPC: AF G-allel 50%, OR= 0.89 [95%CI 0.45-1.75]; $P = 0.74$).

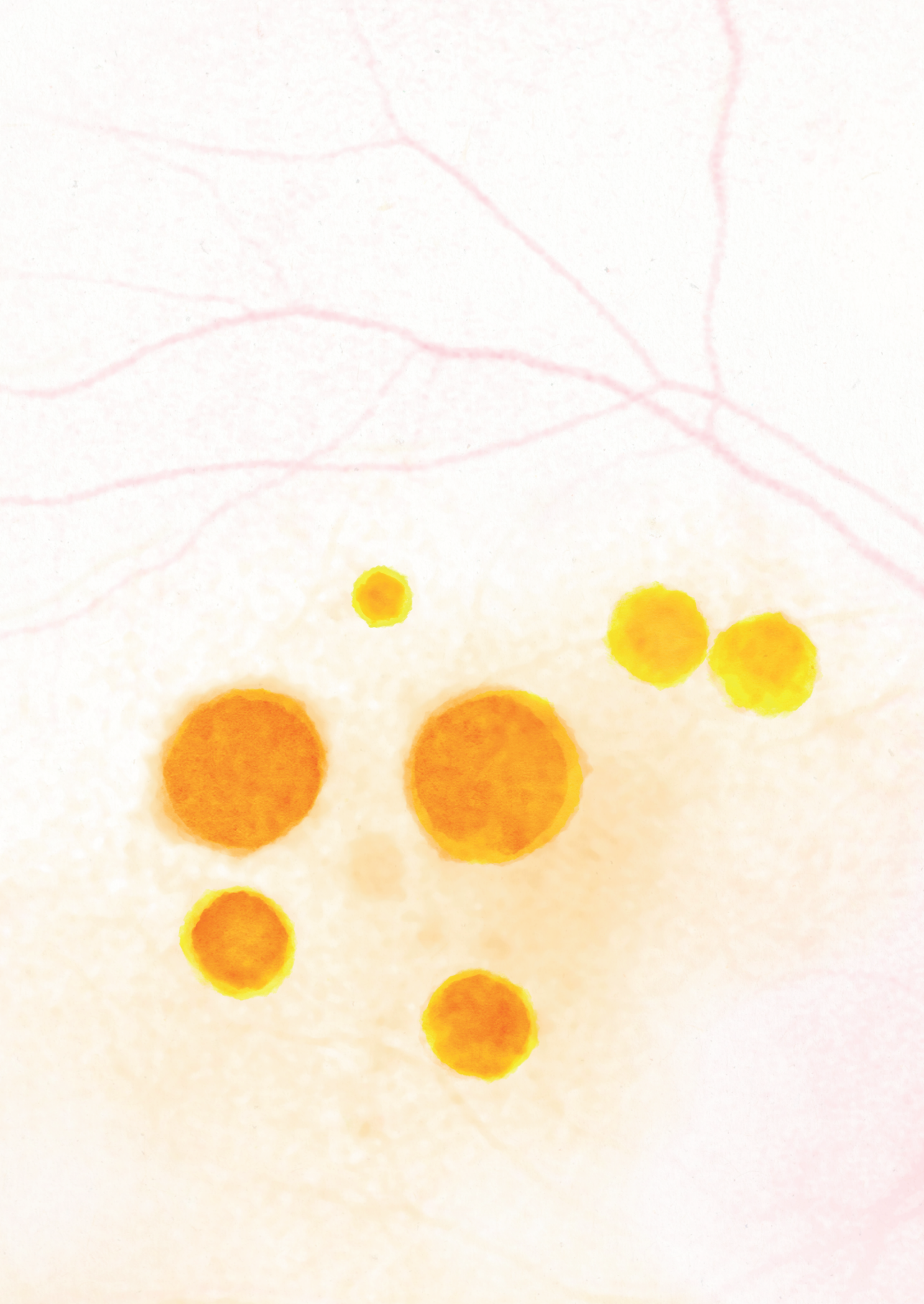

Appendices

DANKWOORD

Onderzoek doen doe je natuurlijk nooit alleen. Vele mensen hebben mij de afgelopen jaren geholpen en daarmee direct of indirect bijgedragen aan het tot stand komen van dit proefschrift. Ik wil dan ook iedereen bedanken die, op wat voor een manier dan ook, heeft meegeholpen aan het realiseren van dit proefschrift. Een aantal mensen wil ik graag in het bijzonder bedanken met een persoonlijk dankwoord.

Om te beginnen wil ik alle patiënten bedanken die aan het onderzoek hebben bijgedragen. Gezien de zeldzaamheid van de oogziekte die we in dit proefschrift hebben onderzocht, had dit proefschrift nooit tot stand kunnen komen zonder jullie hulp. Patiënten uit alle uithoeken van Nederland hebben meegewerkt, en jullie bijdrage staat dan ook aan de basis van dit proefschrift. Ik hoop dat er in de toekomst steeds meer aandacht zal zijn voor jullie ziektebeeld en er antwoorden komen op de vragen die vele van jullie nog steeds dagelijks bezig houden.

Beste promotieteam: Joke, Carel, Annette, en Jonas, in de afgelopen 4 jaar heb ik veel van jullie mogen leren en ik kijk dan ook terug op hele leuke en leerzame jaren. Bij ieder van jullie kon ik altijd terecht met vragen en ik wil jullie dan ook bedanken voor al jullie hulp en geduld. Jullie zijn een geweldig team en vullen elkaar heel goed aan en ik hoop in de toekomst nog veel met jullie te mogen samenwerken.

Geachte prof. dr. de Boer, Beste Joke, eigenlijk vanaf de eerste dag dat ik met mijn promotietraject begon, heb ik me erg op mijn gemak gevoeld bij jou. Hoewel ik soms door de bomen het bos niet meer zag, wist jij mij altijd gerust te stellen en een stukje overzicht te bieden. De combinatie van jouw enorme wetenschappelijke kennis, ervaring en betrokkenheid maakt jou een geweldige begeleider. Ik hoop dan ook tijdens de opleiding nog veel meer van je te leren, maar voor nu wil ik je bedanken voor je begeleiding de afgelopen 4 jaar.

Geachte dr. Ossewaarde-van Norel, Beste Annette, waar te beginnen. Vanaf moment 1 heb ik me altijd door jou gesteund gevoeld en heb je me het vertrouwen gegeven en geleerd om kritisch te durven zijn. Ik durf heel zeker te stellen dat zonder jouw aanstekelijke enthousiasme en extreme betrokkenheid, dit proefschrift niet had bestaan of een heel stuk dunner zou zijn geweest. Jouw gedrevenheid om de zorg van deze patiëntengroep te verbeteren, is bewonderenswaardig. En hoewel jouw agenda soms erg vol kon zijn, wist je altijd een gaatje voor mij te vinden. Ik denk dat we de afgelopen jaren een goed team waren, en we vormden dan ook een heel herkenbaar krullen duo als we door de gangen liepen (collega's begonnen me zelfs mini-Annette te noemen). Ik

ben erg trots dat ik met jou heb mogen samenwerken, al ben ik er van overtuigd dat ik ook in de toekomst nog heel veel dingen van jou ga leren.

Geachte dr. Kuiper, Beste Jonas, hoewel jij niet vanaf het begin van het promotietraject betrokken was bij dit onderzoek, denk ik dat jouw bijdrage onmisbaar is geweest. Ik ben dan ook erg blij dat jij je bij mijn promotieteam hebt gevoegd, want ik durf te stellen dat ik zonder jouw hulp weinig chocola had kunnen maken van de gigantische hoeveelheid genetische en hematologische data. Middels jouw welbekende white board weet jij de meest complexe concepten en ideeën te vereenvoudigen, mijn inziens een talent op zich. Ik wil je bedanken voor jouw hulp en geduld en het soms meerdere keren uitleggen van een techniek of analyse voordat het kwartje bij mij viel.

Geachte prof. dr. Hoyng, Beste Carel, hoewel we de afgelopen jaren niet heel veel hebben samengewerkt, wil ik je heel hartelijk bedanken voor de intensieve samenwerking die we hebben op gezet tussen het UMC Utrecht en het Radboudumc. Ik weet zeker dat dit zonder jouw hulp nooit was gelukt. Jouw interesse in dit ziektebeeld is cruciaal geweest voor het tot stand komen van dit proefschrift en ik wil je hiervoor dan ook hartelijk bedanken.

Geachte leden van de beoordelingscommissie en/of promotiecommissie: prof. dr. Hamann, prof. dr. Klaver, prof. dr. Imhof, dr. van Velthoven, prof. dr. Veldink, prof. dr. Boon, en prof. dr. van Genderen. Graag wil ik jullie bedanken voor het lezen en het beoordelen van dit proefschrift en zitting te nemen in de commissie.

Lieve (oud)-collega's, wat waren het een saaie 4 jaren geweest zonder jullie. En hoewel we veel jaren vanuit huis hebben moeten werken, denk ik dat we elkaar altijd wisten te vinden voor vragen, hulp of advies. Om maar bij het begin te beginnen, vanaf het eerste moment heb ik me erg thuis gevoeld in de onderzoeksgroep waarmee ik startte. Kamil, Anna en Sara, jullie als oudste onderzoekers wisten mij snel wegwijs te maken in het onderzoek. Anna, jouw heerlijke bonbons en zelfgemaakte taarten, maar ook de zeer specifieke geur van jouw rookthee, zal ik nooit vergeten. Sara, jij als mede promovenda bij Annette hebt mij heel veel geholpen met het eigen maken van de beeldvormende technieken en met jouw aanstekelijke enthousiasme voor wetenschappelijk onderzoek wist jij mij altijd ook weer te motiveren. Brendan, we zijn bijna tegelijkertijd begonnen en ik heb dan ook door de jaren heen veel aan jouw hulp en gezelligheid gehad (ook al waren onze werkplekken enkele honderden meters van elkaar verwijderd). Hopelijk gaan we nog een keertje samen varen door Amsterdam, al moeten we dan wel eerst uitvechten welke boot we pakken. Ik kijk er naar uit om samen de opleiding te gaan starten! En dan natuurlijk de B-hokkers, Bas, Myrthe en Roos. Zeker het eerste jaar hebben we eindeloos

veel tijd met elkaar doorgebracht in de zeer gelimiteerde ruimte van het B-hok. Bas, jouw aanstekelijke geklets maakte iedere dag een stukje gezelliger. Ik ga de foto's van Nala en het uitgebreid evalueren van de weekenden absoluut missen. Roos, tijdens mijn onderzoek was jij toch een beetje mijn voorbeeld. Hoe jij jouw enorme werkethos weet te combineren met een hele hoop gezelligheid, blijf ik bewonderenswaardig vinden. Ook hebben we erg veel plezier gehad met het organiseren van DOPS! Myrthe, ik wil jou vooral bedanken voor de gezelligheid van het laatste jaar. Ik ben heel blij dat ik zo nu en dan even mijn frustraties kon uiten bij jou (en vice versa uiteraard). Hoewel je helaas het UMCU hebt verlaten, hoop ik dat we in de toekomst nog contact houden. En is wens je natuurlijk vooral heel veel succes bij de kindergeneeskunde! Cansu, Wouter, Lude, Sanne en Els, ik wil jullie bedanken voor alle hulp en gezelligheid. En de cornea boys, Janneau en Casper, ook al hadden we wetenschappelijk gezien niet heel veel raakvlakken, ik ben blij dat ik met jullie heb mogen samen werken. Carlyn, wat hebben wij wat uren samen doorgebracht met het scoren van foto's. Ik wil je heel erg bedanken voor onze samenwerking, zonder jouw inzet en geduld weet ik niet of we door alle foto's heen waren gekomen. Jytte en Nienke, we hebben niet heel lang samengewerkt maar ik wens jullie allebei heel veel succes met jullie onderzoeken!

Tamara en Marianne, dank jullie wel voor het helpen bij het opzetten van de verschillende onderzoeken en het uitleggen van alle logistieke zaken die bij onderzoek doen komen kijken. Dax en Nivard, hartelijk dank voor jullie bijdrage aan het opstellen van de verschillende datamanagement plannen. Door jullie bijdrage blijft alle data beschikbaar voor toekomstig onderzoek.

Suzan en Petra, bedankt dat ik altijd bij jullie terecht kon met al mijn vragen en logistieke problemen! Beste fotografen, heel veel dank voor de moeite die jullie de afgelopen jaren hebben gestopt in het compleet aanleveren van alle imaging. Vooral tijdens de coronapandemie kon dit af en toe een uitdaging zijn. Beste stafartsen en AIOS, heel veel dank voor alle interesse die jullie de afgelopen jaren hebben getoond in mijn onderzoek. Maar ook jullie hulp bij het includeren van patiënten is onmisbaar geweest. In het bijzonder wil ik Ninette bedanken voor de tijd en moeite die je hebt gestopt in het scoren van de vele foto's. Ook Ina en Angelique wil ik bedanken voor jullie hulp bij het includeren van patiënten.

Beste uveitiswerkgroep, bedankt voor jullie interesse in mijn onderzoek, jullie input voor de onderzoeksopzet en de mogelijkheid om mijn resultaten met jullie te delen.

Beste coauteurs, bedankt voor jullie onmisbare bijdrage aan dit proefschrift. Beste Yvonne de Jong-Hesse, Camiel Boon, Leonie Los, Alberta Thiadens, Magda Meester,

en Ramon van Huet, zonder jullie inzet hadden we nooit zoveel patiënten kunnen includeren verspreid over heel Nederland. Ik ben erg trots dat we uiteindelijk zo een groot patiëntencohort hebben kunnen creëren. Kristel van Eijk, bedankt voor jouw geduld en begeleiding bij het uitvoeren van de GWAS analyses. Saskia Haitjema, bedankt voor jou hulp en expertise op het gebied van de hematologische data van UPOD.

Lieve JC Indigo, ik wil jullie bedanken voor de interesse in mijn proefschrift en de gezelligheid van de afgelopen jaren. We hebben een aantal moeilijke momenten meegemaakt samen, maar ik vind het heel mooi om te zien dat we daardoor alleen maar hechter zijn geworden. Ik hoop dat we elkaar nog vele jaren blijven zien.

Lieve oudhuisgenootjes, dankjewel voor alle gezelligheid van de afgelopen jaren. Ondanks dat we inmiddels al heel wat jaren geen huisgenoten meer zijn, ben ik heel blij dat we elkaar nog steeds zo veel spreken. In het bijzonder wil ik Britt bedanken, zonder jouw Brabantse gezelligheid en worstenbrood ontbijtjes, zou het leven toch een stuk ongezelliger zijn. En lieve Colette, de hoeveelheid uren die wij hebben doorgebracht samen als studiemaatjes, huisgenoten en clubgenoten is eindeloos. Ik durf dat ook wel te zeggen dat je inmiddels meer familie bent dan een vriendin. Inmiddels zit je alweer bijna een jaar in Amerika en ik ben heel trots dat je je hart hebt gevolgd en deze spannende stap hebt durven nemen. Ook al spreken we elkaar nu niet meer dagelijks, ik weet dat ik altijd op je kan rekenen.

Lieve Jade, Zulema, Dick, Milo en Jens, dankjewel voor jullie vriendschap en de vele gezellige vakanties van de afgelopen jaren. Bij jullie kan ik altijd terecht en ik ben heel blij dat ik jullie in mijn leven heb. Ik hoop dat we nog vele jaren samen op vakantie blijven gaan!

Lieve DDF, Lieve Marilou, Inga, Jetske, Iris, Nikki en Sara, ik vind het heel speciaal hoe wij al zoveel jaren een goede vriendschap hebben en elkaar door de jaren heen eigenlijk alleen maar meer zijn gaan zien. Allemaal anders maar toch heel hecht. Ik ben heel trots op wat jullie allemaal al hebben bereikt en ik kan niet wachten om te zien wat de toekomst ons nog gaat brengen. Twee dingen weet ik zeker, wijn zal nooit ontbreken en jullie zullen altijd onderdeel van mijn leven blijven. Heel veel dank voor jullie vriendschap en gezelligheid.

Lieve schoonfamilie, dank jullie wel dat ik onderdeel mag zijn van jullie familie en de interesse die jullie altijd hebben getoond in mijn onderzoek.

Lieve familie en in het bijzonder lieve opa en oma, ik wil jullie graag bedanken voor de interesse die jullie in mij tonen. De vele tradities die wij inmiddels hebben opgebouwd als familie zijn mij heel dierbaar. Ik hoop dan ook dat deze tradities nog vele jaren blijven bestaan en we in de toekomst nog heel veel tijd met elkaar mogen doorbrengen!

Lieve Papa, Mama, Freek, Alex en Bridget, ik wil jullie graag bedanken voor alle mooie herinneringen die we hebben samen. Ik voel mij altijd thuis bij jullie en ik ben dan ook heel blij dat jullie mijn familie zijn. Papa en Mama, jullie onvoorwaardelijk steun en interesse in mijn werk heeft me geholpen om door te gaan en de juiste keuzes te maken in het leven. Lieve Freekie, in veel dingen lijken we op elkaar maar zijn we toch ook verschillend. Ik hoop dat in de toekomst onze band altijd hecht zal blijven en ik kan niet wachten om te zien wat het leven voor ons in petto heeft.

Lieve Sara, inmiddels al weer ruim 4 jaar geleden zijn wij allebei begonnen aan een PhD. Jij in Kopenhagen en ik in Nederland. Inmiddels zijn we honderden telefoonuren verder waarin we gewoon bij kletsten maar waar we ook onze frustraties konden delen. Ondanks de afstand, denk ik dat onze band de afgelopen jaren alleen maar sterker is geworden en ik ben dan ook heel trots dat jij mijn paranimf bent. Inmiddels heb je Kopenhagen ingeruild voor het Zweedse leven, maar ik heb er alle vertrouwen in dat wij elkaar altijd zullen blijven zien en spreken.

Lieve Wilbert, jij haalt altijd het beste in mij naar boven en we vullen elkaar zo ontzettend goed aan. Jouw bijdrage aan dit proefschrift, in de vorm van onvoorwaardelijke liefde en steun, is nog zo veel groter dan je zelf denkt. Een leven zonder jou kan ik me niet voorstellen, het zou in ieder geval een stuk minder gezellig zijn. Ik hoop nog vele jaren bij jou thuis te komen en ik kijk ontzettend uit naar onze toekomst samen.

ABOUT THE AUTHOR

Evianne de Groot was born on 24th of February 1994 in Leiden, the Netherlands. She is the daughter of René and Jeanet and has a younger brother, Freek. In 2012 she graduated from secondary school at the Stedelijk Gymnasium in Leiden. In the same year she moved to Utrecht and started her medical training at the University of Utrecht.

The first time Evianne came in contact with the specialty of ophthalmology, was during her short internship at the Rivierenland in Tiel. After this internship, Evianne decided to further explore her interest in Ophthalmology and she was specifically interested in the ophthalmological patient care outside well-developed countries. Therefore, she travelled to Nepal and did her internship at the Tilganga Institute of Ophthalmology in Katmandu, Nepal. Here, she attended several "eye camps" to remote parts of Nepal were she learned about the impact of eye diseases on the life of patients without immediate access to ophthalmological care. In 2018 she did her master thesis under supervision of Jeannette Ossewaarde-van Norel regarding the efficacy of immunomodulatory therapy in patients with idiopathic multifocal choroiditis, **Chapter 3** of this thesis. Evianne really enjoyed the collaboration with Jeannette and was intrigued by the subject of her master thesis; the rare ophthalmological disease "Multifocal choroiditis". This resulted in the start of a PhD track at the Ophthalmology Department of the University of Utrecht regarding the clinical, immunological and genetic aspects of multifocal choroiditis in an attempt to further unravel the pathophysiology of this rare disease. During her PhD, she received the price for the "Best Free Paper award" for her presentation regarding the genetic associations in multifocal choroiditis (**Chapter 9**) at the International Uveitis Symposium. In addition to her research activities, she was the treasurer of the committee of the Dutch Ophthalmology PhD Students (DOPS) and organized the DOPS conference in 2020.

In April 2023, she continues her journey in the field of Ophthalmology and she will start with the residency in Ophthalmology at the UMC Utrecht.

LIST OF PUBLICATIONS

de Groot EL, de Boer JH, Ossewaarde-van Norel J. Idiopathic Multifocal Choroiditis and Punctate Inner Choroidopathy – Evaluation of Risk Factors for Increased Relapse Rate: A 2-Year Prospective Observational Cohort Study. Ophthalmologica 2022;245(5):476-486.

de Groot EL, ten Dam-van Loon NH, de Boer JH, Ossewaarde-van Norel J. The efficacy of corticosteroid-sparing immunomodulatory therapy in treating patients with central multifocal choroiditis. Acta Ophthalmol. 2020;98(8):816-821.

de Groot EL, Ossewaarde-van Norel J, Ho L, ten Dam-van Loon NH, de Boer JH. The efficacy of adalimumab in treating patients with central multifocal choroiditis. Am J Ophthalmol Case Rep. 2020; 20: 100921.

de Groot EL, van Huet RAC, Bloemenkamp KWM, de Boer JH, Ossewaarde-van Norel J. Idiopathic multifocal choroiditis and punctate inner choroidopathy: an evaluation in pregnancy. Acta Ophthalmol. 2022;100(1):82-88.

de Groot EL, ten Dam-van Loon NH, Kouwenberg CV, de Boer JH, Ossewaarde-van Norel J. Exploring imaging characteristics associated with disease activity in idiopathic multifocal choroiditis: a multimodal imaging approach. Am J Ophthalmol. 2023; S0002-9394(23)00136-8.

de Groot EL, Ossewaarde-van Norel J, Hoefer IE, Haitjema S, de Boer JH, Kuiper JJW. Central Multifocal Choroiditis: Platelet Granularity as a Potential Marker for Treatment With Steroid-Sparing Immunomodulatory Therapy. Front. Ophthalmol. 2021; 784848.

de Groot EL, Huisman A, van Solinge WW, Ossewaarde-van Norel J, Haitjema S. Fluorescein angiography leads to increased fluorescence of blood cells and may hamper routine haematology analysis of ophthalmology patients. Int J Lab Hematol. 2022 Jun;44(3):e91-e94.